

MAST CELL STING ACTIVATION IN INFECTION AND CANCER IMMUNITY

by

Haya Al Bitar

Submitted in partial fulfilment of the requirements
for the degree of Master of Science

at

Dalhousie University
Halifax, Nova Scotia
April 2025

Table of Contents

List of Tables	vii
List of Figures	viii
Abstract	xi
List of Abbreviations and Symbols	xii
Acknowledgements	xv
<u>Chapter 1 : INTRODUCTION</u>	1
1.1 MAST CELLS	1
1.1.1 Mast cells as immune sentinels	1
1.1.2 Mast cell differentiation, subsets, activation, and mediator production.....	2
1.1.3 Mast cells during infection	5
1.1.4 Mast cells in cancer	6
1.1.5 The modulation of mast cells for cancer immunotherapy	8
1.1.6 <i>In vitro</i> models to study mast cell biology	10
1.1.7 Murine mast cell-deficient models	11
1.2 THE CGAS-STING PATHWAY	13
1.2.1 Introduction to the cGAS-STING pathway	13
1.2.2 Type I IFN signaling	14
1.2.3 Functional implications of STING on the immune system	16
1.2.4 Loss-of-function/gain-of-function mutations	17
1.2.5 STING signaling in mast cells.....	18
1.3 STING IN BACTERIAL INFECTION	20
1.3.1 Overview of STING in bacterial infection	20
1.3.2 Introduction to <i>Shigella</i>	22
1.3.3 Immune responses to <i>Shigella</i> infection.....	23

1.4 STING IN OVARIAN CANCER IMMUNOTHERAPY	25
1.4.1 Introduction to ovarian cancer	25
1.4.2 First-line and novel therapeutic approaches	27
1.4.3 Immunotherapy.....	29
1.4.4 Anti-tumor effects of STING activation.....	30
1.4.5 Limitations/downfalls of STING agonist therapy	33
1.4.6 Murine models of ovarian cancer	35
1.5 RATIONALE AND RESEARCH OBJECTIVES	38
<u>Chapter 2 : MATERIALS & METHODS</u>.....	41
2.1 ANIMALS	41
2.2 ANTIBODIES.....	41
2.3 REAGENTS.....	42
2.4 CELL CULTURE	44
2.4.1 Bone marrow-derived mast cells	44
2.4.2 Cord blood-derived mast cells	44
2.4.3 Peritoneal cavity-derived mast cells	45
2.4.4 RAW 264.7 macrophages.....	46
2.4.5 ID8 ovarian cancer cell line.....	46
2.4.6 U-2 OS cells	46
2.4.7 293T cells	47
2.5 PRODUCING STING-TRANSDUCED CELLS	47
2.5.1 DNA cloning vector and gene inserts.....	47
2.5.2 DNA cloning procedure	47
2.5.3 Transfection to produce lentivirus	50
2.5.4 Transduction of cells	51

2.6 MAST CELL ACTIVATION	53
2.6.1 STING and cGAS agonists.....	53
2.7 SHIGELLA INFECTION OF MAST CELLS.....	54
2.8 SURVIVAL OF MICE IN AN OVARIAN CANCER MODEL.....	55
2.8.1 Preparation and injection of ID8 cells	55
2.8.2 ID8 harvest	56
2.8.3 <i>In vivo</i> reconstitution with transduced and WT mast cells.....	57
2.8.4 Harvest of mesenteric lymph nodes and peritoneal washes	57
2.9 GENE EXPRESSION AND PROTEIN ANALYSES.....	58
2.9.1 RNA isolation from cells.....	58
2.9.2 Complementary DNA (cDNA) synthesis.....	59
2.9.3 Quantitative polymerase chain reaction (qPCR) and analyses.....	59
2.9.4 Protein isolation and concentration measurement	60
2.9.5 Western blotting	61
2.9.6 Luminex and ELISA.....	61
2.9.7 Immunofluorescence staining and imaging.....	61
2.10 FLOW CYTOMETRY	62
2.10.1 Annexin V Apoptosis Assay	62
2.10.2 Staining procedure for peritoneal cells and mesenteric lymph nodes	63
2.10.3 Flow cytometry panels and analysis.....	64
2.11 DATA REPRESENTATION AND STATISTICAL ANALYSES	64
<u>Chapter 3 : RESULTS.....</u>	66
3.1 <i>IN VITRO</i> CHARACTERIZATION OF STING SIGNALING IN MAST CELLS.....	66
3.1.1 Characterizing transcriptional changes following STING agonist activation in mast cells	66

3.1.2 Assessing cGAS activation of mast cells	75
3.1.3 Detection and activation of STING protein.....	76
3.1.4 Mast cell production of IFN and chemokines following STING activation	78
3.2 THE ROLE OF STING ACTIVATION IN MAST CELL RESPONSES TO SHIGELLA INFECTION IN VITRO	79
3.3 CHARACTERIZING THE EFFECT OF STING ACTIVATION ON IMMUNE RESPONSES IN VIVO.....	87
3.3.1 STING agonist (ADU-S100) dosing in C57BL/6 mice	87
3.3.2 STING agonist (ADU-S100) kinetics in C57BL/6 mice.....	90
3.3.3 Assessing STING activation kinetics in mast cell-deficient mice.....	96
3.4 THE ROLE OF STING AGONIST THERAPY IN THE ID8 MODEL.....	98
3.4.1 ID8 survival in wild-type mice with STING agonist therapy	98
3.5 THE ROLE OF MAST CELLS IN STING AGONIST EFFICACY IN THE ID8 MODEL.....	100
3.5.1 Survival of the ID8 model in MC-deficient mice.....	100
3.5.2 The role of mast cells in STING agonist therapy on the survival of the ID8 model	103
3.6 GENETIC MODIFICATION OF BMMCS BY TRANSDUCTION WITH LENTIVIRUSES EXPRESSING WILD-TYPE STING AND STING MUTANTS	105
3.6.1 Testing induction of target genes and protein production in U-2 OS cells <i>in vitro</i>	106
3.6.2 Testing induction of target genes and protein production by transduced BMMCs <i>in vitro</i>	107
3.6.3 Testing induction of target genes by transduced BMMCs <i>in vivo</i>	114
3.7 THE EFFECT OF WT STING-TRANSDUCED BMMCS ON ID8 SURVIVAL IN VIVO.....	115
<u>Chapter 4 : DISCUSSION.....</u>	120
4.1 SUMMARY OF MAJOR FINDINGS.....	120

4.2 RESULTS IN THE CONTEXT OF ESTABLISHED LITERATURE.....	123
4.2.1 Activation and overexpression of STING in mast cells	123
4.2.2 Mast cell responses to <i>Shigella</i> infection and the role of the STING pathway	125
4.2.3 The role of MCs and STING activation in ovarian cancer.....	129
4.3 CRITIQUES AND LIMITATIONS	132
4.4 CLINICAL IMPLICATIONS.....	133
4.5 FUTURE RESEARCH DIRECTIONS.....	136
4.5.1 Characterization of STING signaling in mast cells	136
4.5.2 Unraveling the role of mast cells in <i>Shigella</i> infection	137
4.5.3 Elucidating the role of mast cells in ovarian cancer	139
4.6 CONCLUDING REMARKS.....	141
REFERENCES.....	143

List of Tables

Table 1. Mast cell receptors and their corresponding ligands.....	2
Table 2. Reagents used for cell culture and <i>in vitro</i> activations	43
Table 3. Amino acid sequences of GFP, WT STING, V154M, and N153S transcripts ...	50
Table 4. Antibodies for flow cytometry to examine lymphoid immune cell populations (Panel 1).....	65
Table 5. Antibodies for flow cytometry to assess innate immune cell populations (Panel 2)	65

List of Figures

Figure 1. Pro-tumorigenic and anti-tumorigenic functions of mast cells in cancer.....	8
Figure 2. Schematic illustrating the mechanism of STING activation.	15
Figure 3. The innate immune response to <i>Shigella</i> infection.....	25
Figure 4. Anti-tumor functions of the STING pathway in the immune system.....	33
Figure 5. Overview of the pLJM1_Bla_TRE DNA vector for inducible STING expression in mast cells.....	52
Figure 6. Type I IFN, ISG, and cytokine transcript levels were increased in mast cells following STING activation with ADU-S100	67
Figure 7. Mast cells upregulate type I IFN and ISG gene expression following STING activation with diABZI.	68
Figure 8. RAW264.7 macrophages upregulate <i>Ifit1</i> but not <i>Ifnb1</i> mRNA following activation with STING agonists.....	70
Figure 9. STING agonist treatment does not cause changes in cell death or viability in mast cells.	71
Figure 10. STING agonist-induced transcriptional changes were dampened by inhibitor H-151 and are absent in STING KO mast cells.	73
Figure 11. Human mast cells responded to STING activation by upregulating type I IFN-related transcript levels.	74
Figure 12. Mast cell cGAS activation leads to increases in type I IFN and ISG transcript levels.	75
Figure 13. Murine mast cells express intracellular STING protein that is phosphorylated upon activation.....	77
Figure 14. STING activation causes IFN- β and CCL2 production by mast cells.....	79
Figure 15. Murine mast cell type I IFN responses to <i>Shigella</i> infection are STING-dependent	82
Figure 16. Kinetics of <i>Shigella</i> infection in murine mast cells.....	84
Figure 17. Human mast cells promote a STING-independent type I IFN response to <i>Shigella</i> infection.	86

Figure 18. STING activation increases <i>Cxcl10</i> and <i>Ift1</i> gene expression in peritoneal cells.	88
Figure 19. STING activation increases T cell activation in the peritoneum.	90
Figure 20. STING activation promotes transient increases in type I IFN-related transcriptional changes in peritoneal cells.	92
Figure 21. STING activation promotes the production of type I IFNs, CXCL10, CXCL1, and IL-6 by peritoneal cells.	93
Figure 22. STING activation increases macrophage activation and neutrophil infiltration <i>in vivo</i>	94
Figure 23. STING agonist treatment increases T cell activation <i>in vivo</i>	95
Figure 24. Mast cells play a selective role in transcriptional changes in response to STING activation <i>in vivo</i>	97
Figure 25. STING agonist therapy improves overall survival in the ID8 murine ovarian cancer model.	99
Figure 26. Mast cells influence the overall survival of the ID8 ovarian cancer model.	102
Figure 27. Mast cells do not provide a survival advantage with STING agonist therapy in the ID8 ovarian cancer model.	104
Figure 28. U-2 OS cells transduced with wild-type STING and constitutively active STING mutants (V154M, N153S) showed successful DOX-dependent increases of STING protein <i>in vitro</i>	108
Figure 29. Mast cells transduced with WT STING showed successful DOX-dependent induction of total STING, phosphorylated STING, and FLAG tag protein expression <i>in vitro</i>	110
Figure 30. Mast cells transduced with WT STING showed DOX-dependent induction of ISG mRNA expression <i>in vitro</i>	111
Figure 31. Mast cells transduced with WT STING showed rapid kinetics of DOX-dependent induction of STING (<i>Tmem173</i>) and ISG mRNA expression <i>in vitro</i>	112
Figure 32. Mast cells transduced with WT STING do not exhibit enhanced sensitivity to STING agonist activation.	113
Figure 33. <i>In vivo</i> reconstitution with WT STING-transduced increases STING levels in the peritoneal cavity.	115

Figure 34. *In vivo* reconstitution of WT STING-transduced mast cells does not improve ID8 survival. 118

Figure 35. *In vivo* reconstitution of WT STING-transduced mast cells does not enhance STING agonist therapy in the ID8 model. 119

Figure 36. Summary of the impact of mast cells on ID8 ovarian cancer survival. 122

Figure 37. Schematic summary of findings on mast cell STING activation and the implications on bacterial and tumor immunity. 142

Abstract

Mast cells (MCs) are long-lived, tissue-resident immune cells essential for host defense. The STING pathway, a key innate immune response to infection and cellular stress, promotes strong type I interferon (IFN) and pro-inflammatory responses. While the STING pathway holds therapeutic potential in cancer and infection, its role in MCs remains underexplored. Our study demonstrates that MCs trigger type I IFN and NF- κ B responses upon STING activation. We show that MCs are susceptible to *Shigella flexneri* infection, leading to an upregulation of type I IFN and interferon-stimulated gene expression, partially dependent on STING. In a murine ovarian cancer model, MC deficiency led to longer survival, whereas reconstituted MC-deficient mice surprisingly showed improved survival. Treatment with a STING agonist increased survival, but overexpressing STING in MCs within tumors provided no additional benefit. These findings offer valuable insights into STING-mediated immunity in MCs and highlight potential avenues for future therapeutic exploration.

List of Abbreviations and Symbols

7-AAD	7-amino actinomycin D
ANOVA	Analysis of variance
APC	Antigen presenting cell
BMMC	Bone marrow-derived mast cells
BV	Brilliant Violet
CBMC	Cord blood-derived mast cells
CCL	Chemokine (C-C) ligand
CCR	C-C chemokine receptor
CD	Cluster of differentiation
CDN	Cyclic dinucleotide
cDNA	Complementary deoxyribonucleic acid
cGAMP	Cyclic GMP-AMP
cGAS	Cyclic GMP-AMP synthase
CO ₂	Carbon dioxide
Cpa3	Carboxypeptidase A3
CXCL	Chemokine C-X-C motif ligand
CXCR	Chemokine C-X-C motif receptor
Cy7	Cyanine 7 conjugate
DAMP	Damage-associated molecular pattern
DC	Dendritic cell
DNA	Deoxyribonucleic acid
DOX	Doxycycline
ECM	Extracellular matrix
EOC	Epithelial ovarian cancer
ER	Endoplasmic reticulum
ERGIC	Endoplasmic Reticulum-Golgi Intermediate Compartment
FACS	Fluorescence-activated cell sorting
FcεRI	Fc epsilon receptor I
FITC	Fluorescein isothiocyanate
FVD	Fixable viability dye
GFP	Green fluorescent protein
GI	Gastrointestinal
GUSB	glucuronidase beta
HGSC	High-grade serous carcinoma
HK	Hello kitty
HKLM	Hello kitty littermate
HPRT	Hypoxanthine-guanine phosphate
HRR	Homologous recombination repair

I.p.	Intraperitoneal
ICB	Immune checkpoint blockade
IFIT	Interferon induced protein with tetratricopeptide repeats 1
IFN	Interferon
IFNAR	Interferon alpha receptor
Ig	Immunoglobulin
IL	Interleukin
IRF	Interferon regulatory factor
ISG	Interferon-stimulated gene
IVIS	<i>In vivo</i> imaging system
KO	Knock-out
LPS	Lipopolysaccharide
MC	Mast cell
Mcl-1	Induced myeloid leukemia cell differentiation protein 1
MDSCs	Myeloid-derived suppressor cells
MHC	Major histocompatibility complex
mLNs	Mesenteric lymph nodes
MMP	Matrix metalloproteinase
MOI	Multiplicity of infection
MRGPRX2	MAS-related G protein coupled receptor-X2
NETs	Neutrophil extracellular traps
NF- κ B	Nuclear Factor kappa B
NK	Natural killer
NLR	NOD-like receptor
NR	Non-reconstituted
OD	Optical density
PAMP	Pattern-associated molecular patterns
PARP	Poly-ADP ribose polymerase
PCCs	Peritoneal cavity cells
PCMC	Peritoneal cavity-derived mast cells
PCR	Polymerase chain reaction
PDX	Patient-derived xenograft
PE	Phycoerythrin
PRR	Pattern recognition receptors
R. HKs	Reconstituted hello kitty
RBC	Red blood cell
RIG-I	Retinoic acid-induced gene I
RNA	Ribonucleic acid
ROS	Reactive oxygen species
RT-qPCR	Real time quantitative polymerase chain reaction
rtTA	Reverse tetracycline controlled transactivator

SAVI	STING-associated vasculopathy with onset in infancy
SEM	Standard error of the mean
STING	Stimulator of interferon genes
T3SS	Type 3 secretion system
TAMs	Tumor-associated macrophages
TBK1	TANK-binding kinase 1
Tet-On	Tetracycline-On
TGF- β	Transforming growth factor-beta
TLR	Toll-like receptors
TME	Tumor microenvironment
TNF	Tumor necrosis factor
TRE	Tetracycline response element
Tregs	Regulatory T cells
TRIF	TIR domain-containing adaptor inducing interferon- β
UPR	Unfolded protein response
VEGF	Vascular endothelial growth factor
WT	Wild type
mRNA	Messenger RNA
dsRNA	Double-stranded RNA
α	Alpha
β	Beta
ε	Epsilon
γ	Gamma
xg	Gravity
κ	Kappa
λ	Lambda
$^{\circ}C$	Degrees Celsius
g	Grams
ng	Nanogram
μg	Microgram
mg	Milligram
μL	Microlitre
mL	Milliliter
μM	Micromolar
mM	Millimolar

Acknowledgements

I would like to express my deepest gratitude to my supervisors, Dr. Jean Marshall and Dr. Ian Haidl, for their unwavering guidance, support, and encouragement throughout my master's journey. Their expertise, thoughtful feedback, and commitment to my growth have been invaluable. I am truly grateful for the time and energy they invested in helping me navigate through challenges, and for pushing me to expand my thinking and reach my potential. The knowledge and skills I gained under their mentorship have not only shaped this thesis but also profoundly impacted my academic and personal development. I would also like to express my sincere gratitude to my committee members, Dr. Craig McCormick and Dr. Paola Marcato, for their insightful feedback and invaluable contributions to this research. I would like to thank Dr. John Rohde for his collaboration and expertise in the *Shigella* work highlighted in this thesis.

I would like to extend my gratitude to Dr. Edwin Leong, who has been an incredible role model and source of support throughout my undergraduate studies and now my master's. Edwin has consistently gone above and beyond, always there to lend a helping hand with experiments, offer encouragement, and provide guidance whenever needed. Edwin has played a pivotal role in shaping my academic journey, and I truly appreciate everything he has done to help me succeed. Edwin, thank you- my experience in research would not have been the same without you.

I would like to extend my thanks to members of the Marshall Lab for fostering such a positive and encouraging environment to learn and grow. I would also like to thank the laboratory technical staff from the Marshall lab, Nong Xu and Alexander Edgar, for their assistance in this project, as well as everything they do behind the scenes. I would also like to thank CORES facility members Derek Rowter and Gerard Gaspard for their assistance with data acquisition, and all the staff at the Charles Tupper Animal Care Facility.

Finally, I would like to thank my parents, Sami, and Mustafa, whose support has been the foundation of everything I've accomplished. This journey would not have been possible without them. They have been my constant source of strength, always there to listen to my presentations, provide a warm meal, and even drive me to the lab late at night. Their positivity and encouragement have kept me going through every challenge. To my

dear friends, Jason and Phoebe, thank you for always lending an ear and continuously supporting me throughout all that I pursue. It truly took a village, and I am forever grateful for their love, support, and belief in me.

Chapter 1: INTRODUCTION

1.1 MAST CELLS

Mast cells (MCs) are densely granulated immune cells most often derived from circulating CD34⁺ bone marrow myeloid progenitors, which migrate to peripheral tissues where they terminally differentiate and mature under the influence of environmental stimuli¹. These cells exhibit phenotypic and functional heterogeneity that is heavily influenced by the cellular and signaling interactions within their microenvironment and epigenetics, which promotes MC populations with dynamic receptor expression and activity². Mast cells are found in virtually all tissues throughout the body and possess the distinct property of being able to live for months to years³. Although notorious for their role in allergy⁴, MCs have multifaceted roles in physiological homeostasis, response to pathogens, and disease².

1.1.1 Mast cells as immune sentinels

Mast cells are strategically located at host junctions in contact with the external environment such as the skin, lungs, and gastrointestinal tract⁵. This placement allows them to serve as a first line of defense against invading microorganisms and initiate immune responses to clear pathogens². Mast cells are equipped with a diverse array of cell-surface receptors and intracellular sensors, some highlighted in **Table 1**, that give them the ability to recognize several classes of pathogens³. These receptors also enable MCs to respond to damage-associated molecular patterns (DAMPs) due to tissue injury and cell stress. Examples include TLR4 detection of host-derived chaperone proteins like high mobility group box 1⁶ and ST2 binding to IL-33 release by necrotic cells⁷.

Within tissue sites, MCs are localized around blood and lymphatic vessels, which allows them to initiate systemic responses to local stimuli¹. Through the release of mediators, MCs can promote vasodilation, angiogenesis, and increase vascular permeability. These changes in vessel integrity allow for rapid influx of effector immune cells to the site of infection².

Table 1. Mast cell receptors and their corresponding ligands.

Receptor/Sensor	Ligands
FcεRI	Immunoglobulin E (IgE)
FcγRI/FcγRII	Immunoglobulin G (IgG)
KIT	Stem cell factor (SCF)
MRGPRX2	Neuropeptides, antimicrobial peptides, Compound 48/80
TLRs (1-10)	Microbial components and DAMPs (e.g., LPS, peptidoglycan, flagellin, viral RNA)
RIG-I, MDA5	dsRNA
C5aR/C3aR	Complement fragments C5a and C3a
ST2 (IL-33R)	IL-33
Dectin-1	Fungal components (β-glucan, chitin)
Histamine Receptors (H1, H2, H3, H4)	Histamine
Chemokine receptors (CCR2, CCR3, CCR5, etc.)	CCL2 (MCP-1), CCL5 (RANTES)

1.1.2 Mast cell differentiation, subsets, activation, and mediator production

Mast cells in adults originate from both the embryonic yolk sac and bone marrow⁸. However, the majority of MCs develop from bone marrow hematopoietic stem cells through a multi-potent progenitor, progressing through the common myeloid progenitor and granulocyte-monocyte progenitor stages⁹. In mice, MCs arise from a specific sub-

population of progenitors within the granulocyte-monocyte lineage, whereas in humans, a basophil-mast cell common progenitor gives rise to MC progenitors characterized by CD34^{high}/CD117^{intermediate/high}/FcεRI⁺ expression^{8,10}. These non-granulated MCs precursors circulate in blood and home to tissues in an immature state⁹.

Mast cells differ in the extent and nature of granule content. Specifically, proteases found in granules can be used to classify different populations found throughout the body. Traditionally, human MCs are categorized based on their protease content into tryptase-only (MCT), chymase-only (MCC), or both tryptase- and chymase-positive (MCTC) subtypes². However, recent advances in single-cell RNA sequencing have provided a more detailed understanding of MC diversity. A comprehensive pan-organ analysis has identified six distinct MC states across 12 organs, each with unique transcriptomic signatures that highlight the diverse populations found in different tissue sites¹¹. Additionally, variations in protease content are linked to differences in MC responses to activating agents, particularly ligands of the MRGPRX2 receptor^{12,13}. In rodents, MCs are generally classified as either mucosal-type MCs, which express tryptase, or connective tissue-type MCs, which express both tryptase and chymase⁸. Rodents exhibit a broader range of proteases in their MC granules compared to humans, reflecting species-specific differences in function and response^{14,15}.

Upon activation, MCs can respond to sequentially produce different mediators over time by: 1) immediate release of granules (degranulation), 2) quick synthesis of lipid mediators, and 3) synthesis of cytokines, chemokines, and growth factors over the longer-term. Degranulation occurs rapidly after activation to releases a broad spectrum of pre-formed mediators through a calcium flux-dependent process¹⁶. Two types of degranulation

include piecemeal and anaphylactic degranulation, with the former referring to the selective, slower, release of granule content and the latter involving the classical expulsion of entire granules to the extracellular environment¹⁶. The pre-formed mediators found within the granules include histamine, proteases, heparin, TNF, and VEGFA¹⁶.

Mast cells produce newly synthesized lipid mediators, including prostaglandins and leukotrienes, within minutes of activation. These have diverse functions in allergy and host defense¹⁶. Notably, prostaglandins, like PGD₂, promote vasodilation and vascular permeability, making them particularly involved in inflammatory responses¹⁷. Leukotrienes, including LTC₄, are involved in bronchoconstriction, mucus secretion, and airway inflammation, which are central to asthma pathophysiology¹⁸. Beyond their role in allergic reactions, leukotrienes also facilitate the chemotaxis and activation of immune cells during infections^{18,19}.

Lastly, MCs can *de novo* synthesize an extensive range of cytokines, chemokines, and growth factors that are released over a period of hours to days. These mediators have roles in several physiological settings including immune responses to infection, tissue repair, and cancer. Some examples include type I interferons (IFNs), type III IFNs, CCL2, CXCL10, IL-6, GM-CSF, and TGF- β ²⁰.

The magnitude of responses and repertoire of mediators released can vary depending on the cytokine microenvironment and specific MC receptors that are activated². In addition to receptor activation, MC mediator production can be regulated by other leukocytes. For example, direct contact with regulatory T cells can suppress MC degranulation²¹. Hence, it is the net combination of these signals that determines the final response mounted.

1.1.3 Mast cells during infection

Mast cells play a functional role in initiating defensive immune responses to viral, bacterial, and fungal infections⁵. Mast cells express pattern recognition receptors (PRRs) that detect pathogen-associated molecular patterns (PAMPs) and DAMPs. These PRRs include “Toll-like receptors” (TLRs) that bind pathogen components or products, and endogenous products released during cell death. During infection, MCs release mediators to respond to the pathogen directly, as well as recruit and activate other immune cells. They can also directly activate acquired immunity through MHCI and MHCII antigen-presentation to activate dendritic cells and T cells²²⁻²⁴.

Mast cells can detect and respond to several classes of viruses, including DNA and RNA viruses. They possess cytosolic sensors, such as members of the retinoic acid-induced gene I (RIG-I) family, that recognize viral genomic material⁵. During viral infections, MCs are an underappreciated source of type I and type III IFNs^{5,25-27} which are crucial in facilitating anti-viral responses by inhibiting viral replication and promoting CD8⁺ T cell and natural killer (NK) cell cytotoxicity^{28,29}. Additionally, MCs release various chemotactic and activating mediators, including CXCL10, CCL2, and CCL5, in response to infections like respiratory syncytial virus, influenza A, and dengue virus³⁰⁻³². Degranulation products, and newly formed cytokines, such as TNF and IL-1 β , can facilitate leukocyte trafficking to the infection site by enhancing endothelial adhesion³³. Although MCs have a protective role by alerting and coordinating other immune responses, they contribute to virus-induced inflammation and pathology in some settings. For instance, MC activation and vasoactive mediators in the plasma are correlated with increased disease

severity in dengue infection, where they exacerbate intravascular coagulation and vascular leakage^{34,35}.

Mast cells play a crucial role in defending against a variety of bacterial infections³⁶. The expression of TLRs enables them to recognize a wide range of bacterial components, triggering the synthesis and secretion of inflammatory effectors such as TNF, IL-1 β , and IL-6³⁶. Additionally, MCs can indirectly detect pathogenic products bound to antibodies via activation of surface Fc receptors³⁷. Several papers have indicated the role of MC-derived TNF, proteases, and prostaglandins in the prompt recruitment of neutrophils for bacterial clearance³⁸⁻⁴⁰. Mast cells also help mobilize dendritic cells (DCs), which are crucial in initiating adaptive immune responses. This was observed in responses to *S. aureus* peptidoglycan, where MCs were involved in the trafficking of certain DC subsets into the lymph node⁴¹. For direct killing, MCs can generate antimicrobial nets^{42,43}, release cathelicidins⁴⁴, and phagocytose bacteria⁴⁵.

1.1.4 Mast cells in cancer

Recent literature has shed light on MCs as orchestrators of tumor immunity^{1,46-48}. Mast cells accumulate around solid tumors, driven by the abundant growth factors and chemotactic mediators within the tumor microenvironment (TME), and are linked to the angiogenic process^{48,49}. Their presence correlates with diverse prognostic outcomes, which depend on factors such as cancer type, stage, anatomical location, and the specific location of MCs within the tumor¹. Mast cells can have pro-tumorigenic and anti-tumorigenic roles in cancer through direct interaction with cancer cells, the tumor stroma, as well as surrounding immune cells, as displayed in **Figure 1**. Ultimately, the balance between

inhibitory and activating signals determines the overall impact of MCs on tumor progression¹.

To skew immunity toward an anti-tumor response, MCs can release chemokines and cytokines to recruit and activate cytotoxic leukocytes⁴⁹. For instance, the release of CXCL8, CCL4, and CXCL10 by MCs^{30,50} recruits NK cells and T cells to the tumor microenvironment¹. In a mouse model of melanoma, MC-derived CXCL10 was essential in recruiting tumor-infiltrating T cells to establish tumor control⁵¹. Another report indicates a role for MCs in recruiting plasmacytoid DCs by CCL2 production to indirectly enhance tumor killing⁵². Mast cells can also directly induce tumor cell cytotoxicity via the release of TNF, while MC-derived tryptase has been shown to inhibit melanoma cell proliferation^{53,54}.

On the other hand, MCs can promote angiogenesis, extracellular matrix (ECM) degradation, and immune suppression, which allows for cancer dissemination⁴⁹. MC proteases activate latent matrix metalloproteinases (MMPs), which degrade ECM components⁵⁵ and activate latent TGF- β ⁵⁶, thereby enabling cancer cells to spread beyond the primary tumor site. Moreover, MC granule products, including VEGF and tryptase, can stimulate angiogenesis^{57,58} to supply tumors with nutrients, facilitating tumor cell proliferation⁵⁹.

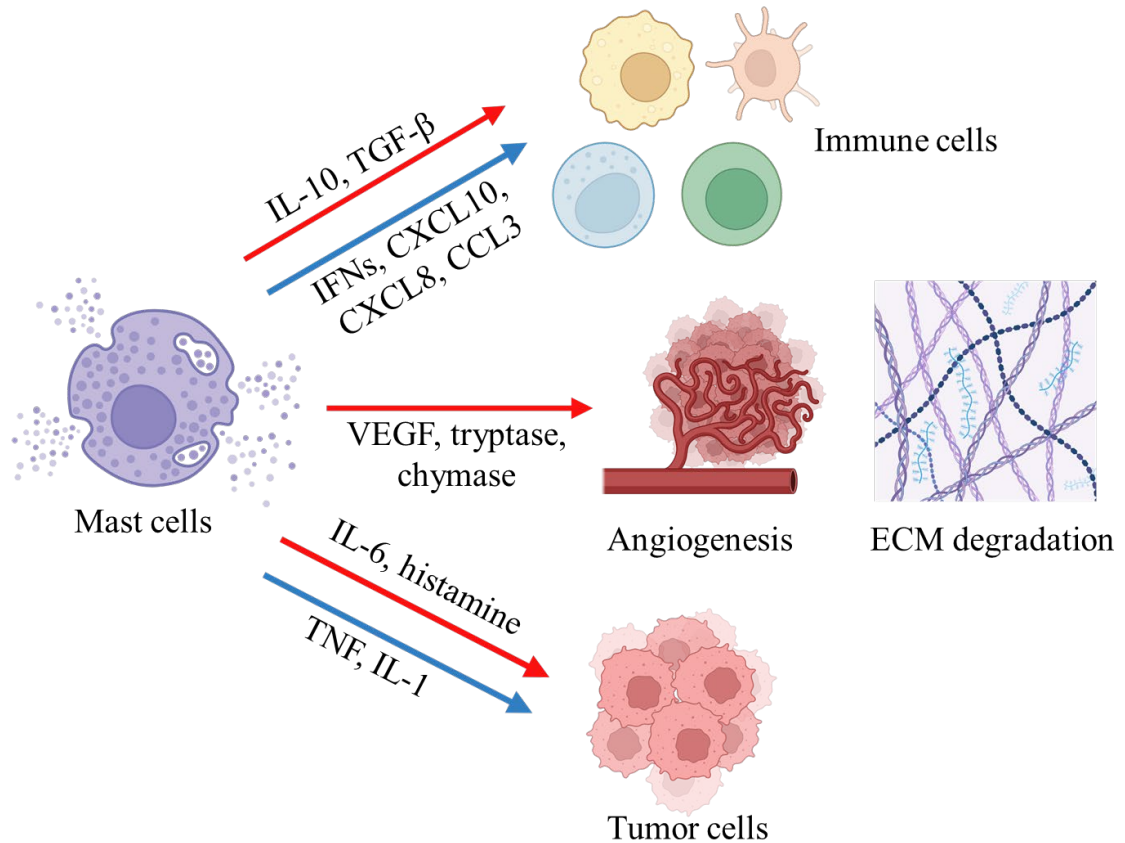


Figure 1. Pro-tumorigenic and anti-tumorigenic functions of mast cells in cancer.

This diagram depicts the complex functions of mast cells in the tumor microenvironment, illustrating both their pro-tumorigenic and anti-tumorigenic roles. Red lines highlight mediators released by mast cells that promote tumor progression, including factors that enhance tumor cell proliferation, immune suppression, and angiogenesis. Blue lines represent mediators that support tumor regression, such as those that stimulate immune activation and tumor cell apoptosis. The diagram shows the impact of mast cell-derived mediators on immune cells, the ECM, vasculature, and direct tumor cell behaviors, emphasizing the multifaceted role of mast cells in either promoting or inhibiting cancer growth, depending on the tumor context.

1.1.5 The modulation of mast cells for cancer immunotherapy

Given that MCs are increased in many solid tumors, found in virtually all tissues, and possess highly dynamic functionality, they are a compelling target for manipulation to

achieve an anti-tumor effect in cancer immunotherapy. There are a few proposed avenues of MC manipulation that could be utilized based on the evaluation of several unique MC properties.

Selectively activating MCs could be a strategy to boost anti-tumor responses. This could be accomplished with the use of MC receptor agonists. For example, TLR2 agonist activation was shown to inhibit tumor growth of melanoma in a MC-dependent manner⁶⁰. Similar findings were observed with TLR4 activation of MCs resulting in a reduction of tumor growth⁵¹. Mast cell overexpression of cytokines or genetic modifications to produce tumor antigens to stimulate immunity are other avenues that should be further explored⁶¹. Adoptive cell transfer and CRISPR-Cas9 editing are continuously advancing techniques in cancer immunotherapy that could be used to achieve this^{61,62}. Since MCs play a significant role in allergy and inflammation, activation must be regulated and selective to offset any potential negative side effects.

In cases where MCs may be detrimental, reducing their numbers or limiting their activation can be beneficial. This approach is used in other diseases such as systemic mastocytosis. MC stabilizers can be used to impair degranulation while tyrosine kinase inhibitors are useful in inhibiting MC maturation and survival. One caveat is that these drugs are not selective for MCs and may be associated with other abnormalities⁶³. Another avenue is MC depletion which could be accomplished with antibodies targeting c-kit, such as Barzolvolimab, which has been shown to improve disease activity in chronic urticaria in clinical trials⁶⁴. Limiting MC recruitment to tumor sites by blocking CXCR4 has demonstrated the ability to suppress cancer growth *in vivo*⁶⁵. Directly targeting MC mediators may also help limit cancer progression, with studies indicating that tryptase

inhibitors hold promise in reducing metastasis by decreasing angiogenesis and MMP activity⁵⁸.

1.1.6 *In vitro* models to study mast cell biology

The ability to study MCs *in vitro* is valuable in characterizing MC biology in isolation or in combination with other cell types, particularly in the context of immunological pathways and responses to infections. There are several MC cell lines available, and primary MC monocultures can also be derived from rodent and human stem cells.

To study MCs in rodents, cell lines such as RBL-2H3 and MC/9 can be used^{66,67}. However, there are limitations to their translatability as a result of several differences from primary MCs, including protease profile and cytokine release in response to allergen⁶⁸. Primary MC cultures can be derived from bone marrow progenitors and serve as a widely used model⁶⁹. These bone marrow-derived mast cells (BMMCs) are generally regarded as being skewed toward a mucosal phenotype, although they do not fully encapsulate all the distinct characteristics of either connective tissue-type or mucosal-type MCs¹⁴. Rather, it is widely considered that BMMCs can adopt a phenotype dependent on the conditions they are cultured in, or from tissue-specific microenvironmental cues^{14,70}. An alternative source of MCs is the peritoneal cavity, where cells within can be isolated, enriched, and differentiated to generate peritoneal cavity-derived MCs (PCMCs)^{71,72}. The phenotype exhibited by PCMCs is more similar to that of connective tissue-type MCs, and they have transcriptomic profiles that are distinct from BMMCs including receptor expression, differences in protease expression, and lipid mediator production⁷³.

Studies of MCs in humans can be conducted using cell lines such as HMC-1 and LAD2, but they also have their own limitations. For instance, HMC-1 cells lack functional IgE receptors and exhibit reduced degranulation activity, which makes them less suitable for studying certain MC functions, such as IgE-mediated allergic responses^{74,75}. The protease profile within the cell lines also differs from tissue-resident MCs such as in the skin⁷⁵, which further emphasizes these limitations. Primary cultures of human MCs can be generated from stem cells isolated from peripheral blood, bone marrow, and umbilical cord blood⁷⁶. The latter are termed cord blood-derived mast cells (CBMCs) and provide a model for studying human-specific MC functions. Although there exists some donor-dependent MC heterogeneity, many functional properties are intact in CBMCs including IgE mediated degranulation, MC-specific genes associated with protease profiles, lipid mediator synthesis, and cytokine and chemokine production⁷⁷.

It remains difficult to isolate tissue-specific MCs and maintain these specific phenotypes because of their complex incorporation within the tissue microenvironment, integrating with other cell types and extracellular matrix. Therefore, when studying MC biology, it is important to select the appropriate source and type that best establishes translatability and relevance to MCs in physiological settings.

1.1.7 Murine mast cell-deficient models

Although *in vitro* studies are useful in studying aspects of MC biology in isolation, animal models are needed to fully capture the role of MCs in physiological systems. The use of MC-deficient models has been extremely useful in evaluating the contribution of MCs to biological processes⁷⁸. Although several models of MC-deficiency exist, our work focused on two: *Kit^{W-sh/W-sh}* and “Hello Kitty” *Cpa3-Cre; Mcl-1^{fl/fl}*.

The *Kit*^{W-sh/W-sh} mouse model has an inversion mutation affecting a large segment of the genome including the transcriptional regulatory elements of the c-kit locus that affects c-kit transcription⁷⁹. The c-kit receptor binds to stem cell factor, which is a cytokine essential for hematopoietic development. Therefore, it is highly expressed in hematopoietic stem cells⁷⁸. While other cells lose this receptor as they undergo differentiation, MCs are one of the only terminally differentiated immune cells that retain c-kit⁷⁸. Since c-kit is essential for MC development and survival, *Kit*^{W-sh/W-sh} exhibit MC deficiency in all tissues⁷⁹. Although this model is fertile and has fewer phenotypic abnormalities compared to other Kit-dependent models, there are still reported increased numbers of neutrophils and basophils which must be taken into consideration⁷⁸.

The “Hello Kitty” *Cpa3-Cre; Mcl-1*^{fl/fl} strain of MC-deficiency is independent of the *Kit* gene. This mouse model involves the selective deletion of myeloid cell leukemia sequence 1 (Mcl-1) using a Cre-lox system⁸⁰. Mcl-1 is an anti-apoptotic factor required for MC survival; however, it is also expressed by other granulocytes and basophils⁸¹. The Cre recombinase is expressed under the control of the carboxypeptidase A3 (*Cpa3*) promoter, a protease that is highly expressed in MCs. *Cpa3-Cre* transgenic mice were crossed with mice containing floxed Mcl-1 genes, where two loxP sites flank exon 1. Therefore, in *Cpa3*-expressing cells, primarily MCs, exon 1 is deleted, resulting in the complete absence of Mcl-1. This model leads to a 92-100% depletion of MCs in various tissues. However, there is also a 58-78% reduction in basophils⁸⁰.

Adoptive transfer of MCs into MC-deficient mice (MC knock-in) is a necessary approach used to confirm that any changes seen in the MC-deficient animals are truly due to the absence of MCs instead of off-target effects⁸². If the wild-type phenotype can be

rescued by reconstitution of MCs into MC-deficient tissues, this confirms MC-specific contributions. Taking it a step further, culturing MCs from mice deficient in expression of a specific protein, and then reconstituting them into MC-deficient mice, allows for the experimental determination of the effects of that protein produced by MCs in an *in vivo* setting².

1.2 THE CGAS-STING PATHWAY

1.2.1 Introduction to the cGAS-STING pathway

Discovered in 2008, the STING (Stimulator of Interferon Genes) pathway is a key player of the innate immune system⁸³. It is typically activated by infection or cellular stress⁸⁴ and is widely expressed in immune cells, as well as epithelial and endothelial cells⁸⁵. STING signaling is initiated by cGAS, an intracellular sensor, that detects the presence of cytosolic microbial or host genomic material⁸⁴. Upon direct binding to DNA, cGAS synthesizes the cyclic dinucleotide (CDN) secondary messenger cyclic GMP-AMP (cGAMP) from GTP and ATP⁸⁶, which is the endogenous ligand for the STING protein. STING can also be activated independently of cGAS by bacterial-derived CDNs, although with a lower affinity^{87,88}.

STING is a transmembrane protein that resides in the endoplasmic reticulum (ER) as a monomer⁸⁴. Upon ligand binding and activation, STING undergoes dimerization and translocates from the ER to the Golgi apparatus, where it recruits TANK-binding kinase 1 (TBK1) and becomes phosphorylated⁸⁹. TBK1 then phosphorylates the transcription factor interferon regulatory factor 3 (IRF3), which dimerizes and translocates to the nucleus to drive the transcription of type I interferons, such as interferon- β (IFN- β)⁸⁹. The inhibitor of

NF- κ B (I κ B) kinase is also phosphorylated, resulting in the release and subsequent nuclear translocation of NF- κ B. This process triggers the expression of pro-inflammatory cytokines and chemokines, further amplifying the immune response⁸⁶.

Overall, STING plays a pivotal role in mediating immune responses to double-stranded DNA viruses, such as herpes simplex virus 1 (HSV-1), cytomegalovirus, and adenoviruses⁹⁰⁻⁹². While less extensively studied, this pathway can also be activated by retroviruses and RNA viruses^{93,94}. Activation of STING is also linked to other cellular processes such as autophagy and apoptosis⁸⁶. Although initially discovered for its role in host defense, STING is now being explored for its involvement in inflammatory diseases, autoimmunity, and tumor immunity. As a result, it is being investigated as a potential therapeutic target for modulation^{95,96}.

1.2.2 Type I IFN signaling

Interferons (IFNs) are a family of pleiotropic cytokines known for the role in orchestrating anti-viral immunity. IFNs are categorized into 3 groups: type I, II, and III. The type I IFN family consists of IFN- α , which has 13 subtypes in humans and 14 in mice, as well as IFN- β , IFN- ϵ , IFN- κ , and IFN- ω ⁹⁷. The production of type I IFNs is induced by the activation of PRRs by pathogens, including TLRs, NLRs, and RIG-I⁹⁸. There are diverse downstream signaling processes that result in type I IFN production depending on the sensor activated. For example, TLR signaling utilizes the adaptor protein TIR-domain containing adaptor protein-inducing IFN- β (TRIF), whereas RIG-I signals through mitochondrial antiviral signaling protein (MAVS)²⁹. However, the phosphorylation, activation, and dimerization of IRF3 and IRF7 is central to gene transcription of type I IFNs²⁹.

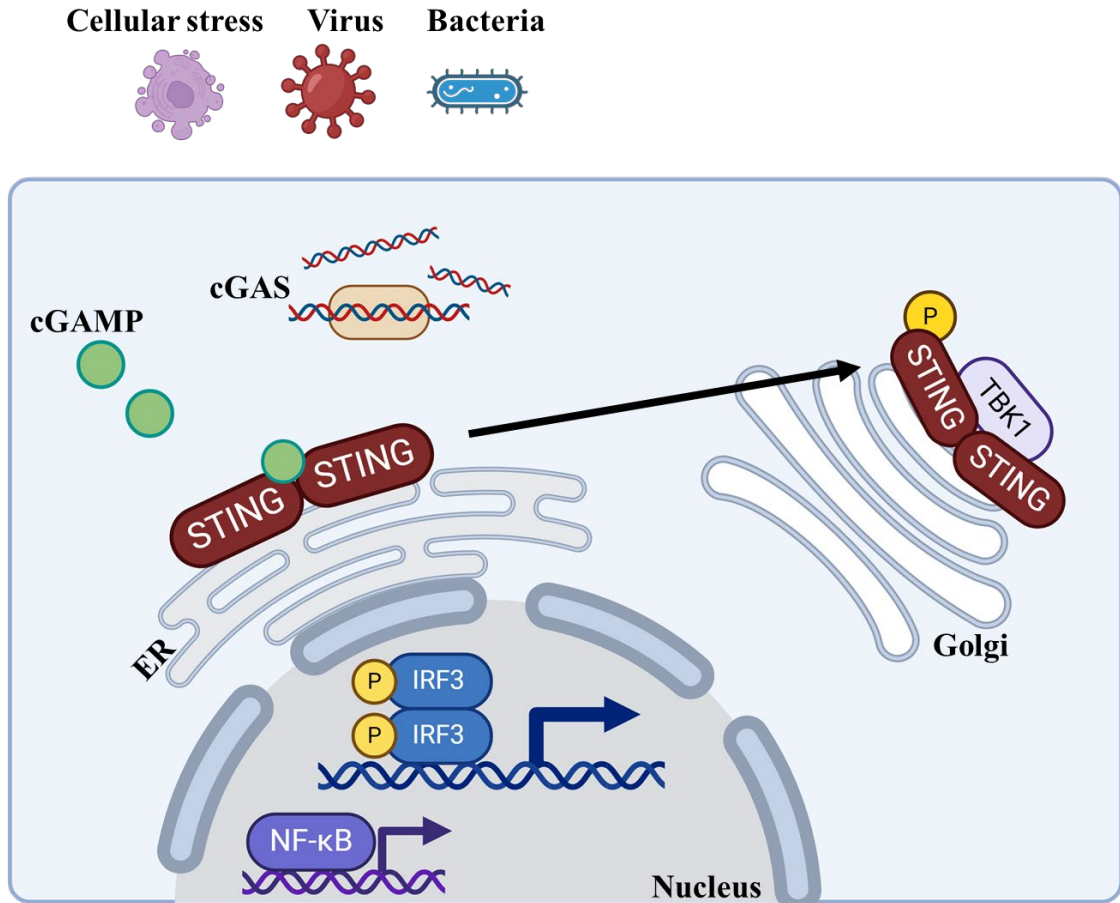


Figure 2. Schematic illustrating the mechanism of STING activation.

This diagram illustrates the key steps involved in STING signaling. Upon detection of cytosolic DNA, the sensor cGAS synthesizes cGAMP, which binds to and activates STING located in the endoplasmic reticulum. Activated STING translocates to the Golgi apparatus, where it recruits and activates TBK1, leading to the phosphorylation of IRF3 and activation of NF-κB. This response results in the production of type I interferons and pro-inflammatory mediators, which play a crucial role in modulating immune responses.

Once secreted, type I IFNs signal through the heterodimeric interferon- α receptor (IFNAR), which is composed of subunits IFN- α receptor 1 (IFNAR1) and IFN- α receptor 2 (IFNAR2)²⁹. Upon receptor binding, Janus kinase I (JAK1) and tyrosine kinase 2 (TYK2) are activated and phosphorylate cytosolic signal transducer and activator of transcription 1 (STAT1) and STAT2 proteins⁹⁸. STAT1 and STAT2 dimerize and form a transcription complex with IRF9, ISGF3, which translocates into the nucleus and binds the IFN-stimulated response element (ISRE)⁹⁸. This promotes the expression of interferon-stimulated genes (ISGs) that encode immune mediators and effector proteins that interfere with the viral replication cycle^{97,99}. Downstream signaling of type I IFNs also acts in an autocrine and paracrine fashion⁹⁸ in which ISGs also act as positive regulators to reinforce and propagate more IFN production⁹⁹.

1.2.3 Functional implications of STING on the immune system

Activation of STING can boost innate and adaptive immunity by promoting immune cell maturation, cytotoxicity, and improved antigen presentation¹⁰⁰. A significant portion of these effects is mediated by the production of type I IFNs.

Activation of the STING pathway enhances NK cell cytotoxicity, as evidenced by increased levels of IFN- γ , granzyme B, and the degranulation marker CD107a¹⁰¹. In addition, STING plays a key role in priming IFN- γ -producing CD8⁺ T cells, a process also driven by type I IFN production¹⁰². When CD8⁺ T cells are primed with a STING agonist, they exhibit elevated T-bet expression, along with increased levels of perforin, granzyme B, and enhanced lytic activity¹⁰³. This effect is partly attributed to STING-induced maturation of DCs, leading to upregulation of co-stimulatory molecules like CD86, CD80, and MHC class I molecules^{102,103}. This boosts the ability of DCs to process and present

antigens to T cells, thus facilitating more effective immune responses. Furthermore, STING activation is implicated in the recruitment and polarization of macrophages toward an inflammatory M1 phenotype, characterized by elevated F4/80 expression, TNF production, and enhanced phagocytic activity¹⁰⁴. The STING-induced production of CXCL1/2 and type I IFNs contributes to neutrophil migration and increased cytotoxicity, including the generation of reactive oxygen species (ROS)¹⁰⁵. Together, these effects highlight some of the pivotal roles of STING in amplifying both innate and adaptive immune responses.

Although type I IFNs, inflammatory cytokines, and chemokines play a protective role, prolonged signaling can be detrimental and cause tissue damage and immune dysfunction. In fact, overactivation can result in apoptosis, metabolic dysfunction, and decreased proliferation, as described in T cells^{106,107}. Hence, regulatory mechanisms, such as post-translational modifications and lysosomal degradation, are essential to ensure balanced immune responses^{108,109}.

1.2.4 Loss-of-function/gain-of-function mutations

The STING protein is encoded by the gene *TMEM173* that is highly heterogenous in the human population¹¹⁰. The most common human alleles are *R232*, *H232*, and *HAQ* (*R71H-G230A-R293Q*), with the latter expressing low levels of STING protein and impaired responses to CDNs^{111,112}. While the implications of null mutations on infection susceptibility remains to be fully explored, existing literature suggests that such mutations may impair IFN production in response to pathogens and bacterial products^{113,114}.

There are inherited and *de novo* gain-of-function mutations in STING that cause constitutive dimerization of STING¹¹⁰, leading to continuous activation of the pathway

independent of cGAMP⁸⁶. These mutations lead to autoimmune and inflammatory diseases such as STING-associated vasculopathy with onset in infancy (SAVI)¹¹⁰. The most common SAVI-associated mutations are V155M and N154S¹¹⁵. SAVI is described as a type I interferonopathy and characterized by systemic inflammation, interstitial lung disease, skin lesions, and T cell cytopenia¹¹⁶. Mouse models of SAVI have been developed by the generation of STING N153S and V154M knock-in mice^{117,118}, which present with lymphopenia, lung disease, and premature death.

Mutations in STING are also described in different cancers; however, these are rare and likely do not contribute to the progression of disease¹¹⁰. On the other hand, levels of *TMEM173* expression are being evaluated as a prognostic marker and in correlation with responsiveness to varying cancer therapies^{119,120}. This would be relevant to predict patient sensitivity to STING agonist therapy or other cancer treatments¹²¹. For example, higher STING levels may be beneficial in the context of radiation where there is DNA release from damaged cells that can boost immune responses via STING stimulation¹²². Alternatively, oncolytic DNA viruses are a more appealing therapy in cancers that are defective in STING signaling¹²³. Overall, the diverse genetic variations highlight the complex role of STING in immune regulation and its potential as both a therapeutic target and a biomarker for disease prognosis.

1.2.5 STING signaling in mast cells

Despite the well-established role of STING signaling in immune responses, its involvement in MCs remains underexplored. This leaves a gap in our understanding of how STING signaling affects MC biology and the contribution of MCs to immune responses mounted through this pathway. Goldmann *et al.* describe STING-dependent IFN- α

production in a MC cell line, HMC-1, in response to *S. aureus* internalization¹²⁴. Furthermore, the subsequently secreted type I IFNs signaled, in an autocrine manner, to improve the MC's ability to control bacterial burden¹²⁴. This paper provided novel insight since MCs are not typically described to produce type I IFNs in response to bacterial infection due to the inability of bacteria to enter the cell¹²⁵. One caveat is the cell line is phenotypically distinct compared to MCs in physiological settings and it would be important to recapitulate these findings using primary cells.

Another paper by Graham *et al.* demonstrated that cytokine and chemokine expression by bone marrow-derived MCs in response to influenza A virus was partially STING-dependent³¹. More specifically, they showed that there was a reduction in IL-6, CCL2, and CCL4 production by STING-deficient MCs compared to wild-type C57BL/6 MCs. However, there was no indication of STING-mediated type I IFN production in these primary murine cells. A similar phenomenon has been described where virus-induced activation of STING signals through STAT6 to produce chemotactic mediators but not type I IFNs¹²⁶.

Lastly, Martin *et al.*, showed that 3'3'-cGAMP, a CDN, promoted immunity against anthrax toxins when used as an adjuvant¹²⁷. They reported that MCs make up the largest proportion of immune cells analyzed in the sublingual tissues, where the mice were immunized. Since MCs have been described to enhance mucosal IgA responses¹²⁸⁻¹³⁰, it would be worth investigating whether MC stimulation by the CDN contributes to the increased antibody production. Since MCs are found in abundance at sites where viral and bacterial infections occur, unraveling this pathway would shed light on an underappreciated mechanism in which MCs promote the clearance of pathogens.

1.3 STING IN BACTERIAL INFECTION

1.3.1 Overview of STING in bacterial infection

Although type I IFNs are essential in mediating antiviral immunity, their role in bacterial infections is contradictory depending on the pathogen^{131,132}. Bacterial infections stimulate STING activation through a few mechanisms which are highlighted below.

Bacteria produce CDNs as secondary messenger molecules, which play essential roles in their lifecycle, particularly in virulence¹³³. These CDNs can directly activate STING, but the effects of this activation vary depending on the type of infection. A well-studied example is *Listeria monocytogenes*, where CDN detection triggers the production of type I IFNs and IL-6 in a STING-dependent manner. In a model of *L. monocytogenes* enterocolitis, STING was reported to play a protective role by promoting the recruitment of monocytes¹³⁴, which are crucial for bacterial clearance and reducing bacterial burden¹³⁵. In contrast, *Staphylococcus aureus* activation of STING by CDNs led to STING-dependent type I IFN production, but this response promoted bacterial survival within macrophages¹³⁶. In a cutaneous *S. aureus* infection setting, STING activation has been shown to suppress neutrophil chemotaxis and consequently impair bacterial clearance¹³⁷. Thus, while CDN-STING signaling can be protective in some infections, it can also have detrimental effects in others.

The direct detection of bacterial or host DNA can stimulate type I IFN production via STING¹³⁸⁻¹⁴⁰. For example, recognition of *Streptococcus pyogenes* nucleic acids can trigger type I IFN production. This led to enhanced survival, improved tissue pathology, and was associated with reduced neutrophil recruitment in a cellulitis infection model¹⁴¹. A similar effect was observed in soft tissue infection, where type I IFN production played

a protective role by limiting hyperinflammation and dampening the production of IL-1 β , thus preventing tissue damage¹⁴². *Pseudomonas aeruginosa* DNA has been described to be sensed by cGAS to activate STING, which dampened excessive inflammation and played a role in the unfolded protein response (UPR) to decrease lung injury¹³⁹. *Streptococcus pneumoniae* toxin pneumolysin can cause mitochondrial stress and subsequent DNA release to stimulate type I IFN production¹⁴³. Similarly, bacterial products like LPS can induce mitochondrial stress and increase levels of ROS, TNF, and IL-1 β through STING signaling, which aggravated lung injury¹⁴⁴.

STING also participates in bacterial infections by affecting other physiological processes. For example, STING activation induced autophagy in macrophages during *Mycobacterium tuberculosis* infection as a mechanism to limit growth and kill intracellular bacteria^{140,145}. Moreover, IFN-independent STING signaling promoted coagulation in a mouse model of sepsis, through ER-calcium release which worsened survival¹⁴⁶.

Similar to *Listeria*, *Shigella* is a known intracellular bacterium. STING activation is not as well described in *Shigella* infection; however, it has been shown that *Shigella* has evolved mechanisms to modulate the immune pathway. Bacterial effectors, IpaJ and VirA, inhibit the translocation of STING from the ER to the Golgi, thus dampening host IFN production¹⁴⁷. Another mechanism is the targeting of TBK1 for ubiquitination and subsequent proteasomal degradation¹⁴⁸. However, the immune cells that respond to *Shigella* through STING activation have not been extensively elucidated and is an area of study to pursue.

1.3.2 Introduction to *Shigella*

Shigella is a gram-negative enteric bacterial pathogen. The genus comprises four distinct species: *Shigella dysenteriae*, *Shigella flexneri*, *Shigella boydii*, and *Shigella sonnei*¹⁴⁹. *Shigella* primarily targets the intestinal lining¹⁴⁹ causing a diarrheal gastrointestinal (GI) disease called shigellosis. The disease is primarily caused by *S. flexneri*, accounting for approximately 60% of cases¹⁴⁹. Shigellosis is characterized by inflammation of the colon, ulcerations in the mucosal lining, and a disruption of the intestinal barrier function¹⁴⁹. Although shigellosis is typically self-limiting, treatment often includes antibiotics and supportive care; however, antibiotic resistance is becoming a concern¹⁵⁰. *Shigella* is a highly virulent pathogen with a remarkably low infectious dose of 10-100 bacteria¹⁵⁰. Transmission occurs primarily through contaminated food or water, and through the fecal oral route¹⁵⁰. Disease is prevalent in developing countries and among pediatric populations, where access to sanitation and healthcare resources may be limited¹⁵⁰.

Shigella employs sophisticated mechanisms to subvert host cells and propagate infection¹⁵¹. A large plasmid encodes multiple virulence factors including the type III secretion system (T3SS)¹⁵², a needle-like projection that is anchored into the bacterial cell wall¹⁵³. To infect a host cell, the T3SS is injected into the plasma membrane and enables the delivery of bacterial effector proteins into the host's cytoplasm¹⁵³. These effector proteins promote bacterial entry into the host cell by inducing actin rearrangement to drive endocytosis for internalization. Despite being non-flagellated, *Shigella* utilizes this actin rearrangement to facilitate movement within and between cells, a process known as 'actin-based' motility¹⁵⁴. Moreover, the effector proteins further promote bacterial dissemination

by manipulating host cell processes to create a replicative niche. For example, they are involved in dampening host inflammatory responses and ensuring host cell survival¹⁵¹.

1.3.3 Immune responses to *Shigella* infection

To establish an infection and colonize the intestine, *Shigella* must traverse the epithelial barrier. This is accomplished by crossing from the apical (luminal) side to the basolateral side of the epithelial layer through microfold (M) cells¹⁵⁵. M cells are specialized epithelial cells of the GI tract's immune surveillance system that selectively transport pathogens and antigens from the lumen to the underlying immune cells on the basolateral side¹⁵⁶. Antigen presenting cells near the M cells, including macrophages¹⁵⁶, phagocytose the bacteria; however, *Shigella* can escape the phagosome within the host cell through the T3SS system and replicate in the host cytoplasm^{157,158}.

Invasion and replication of *Shigella* within the host cell triggers NLR inflammasome activation which promotes pro-inflammatory cytokine maturation and cell death¹⁵⁹⁻¹⁶¹. *Shigella* effectors, such as MxiI, are also recognized by inflammasome receptors like NLRC4 and NLRP3, further amplifying the host immune response^{159,162}. As a consequence of capsase-1 activation and bacterial effectors, the host cell undergoes pyroptosis which is a form of lytic and inflammatory cell death that releases additional DAMPs and mediators, prominently IL-1 β and IL-18^{163,164}. From there, *Shigella* goes on to infect adjacent epithelial cells along the basolateral surface by actin polymerization. These cytokines promote inflammation, vasodilation, and the recruitment and activation of immune cells, like NK cells and neutrophils, to then kill the now accessible bacteria^{156,165}. *Shigella* can also activate TLR2 and TLR4, due to lipoproteins and LPS on the outer membrane of the bacteria, respectively. This leads to subsequent NF- κ B activation and

release of TNF- α , IL-1 β , and IL-6¹⁶⁶⁻¹⁶⁸. TLR2 activation in macrophages also orchestrates IFN- γ production to limit bacterial replication¹⁶⁹.

Neutrophils have been long described as central immune cells in controlling *Shigella* infection through several mechanisms. In response to CXCL8 produced by intraepithelial immune cells and infected and bystander epithelial cells¹⁷⁰, neutrophils transmigrate from the bloodstream toward the luminal side of the epithelium^{171,172}. Neutrophils can mediate the resolution of infection by phagocytosis and degranulation to release antimicrobial proteins such as elastase and defensins¹⁷³⁻¹⁷⁵. Lastly, the release of neutrophil extracellular traps (NETs) which consists of enzymes, bactericidal proteins, and chromatin, are also involved in *Shigella* killing¹⁷⁶. Despite being essential for bacterial clearance, neutrophil transmigration induces extensive tissue damage to the colonic mucosa, which can further enable bacterial crossing of the epithelium¹⁷⁷.

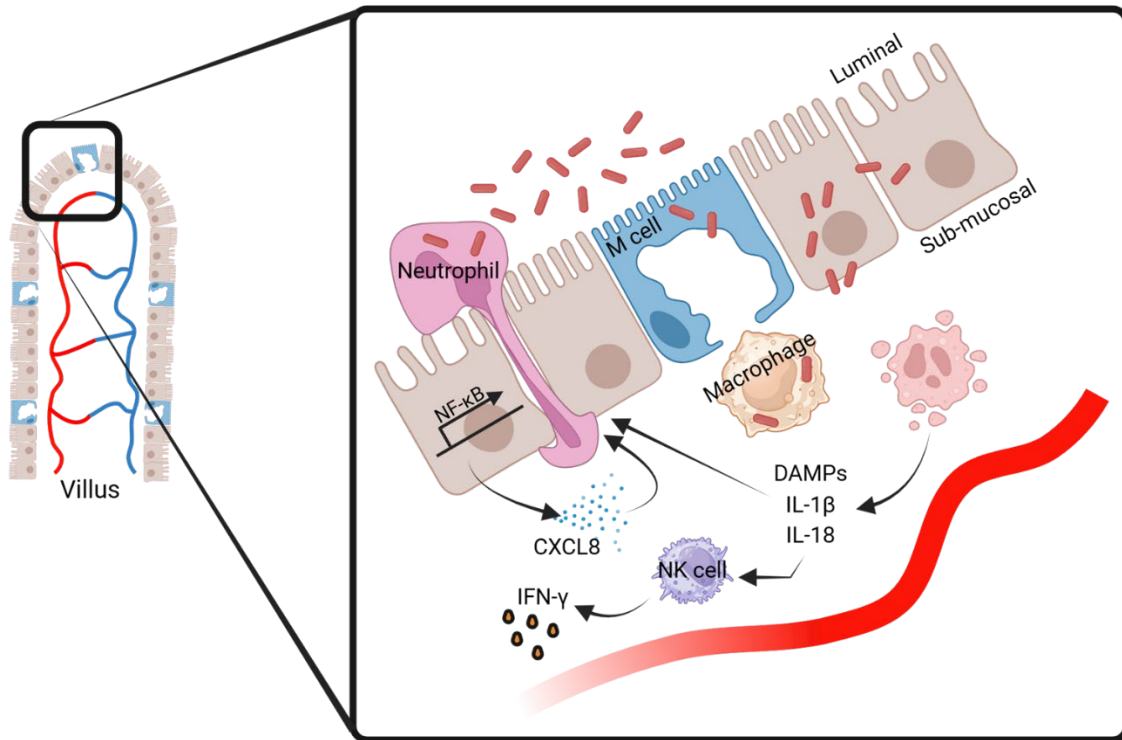


Figure 3. The innate immune response to *Shigella* infection.

Upon invasion of the intestine, *Shigella* crosses the epithelial layer, where it is recognized by PRRs, triggering inflammatory pathways. This activates the recruitment of immune cells, cytokine release, and the initiation of host defense mechanisms. Key cellular responses are illustrated, highlighting the role of macrophages and DCs in controlling bacterial spread.

1.4 STING IN OVARIAN CANCER IMMUNOTHERAPY

1.4.1 Introduction to ovarian cancer

Ovarian cancer is the most lethal gynecologic malignancy with a devastating 5-year survival rate under 50%¹⁷⁸. Patients often present with subtle clinical presentations including bloating and abdominal discomfort and unlike cervical cancer, there is a lack of effective routine screening¹⁷⁹. This combination of non-specific symptoms and the absence of early detection measures leads to delayed diagnoses, resulting in over 80% of women being diagnosed at stage III or IV when the tumor has metastasized throughout the

peritoneum and beyond, which significantly reduces the chances of successful treatment^{180,181}.

Ovarian cancer is typically classified into three main types: epithelial (EOC), germ cell, and sex-cord stromal tumors¹⁷⁸. Among these, EOCs account for approximately 90% of cases and can be further divided into five subtypes that are distinct in their molecular, histologic, and immune profile: high-grade serous (HGSC), endometrioid, clear cell, low-grade serous, and mucinous carcinomas¹⁷⁸. HGSC is the most common and aggressive subtype, associated with a particularly poor prognosis¹⁷⁸. Hence, ovarian cancer is a highly heterogeneous disease at the cellular, molecular, and immunological level, making it complex to treat¹⁸².

Several risk factors are associated with the development of ovarian cancer with age, genetic predisposition, and family history being the most well-established¹⁸³. Ovarian cancer is a heritable disease that is linked to germline mutations in genes involved in DNA repair¹⁸¹. Prominent genes implicated in this process include *BRCA1* and *BRCA2*, which are involved in repairing DNA double-strand breaks through a process called homologous recombination repair (HRR) to maintain genomic stability¹⁸¹. Alterations in these genes impair DNA damage repair mechanisms and lead to an accumulation of mutations which increases the risk of cancer development¹⁸¹. In addition to mutations, individuals with a family history of ovarian cancer or breast cancer are at an elevated risk and are typically monitored more closely for early signs of the disease¹⁸³.

The progression of ovarian cancer and responses to therapy are deeply influenced by the tumor microenvironment (TME). The TME is a dynamic and heterogeneous mix of cellular and acellular components, including cancer cells, immune cells, stromal cells,

blood vessels, ECM material, and soluble mediators¹⁷⁹. In ovarian cancer, the TME exhibits both inter- and intra-tumoral variability, especially in the metastases spread throughout the peritoneum, each surrounded by distinct microenvironments¹⁸². Due to extensive metabolic activity and abnormal angiogenesis, the TME is acidic and hypoxic, which is associated with the infiltration of immunosuppressive immune populations. Ovarian cancer is often considered ‘immunologically cold’ due to lack of anti-tumor immune cells and immunosuppressive environment^{179,184}. Inhibitory immune cells including myeloid-derived suppressor cells (MDSCs), tumor associated macrophages (TAMs), and regulatory T cells (Tregs) constitute a significant portion of the TME and produce inhibitory cytokines, such as IL-10 and TGF- β , that repress T-cell function, as well as promote tumor angiogenesis and tissue remodeling^{179,185,186}. This creates an environment where anti-tumor immune cells are either excluded from the tumor or rendered ineffective. The complex immune landscape plays a major role in determining the tumor's response to therapy and its potential for metastasis.

1.4.2 First-line and novel therapeutic approaches

The efficacy of treatments for ovarian cancer is variable depending on the genetic profile, histological subtype, and stage of cancer¹⁷⁸. The standard first-line therapy typically includes cytoreductive surgery to remove as much of the tumor as possible, followed by chemotherapy using platinum or taxane-based drugs¹⁸¹. Despite initial responses, over 70% of patients relapse due to acquired chemotherapy resistance and experience disease recurrence^{185,187}. This underscores the need for novel therapeutic approaches, including targeted therapies and immunotherapy.

Poly (ADP-ribose) polymerase (PARP) inhibitors, like Olaparib, have emerged as a promising therapeutic and been approved as a concurrent or maintenance targeted therapy following chemotherapy¹⁸⁸. These inhibitors block base excision repair in cancer cells, which is a DNA repair mechanism¹⁸⁹. These are particularly impactful in patients with mutations in *BRCA1/2* as these already impair the cancer cells' ability to repair DNA through HRR, making them more reliant on PARP enzymes¹⁸⁹. Hence, inhibiting PARP enzymes leads to an increased accumulation in DNA damage, ultimately leading cancer cells to undergo programmed cell death through synthetic lethality¹⁹⁰. However, only 10-15% of EOC patients carry a mutation in *BRCA1/2* and alternative approaches are needed that can be used more broadly¹⁹¹.

Another avenue of treatment are drugs that target angiogenesis to limit tumor growth and spread¹⁸⁵. The formation of new blood vessels is an important process for cancers to increase nutrient supply and remove metabolic waste¹⁸⁵. An example is a monoclonal antibody called Bevacizumab which targets the pro-angiogenic factor VEGF and prevents binding to its receptor and signaling¹⁸⁵. In addition to reducing blood vessel formation, this reduces vascular permeability and improves the delivery of chemotherapy to the tumor¹⁸⁵.

Folate receptor inhibitors are another class of therapeutics that directly kill cancer cells¹⁹². Folate receptor alpha (FR α) is a glycoprotein overexpressed on the surface of most ovarian cancer cells¹⁹². Mirvetuximab soravtansine is an approved antibody-drug complex used to treat chemotherapy-resistant patients¹⁹². Once the antibody binds to the receptor on the cancer cell, the complex is internalized, and a cytotoxic drug called DM4 (which prevents microtubule formation) is released and interferes with cell division, leading to cell

death¹⁹². Overall, this therapy minimizes damage to normal cells compared to conventional chemotherapy but is still under investigation.

1.4.3 Immunotherapy

Immunotherapy refers to the manipulation of the immune system to treat disease. In cancer, one strategy is to enhance the ability of immune cells to detect and eliminate cancer cells¹⁹³. Several immunotherapies have been developed and shown efficacy in various cancers. Some examples that have been studied in the context of ovarian cancer include CAR T-cell therapy and point blockade (ICB), which will be briefly discussed below¹⁹³.

CAR T-cell therapy was first introduced in 2017 and has transformed the landscape of treatment for hematologic malignancies like leukemia and lymphoma¹⁹³. It involves genetically modifying T cells to better recognize cancer cells. T cells are isolated from patient's blood and modified to express a recombinant receptor for a tumor antigen¹⁹⁴. Following reinfusion into the body, the receptor precisely recognizes the tumor antigen on cancer cells and will induce the CAR-T cell to release of cytotoxic mediators like perforin to lyse the tumor cells. Current studies are investigating CAR T cells that target FR α and mesothelin, but these are still in the early phases¹⁹⁴. One barrier to the efficacy of CAR-T cells in ovarian cancer is the vast tumor heterogeneity and antigen escape¹⁹⁴. This makes it difficult to identify a suitable antigen that could successfully target all tumor cells and avoid non-pathologic tissues¹⁹⁴.

Immune checkpoint inhibitors (ICIs) are an immunotherapy, first approved in 2011, that have shown success clinically for solid tumors, especially in melanoma¹⁹⁵. Immune checkpoint proteins, normally expressed on the surface of healthy cells, bind to receptors

on T cells to initiate inhibitory signals that prevent T cell activation and autoimmunity¹⁹⁵. These receptors include surface proteins programmed cell death protein 1 and cytotoxic T-lymphocyte-associated protein 4 on T cells and programmed cell death ligand 1 (PD-L1), CD80, and CD86 on APCs¹⁹⁶. As a form of immune evasion, cancer cells also upregulate these checkpoint inhibitor molecules, like PD-L1, to avoid being targeted by cytotoxic T cells¹⁹⁶. Hence, ICI block the surface proteins on cancer or immune cells to allow immune responses to proceed. Despite success in other cancers, little success has been observed in ovarian cancer¹⁹⁷, which is partially attributed to the lack of tumor-infiltrating lymphocytes and low tumor mutational burden¹⁹⁸.

Overall, it is believed that the immunosuppressive TME limits the efficacy of these immunotherapies that rely on the adaptive immune system. Given this, an ideal approach worth investigating would be to use a treatment modality that dampens the immunosuppressive limitations and facilitates the cytotoxic activity of immune cells within the TME.

1.4.4 Anti-tumor effects of STING activation

The immune boosting properties of STING activation have made it a promising target for immunotherapy. Over the past decade, preclinical studies have highlighted the potent anti-tumor effects of STING activation in multiple cancer models¹⁹⁹⁻²⁰¹. These results led to the development of early-phase clinical trials, where STING agonists are being evaluated both as monotherapies and in combination with other established cancer treatments²⁰². As previously mentioned, many of these anti-tumor functions are attributed to the production of type I IFNs²⁰³. In fact, IFN- α 2 was the first immunotherapeutic agent that was approved in 1986¹⁹⁶. STING activation holds promise as it results in a breadth of

type I IFNs being produced, alongside other inflammatory chemokines and cytokines, which amplifies the immune system on multiple fronts.

STING is involved in regulating the tumor-immunity cycle through a variety of mechanisms²⁰³. The pathway has been shown to promote the maturation of DCs and upregulation of surface molecules that enhance the ability to process and present tumor antigens to T cells^{204,205}. STING activation is also involved in maintaining the stemness of CD8⁺ T cells, as well as increasing their cytotoxic and memory functions, which is important for the clearance of tumor cells^{206,207}. Agonist treatment promoted the accumulation of NK cells within tumors and increased their lytic mediators and ability to establish control¹⁰¹, while suppressing the differentiation of MDSCs²⁰⁸.

Activation of STING is important in boosting the presence of immune cells within the microenvironment to clear cancer cells²⁰⁹. Downstream chemokines CXCL9 and CXCL10 are involved in the recruitment of T cells and NK cells into solid tumors^{210,211}. This has been shown in mouse models of melanoma and colorectal cancer, where STING agonist injections increased intratumoral CD8⁺ T cells^{199,212}. To further promote the trafficking of immune cells to the tumor, STING agonists can modulate the vasculature within the TME by upregulating endothelial adhesion molecules like vascular cell adhesion protein 1 (VCAM-1)²¹³, to enhance the extravasation of T cells. Treatment with a CDN increased NK cells within tumors and draining lymph nodes and demonstrated enhanced effector functions¹⁰¹. Additionally, STING activation can remodel the immunosuppressive environment by reducing Tregs²¹⁴ and reprogramming M2 macrophages to a M1 phenotype²¹⁵.

In addition to stimulating immune cells, type I IFNs can have direct effects on tumor cells. Intrinsic STING signaling within cancer cells has been shown to directly inhibit tumor cell proliferation²¹⁶ by impeding the cell cycle and increase their sensitivity to checkpoint blockade²¹⁷. Signaling can also enhance the recognition of cancer cells by inducing the upregulation of MHC class I and NKG2D on the cell surface, increasing the susceptibility of tumor cell lysis by T cells and NK cells^{218,219}. STING can increase tumor immunogenicity due to the release of tumor antigens and DAMPs from dying cancer cells²²⁰. Intratumoral STING agonist injection decreased the vascularization of the TME, indicated by lower blood vessel density in a Lewis lung carcinoma model²²¹. Overall, these effects can also enhance responses to other cancer treatments, implicating the potential use of STING as a combination therapy.

Due to the poor chemical properties of natural STING agonists, several synthetic CDNs and non-nucleotide small molecule drugs have been developed to bind STING with a higher affinity and greater stability²²². These agonists have been approved for clinical trials. ADU-S100 was the first STING agonist that was approved to proceed to human clinical trials as a monotherapy²²³. Although the therapeutic efficacy of STING agonists is not as robust in humans as a monotherapy, it is being explored with existing immunotherapies where there may be synergistic effects²²³. For example, it could boost responses to ICIs where efficacy may be dampened in immunologically cold tumors^{204,220}.

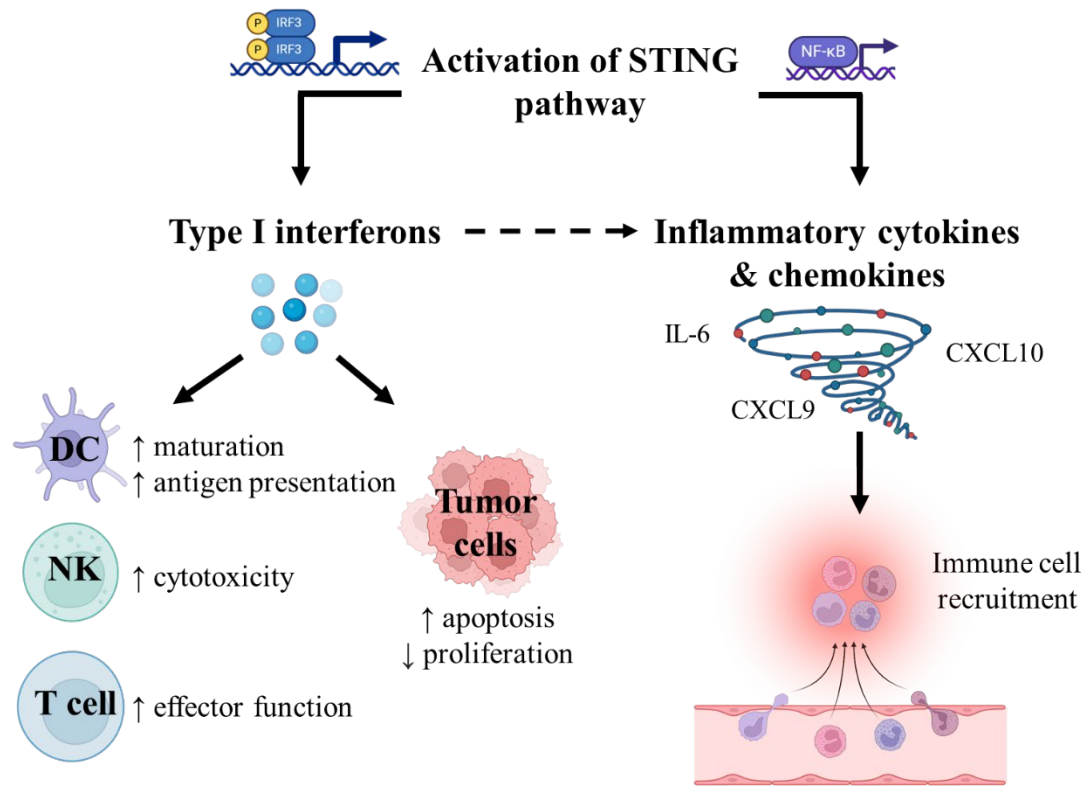


Figure 4. Anti-tumor functions of the STING pathway in the immune system.

This diagram highlights some key mechanisms through which the STING pathway enhances anti-tumor immunity. Upon activation, STING induces the production of type I interferons, leading to the activation of DCs, NK cells, and T cells. Additionally, the STING pathway induces apoptosis and limits the proliferation of tumor cells, further contributing to the suppression of tumor growth. Lastly, the release of pro-inflammatory cytokines contributes to the recruitment of immune cells to the tumor site for tumor elimination. There also exists crosstalk between type I interferons and pro-inflammatory mediators, as indicated by the dashed arrow.

1.4.5 Limitations/downfalls of STING agonist therapy

The efficacy of STING agonists is context dependent and has its limitations. Despite mounting a type I IFN response in T cells, STING activation is also documented to cause T cell stress and death. Stimulation of STING in T cells increased genes associated with apoptosis, the caspase cascade, ER stress, and the UPR response¹⁰⁶. In response to STING agonist DMXAA, T cells exhibit reduced proliferation²²⁴ and increased cell

death¹⁰⁶. Overall, the STING agonist cytotoxicity in T cells would prove counterproductive to the goal of enhancing anti-tumor T cell responses.

The effectiveness of STING targeted therapy is variable between cancers and is not suitable for all tumors. STING activation can induce tolerogenic immune responses. For example, STING-induced indoleamine 2, 3-dioxygenase production by DCs was involved in suppressing effector T cells and promoting the differentiation of Tregs²²⁵. Moreover, it can also reduce tumor infiltrating immune cells dependent on tumor antigenicity²²⁶. Other studies have shown that STING signaling can support metastasis in models of breast and brain cancer^{227,228}. This may be attributed to NF-κB activation in tumor cells which can promote proliferation, suppress apoptosis, and induce epithelial-mesenchymal transition²²⁹. These studies emphasize the role of tumor settings and the importance of more targeted activation of the pathway within certain cell types.

Due to the lack of tissue or cell specificity, the activation of the STING pathway is broadly associated with adverse reactions²²². Hence, another obstacle to STING-targeted therapy includes finding a route of administration that is effective while avoiding tissue toxicity, autoimmunity, and uncontrolled inflammation²²². Most clinical studies are injecting agonists intratumorally. However, this method is only useful for patients that have accessible solid tumors and would not reach distal metastases²²². Intravenous administration may lead to systemic inflammation and, due to the short serum half-life of STING activators, there is the potential for low tumor accumulation²²². The poor physiochemical properties of the STING agonists are a significant barrier leading to the reduced efficacy observed in clinical trials. For example, intratumoral ADU-S100 was unfortunately found to be absorbed rapidly with a short half-life of 10 to 23 minutes²²³.

Researchers are trying to develop enhanced delivery systems of STING agonists, including nanoparticles and liposomes, to increase stability and cell entry²³⁰. Another avenue is the targeted delivery of agonists to specific cell types based on different receptor expression²³⁰.

1.4.6 Murine models of ovarian cancer

Preclinical mouse models have been instrumental in advancing our understanding of the pathophysiology of ovarian cancer and the development of novel therapies. Various models are available, each with their own benefits and limitations, that recapitulate the molecular mechanisms of cancer progression and response to treatment as reviewed by Karakshav and Zhang²³¹. The most used murine models include syngeneic and xenograft models, which will be highlighted below.

Three important factors in xenograft and syngeneic models are the tumor cell source, the location of engraftment, and the immune status of the strain²³². The common routes of cancer cell administration are subcutaneous, intraperitoneal, and orthotopic injections²³². Subcutaneous injections lead to the formation of a tumor that is localized around the injection site²³¹. These can be useful in studies that require the measurement and quantification of tumor growth and solid tumor sections for histological analyses²³². However, it is less physiologically relevant in terms of cancer progression and anatomical location. Intraperitoneal injections are beneficial in recapitulating the metastatic nature of EOC²³². Injection into the peritoneum results in a disseminated cancer model with the formation of ascites and cancer foci throughout the peritoneum, coating the spleen and liver²³¹. This pathology is similar to that seen clinically in advanced stages of ovarian cancer, making this method of engraftment particularly relevant to human disease²³¹. However, it cannot be used to examine earlier stages of disease and it is more difficult to

study the cancer itself as there is no primary tumor formation²³¹. Orthotopic engraftment refers to the implantation of tumor cells in the anatomical location from which they are derived²³². Hence, it refers to injections into the ovarian lining, also known as the bursa, which allows tumors to develop in physiologically relevant environments²³². Intrabursal injections are useful for studying all stages of cancer growth since the growth on the ovary disseminates from the primary site to then develop ascites²³¹. However, intrabursal injections are technically more difficult and time consuming, which makes it difficult to achieve larger sample sizes²³¹.

In syngeneic models, tumor cells derived from an inbred strain are engrafted into hosts of genetic similarity, ensuring that the immune system remains intact²³³. The ID8 model is an established cell line and widely used murine model of epithelial ovarian cancer²³⁴. Mouse ovarian surface epithelial (MOSE) cells derived from the bursa, the lining of the ovaries, were cultured *in vitro* until they transformed and adopted cancerous phenotypic changes²³⁴. Administration of these cells into mice leads to ovarian cancer development with pathology depending on the method of engraftment. Additionally, Walton and colleagues have developed genetically modified ID8 sublines that contain frequently found mutations in observed in human patient populations such as those in *Trp53*, *Brca1*, and *Brca2*^{235,236}. These mutations are known to influence responses to treatment and the immune microenvironment; hence, these modified cells provide a more nuanced understanding of ovarian cancer biology, including insights into how genetic alterations affect tumor behavior and therapy outcomes^{237,238}. Another useful alteration in the ID8 model includes transfecting the cells with luciferase, which enables non-invasive tracking of tumor burden and metastasis using *in vivo* imaging systems (IVIS) that detect

bioluminescence²³⁹. One key advantage of this model is that the host mice are immunocompetent, which allows for the study of immune responses to ovarian cancer and treatments²³³. This ovarian cancer model offers several advantages including fast tumor growth and relatively low costs compared to other models²³¹. However, a key limitation is that the ID8 model lacks tumor heterogeneity, which is commonly seen in human ovarian cancer, making it more difficult to fully replicate the complexity seen in patient tumors²³².

Xenograft models entail the transplantation of human ovarian cancer cells or tumors into mice²³³. However, these models require immunodeficient mice strains, such as the severe combined immunodeficiency (SCID) model, to ensure that the mice do not reject the human tissue²³¹. In patient-derived xenografts (PDX), clinical samples are engrafted into the mice²³³. Using whole tumors resected during surgery is beneficial in retaining the cellular integrity and heterogeneity from the original tumor²³³. Following transplantation into the mouse, the tumor is left to grow for months, before it is excised and implanted into other mice for *in vivo* experiments²³¹. Due to the immunodeficiency in the mouse strains, these models are not used to study immunotherapies which have been revolutionary in the field of cancer²³¹. However, the emergence of humanized mouse models has tackled this obstacle and allowed for immunotherapeutic testing. This model involves generating mice with intact immune systems that resemble the human system by infusing human leukocytes or hematopoietic stem cells before the engraftment of the clinical sample^{233,240}. Some limitations of PDX models are the lengthy experimental times, high cost, and access to clinical sample sources²³².

The ID8 model was chosen in our studies as it resonates most with our research question. With an intact immune system, we are able to accurately evaluate the efficacy of STING immunotherapy in a model that resembles the late stages of cancer.

1.5 RATIONALE AND RESEARCH OBJECTIVES

Considering all the above information together, this introduction has described three broad areas that have been integrated to define the research objectives and hypotheses: 1) MCs, 2) STING pathway activation, and the 3) potential functional roles for MC STING activation in *Shigella* infection and ovarian cancer.

To briefly summarize, MCs are sentinel immune cells that are pivotal in initiating immune responses to pathogens by producing a wide array of mediators that recruit and activate both innate and adaptive leukocytes to clear infection. Moreover, MCs are present in increased numbers within the tumor microenvironment, where they play complex and sometimes paradoxical roles in modulating tumor progression and immune surveillance.

The STING pathway is a critical component of the innate immune response to microbial infections that is well-documented to boost immune responses by increasing leukocyte mobilization and cytotoxicity. The robust production of type I IFNs, cytokines, and chemokines makes STING a strong modulator of immunity, with implications in enhancing antiviral, antitumor, and antibacterial responses. Although this pathway has been described in other immune cells, it has not been described in MCs before.

Given the central role of MCs in early immune activation and their widespread presence in tissues, understanding how the STING pathway operates within these cells could reveal new insights into their function as immune sentinels in ovarian cancer and intracellular bacterial infection. Moreover, it could open avenues for innovative therapies

that harness the potential of MCs to modulate immune responses, including cancer immunotherapy. **We hypothesized that mast cell STING activation promotes a type I IFN response that has a functional role in infection and anti-tumor immunity.**

This investigation can be summarized in three primary aims:

1. Investigate the functionality of the STING pathway in mast cells and characterize their responses to STING activation *in vitro*.

This aim allowed us to determine whether MCs express functional STING and how its activation influenced gene expression, mediator production, and overall immune responses. This allowed us to begin to elucidate the type of response and influence MCs may have in biological settings.

2. Assess the role of STING activation in mast cell responses to *Shigella* infection.

Given the abundance of MCs in mucosal tissues, such as the intestine, which are frequently exposed to pathogens like *Shigella*, this aim investigated how STING activation influenced MC responses to bacterial infection. This provides new insights into their role in mucosal immunity.

3. Assess the ability of mast cells that inducibly express activated STING to inhibit ovarian cancer.

This aim explored the potential of MC-mediated STING activation as a targeted cancer immunotherapy. We assessed the effects of localized STING activation in MCs within the ovarian tumor microenvironment, where STING agonists are being tested as promising therapeutic agents. By genetically modifying MCs to inducibly express either wild-type or constitutively active STING, we aimed to circumvent the systemic side effects associated

with broad STING activation such as systemic toxicity and unwanted activation in other cells. This research will help elucidate whether MC-mediated STING delivery can impede tumor development and contribute to the development of targeted cancer immunotherapies. The completion of these research aims provided valuable insights into STING-associated immunity mediated by MCs, establishing a strong foundation for future studies to explore its therapeutic potential.

Chapter 2: MATERIALS & METHODS

2.1 ANIMALS

Female mice were used between the ages of 8-11 weeks for all experiments. Wild-type C57BL/6 mice were obtained from Charles River Laboratories (Quebec, Canada) or obtained from in-house breeding colonies at the Carleton Animal Care Facility (CACF) at Dalhousie University. *KitW-sh*/HNihrJaeBsmJ (*KitWsh/Wsh*; Wsh), C57BL/6-Cpa3-Cre; *Mcl-1fl/fl* (Hello Kitty; HK) and wild-type littermate (HKLM) mice were obtained from in-house breeding colonies at the CACF from founder animals provided by Dr. S. Galli (Stanford University). STING KO (C57BL/6J-*Sting1^{g^t}*/J) and B6.Cg-*Gt(ROSA)26Sor^{tm1.1(CAG-rtTA3)Slowe}*/LdowJ (Rosa26-rtTA) mice were purchased from Jackson Laboratories (Bar Harbor, ME). Mice from the HK breeder colonies were genotyped at 4-5 weeks of age by PCR to identify mast cell-deficient mice from wild-type littermate controls. All animal procedures were approved by the Dalhousie University Committee on Laboratory Animals, following guidelines from the Canadian Council for Animal Care.

2.2 ANTIBODIES

Primary antibodies for western blotting and immunofluorescence were anti-STING (1:2500, D1V5L, Rabbit mAb; Cell Signaling Technology, Danvers, MA), anti-TBK1 (1:1000, D1B4, Rabbit mAb, Cell Signaling Technology), anti-phospho-STING (1:1000, S365, D8F4W, Rabbit mAb, Cell Signaling Technology), anti-phospho-TBK1 (1:1000, S172, D52C2, Rabbit mAb, Cell Signaling Technology), anti-vinculin (1:3000, E1E9V, Rabbit mAb, Cell Signaling Technology), anti- β -actin (Clone: AC-15, Mouse mAb, Sigma

Aldrich, St. Louis, MO), and anti-FLAG[®] (1 µg/mL, M2, Mouse mAb, Sigma-Aldrich). Secondary antibodies for western blots were mouse anti-rabbit (Jackson ImmunoResearch, West Grove, PA) and donkey anti-mouse (Jackson ImmunoResearch) and used at a 1:5000-1:10,000 dilution. The secondary antibody for immunofluorescence was goat anti-rabbit AF555 and used at 1:1000.

2.3 REAGENTS

Sources of cell culture reagents, activators, and inhibitors can be found in **Table 2**.

Table 2. Reagents used for cell culture and *in vitro* activations.

Reagent	Source
Dulbecco's Modified Eagle Medium (DMEM)	Gibco, Thermo Fisher Scientific
Rosewell Park Memorial Institute 1640 (RPMI)	Gibco, Thermo Fisher Scientific
Penicillin-Streptomycin (P/S)	Hyclone, Cytiva (Marlborough, MA)
4-(2-hydroxyethyl)-1-piperazineethanesulfonic acid (HEPES)	Hyclone, Cytiva
Fetal Bovine Serum (FBS)	Gibco, Thermo Fisher Scientific
Prostaglandin E2 (PGE ₂)	Tocris Bioscience (Bristol, UK)
Recombinant mouse IL-3 (rmIL-3)	BioLegend (San Diego, CA)
Recombinant human stem cell factor (rhSCF)	Peprtech (Cranbury, NJ)
Recombinant human IL-3 (rhIL-3)	Peprtech
Nonessential amino acids (NEAA)	Hyclone, Cytiva
Human IL-6 (hIL-6)	Peprtech
Recombinant mouse stem cell factor (rmSCF)	BioLegend
β-mercaptoethanol (β-ME)	Sigma-Aldrich
TrypLE™ Express	Gibco, Thermo Fisher Scientific
Ethylenediaminetetraacetic acid disodium salt dihydrate (EDTA)	Sigma-Aldrich
Phosphate-Buffered Saline (PBS)	Sigma-Aldrich
Soybean Trypsin Inhibitor (STI)	Millipore, Sigma (Burlington, MA)
Blasticidin	InvivoGen (San Diego, CA)
Poly(I:C)	InvivoGen
ADU-S100	InvivoGen
diABZI	Cayman Chemical Company (Ann Arbor, MI)
G3-YSD	InvivoGen
H-151	InvivoGen

2.4 CELL CULTURE

2.4.1 Bone marrow-derived mast cells

Bone marrow-derived mast cells (BMMCs) were differentiated from mononuclear cells isolated from female C57BL/6, Rosa26-rtTA, and STING KO mice. Mice were euthanized by anesthetization with isoflurane followed by CO₂ asphyxiation. Under aseptic conditions, tibiae and femurs were harvested, and bone marrow was flushed out using a 27-gauge needle and sterile, endotoxin-free RPMI 1640 media. The cell suspension was then filtered through a 40-micron filter to remove debris. The cells were centrifuged at 300 x g for 10 minutes at 4°C and cultured in media consisting of RPMI 1640 with L-glutamine and sodium bicarbonate, 10% heat-inactivated FBS, 1% P/S, 200 μM PGE₂, 50 μM β-ME, and 15% WEHI3-B cell line supernatant as a source of IL-3. Cells were cultured at a density of 0.5 x 10⁶/mL, with fresh media provided twice per week, and incubated at 37°C in 5% CO₂. BMMCs were assessed for maturity after 4 weeks by analyzing the expression of CD117 and FcεRIα using flow cytometry. Cultures were considered mature and suitable for experimentation when ≥ 95% of the cells were CD117⁺ and FcεRIα⁺.

2.4.2 Cord blood-derived mast cells

Human primary mast cells were derived from human umbilical cord blood obtained from consenting mothers at the IWK Health Centre in Halifax, Canada. Heparin-treated blood was diluted in PBS and layered over Lympholyte[®]-H Cell Separation Media (Cedarlane, Burlington, Canada), followed by centrifugation at 480 x g for 25 minutes, with no brake. The buffy coat containing mononuclear leukocytes was harvested, washed with PBS, and spun at 300 x g for 20 minutes. Following red blood cell (RBC) lysis through

addition of sterile distilled H₂O, mononuclear cells were cultured at 1.0 x 10⁶ cells/mL in StemSpan™ SFEM serum-free medium (Stem Cell Technologies, Vancouver, Canada) supplemented with 100 ng/mL rhSCF and 10 ng/mL hIL-6. For the first week of culture, 10 ng/mL rhIL-3 was added. After the first week, cells were cultured at 0.5 x 10⁶/mL and passaged weekly under 5% CO₂ at 37°C. After 5 weeks, cells were cultured in RPMI medium supplemented with 10% FBS, 1X P/S, 15 mM HEPES, 0.1 mM NEAA, 100 ng/mL of rhSCF, 10 ng/mL of rhIL-6, and 50 μM of β-ME. At week 6, MC purity was assessed by CD117 expression via flow cytometry, with cultures subsequently used in experiments when purity reached ≥ 95%.

2.4.3 Peritoneal cavity-derived mast cells

A pure culture of peritoneal cavity-derived mast cells (PCMCs) was isolated from male C57BL/6 mice. Following euthanasia as described previously, a ventral vertical incision was made to expose the peritoneal cavity under aseptic conditions. A 22G needle was used to inject 5 mL of ice-cold wash buffer, consisting of 0.5% BSA (Sigma-Aldrich), 5 mM EDTA, and PBS, into the peritoneal cavity. The peritoneal cavity was gently massaged to suspend the intraperitoneal cells into the solution, which was then aspirated and transferred to a conical tube. The cells were centrifuged at 300 x g for 10 minutes at 4°C, then resuspended in RPMI 1640 media supplemented with 30 ng/mL rmSCF, 10 ng/mL rmIL-3, 10% FBS, 1X P/S, and 15 mM HEPES. On the following day, suspension cells were discarded, and the same volume of complete media was replaced. Three days later, suspension cells were combined with adherent cells that were detached using TrypLE™ (Gibco, Thermo Fisher Scientific, Waltham, MA) and then centrifuged at 200 x g for 10 minutes at 4°C. Cells were cultured at a density of 0.3 x 10⁶ cells/mL in complete

media at 37°C and 5% CO₂, with media changes occurring twice a week. PCMC development and maturity were assessed starting at 2 weeks by flow cytometry (FACS), probing for CD117 and FcεRI. Cultures were determined as mature when purity was greater than 95%.

2.4.4 RAW 264.7 macrophages

The macrophage cell line RAW 264.7 (ATCC®, TIB-71™) was cultured in complete DMEM supplemented with 10% FBS and maintained at 37°C in 5% CO₂. Cells were detached using a cell scraper and passaged every 3 days at a ratio of 1:3 to 1:6.

2.4.5 ID8 ovarian cancer cell line

The ID8 mouse ovarian cell line was provided by Dr. Shashi Gujar at Dalhousie University and cultured in complete DMEM supplemented with 10% FBS. Once the cells reached approximately 80% confluency, the flask was rinsed with PBS, and cells were detached by incubating them with TrypLE™ for 5 minutes at 37°C. After centrifugation at 300 x g for 10 minutes, the cells were resuspended in fresh media and split at a 1:10 ratio. Cultures were maintained at 37°C in 5% CO₂ and used for experiments until they reached 15 passages.

2.4.6 U-2 OS cells

The human bone osteosarcoma cell line, U-2 OS (ATCC®, HTB 96™), was cultured in complete DMEM containing 10% FBS. Cells were detached using TrypLE™ and passaged every 3 to 4 days at a ratio of 1:3 to 1:6. Cultures were maintained at 37°C in 5% CO₂ conditions.

2.4.7 293T cells

The human epithelial-like 293T cell line (ATCC®, CRL-3216™) was cultured in DMEM supplemented with 10% FBS. Cells were passaged every three days following detachment with TrypLE™ and sub-cultured at ratios ranging from 1:3 to 1:8. Cultures were incubated at 37°C and 5% CO₂.

2.5 PRODUCING STING-TRANSDUCED CELLS

2.5.1 DNA cloning vector and gene inserts

The DNA lentiviral vector pLJM1_Bla_TRE was optimized and generously provided by Dr. Ben Johnston in Dr. Craig McCormick's laboratory at Dalhousie University. This vector contains three key features: 1) an ampicillin resistance marker for selecting transformed bacteria used to amplify the vector, 2) an inducible tetracycline response element (TRE) that enables controlled expression of the inserted genes, and 3) a blasticidin resistance marker for positively selecting successfully transduced cells in culture. Wild-type STING and constitutively active STING mutants (V154M, N153S) were the genes of interest inserted into the vector. A green fluorescent protein (GFP) transcript was included as a control to assess transfection and transduction efficiency, and to serve as a negative control for STING expression in experiments. The amino acid sequences of the selected transcripts used for vector cloning are shown in **Table 3**.

2.5.2 DNA cloning procedure

The mRNA sequence for murine wild-type STING was retrieved from NCBI Gene Bank. Using SnapGene® 3.3.4 (GSL Biotech LLC, San Diego, CA), an EcoRI restriction cut site was inserted upstream of the sequence, while preserving the Kozak sequence. Sites

for XbaI, MluI, and SalI were added downstream of the sequence. The wild-type STING and mutant STING sequences (V154M, N153S) were ordered from TWIST Bioscience (San Francisco, CA), delivered in cloning plasmids containing ampicillin resistance genes.

To amplify the DNA, DH5- α competent *E. coli* (New England Biolabs, Ipswich, MA) were transformed with the plasmids. After adding the plasmids, the tubes were flicked to mix, then placed on ice for 30 minutes to allow plasmid dispersion and attachment to bacterial membranes. The bacteria were then heat-shocked at 42°C for 30 seconds to facilitate plasmid uptake, followed by a 5-minute incubation on ice. Super optimal medium with catabolite repression (SOC, NEB) was added to the mixture, which was then shaken at 37°C for 1 hour. After incubation, the bacteria were spread onto agar plates containing 100 μ g/mL ampicillin and incubated overnight at 37°C.

Resistant colonies were picked and transferred individually to lysogeny broth (LB, Fisher Bioreagent) supplemented with 100 μ g/mL ampicillin and allowed to grow overnight. Plasmid purification was then performed using the QIAprep Spin Miniprep Kit (Qiagen, Hilden, Germany), following the manufacturer's instructions. Briefly, bacteria were centrifuged, the supernatant discarded, and cells were lysed to release plasmid DNA. The lysates were separated from the pellet (containing cell walls and genomic DNA) and passed through columns with silica membranes for plasmid isolation. The columns were washed to remove impurities, and the pure plasmid was eluted.

To retrieve the purified gene inserts, plasmids were digested with XbaI and EcoRI restriction enzymes in CutSmart® Buffer (New England Biolabs). The vector DNA was also digested with these enzymes and treated with phosphatase (Quick CIP) to prevent re-ligation. The digested vector and gene inserts were analyzed on a 1.2% agarose gel

containing RedSafe™ (1:20,000) for nucleic acid detection. The gel was imaged on an Alpha Innotech Red™ Imaging System to confirm the predicted fragment sizes. DNA fragments of interest (the vector and inserts) were excised from the gel using a scalpel, and the DNA was purified using the QIAquick Gel Extraction Kit (Qiagen), following the manufacturer's protocol. The Quick Ligation™ Kit (New England Biolabs) was used to ligate the vector and inserts. Briefly, 10 µL ligation reactions were prepared, containing Quick Ligase Reaction Buffer, vector DNA, insert DNA, nuclease-free water, and Quick Ligase. The insert and vector were mixed at a 3:1 molar ratio and incubated at room temperature for 5 minutes.

The ligation products were transformed into *E. coli* for plasmid amplification, as previously described. Colonies were picked and cultured in LB broth containing ampicillin overnight at 37°C. After centrifugation, the bacteria were lysed and plasmids purified using the QIAprep Spin Miniprep Kit. DNA constructs were analyzed by gel electrophoresis after restriction enzyme digestion to confirm successful ligation and the presence of desired products. Representative colonies were sequenced at GeneWiz (South Plainfield, NJ), positive colonies were grown in larger cultures, and plasmid purification was performed using the QIAGEN Plasmid Maxi Kit. The resulting plasmids were then used for the generation of lentiviral particles.

Table 3. Amino acid sequences of GFP, WT STING, V154M, and N153S transcripts.

Target Gene	Amino Acid Sequence
GFP	MVSKGEELFTGVVPILVELDGDVNGHKFSVSGEGEGDATYGK LTLKFICTTGKLPVPWPTLVTTLTLYGVQCFSRYPDHMKQHFFK SAMPEGYVQERTIFFKDDGNYKTRAEVKFEKDTLVNRIELKGI DFKEDGNILGHKLEYNNSHNVYIMADKQKNGIKVNFKIRHNI EDGSVQLADHYQQNTPIGDGPVLLPDNHYLSTQSALS KDPNEK RDHMLVLEFVTAAGITLGMDELYK
WT STING	MPYSNLHPAIPRPRGHR SKYVALIFLVA SLMILWVAKDPPNHTL KYLALHLASHELGLLLKNLCC LAEELCHVQSRYQGSYWKAVR ACLGCPHHC MAMILLSSYFYFLQNTADIYLSWMFGLLVLYKSLS MLLGLQSLTPAEVSAVCEEK LNV AHGLAWSYYIGYLRILPGL QARIRMFNQLHNNMLSGAGSRRLYILFPLDCGVPDNL SVVDPNI RFRDMLPQQNIDRAGIKNRVYSNSVYEILENGQPAGVCILEYAT PLQTLFAMSQDAKAGFSREDRLEQAKLFCRTLEEILEDVPESRN NCRLIVYQEPTDGNSFSLSQEVL RHIRQEEKEEVTMNAPMTSVA PPPSVLSQEPRL LISGMDQPLPLRTDLI

Note: **Bolded and boxed** amino acids indicate sequence differences between WT STING and constitutively active mutants (V154M, N153S).

2.5.3 Transfection to produce lentivirus

Lentiviruses were produced using a second-generation lentiviral system, which involved two helper plasmids: psPAX2 as the packaging plasmid and pMD.2 as the envelope plasmid. Transfection of HEK293T cells was performed using jetOPTIMUS® DNA Transfection Reagent (Polyplus, Illkirch, France). HEK293T cells were seeded at a density of 0.9×10^6 cells per well in four separate wells of a 6-well plate, one well for each vector, in DMEM supplemented with 10% FBS. The cells were cultured overnight at 37°C to allow adherence to the plate. In four separate tubes, 1.32 µg of pPAX2, 0.64 µg of pMD.2, and 1.7 µg of the transfer vector were mixed with 200 µL of jetOPTIMUS buffer. Each tube received 4.5 µL of JetOptimus reagent and the contents were vortexed briefly and then incubated at room temperature for 10 minutes. The DNA complex was then added

dropwise to the corresponding wells containing HEK293T cells. After a 6-hour incubation, the transfection medium was aspirated and replaced with DMEM supplemented with 2% FBS for 48 hours. Transfected cells were spun down at 300 x g for 10 minutes to collect lentivirus containing supernatant. Transfection efficiency was determined by assessing the percentage of GFP-positive cells by flow cytometry. This GFP-positive population served as an estimate of the transfection efficiency for cells transfected with the STING constructs.

2.5.4 Transduction of cells

The lentiviral supernatant was transferred and passed through a 0.45 μ M syringe filter to remove any cell clumps. Polybrene (Sigma-Aldrich) was added to the medium at a final concentration of 5 μ g/mL to help viral particles attach to the cell membrane. The lentiviruses containing GFP, WT STING, STING V154M, and STING N153S were used to transduce Rosa26-rtTA BMMCs and U-2 OS cells, which express reverse tetracycline controlled transactivators (rtTA).

U-2 OS cells were seeded at 0.5 million cells per well into 6 well-plates, with tetracycline-free 10% FBS (Gibco, Thermo Fisher Scientific) DMEM overnight. The next day, the media was replaced with lentiviral-containing supernatant. BMMCs were resuspended in the virus-containing media and loaded onto 6-well plates. The plates were covered, sealed, and then centrifuged at 2000 rpm for two hours at room temperature to facilitate viral uptake. After centrifugation, the supernatant was discarded, and the BMMCs and U-2 OS cells were resuspended in their respective culture media. After 24 hours, transduced cells were positively selected by adding 12 μ g/mL blasticidin into the culture.

To induce transcription of the genes of interest, cells were treated with 0.5 $\mu\text{g}/\text{mL}$ doxycycline (Sigma-Aldrich).

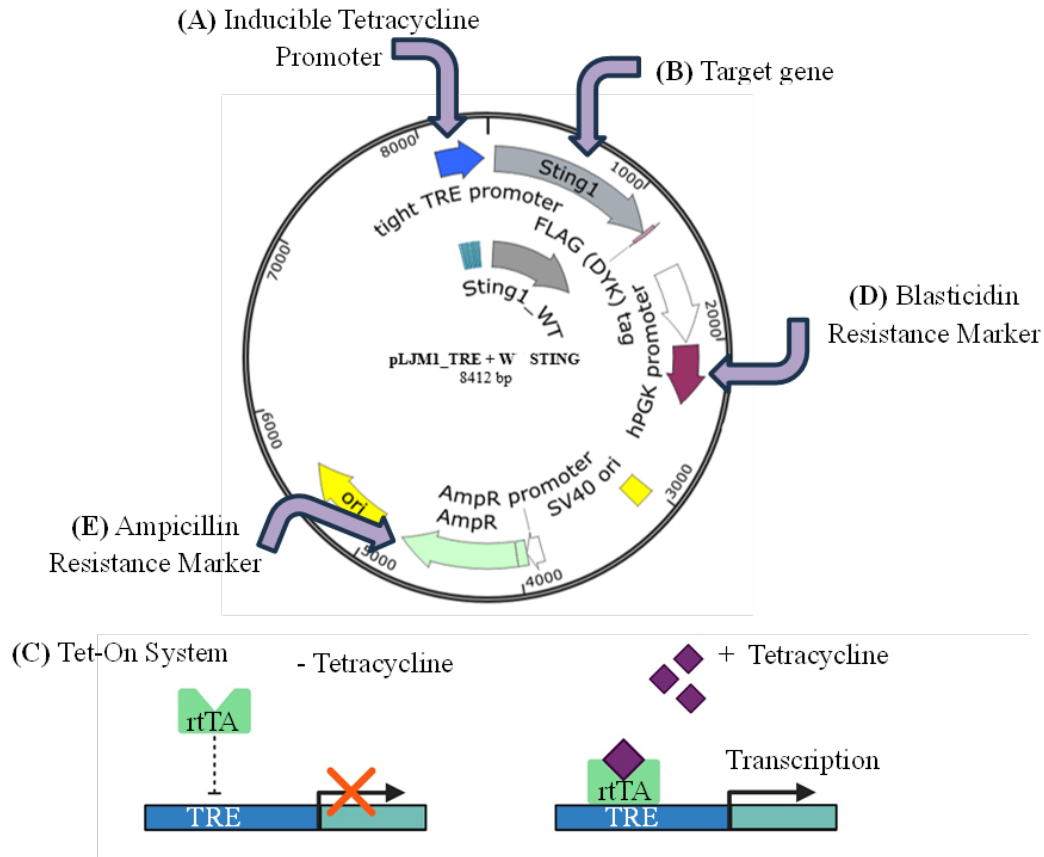


Figure 5. Overview of the pLJM1_Bla_TRE DNA vector for inducible STING expression in mast cells.

A 2nd generation lentiviral system was used to transduce target cells with the pLJM1 DNA vector enabling inducible expression of STING variants (WT STING, V154M STING, N153S STING). This vector incorporates a (A) tetracycline-responsive element (TRE) upstream of the (B) gene of interest, which operates through a (C) tetracycline “ON” system. Cells expressing the reverse tetracycline-controlled transactivator (rtTA) protein are capable of inducing expression of the target gene upon exposure to tetracycline or its derivatives. The presence of a (D) blastocidin resistance marker facilitates the positive selection of successfully transduced cells *in vitro*. Additionally, the (E) ampicillin resistance marker aids in the selection of transformed bacteria during the cloning process of the DNA vector in preparation for transduction. This inducible system allows for the precise control of STING expression, facilitating studies on its functional role in mast cell immune responses.

2.6 MAST CELL ACTIVATION

Prior to all *in vitro* experiments, BMDCs and PCMCs were counted, washed, and resuspended in fresh media at a density of 1×10^6 cells/mL. BMDCs were pre-incubated overnight in resting media, consisting of RPMI, 10% FBS, 50 mM β -ME, 1% P/S, and 15% WEHI supernatant, before activation. After the resting period, BMDCs were resuspended in activation media (RPMI with 2% FBS, 1% P/S, 15 mM HEPES, 3 ng/mL rIL-3, and 100 μ g/mL STI) for the duration of the experiment. PCMCs, on the other hand, were not rested overnight and were activated directly in the same media described in **Section 2.4.3**, with the addition of 100 μ g/mL STI.

2.6.1 STING and cGAS agonists

Mast cells resuspended in activation media were treated with STING agonists ADU-S100 (0.08 μ g/mL, 0.4 μ g/mL, 2 μ g/mL, 10 μ g/mL) and diABZI (0.08 μ M, 0.4 μ M, 2 μ M, 10 μ M) to evaluate the dose-dependent effects of STING activation. The cGAS agonist G3-YSD (0.1 μ g/mL, 0.3 μ g/mL, 0.9 μ g/mL, 2.7 μ g/mL) and Poly(I:C) (10 μ g/mL) were transfected into cells using Lipofectamine™ 2000 Transfection Reagent (LF2000, Thermo Fisher Scientific). Cells that remained in activation media for the duration of the experiment were used as unstimulated (mock) controls.

To perform transfection, LF2000 was added to OPTI-MEM media (Thermo Fisher Scientific) and incubated for 5 minutes at room temperature (Tube A). In a separate tube, G3-YSD or Poly(I:C) was diluted in OPTI-MEM (Tube B). Tubes A and B were mixed and incubated at room temperature for 20 minutes to allow the DNA complex to form, after which the mixture was added to the cells. Cells were incubated in 5% CO₂ at 37°C for varying time points.

At indicated time points, cells were centrifuged at 400 x g for 5 minutes. Supernatants were collected and stored at -80°C, while cell pellets were taken for RNA or protein isolation. For STING inhibitor experiments, cells were pre-incubated with H-151 (0.11 µM, 0.33 µM, 1 µM, 3 µM, 9 µM) for 1 hour before the addition of ADU-S100 (2 µg/mL) or Poly(I:C).

2.7 SHIGELLA INFECTION OF MAST CELLS

Shigella flexneri strains (wild-type, ipaJ^{-/-}, and mxiD^{-/-}) were kindly provided by Dr. John Rohde from Dalhousie University. Gentamicin protection assays were conducted to assess bacterial invasion, survival, and immune signaling in MCs. The day before the experiments, a single colony of each bacterial strain was selected from tryptic soy broth (TSB) plates and inoculated into 3 mL of TSB broth, followed by incubation at 37°C and shaking at 200 rpm. Wild-type and STING KO BMMCs or PCMCs were cultured overnight in resting media containing 4 ng/mL IL-3, without P/S.

On the day of the experiment, the bacteria were diluted 1:25 in fresh TSB and incubated at 37°C with shaking at 200 rpm for approximately 3 hours until the optical density at 600 nm (OD₆₀₀) was measured to be 1.0 (density of 5 x 10⁸/mL). To achieve different multiplicities of infection (MOI), the bacteria were further diluted in PBS to achieve densities of 1 x 10⁸/mL and 2 x 10⁷/mL for infections at MOIs of 20 and 4, respectively.

To prepare MCs for infection, cells were centrifuged and washed twice with RPMI. Diluted bacteria were added to 1 x 10⁶ cells in RPMI containing 5% FBS and 4 ng/mL IL-3. Blank PBS was added to uninfected (control) cells. The cells were incubated for 60 minutes to allow bacterial infection to occur, after which they were centrifuged at 400 x g

for 5 minutes at room temperature. The supernatants were discarded, and fresh RPMI media supplemented with 5% FBS and 4 ng/mL IL-3 was added. Gentamicin (100 µg/mL) was introduced to the media to eliminate any remaining extracellular bacteria. The cells were then incubated for 4, 8, or 18 hours post-initial infection. At selected timepoints, cells were examined under the microscope for signs of cell death following trypan blue staining, then centrifuged at 400 x g for 5 minutes at room temperature. The supernatants were aliquoted and stored at -80°C, while cells were lysed in TRI Reagent® (Sigma-Aldrich) for RNA isolation.

2.8 SURVIVAL OF MICE IN AN OVARIAN CANCER MODEL

2.8.1 Preparation and injection of ID8 cells

ID8 cells were cultured as described in **Section 2.4.5**. In preparation for injections, the media was discarded, and cells were rinsed with PBS. TrypLE™ was used to detach cells by incubation at 37°C for 5 minutes. After detachment, cells were collected, and DMEM was used to rinse the bottom of the flasks to recover any remaining cells, which were pooled with the detached cells. The cells were centrifuged at 300 x g for 10 minutes and washed twice with DMEM. Aliquots were taken for cell counting before each spin. After the final cell count, the cells were resuspended in DMEM with 15 mM HEPES to reach a cell density of 15×10^6 cells/mL. The cell suspension was loaded into 1 mL syringes with 27G needles. Mice were injected intraperitoneally with 200 µL of the suspension, delivering 3.0×10^6 ID8 cells per mouse. The mice were monitored for the development of ascites or signs of morbidity every 2 days for up to 100 days. Signs of distress included

lack of activity, hunched posture, breathing difficulties, weight loss, ruffled hair, or a swollen abdomen.

2.8.2 ID8 harvest

Mice were euthanized by CO₂ asphyxiation and a ventral vertical incision was made to expose the peritoneal cavity. Ascites was collected from the peritoneum using a 5 mL syringe with a 21G needle into a conical tube and centrifuged at 500 x g for 10 minutes at 8°C. The ascites supernatant was aliquoted and stored at -80°C. The pellet was vortexed, and 3 mL of red blood cell (RBC) lysis buffer (8.02 g ammonium chloride, 0.84 g potassium bicarbonate, and 0.37 g ethylenediaminetetraacetic acid disodium salt dissolved in 1000 mL distilled water) was added for a 3-minute incubation at room temperature. PBS was added to the conical tube and the sample was mixed by inversion. The sample was left for 5 minutes to allow any ID8 cell clumps to settle as a pellet at the bottom of the tube. The remaining supernatant, excluding the pellet, was transferred into another tube for centrifugation at 400 x g for 10 minutes at 8°C.

After centrifugation and aspiration of the supernatant, a second RBC lysis was performed with 2 mL of buffer. Samples were incubated for 3 minutes at room temperature, washed with PBS, and allowed to sit for 5 minutes to let any residual ID8 cells settle on the bottom. The remaining supernatant was transferred into a new tube and spun down. The cells were then resuspended in PBS and split into two tubes; at which time an aliquot was collected for cell counting. Following the final spin, one tube of peritoneal cavity cells was resuspended in 1% PFA, while the other was resuspended in TRI Reagent®.

To wash the ID8 cell pellet, PBS was added to the tube, and cells were allowed to settle again. The PBS was aspirated and ID8 cells were separated into two tubes: one for

resuspension in 1% paraformaldehyde (PFA) and the other for resuspension in TRI Reagent®.

2.8.3 *In vivo* reconstitution with transduced and WT mast cells

Kit^{Wsh/Wsh} and C57BL/6-Cpa3-Cre; *Mcl-1^{fl/fl}* mice were peritoneally reconstituted with wild-type BMMCs or transduced BMMCs. BMMCs were cultured as described in **Section 2.4.1** and washed with PBS once before use. Following centrifugation at 300 x g for 10 minutes, cells were resuspended in DMEM with 15 mM HEPES at a density of 3 x 10⁶ cells/ 200 µL. Cells were loaded into 1 mL syringes with 27G needles and mice received 3 x 10⁶ cells by intraperitoneal injections. Injected mice were used four weeks following reconstitution, allowing the injected MCs to populate the peritoneum and adapt to the microenvironment. The success and extent of reconstitution was assessed by qPCR analysis of *Tpsb2* expression in peritoneal cavity cells collected at endpoint. Mice that were reconstituted with transduced cells were provided with doxycycline (DOX) chow (2 mg/kg, Bio-Serve, Flemington, NJ) to induce expression from the Tet-On promoter in the lentiviral construct.

2.8.4 Harvest of mesenteric lymph nodes and peritoneal washes

Peritoneal cavity cells and mesenteric lymph nodes were collected from mice following intraperitoneal STING agonist injections to analyze immune responses. Mice were euthanized by CO₂ asphyxiation and peritoneal cells were collected by lavage of the peritoneum with 5 mL of buffer (PBS containing 0.5% BSA and 5 mM EDTA). After collecting an aliquot for cell counting, samples were centrifuged at 300 x g for 5 minutes at 4°C. The supernatant was aliquoted and stored at -80°C, and the cells were resuspended

in PBS. A portion of the cells was separated, centrifuged at 400 x g for 5 minutes, and resuspended in TRI Reagent® for RNA isolation. The other portion was stained for FACS analysis as outlined in **Section 2.10.2**.

Mesenteric lymph nodes were harvested and placed into Eppendorfs containing PBS with 2% BSA on ice until processing. The lymph nodes were pressed through a 70 µm mesh screen, and PBS was used to rinse the screen twice into the conical. Samples were split into two tubes and then centrifuged at 400 x g for 10 minutes at 4°C. One tube was resuspended in TRI Reagent® while the other was resuspended in PBS for flow cytometry staining.

Spleen cells were used as unstained and fixable viability dye (FVD) compensation controls for flow cytometry (see **Section 2.10.2**). The collected spleen was filtered through a 70 µm mesh screen, and PBS was used to rinse the screen into a conical tube twice. Half of the cells were heat-killed by incubating at 65°C for 4 minutes, followed by 2 minutes on ice. These heat-killed cells were combined with live cells prior to staining for flow cytometry analysis.

2.9 GENE EXPRESSION AND PROTEIN ANALYSES

2.9.1 RNA isolation from cells

Cells were lysed in TRI Reagent® and stored at -80°C until used for isolations. Following chloroform addition, tubes were mixed by inversion and left at room temperature for three minutes. The samples were centrifuged at 12,000 x g for 15 minutes at 4°C. After centrifugation, the aqueous (top) layer was collected and mixed with an equal volume of RNase-free 70% ethanol. The samples were transferred to RNeasy mini spin

columns, and RNA isolation was performed according to the RNeasy[®] Mini Kit protocol. For samples containing transduced cells, 80 μ L of DNase I from the RNase-free DNase I kit (Qiagen) was added to the samples and incubated at room temperature for 15 minutes after the first wash with RW1 buffer. RNA concentration and purity were assessed using a BioTek plate reader with the corresponding Gen5 software (Agilent Technologies, Santa Clara, CA). The A260/A280 ratio was used to determine RNA purity. Complementary DNA (cDNA) was synthesized immediately from the RNA or RNA samples were stored at -80°C for future use.

2.9.2 Complementary DNA (cDNA) synthesis

Purified RNA (300 ng) was used to synthesize cDNA using a QuantiTect Reverse Transcription Kit (Qiagen) following the manufacturer's protocol. Briefly, RNA was mixed with RNase/DNase-free water to reach a total volume of 12 μ L, before the addition of 2 μ L gDNA Wipeout from the kit. The mixture was incubated at 42°C for 2 minutes to eliminate any genomic DNA. Next, 6 μ L of a mix containing 1 μ L of the kit's primer mix, 1 μ L of Reverse Transcriptase, and 4 μ L of the Reverse Transcription Buffer was added to each RNA sample. The samples were placed in a thermocycler, where they were incubated at 42°C for 30 minutes to allow reverse transcription, followed by 95°C for 3 minutes. cDNA samples were diluted 1:4 or 1:8 with RNase/DNase water before use or storage at -20°C.

2.9.3 Quantitative polymerase chain reaction (qPCR) and analyses

RT-qPCR was carried out using a Bio-Rad CFX384[™] RT-PCR thermocycler with the following cycling conditions: initial denaturation at 95°C for 3 minutes, followed by

40 cycles consisting of 95°C for 20 seconds, 60°C for 30 seconds, and plate reading. A final step was performed at 95°C for 10 seconds, followed by a melt curve analysis. For each reaction, 2 μ L of cDNA was combined with 5 μ L of SYBR® Green Supermix (Bio-Rad Laboratories), 0.25 μ M or 0.5 μ M primers, and RNase/DNase-free water, bringing the final volume to 10 μ L. Samples were loaded into 384-well plates (Bio-Rad Laboratories) in duplicate. Intron-spanning primers were obtained from Bio-Rad or Qiagen and validated prior to use. Reference (housekeeping) genes, *Hprt* and *Gusb*, were used. Cycle values over 35 were considered null expression. Results were processed and exported using CFX Maestro v1.1 software (Bio-Rad Laboratories), analyzed on Microsoft Excel, and graphed using GraphPad Prism (GraphPad, La Jolla, CA).

2.9.4 Protein isolation and concentration measurement

To isolate protein, cells were first centrifuged at 400 x g for 5 minutes, and the resulting pellets were washed once with PBS. Following a second centrifugation, the cells were lysed in Radio-Immunoprecipitation Assay (RIPA) buffer (Sigma-Aldrich), supplemented with phosSTOP phosphatase inhibitor (Roche, Sigma-Aldrich) and cOmplete Mini protease inhibitor (Roche, Sigma-Aldrich). The tubes were incubated on ice for 15 minutes, vortexing every 3 minutes, and then centrifuged at 15,000 x g for 10 minutes at 4°C. The supernatant was collected and kept on ice for protein analysis. Protein concentration was determined using the Pierce BCA Protein Assay Kit (Thermo Fisher Scientific). Absorbance was measured at 562 nm using a plate reader, and concentrations were calculated from a standard curve.

2.9.5 Western blotting

Protein (3 μg – 25 μg) was loaded onto 10% sodium dodecyl sulfate-polyacrylamide gels for electrophoresis. Gels were transferred to a nitrocellulose membrane (Bio-Rad Laboratories). The membrane was blocked with 5% milk in TBST (TBS with 0.1% Tween-20) to prevent non-specific binding. Primary antibodies were then applied, followed by corresponding secondary antibodies. Blots were developed using Clarity Max Western ECL Substrates (Bio-Rad Laboratories), and chemiluminescent signals were detected with a ChemiDoc Imaging System. The exposure times for imaging were automatically determined by the system. Finally, the images were processed and analyzed using ImageLab software (Bio-Rad Laboratories).

2.9.6 Luminex and ELISA

To quantify secreted proteins, supernatants were collected at experimental endpoints. Mouse multiplex magnetic Luminex® assay (Invitrogen, Thermo Fischer Scientific) kits were purchased and run according to the manufacturer's instructions using provided reagents. Plates were read on a Bio-Rad Bio-Plex 200 system. Enzyme-linked immunosorbent assays (ELISAs) were carried out using kits from R&D Systems (Minneapolis, MN), Peprotech, or Thermo Fisher. The ELISAs were performed over 2 days following the manufacturer's instructions. Plates were read at 450 nm using an Epoch Microplate Spectrophotometer and analyzed with Gen 5 software (BioTek, Winooski, VT).

2.9.7 Immunofluorescence staining and imaging

Round coverslips (0.17 mm) were sterilized in 100% ethanol, air dried, and placed into a 12-well plate. Poly-D-lysine (0.1 mg/mL, Sigma-Aldrich) was used to coat the

coverslips, by allowing them to sit in this solution for 30 minutes. The coverslips were then rinsed twice with cell culture-grade water and left to dry for an hour. One million BMMCs were seeded onto the coated coverslips and incubated for 20 minutes before being centrifuged at 300 x g for 10 minutes. Media was discarded and cells were fixed in 4% PFA for 10 minutes at room temperature. The cells were rinsed three times with ice-cold PBS and permeabilized with PBS containing 0.3% Triton-X-100 for 10 minutes at room temperature. Following three washes with PBS, the cells were blocked with 1%-BSA-PBS-0.3% Triton X-100 for 1 hour at room temperature with agitation. The cells were washed with PBS for 5 minutes three times on a plate shaker. Primary antibodies, diluted in 1% BSA-PBS-0.3% Triton X-100, were added and incubated for 1 hour at room temperature with agitation. After three rinses with PBS, the corresponding secondary antibodies, diluted in 1% BSA-PBS-0.3% Triton X-100, were added and incubated for 1 hour in the dark, with agitation on the plate shaker. Coverslips were rinsed with PBS and stained with DAPI (500 nM, Cell Signaling Technology) for 1 minute, excluding the unstained samples. Following PBS washes, coverslips were mounted onto slides using Prolong Gold (Invitrogen) and left to cure at room temperature for 24 hours in the dark. Slides were imaged on a Zeiss LSM 880 confocal laser scanning microscope using the DPSS 561-10 (561 nm, A568 channel) laser with a 100X oil immersion objective. Images were exported as TIFF files, and scale bars were added using ZEISS ZEN lite software.

2.10 FLOW CYTOMETRY

2.10.1 Annexin V Apoptosis Assay

BMMCs were treated with STING agonists for 48 hours before being assessed for apoptosis by Annexin V and 7-Aminoactinomycin D (7-AAD) staining. The Annexin V

Apoptosis Detection Kit (eBioscience, San Diego, CA) was used according to the manufacturer's protocol. Briefly, treated cells were collected into Eppendorf tubes and centrifuged at 400 x g for 5 minutes. The cells were rinsed with PBS, spun again, and resuspended in 1X binding buffer.

For controls, BMDCs were collected from culture, washed with PBS, resuspended in PBS, and split into three tubes. For the positive control, cells were heat-killed by placing one tube at 65°C for 4 minutes, followed by ice for 2 minutes. These heat-killed cells were combined with another tube of live cells, while the third tube was left as an unstained control. Binding buffer was added to all tubes, followed by centrifugation at 400 x g for 5 minutes, and resuspension in buffer. The heat-killed sample was then further split into the following controls: positive control, Annexin V only, and 7-AAD only.

Annexin V-FITC was added to the appropriate samples (5 µL per 100,000 cells), and the tubes were incubated in the dark for 15 minutes. Afterward, cells were washed in binding buffer, centrifuged, and resuspended. Finally, 5 µL of 7-AAD (Thermo Fisher Scientific, stock: 1 mg/mL) was added to each sample 5 minutes before acquisition for flow cytometry analysis.

2.10.2 Staining procedure for peritoneal cells and mesenteric lymph nodes

Cells were stained in FVD eFluor506 (1:1000 in PBS) and incubated for 20 to 30 minutes in the dark at 4°C. Immunofluorescence (IMF) buffer (10 mM sodium azide and 2% FBS in 1X PBS) was added to each tube, and the cells were centrifuged at 300 x g at 4°C for 5 minutes. To block nonspecific binding, cells were resuspended in 3% FBS in PBS for 15 minutes at room temperature. After blocking, the cells were split into two equal volumes, each for a separate staining panel, and transferred to a 96-well plate. Antibody

cocktails for Panel 1 and Panel 2 (**Table 4 & 5**) were added to the samples, and incubation was carried out for 25 minutes at 4°C. Cells were washed with IMF buffer and PBS to remove excess antibodies, followed by fixation in 1% PFA for 30 minutes. The cells were washed once more with PBS and IMF buffer before final resuspension in IMF buffer prior to flow cytometry acquisition. To perform compensation controls, UltraComp beads (Thermo Fisher Scientific) were stained with 0.3 µL of each monoclonal antibody, fixed in 1% PFA, and then resuspended in IMF buffer.

2.10.3 Flow cytometry panels and analysis

Data collection was completed at the Faculty of Medicine CORE flow cytometry facility using the BD FACS Celesta and FACSDIVA software. Analysis was performed using FlowJo software (BD Biosciences, San Jose, CA). The following flow cytometry panels were used to assess the activation and infiltration of immune cells in response to STING agonist ADU-S100 in the peritoneum (**Table 4 & 5**).

2.11 DATA REPRESENTATION AND STATISTICAL ANALYSES

Statistical analyses were complete using GraphPad Prism v9.4.1 software. Data are presented as mean ± SEM. Survival data was assessed by Log-Rank (Mantel-Cox) Test. p-values < 0.05 were considered statistically significant. The specific statistical approach used for each experiment was dependent on data distribution and experimental design, as clarified in figure legends.

Table 4. Antibodies for flow cytometry to examine lymphoid immune cell populations (Panel 1).

Laser (excitation)	Fluorochrome	Marker	Immune cell subset	Dilution	Clone	Supplier
Violet (405 nm)	BV650	CD19	B cells	1:400	6D5	BioLegend
	eF506	FVD		1:1000		Invitrogen
Blue (488 nm)	FITC	CD69	T cell activation	1:400	H1.2F3	BioLegend
	PE-Cy7	CD3e		1:400	145-2C11	eBioscience
	PE	CD8	T cell	1:400	53-6.7	BioLegend
Red (628 nm)	APC	NK1.1	NK cells	1:400	PK136	BioLegend
	AF700	CD4	T cells	1:800	GK1.5	BioLegend

Table 5. Antibodies for flow cytometry to assess innate immune cell populations (Panel 2).

Laser (excitation)	Fluorochrome	Marker	Immune cell subset	Dilution	Clone	Supplier
Violet (405 nm)	BV605	Ly6G	Neutrophils	1:400	1A8	BD Biosciences
	eF506	FVD		1:1000		Invitrogen
Blue (488 nm)	FITC	CD11b	Neutrophils, Macrophages, Monocytes, NK cell activation marker	1:1600	M1/70	eBioscience
	PE-Cy7	F4/80	Resting macrophages	1:1600	BM8	eBioscience
	PE	CD117	Mast cells	1:1200	2B8	eBioscience
Red (628 nm)	APC	FcεRI	Mast cells	1:400	MAR-1	BioLegend
	APC-eF780	Ly6C	Inflammatory monocytes	1:400	HK1.4	eBioscience
	AF700	MHCII	Dendritic cells	1:400	M5/114.15.2	eBioscience

Chapter 3: RESULTS

3.1 *IN VITRO* CHARACTERIZATION OF STING SIGNALING IN MAST CELLS

3.1.1 Characterizing transcriptional changes following STING agonist activation in mast cells

To determine if the STING pathway was functional in MCs, BMMCs were treated with STING agonists and transcriptional changes assessed to determine the type of response elicited. Two types of STING agonists (ADU-S100 and diABZI) were used to define potential differences in activation based on the class of drug. ADU-S100 is a cyclic dinucleotide (CDN) that is a structural analog of the endogenous STING ligand, whereas diABZI is classified as a non-CDN dimeric STING ligand. Poly(I:C), a synthetic dsRNA, was used as a positive control for MC-associated type I IFN induction.

A titration was performed with both STING agonists (ADU-S100: 0.08 µg/mL - 10 µg/mL, diABZI: 0.08 µM - 10 µM), to test the dose-dependency of MC responses. After 6 hours, type I IFN and ISG transcript levels were determined by qPCR. ADU-S100 (10 µg/mL) treatment significantly upregulated the gene expression of type I IFNs (*Ifnb1*, *Ifna11*, *Ifna2*), ISGs (*Ifit1*, *Cxcl10*) and NF-κB-associated transcripts (*Il6*) compared to untreated cells (**Figure 6A**). A pattern of increased gene induction was seen with increasing concentrations of the agonist. Similar results were observed in diABZI-treated BMMCs, demonstrated by increases in *Ifnb1*, *Cxcl10*, and *Ifit1* transcript levels compared to mock-treated BMMCs at 6 hours (**Figure 7A**). Poly(I:C) treatment induced increases in the gene expression of all tested targets, except *Il6*. Overall, these results suggest the STING

pathway is functional in MCs and that activation induces type I IFN-related transcriptional changes which could contribute to promoting effective immune responses.

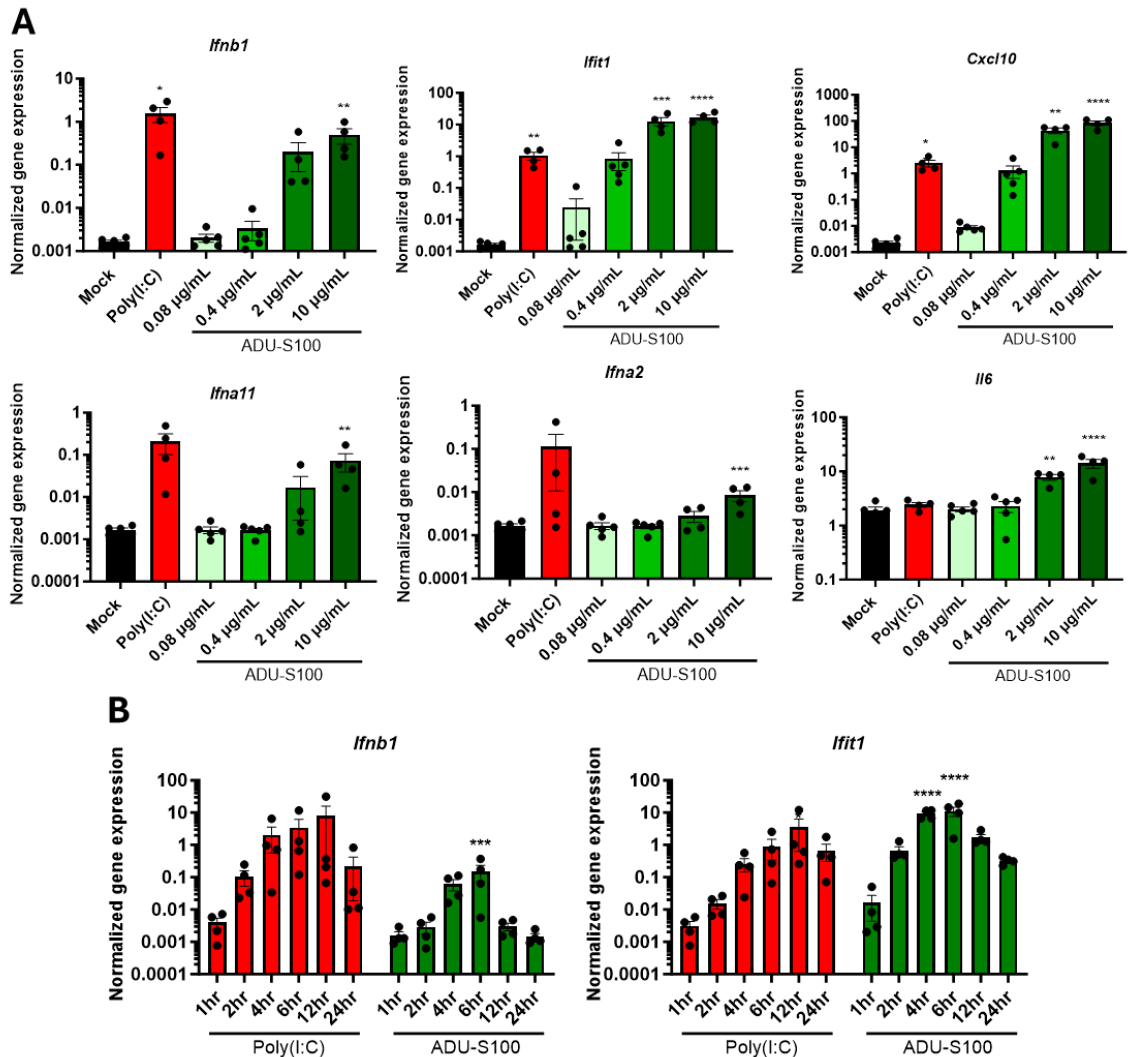


Figure 6. Type I IFN, ISG, and cytokine transcript levels were increased in mast cells following STING activation with ADU-S100.

BMMCs were cultured in activation media and (A) treated with ADU-S100 (0.08, 0.4, 2, 10 µg/mL), Poly(I:C) (10 µg/mL), or left untreated (mock) for 6 hours. (B) BMMCs were treated with 10 µg/mL Poly(I:C) or 2 µg/mL ADU-S100 for 1, 2, 4, 6, 12, and 24 hours. Gene expression of type I IFNs and ISGs was measured using RT-qPCR and normalized to the geometric mean of housekeeping genes *Hprt* and *Gusb*. Statistical significance was determined by: (A) one-way ANOVA followed by Dunnett's multiple comparisons test, comparing agonist doses to mock treatment, while unpaired t-tests were performed to compare Poly(I:C) treatment to mock or (B) two-way ANOVA followed by a Šidák's multiple comparisons test, comparing Poly(I:C) or ADU-S100 treatment to mock at each time point. Data shown as mean ± SEM. n = 3-5 per treatment. * $p < 0.05$; ** $p < 0.01$; *** $p < 0.001$; **** $p < 0.0001$.

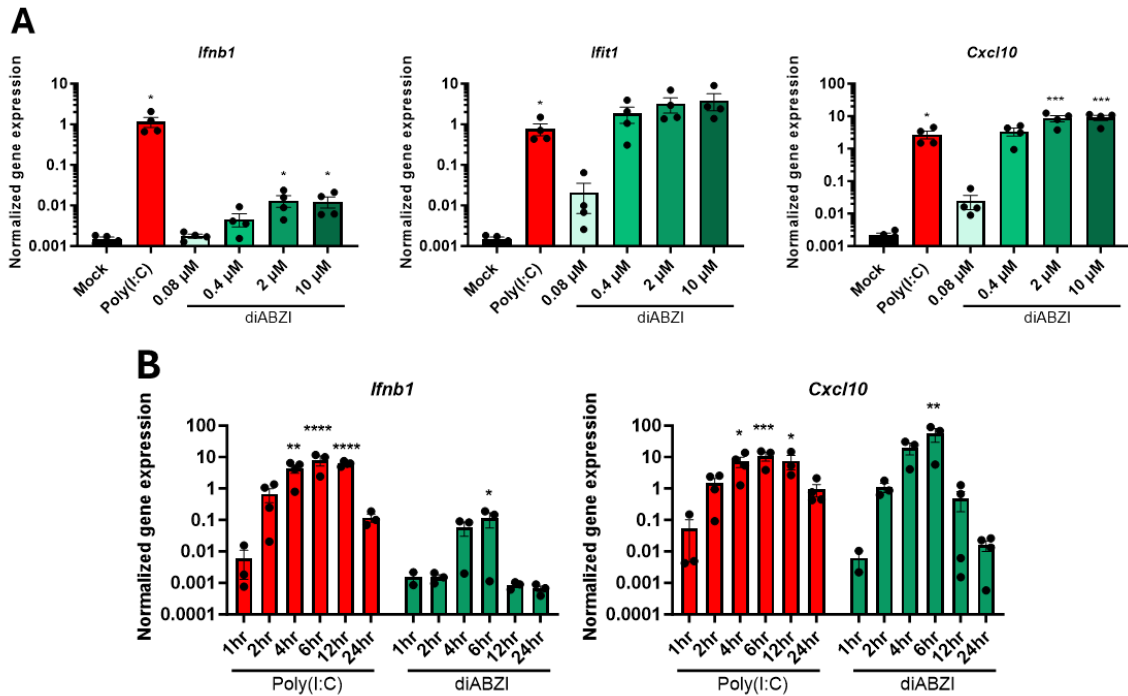


Figure 7. Mast cells upregulate type I IFN and ISG gene expression following STING activation with diABZI.

(A) BMMCs were cultured in activation media and treated with diABZI (0.08, 0.4, 2, 10 μM), Poly(I:C) (10 $\mu\text{g}/\text{mL}$), or left untreated (mock) for 6 hours. (B) BMMCs were treated with 10 $\mu\text{g}/\text{mL}$ Poly(I:C) and 10 μM diABZI for 1, 2, 4, 6, 12, and 24 hours. Gene expression of type I IFNs and ISGs was measured using RT-qPCR and normalized to the geometric mean of housekeeping genes *Hprt* and *Gusb*. Statistical significance was determined by: (A) one-way ANOVA followed by Dunnett's multiple comparisons test, comparing agonist doses to mock treatment, while unpaired t-tests were performed to compare Poly(I:C) treatment to mock or (B) two-way ANOVA followed by a Šídák's multiple comparisons test, comparing Poly(I:C) or diABZI treatment to mock at each time point. Data shown as mean \pm SEM. $n = 3\text{--}5$ per treatment condition. * $p < 0.05$; ** $p < 0.01$; *** $p < 0.001$; **** $p < 0.0001$.

RAW264.7 macrophages were used as a cell-line control as they are described to have functional STING signaling that leads to the phosphorylation of IRF3²⁴¹. These macrophages were treated with both STING agonists, similar to the BMMCs. In response to ADU-S100, there was a dose-dependent trend of increased *Ifit1* gene expression with higher agonist concentrations at 6 hours (Figure 8A). Induction of *Ifit1* was increased with

diABZI treatment but in a smaller magnitude (**Figure 8B**). However, no increase in *Ifnb1* transcription levels was observed following treatment with either agonist, which may be due to a difference in IFN signaling (**Figure 8**). These cells may be primarily upregulating IFN α gene expression or have devoid IFN β signaling in response to STING activation.

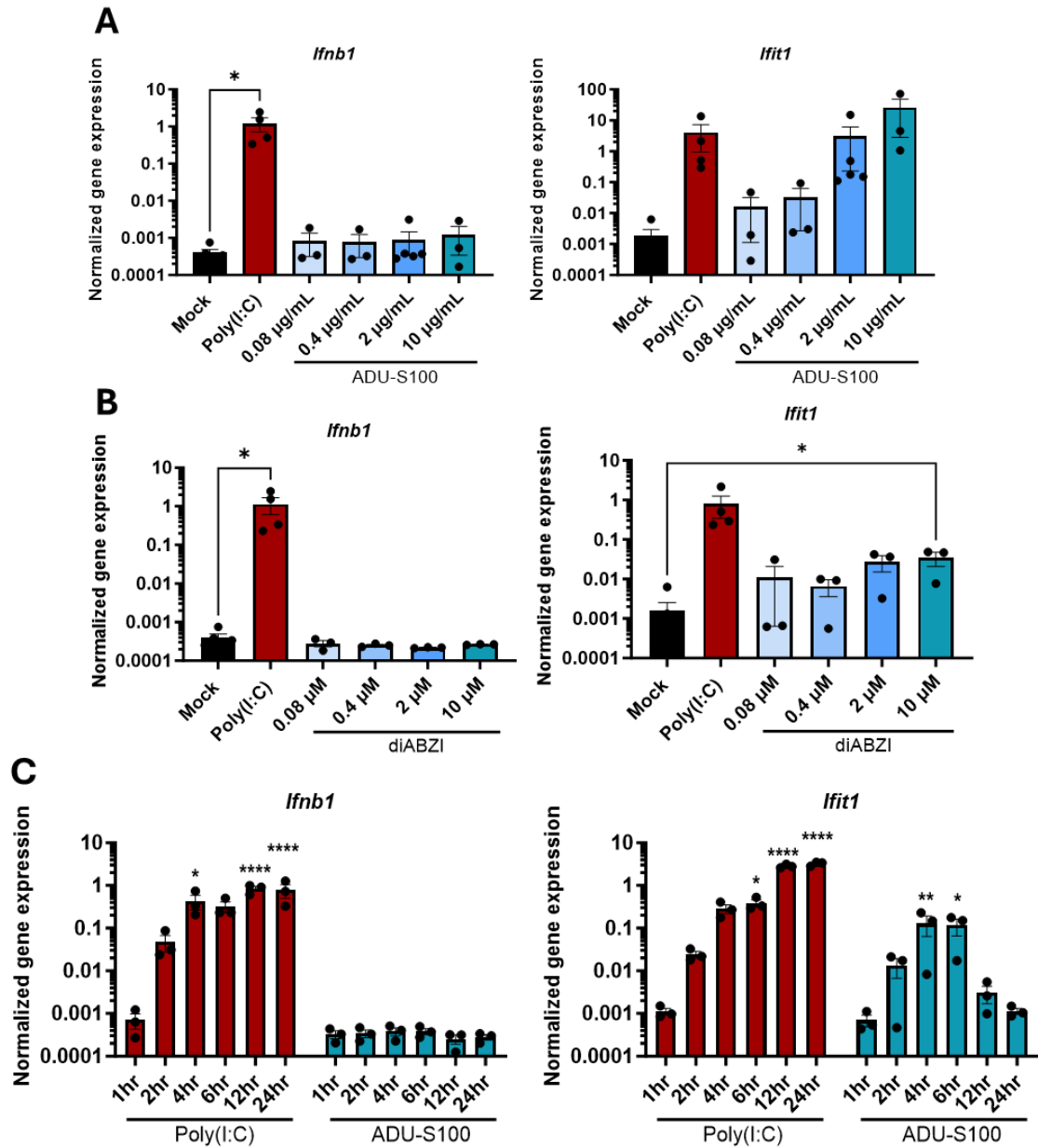


Figure 8. RAW264.7 macrophages upregulate *Ifit1* but not *Ifnb1* mRNA following activation with STING agonists.

RAW264.7 macrophages were cultured in DMEM supplemented with 10% FBS and treated with Poly(I:C) (10 µg/mL), (A) ADU-S100 (0.08, 0.4, 2, 10 µg/mL), (B) diABZI (0.08, 0.4, 2, 10 µM), or left untreated (Mock) for 6 hours. (C) RAW264.7 macrophages were treated with 10 µg/mL Poly(I:C), 10 µM diABZI or 10 µg/mL ADU-S100 for 1, 2, 4, 6, 12, and 24 hours. Gene expression of type I IFNs and ISGs was measured using RT-qPCR and normalized to the geometric mean of housekeeping genes *Hprt* and *Gusb*. Statistical significance was determined by: (A, B) one-way ANOVA followed by Dunnett's multiple comparisons test, comparing agonist doses to mock treatment, while unpaired t-tests were performed to compare Poly(I:C) treatment to mock or (B) two-way ANOVA followed by a Šidák's multiple comparisons test, comparing Poly(I:C) or agonist treatment to mock at each time point. Data shown as mean ± SEM. n = 3–5 per treatment condition. * $p < 0.05$; ** $p < 0.01$; **** $p < 0.0001$.

A time-course experiment was conducted with STING agonist concentrations selected from the titration (2 µg/mL ADU-S100 and 10 µM diABZI) to assess the kinetics of STING activation in MCs. Changes in gene expression were evaluated at 1, 2, 4, 6, 12, and 24-hours post-STING agonist treatment. Gene induction changes occurred rapidly where peak gene expression of *Ifnb1*, *Cxcl10*, and *Ifit1* was observed 4 to 6 hours post-STING agonist treatment (Figure 6B and 7B). These IFN-related transcriptional changes were transient, as *Ifnb1* transcript levels decreased toward baseline by 12 hours after agonist treatment.

To assess whether ADU-S100 caused any cytotoxic effects at the tested doses (2 µg/mL and 10 µg/mL), cell death was evaluated in BMDCs using Annexin V and 7-aminoactinomycin D (7-AAD) staining after 48 hours of treatment. No notable differences were observed in the proportions of apoptotic (Annexin V⁺, 7-AAD⁻) and late apoptotic or necrotic (Annexin V⁺, 7-AAD⁺) cells between the STING agonist-treated group and the control group (Figure 9B and 9D). In contrast, the positive control group, consisting of heat-killed MCs, showed an increase in non-viable cell proportions (Figure 9A),

confirming the reliability of the staining procedure. These results suggest that activation of STING by ADU-S100 does not induce cell death in MCs at the tested concentrations.

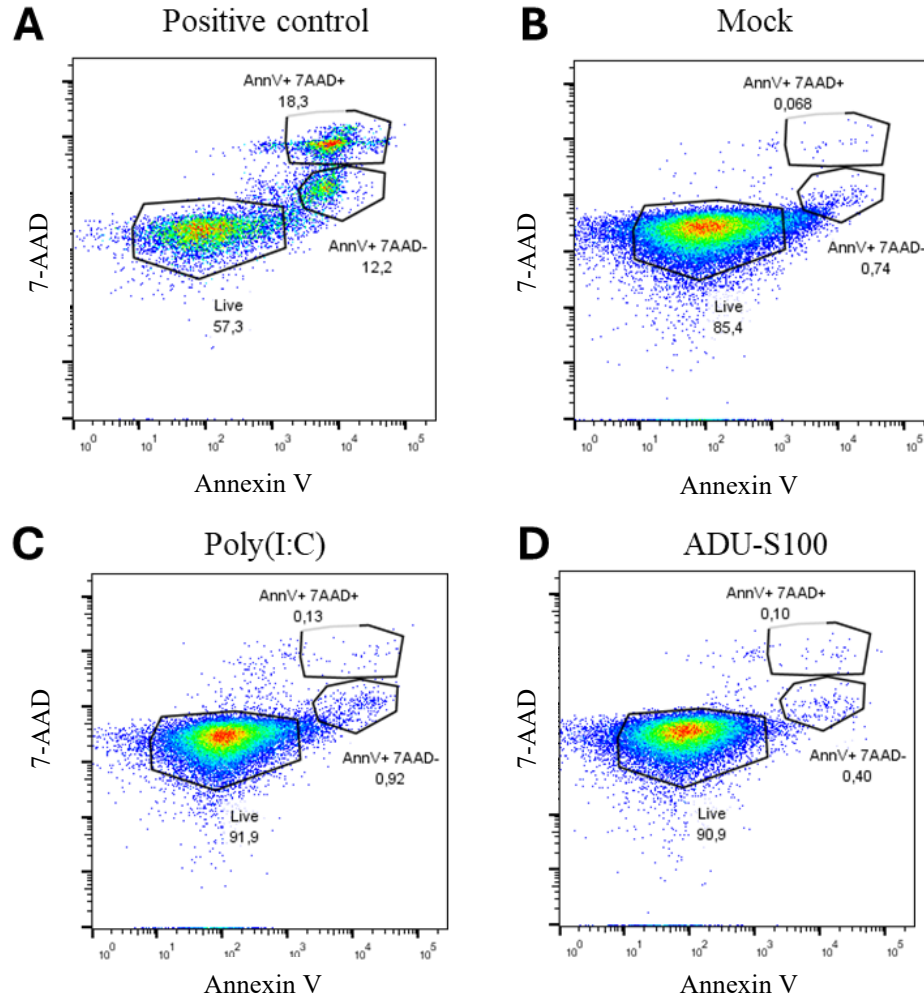


Figure 9. STING agonist treatment does not cause changes in cell death or viability in mast cells.

BMMCs were left untreated (mock), transfected with Poly(I:C) (10 $\mu\text{g}/\text{mL}$), or treated with ADU-S100 (10 $\mu\text{g}/\text{mL}$) for 48 hours. Heat-killed MCs were used as a positive control. Cells were stained for Annexin V and 7-AAD and analyzed by flow cytometry. Representative flow cytometric plots are shown with percentages in the gates as shown.

H-151 is an irreversible STING inhibitor that covalently binds to a transmembrane residue on the STING protein to prevent clustering, which is an essential step for activation.

A dose-response analysis for the impact of H-151 (0.11 μ M, 0.33 μ M, 1 μ M, 3 μ M, 9 μ M) was conducted on BMMCs in conjunction with ADU-S100 (2 μ g/mL). There was a dose-dependent decrease in *Ifnb1* and *Ifit1* gene expression at 6 hours in ADU-S100-treated cells with the addition of the inhibitor (**Figure 10A**). These data suggests that STING signaling follows standard activation in MCs, which can be inhibited as a tool to study STING in our system.

For subsequent experiments, STING-deficient MCs were used to determine the role of MC-derived STING in settings of infection. To confirm their deficiency, peritoneal cavity-derived MCs (PCMCs) were cultured from STING-deficient (Goldenticket, *Tmem173^{gt}*) mice. The response to ADU-S100 (10 μ g/mL) in WT C57BL/6 and STING-deficient MCs showed that the gene expression of *Ifnb1*, *Ifit1*, and *Cxcl10* in the STING-deficient cells was dampened and comparable to mock-treated cells at 6 hours (**Figure 10B**).

To determine whether the STING responses observed in mouse MCs were consistent in human MCs, ADU-S100 agonist dose and kinetic responses were performed with cord blood-derived MCs (CBMCs) in the same manner. Human MCs respond similarly, as indicated by increased transcripts of *IFNB*, *IFIT1*, and *CXCL10* at 6 hours following ADU-S100 treatment. However, this response was only observed with the highest dose (**Figure 11A**). These transcriptional changes, specifically in *IFNB*, were more subtle compared to what was observed in murine MCs and there were no obvious dose-dependent changes. There may be a potential need for higher doses to elicit a notable response due to decreased sensitivity or an increased threshold for activation in human MCs. However, similar to murine MCs, transcriptional increases were most prominent at

6 hours and transient (**Figure 11B**). Additionally, the heterogeneous nature of human samples and polymorphisms can lead to variation in responses. Poly(I:C)-induced increases in *IFNB*, *IFIT1*, and *CXCL10* expression were more robust and remained high at 24 hours, potentially due to numerous receptors being activated (**Figure 11A and 11B**).

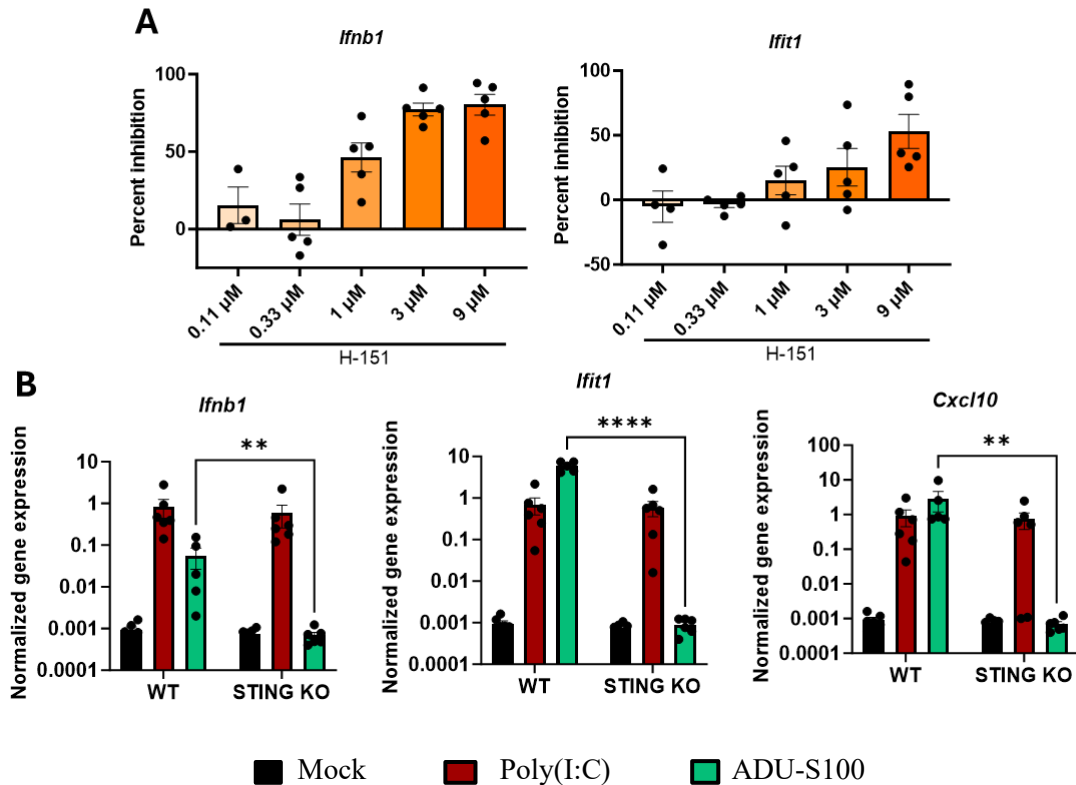


Figure 10. STING agonist-induced transcriptional changes were dampened by inhibitor H-151 and are absent in STING KO mast cells.

(**A**) BMDCs were cultured in activation media and pre-treated with H-151 (0.11, 0.33, 1, 3, 9 μ M) for 1 hour before ADU-S100 (2 μ g/mL) was added for 6 hours. (**B**) WT and STING KO PCMCs were treated with 10 μ g/mL Poly(I:C), 10 μ g/mL ADU-S100, or left untreated (mock) for 6 hours. Gene expression of type I IFNs and ISGs was measured using RT-qPCR and normalized to the geometric mean of housekeeping genes *Hprt* and *Gusb*. Statistical significance was determined by two-way ANOVA followed by a Šidák's multiple comparisons test, comparing responses to treatment between WT and STING KO cells. Data shown as mean \pm SEM. n = 5–6 per treatment condition. ** p < 0.01; **** p < 0.0001.

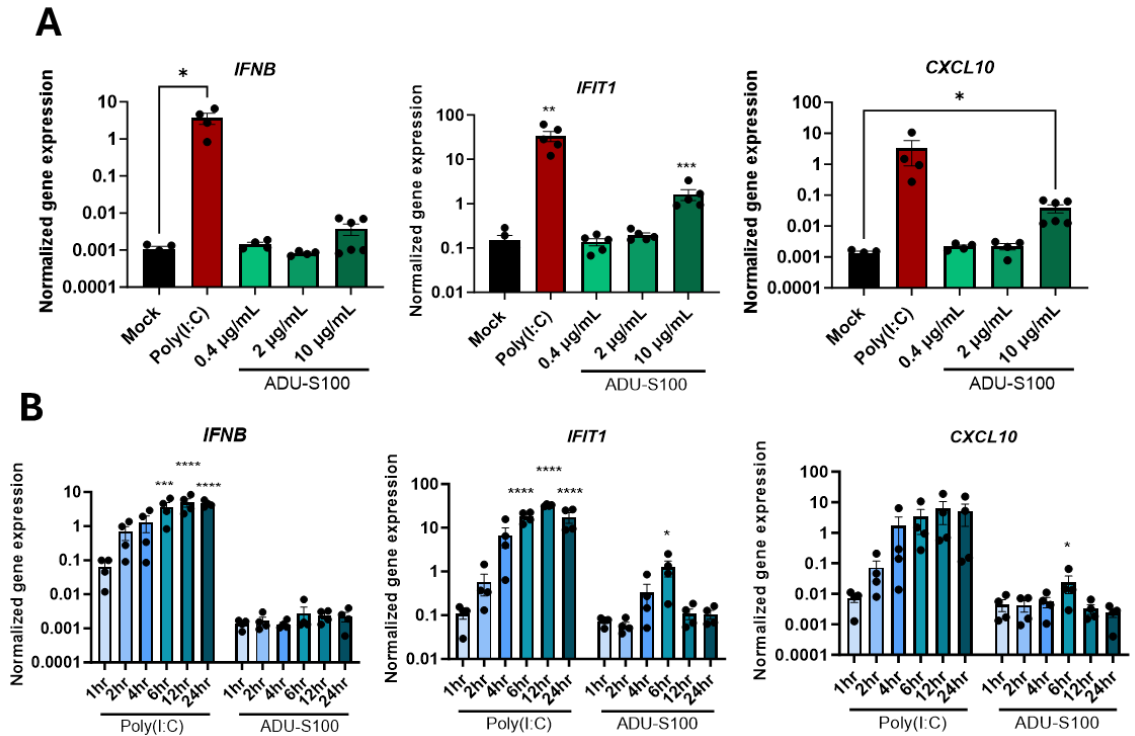


Figure 11. Human mast cells responded to STING activation by upregulating type I IFN-related transcript levels.

CBMCs were cultured in activation media and (A) treated with ADU-S100 (0.4, 2, 10 µg/mL) or Poly(I:C) (10 µg/mL) for 6 hours (B) CBMCs were treated with 10 µg/mL Poly(I:C) or 10 µg/mL ADU-S100 for 1, 2, 4, 6, 12, and 24 hours. Gene expression of type I IFNs and ISGs was measured using RT-qPCR and normalized to the geometric mean of housekeeping genes *HPRT* and *GUSB*. Statistical significance was determined by: (A) one-way ANOVA followed by Dunnett's multiple comparisons test, comparing agonist doses to mock treatment, while unpaired t-tests were performed to compare Poly(I:C) treatment to mock or (B) two-way ANOVA followed by a Šídák's multiple comparisons test, comparing Poly(I:C) or agonist treatment to mock at each time point. Data shown as mean ± SEM. n=4-5 per treatment condition. * $p < 0.05$; ** $p < 0.01$; *** $p < 0.001$; **** $p < 0.0001$.

3.1.2 Assessing cGAS activation of mast cells

To assess the activation of upstream components of the STING pathway, BMDCs were treated with an agonist targeting cGAS, the intracellular sensor that initiates the pathway. G3-YSD is a DNA sequence and known cGAS agonist that was transfected into cells using Lipofectamine 2000. An *in vitro* dose-response (0.1 $\mu\text{g}/\text{mL}$, 0.3 $\mu\text{g}/\text{mL}$, 0.9 $\mu\text{g}/\text{mL}$, and 2.7 $\mu\text{g}/\text{mL}$) was conducted with BMDCs for 6 and 24 hours. Type I IFN (*Ifnb1*) and ISG (*Cxcl10*, *Ifit1*) gene expression were significantly increased 6 and 24 hours post-

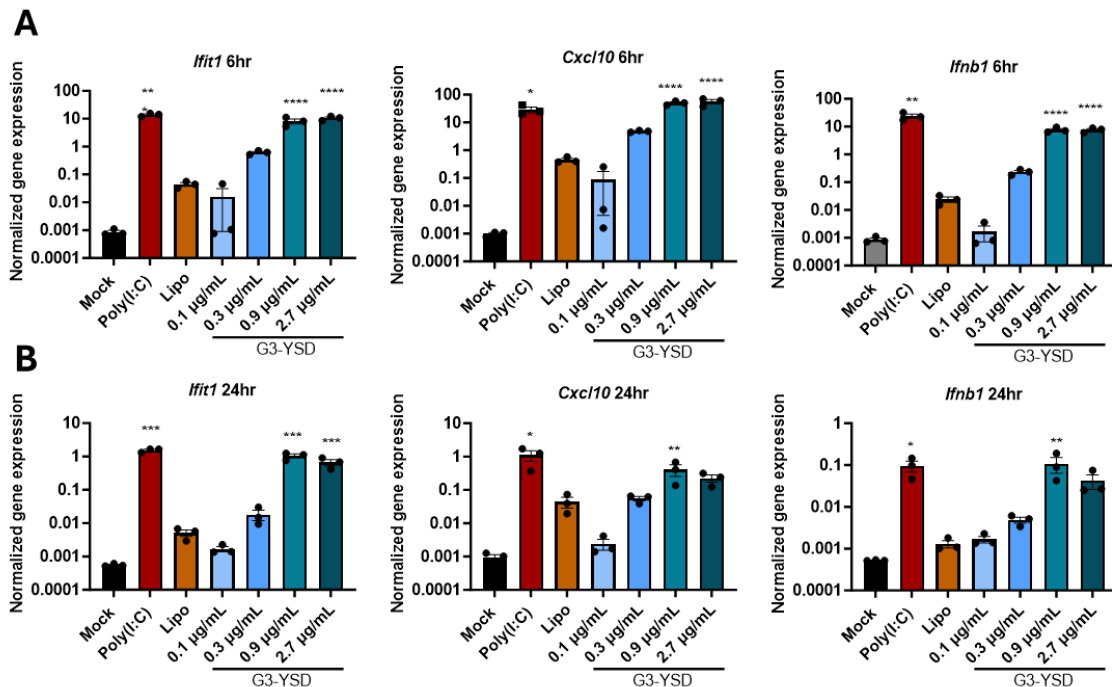


Figure 12. Mast cell cGAS activation leads to increases in type I IFN and ISG transcript levels.

BMDCs were cultured in activation media and transfected with Lipofectamine 2000 alone (Lipo), Poly(I:C) (10 $\mu\text{g}/\text{mL}$), or G3-YSD (0.1, 0.3, 0.9, 2.7 $\mu\text{g}/\text{mL}$) for (A) 6 and (B) 24 hours. Gene expression of type I IFNs and ISGs was measured using RT-qPCR and normalized to the geometric mean of housekeeping genes *Hprt* and *Gusb*. Statistical significance was determined by one-way ANOVA followed by a Dunnett's multiple comparisons test, comparing agonist and lipofectamine transfection to mock treatment. Unpaired t-tests were performed to compare Poly(I:C) treatment to mock. Data shown as mean \pm SEM. $n=3$ per treatment condition. * $p < 0.05$; ** $p < 0.01$; *** $p < 0.001$; **** $p < 0.0001$.

G3-YSD transfection (**Figure 12A and 12B**). The duration of signaling was longer than that seen with the STING agonists, as transcript levels were still high at 24 hours.

3.1.3 Detection and activation of STING protein

To visualize STING at the protein level, antibodies were used to probe STING for western blot and immunofluorescence analysis. Positive staining for STING was observed around the nucleus in fixed and untreated BMMCs via immunofluorescence (**Figure 13C**). To ensure the signal was specific, STING KO BMMCs were stained similarly and little (background) to no fluorescence was observed (**Figure 13C**). These findings are consistent with western blots results where the presence of STING protein was detected at baseline in untreated BMMCs and was absent in STING-deficient BMMCs (**Figure 13A**).

To determine activation of STING protein, lysates were collected from BMMCs treated for 6 and 24 hours with ADU-S100 (10 $\mu\text{g/mL}$), diABZI (10 μM), or G3-YSD (2.7 $\mu\text{g/mL}$) and probed for active phosphorylated STING (Serine 365). Additionally, phosphorylated TBK1 (Serine 172) was probed as another indication of pathway activation. TBK1 is downstream of STING in the pathway and becomes phosphorylated during activation. Increased levels of phosphorylated STING (35 kDa) and TBK1 (84 kDa) protein were detected 6- and 24-hours post-treatment for all three agonist treatments and was absent in untreated and STING-deficient BMMCs (**Figure 13A**). The phosphorylation of STING and TBK1 was most prominent in diABZI- and G3-YSD-treated BMMCs compared to those that were treated with ADU-S100. Moreover, phosphorylated STING and TBK1 levels were decreased at the 24-hour timepoint. A decrease in total STING protein was observed 24 hours after STING agonist treatment, but not cGAS agonist, and was most significant with ADU-S100. This decrease in total protein may be activation-

induced lysosomal degradation. This is one mechanism that is known to terminate STING signaling, where STING is trafficked to the lysosome to be degraded²⁴². Overall, there could be differences in signaling, termination, and recycling depending on the class of

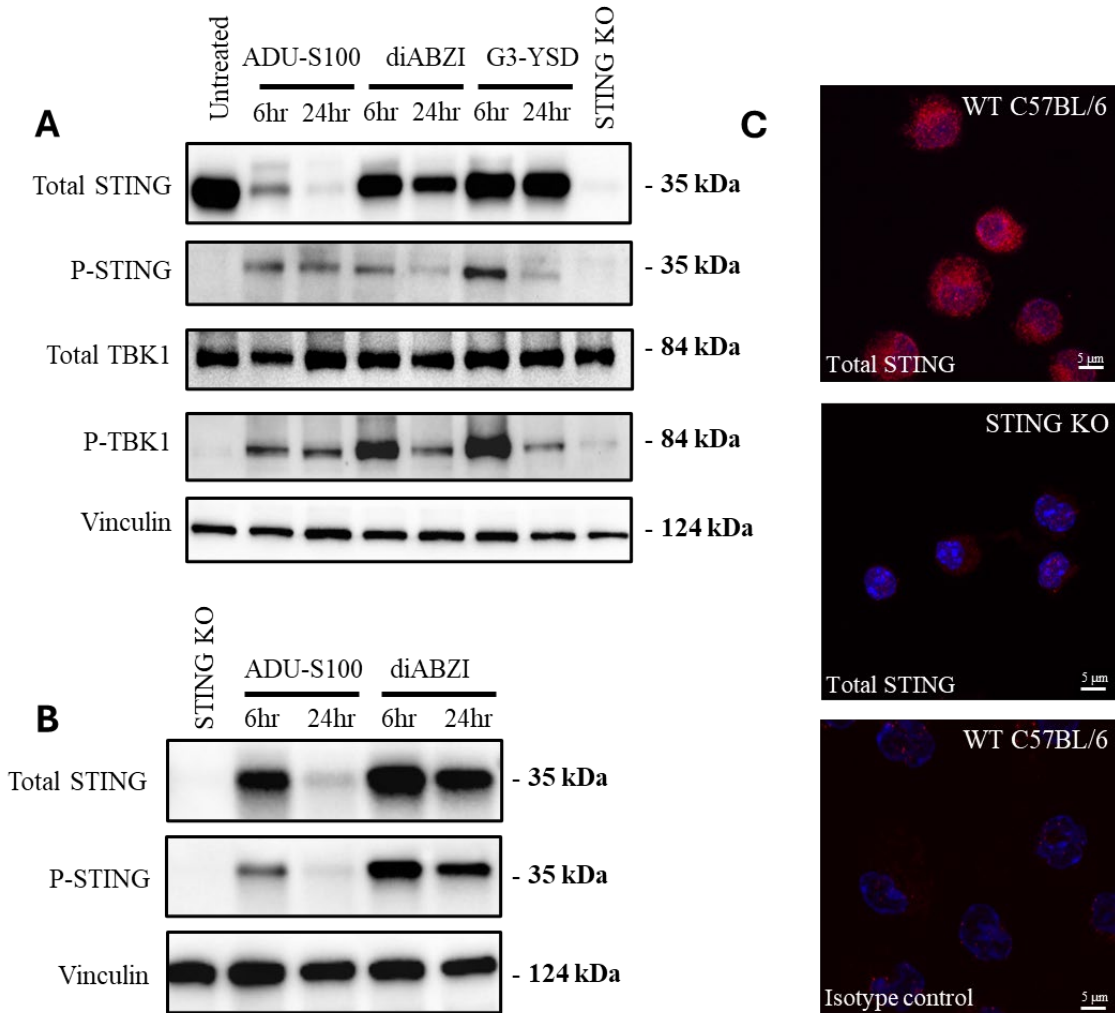


Figure 13. Murine mast cells express intracellular STING protein that is phosphorylated upon activation.

Lysates were collected from (A) BMMCs and (B) PCMCs treated with ADU-S100 (10 μg/mL), diABZI (10 μM), or G3-YSD (2.7 μg/mL) for 6 and 24 hours. Cells were probed for phosphorylated STING and phosphorylated TBK1 protein by western blot. Representative images of blots using vinculin as a loading control are shown. (C) BMMCs were fixed on poly-D-lysine coated coverslips and stained for STING (red; 1:100) and co-labeled with DAPI (blue). The images were captured at a magnification of 1000X. Representative images of immunofluorescence staining are shown on wild-type (WT) C57BL/6 and STING KO BMMCs. Images are representative of 2 to 3 experiments.

agonist. Activation of STING was also assessed in PCMCs where a similar trend of protein phosphorylation was observed with ADU-S100 and diABZI treatment (**Figure 13B**), indicating activation consistency in a different MC population.

3.1.4 Mast cell production of IFN and chemokines following STING activation

When activated, MCs secrete a variety of mediators to promote immune responses. To examine MC mediator production following STING activation, cytokines and chemokines levels were measured in the supernatants of BMMCs treated with ADU-S100 (10 µg/mL) by Luminex and ELISA. IFN-β production was significantly increased 6 and 12 hours following ADU-S100 treatment, although to modest levels, but such IFN production was not observed in diABZI-treated cells (**Figure 14A**). Moreover, CCL2 was significantly elevated at 12 and 24 hours post-ADU-S100 treatment. Similar results were observed with diABZI treatment, with a significant increase of CCL2 at 24 hours (**Figure 14B**). Poly(I:C) transfection resulted in strongest IFN-β and CCL2 production at 12 hours and 24 hours, respectively (**Figure 14A and 14B**). These results suggest that MCs, when activated by STING, can produce mediators that recruit and activate other immune cells, which may be useful in promoting immunity, especially during infection and cancer.

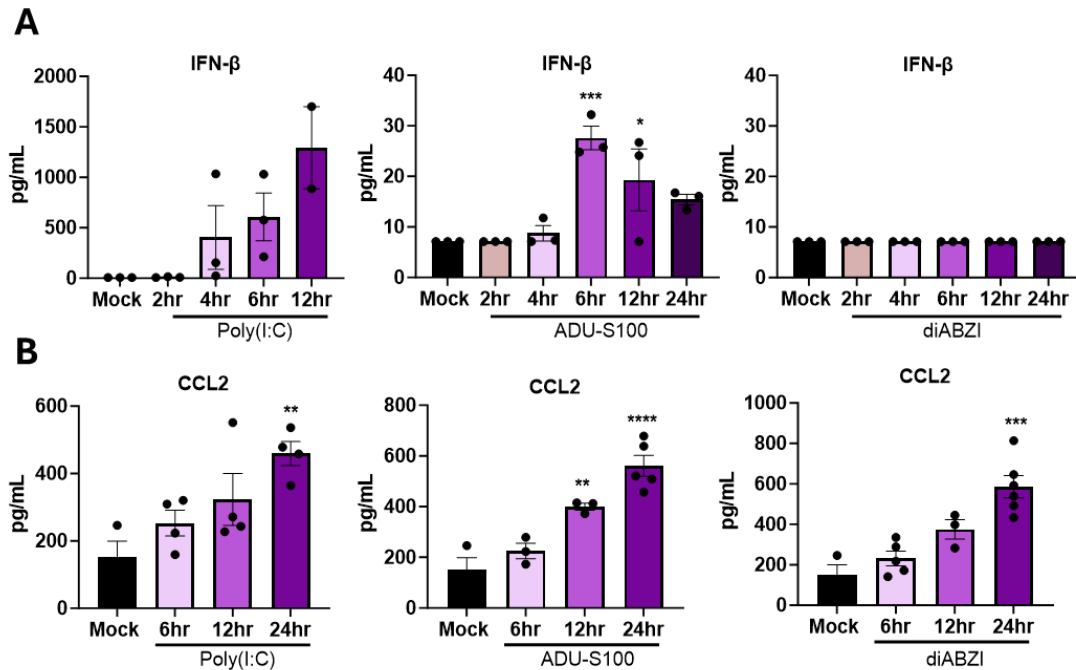


Figure 14. STING activation causes IFN- β and CCL2 production by mast cells.

Supernatants were collected from BMMCs cultured in activation media and treated with ADU-S100 (10 $\mu\text{g/mL}$), diABZI (10 μM), Poly(I:C) (10 $\mu\text{g/mL}$) or left untreated (mock) for 2, 4, 6, 12, and 24 hours. Protein levels of **(A)** IFN- β and **(B)** CCL2 were measured by Luminex and ELISA, respectively. Statistical significance was determined by one-way ANOVA followed by a Dunnett's multiple comparisons test, comparing Poly(I:C) or agonist treatment to mock at each time point. Data shown as mean \pm SEM. $n = 3\text{--}5$ per treatment condition. * $p < 0.05$; ** $p < 0.01$; *** $p < 0.001$; **** $p < 0.0001$.

3.2 THE ROLE OF STING ACTIVATION IN MAST CELL RESPONSES TO *SHIGELLA* INFECTION *IN VITRO*

Given the presence and potential impact of STING signaling in MCs, we aimed to explore its functional relevance in the context of infection. While STING signaling has been shown to have conflicting roles in bacterial infections, its role in *Shigella* infection remains incompletely characterized. As MCs are strategically positioned in the mucosal intestinal lining, they could serve as an early line of defense and underappreciated cells in

mounting immune responses to infection. Therefore, we sought to investigate whether MCs respond to *Shigella* infection and the role of STING in this process.

To address this, 2 mutants of *Shigella*- Δ *ipaJ* and Δ *mxiD*- were used along with the wild-type MT90 strain (WT). IpaJ is a bacterial effector that *Shigella* possesses to manipulate host defense mechanisms. It has been shown to inhibit STING signaling by blocking the translocation of STING to the ERGIC through GTPase demyristoylation¹⁴⁷. As the IpaJ mutant lacks this inhibitory effect, it allows us to better understand the role of STING signaling in MC responses. On the other hand, the *mxiD* mutant lacks a membrane protein essential for the type III secretion system, which *Shigella* uses to infect and enter host cells. As a result, the *mxiD* mutant is unable to enter target cells and provides valuable insight into immune responses that rely on intracellular signaling.

Wild-type and STING KO BMBCs were infected *in vitro* with WT, Δ *ipaJ*, and Δ *mxiD* *Shigella* at a MOI of 20 for 18 hours (**Figure 15A**). At this time point, MCs were assessed for changes in gene expression. We first found that MCs responded to WT *Shigella* infection by upregulating the transcription of *Ifnb1* and *Ifit1*, indicating the activation of a type I IFN response. Infection with the *mxiD* mutant resulted in gene expression levels of these targets similar to those of uninfected cells, suggesting that these IFN-related transcriptional changes are dependent upon bacterial entry. Moreover, this IFN response was observed to be partially STING dependent. MCs infected with Δ *ipaJ*, which cannot block STING signaling, displayed significantly higher levels of *Ifnb1* and *Ifit1* transcripts compared to WT-infected cells. A further indication of this STING-dependency was the lower induction of *Ifnb1* and *Ifit1* in STING KO MCs that were infected with both WT and Δ *ipaJ* *Shigella*. Interestingly, a distinct pattern was observed with *Cxcl10*

transcript upregulation which was robustly increased to similar magnitudes following infection with all three bacterial strains. Since infection with the *mxiD* mutant led to similar *Cxcl10* expression levels, these data suggested that MCs may also respond to *Shigella* infection through extracellular receptors.

These infection experiments were also conducted with PCMCs to determine if phenotypic differences in a different MC population would result in different immune responses (**Figure 15B**). Similar to the results observed in BMMCs, *Shigella* infection induced upregulation of *Ifnb1* and *Ifit1* in WT PCMCs, with this response being dependent on bacterial entry, as evidenced by the lack of gene expression changes following Δ *mxiD* infection. Additionally, the significant increase in transcript levels in response to the IpaJ mutant suggested that STING is involved in mediating MC responses to *Shigella* infection. However, *Cxcl10* transcriptional changes differed in PCMCs compared to BMMCs. In WT PCMCs, infection with the *mxiD* mutant did not result in upregulation of *Cxcl10* gene expression. This discrepancy may be attributed to differences in surface receptor expression between these MC populations, or it could reflect an increased threshold required for activation of extracellular signaling in PCMCs.

To assess MC mediator production, supernatants were collected following infection and used to conduct ELISAs (**Figure 15C**). First, IL-6 production was similarly increased across all three bacterial strains, with no significant difference between WT and STING KO BMMCs. This suggests that MCs contribute to a pro-inflammatory response during *Shigella* infection in a STING-independent manner, likely triggered by extracellular signals. A similar trend was observed with CCL2 production, which highlights a potential role of MCs in recruiting macrophages and DCs, which is crucial for the resolution of

Shigella infection. ELISA was not sensitive enough to detect IFN- β protein, but the significant upregulation of *Ifit1* suggests sufficient type I IFN production to stimulate ISG expression.

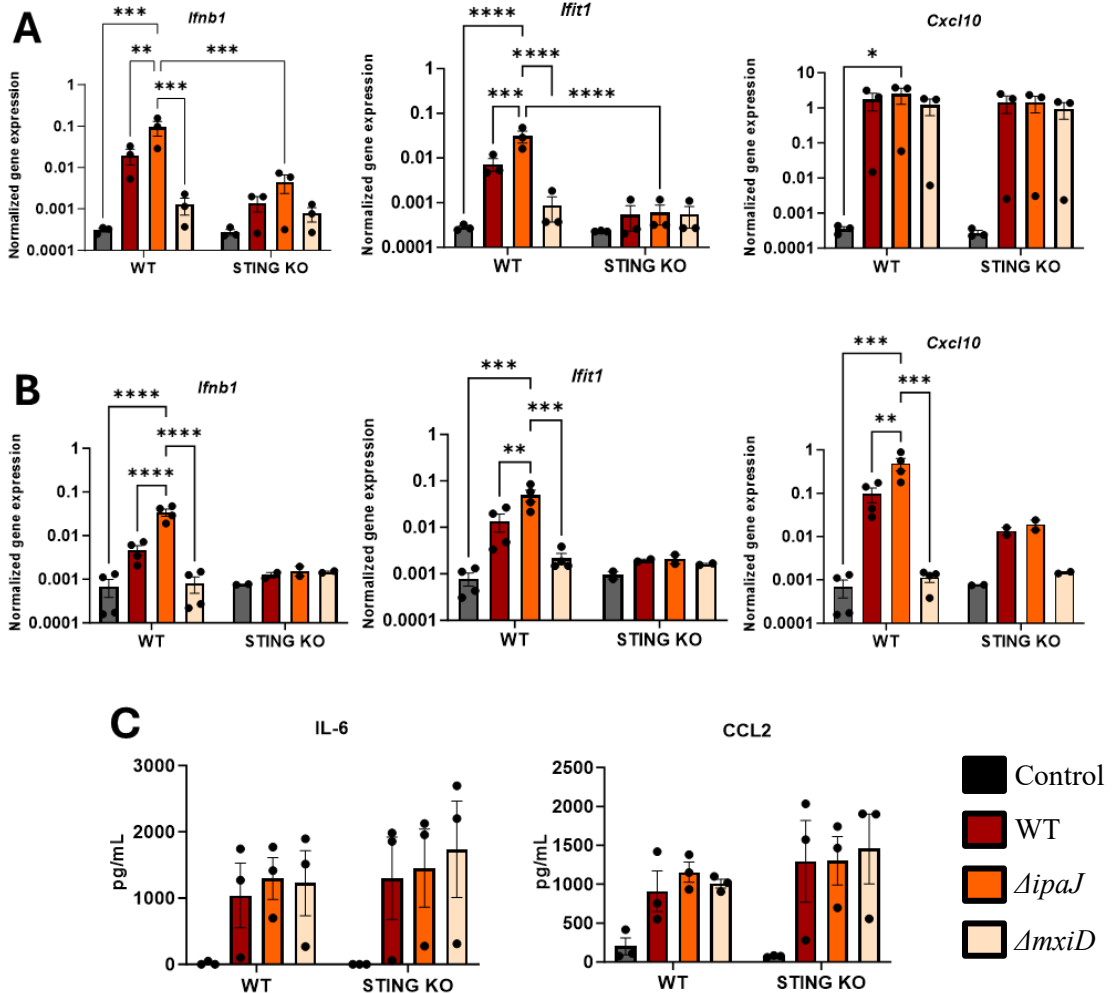


Figure 15. Murine mast cell type I IFN responses to *Shigella* infection are STING-dependent.

Wild-type C57BL/6 and STING KO (A) BMBCs and (B) PCMCs were infected with indicated *Shigella* strains at an MOI of 20 for 18 hours. Gene expression of type I IFNs and ISGs was measured using RT-qPCR and normalized to the geometric mean of housekeeping genes *Hprt* and *Gusb*. (C) Chemokines and cytokines were measured in the supernatant of infected BMBCs for 18 hours via ELISA. Statistical significance was determined by two-way ANOVA followed by a Tukey's multiple comparisons test. Data shown as mean \pm SEM. n = 3 per treatment condition. * $p < 0.05$; ** $p < 0.01$; *** $p < 0.001$; **** $p < 0.0001$.

Experiments were conducted to assess the kinetics of infection, with gene expression changes evaluated at 4, 8, and 18 hours post-infection (**Figure 16**). At the 4-hour timepoint, no significant IFN-related transcriptional changes were observed. However, upregulation of *Ifnb1* and *Ifit1* expression became significant at 8 hours and persisted through 18 hours, displaying the same trends previously observed (**Figure 16A and 16B**). The significant increase in *Ifnb1* and *Ifit1* gene expression in MCs infected with the IpaJ mutant, compared to WT *Shigella*, further suggests that STING plays a key role in mounting this response. Additionally, no changes in *Ifit1* and *Ifnb1* expression were observed in MCs infected with Δ mxiD *Shigella* at any timepoint, reinforcing the need of bacterial entry for inducing type I IFN expression. *Cxcl10* induction was also prominent at 8 hours and significantly increased by 18 hours, with similar expression levels across all three bacterial strains (**Figure 16C**). Moreover, earlier increases in *Il1b* expression were observed at 4 hours in MCs infected with all *Shigella* strains, suggesting that these changes were dependent on extracellular signaling (**Figure 16D**). *Il1b* is a key pro-inflammatory and protective cytokine in *Shigella* infection, and these findings imply that MCs may contribute to its production. Overall, these kinetic data highlight an early, STING-independent pro-inflammatory cytokine response by MCs, followed by a later induction of IFN-related transcripts that partially relied on STING signaling.

To determine if these outcomes are consistent in human cells, *Shigella* infections were conducted in CBMCs for 4 and 18 hours (**Figure 17**). Preliminary results reveal differences in responses compared to murine MCs. First, the upregulation of *IFIT1* expression was similar in CBMCs infected by all three bacterial strains (**Figure 17B**), suggesting that STING signaling or bacterial entry is not essential in this response. Given

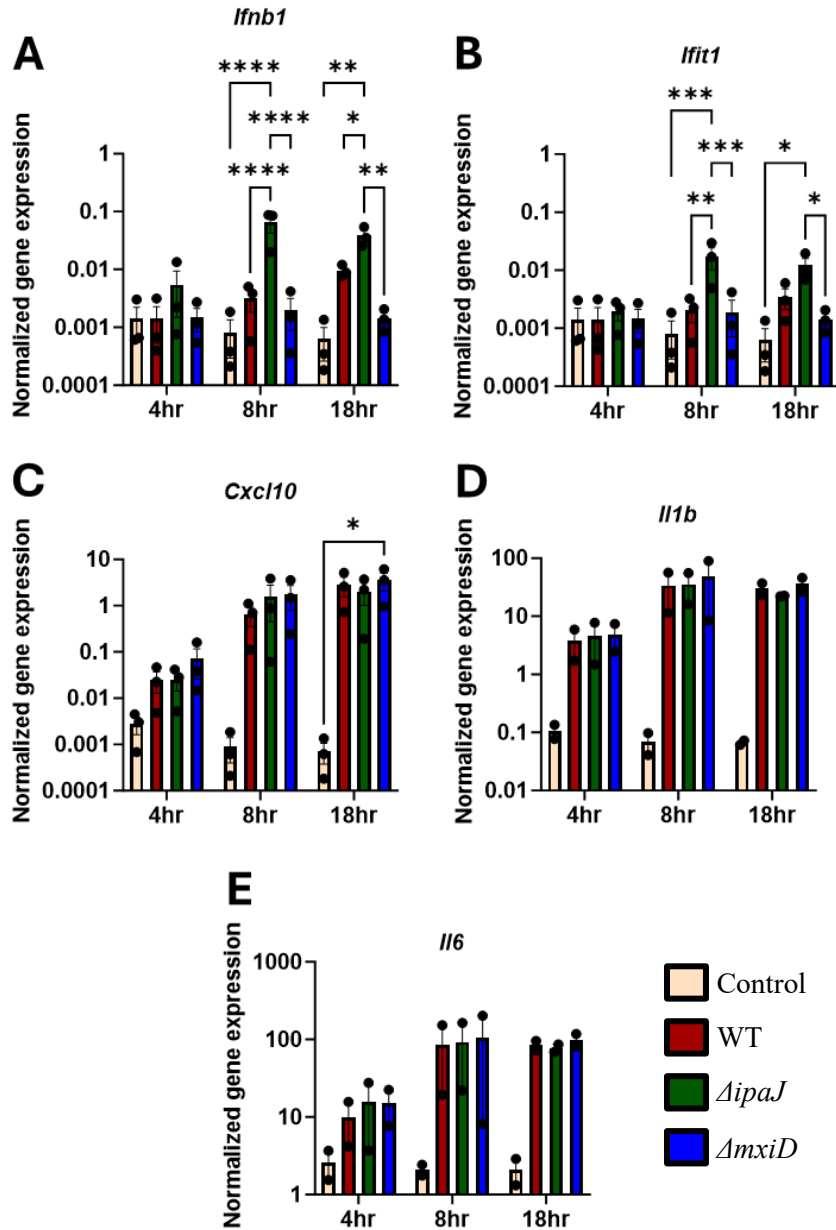


Figure 16. Kinetics of *Shigella* infection in murine mast cells.

Wild-type C57BL/6 BMDCs were infected with indicated *Shigella* strains at an MOI of 20 for 4, 8, or 18 hours. Gene expression of cytokines and ISGs was measured using RT-qPCR and normalized to the geometric mean of housekeeping genes *Hprt* and *Gusb*. Statistical significance was determined by two-way ANOVA followed by a Tukey's multiple comparisons test. Data shown as mean \pm SEM. n = 3 per treatment condition. * $p < 0.05$; ** $p < 0.01$; *** $p < 0.001$; **** $p < 0.0001$.

that transcript levels are comparable in MCs infected with the *mx1D* mutant, there may be an extracellular signal that is driving the type I IFN response in human MCs, a response that is less prominent in murine MCs. Similar findings were observed with *CXCL10* induction, which aligned with the responses seen in murine MCs (**Figure 17C**). In human MCs, *IFIT1* and *CXCL10* were upregulated at 4 hours, with transcript levels returning to baseline by 18 hours. In contrast, murine MCs exhibited significant gene induction only at 18 hours. These faster kinetics in human MCs may reflect the fact that bacterial entry is not required for activation, and extracellular signaling occurs more rapidly. More subtle differences were observed in the induction of *IFNB* and *CCL2* (**Figure 17A and 17D**). Overall, these data suggest that the activation mechanisms in human MCs differ from those in murine MCs. However, additional biological replicates are necessary to determine the statistical significance of these findings.

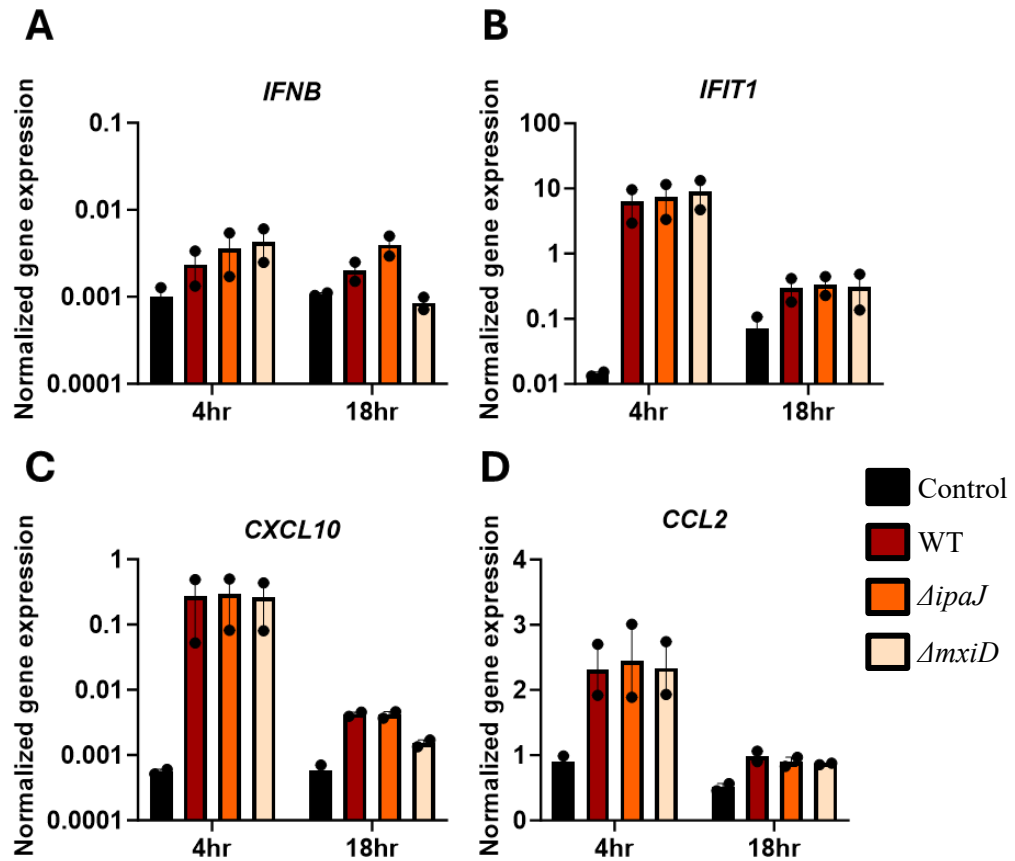


Figure 17. Human mast cells promote a STING-independent type I IFN response to *Shigella* infection.

CBMCs were cultured in activation media and infected with indicated *Shigella* strains at an MOI of 20 for 4 or 18 hours. Gene expression of type I IFNs, ISGs, and chemokines was measured using RT-qPCR and normalized to the geometric mean of housekeeping genes *HPRT* and *GUSB*. Data shown as mean \pm SEM. n=2 per treatment condition.

3.3 CHARACTERIZING THE EFFECT OF STING ACTIVATION ON IMMUNE RESPONSES *IN VIVO*

3.3.1 STING agonist (ADU-S100) dosing in C57BL/6 mice

STING activation is well described to enhance immune responses through the recruitment and activation of leukocytes. We aimed to assess the effects of MC STING activation in the context of cancer and whether MC-specific STING activation could boost *in vivo* immune responses. To achieve this, a baseline characterization of immune responses to STING agonist activation was first determined. Specifically, appropriate doses of STING agonist were established that could elicit a robust immune response *in vivo*, without causing adverse reactions. ADU-S100 was selected as the STING agonist for all subsequent animal studies, as it was more thoroughly characterized in our *in vitro* experiments (**Section 3.1**) and was shown to induce a stronger response in MCs compared to diABZI. The dosing of ADU-S100 was examined in 8-week-old female C57BL/6 mice. Intraperitoneal (i.p.) injections at 0.25 mg/kg, 0.75 mg/kg, or vehicle control (H₂O in PBS) were administered, and mice euthanized at 24 hours. Peritoneal lavages were collected to isolate circulating cells in the peritoneum. Mesenteric lymph nodes (mLNs) within the peritoneal cavity²⁴³ were collected to gauge T cell activation. These samples were used for gene expression and FACS analyses, where two panels were developed for acquisition to assess lymphoid and myeloid cells.

Mice treated with the agonist (both 0.25 mg/kg and 0.75 mg/kg) showed a significant increase in gene expression of *Cxcl10* and *Ifit1* in peritoneal cavity cells (**Figure 18A**). Similar trends in ISG expression were observed in mLNs (**Figure 18B**). These transcriptional changes infer that a type I IFN response was induced; however, type I IFN

gene expression was not detected at the 24-hour timepoint. Given the upregulation of downstream ISGs, it is possible that type I IFN responses were transient and occurred earlier than the time of analysis.

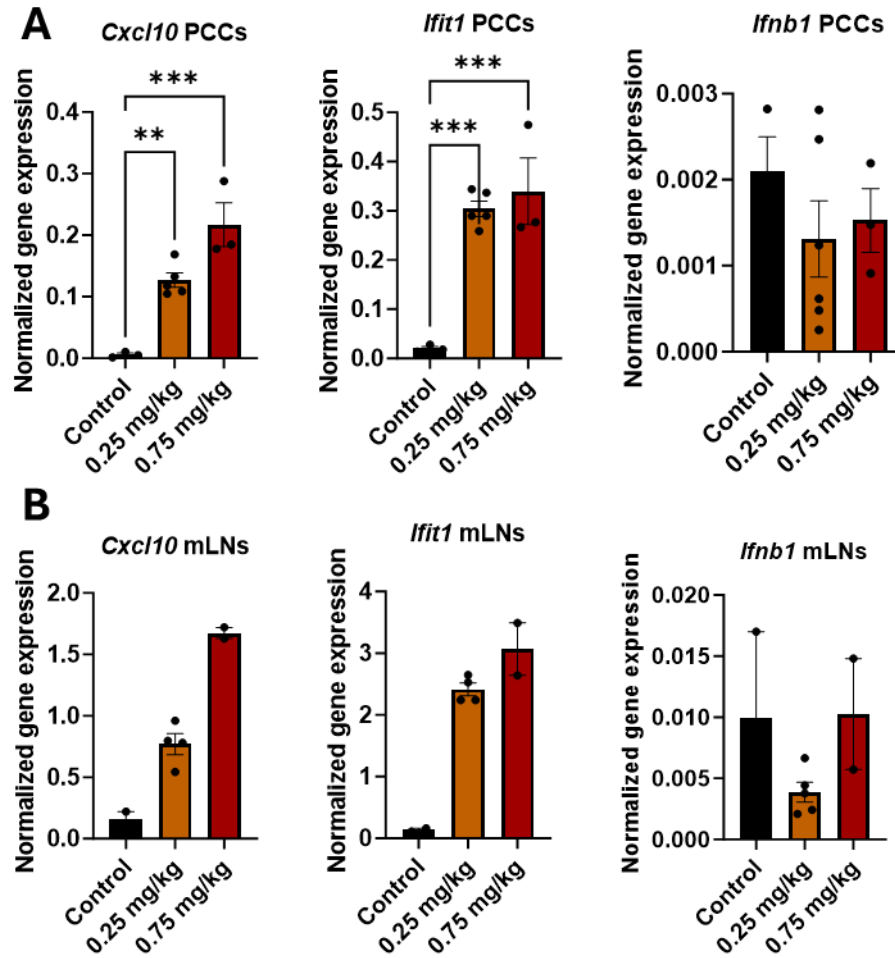


Figure 18. STING activation increases *Cxcl10* and *Ifit1* gene expression in peritoneal cells.

C57BL/6 mice were injected with ADU-S100 (0.25 mg/kg or 0.75 mg/kg) or vehicle control (H₂O in PBS) intraperitoneally (i.p.). Mice were sacrificed 24-hours post-injection to collect mesenteric lymph nodes (mLNs) and peritoneal cavity cells (PCCs) by lavage. Gene expression of *Ifnb1* and ISGs in (A) PCCs and (B) mLNs was measured using RT-qPCR and normalized to the geometric mean of housekeeping genes *Hprt* and *Gusb*. Statistical significance was determined by one-way ANOVA followed by a Dunnett's multiple comparisons test, comparing agonist treatment to control. Data shown as mean ± SEM. n=3-5 per treatment condition. ** $p < 0.01$; *** $p < 0.001$.

Flow cytometry analyses of the peritoneal cells were conducted to assess the infiltration and activation of immune cells in the peritoneum following STING agonist treatment. At 24 hours, ADU-S100 treatment resulted in a decrease in CD3⁺CD4⁺ T cell proportions and cell counts (**Figure 19A**), possibly suggesting migration out of the peritoneum. The proportion of CD8⁺ T cells within CD3⁺ cells was significantly increased with agonist treatment, possibly due to the departure of CD4⁺ T cells. Moreover, there were significant increases in the proportion of CD69 positive cells within both CD4⁺ and CD8⁺ populations, indicated early activation of T cells (**Figure 19A**). This T cell activation may be a result of direct stimulation by the agonist, as well as indirect activation by type I IFNs and other immune cells²⁰³.

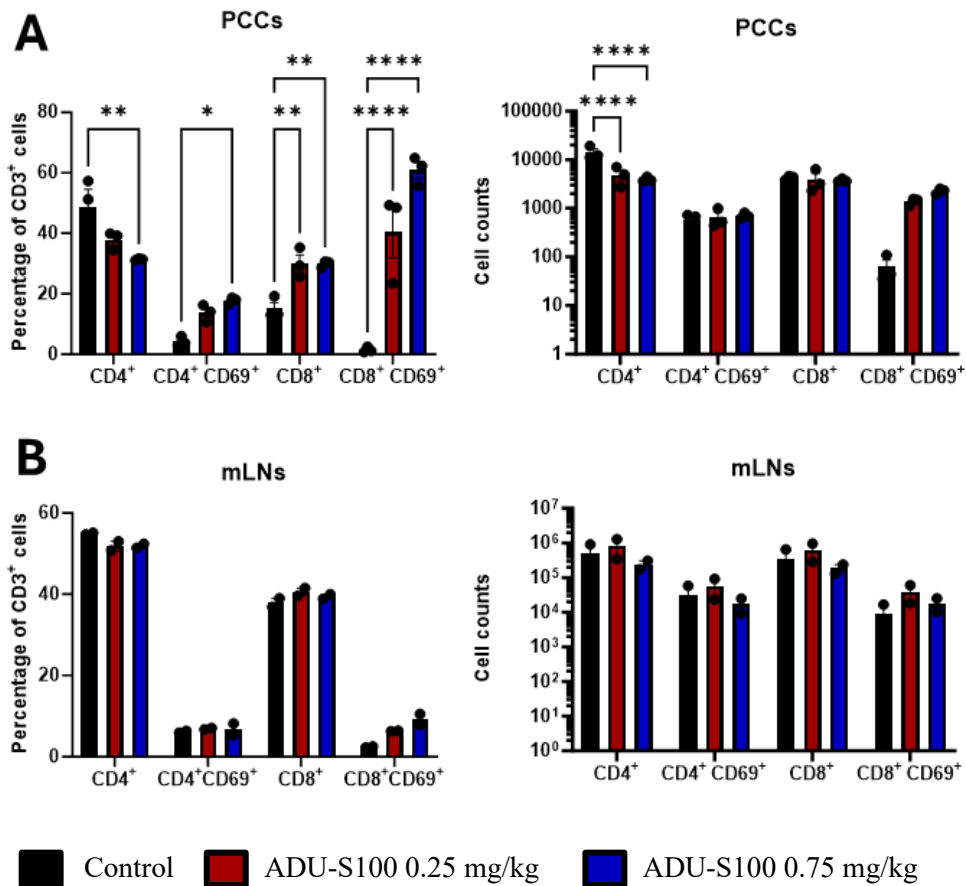


Figure 19. STING activation increases T cell activation in the peritoneum.

C57BL/6 mice were injected (i.p.) with ADU-S100 (0.25 mg/kg or 0.75 mg/kg) or vehicle control (H₂O in PBS). Mice were sacrificed 24-hours post-injection to collect mLNs and PCCs by lavage. Cells were stained with antibodies probing for markers in Panel 1 (**Table 4**) and fixed in 1% PFA to analyze lymphoid immune cell proportions in the peritoneum and mLNs by flow cytometry. Percentages of T cells from CD3⁺ cells and total cell counts in (**A**) PCCs and (**B**) mLNs are displayed. Statistical significance was determined by two-way ANOVA followed by a Dunnett's multiple comparisons test, comparing agonist treatment to control, within each population. Data shown as mean ± SEM. n=2-5 per treatment condition. **p* < 0.5; ***p* < 0.01; *****p* < 0.0001.

Analysis of the mLNs demonstrated no differences in T cell populations (**Figure 19B**), which may be due to the 24-hour time point being too early to detect noticeable differences, or that peritoneal cavity lymphatic drainage to this site was limited. Other lymph nodes within the peritoneal cavity, such as the celiac and periportal lymph nodes, or the mediastinal nodes might exhibit differences²⁴³. Since similar immune responses were observed and no significant differences were observed between the 0.25 mg/kg and 0.75 mg/kg doses of ADU-S100, 0.25 mg/kg was used for the subsequent experiments.

3.3.2 STING agonist (ADU-S100) kinetics in C57BL/6 mice

Since type I IFN gene expression was not detected at 24 hours, an *in vivo* kinetics response was performed, and immune responses investigated at 1, 2, 4, and 6 hours post-agonist injection. Gene expression of *Ifnb1* peaked at 1 hour, whereas *Ifna1*, *Ifna2*, *Ifna6* were significantly increased at 2 hours in peritoneal cavity cells of agonist-treated mice compared to vehicle control (**Figure 20**). The expression of type I IFNs was diminished by 4 hours with mRNA levels comparable to control-treated mice, a finding that is consistent with the rapid kinetics reported in the literature²⁴⁴. The transcript levels of ISGs, *Cxcl10* and *Ifit1*, were significantly upregulated at 2 hours and remained high at 6 hours.

Interestingly, there was increase in the transcription of *Il-28*, a type III interferon (IFN- λ 3), 6 hours post ADU-S100 administration (**Figure 20**). This could be a result of crosstalk between type I and type III IFN signaling^{244,245} or direct induction of type III IFN gene expression by STING²⁴⁶.

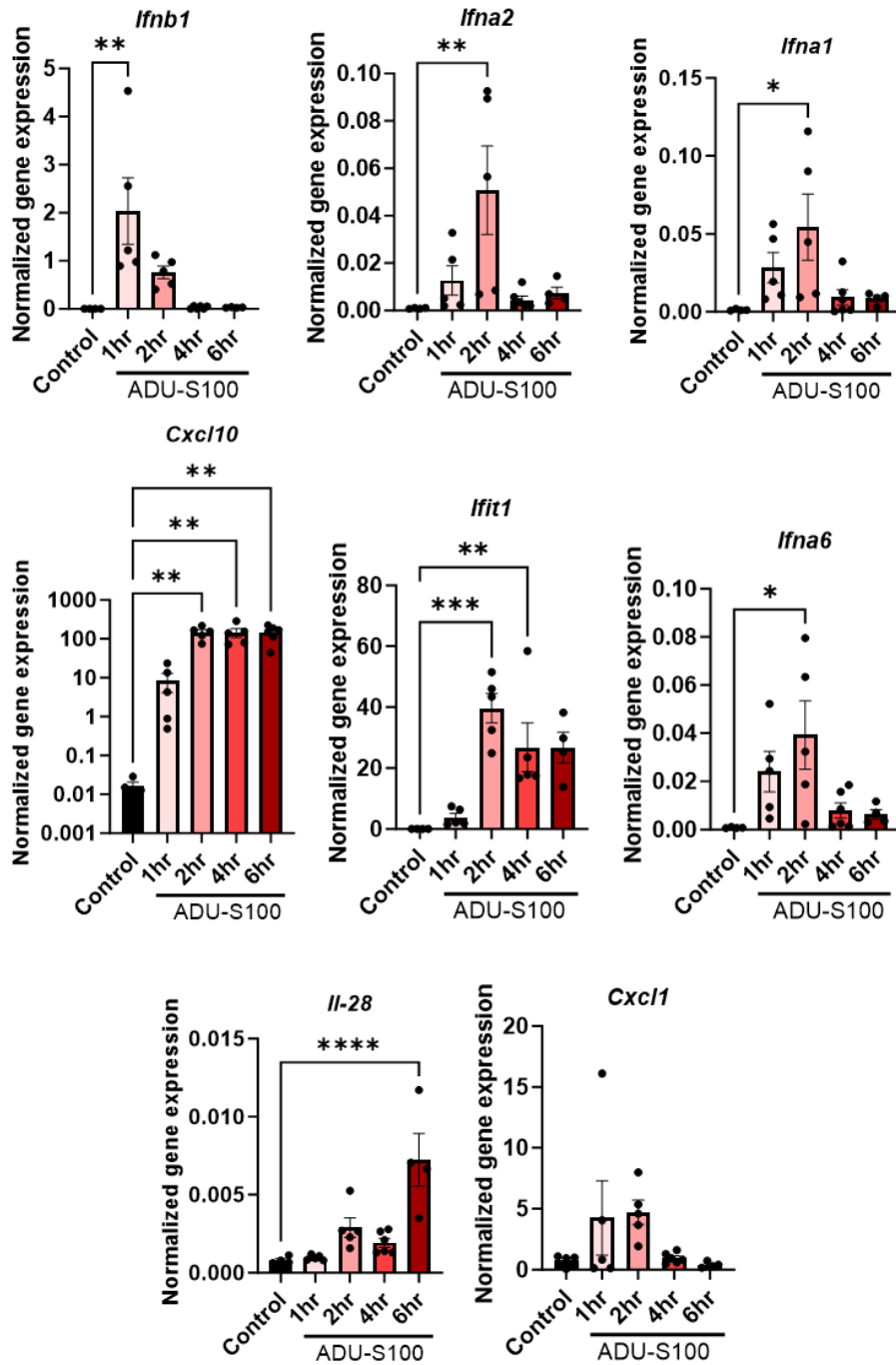


Figure 20. STING activation promotes transient increases in type I IFN-related transcriptional changes in peritoneal cells.

C57BL/6 mice were injected (i.p) with ADU-S100 (0.25 mg/kg) or vehicle control (H₂O in PBS). Mice were sacrificed at 1-, 2-, 4-, and 6-hours post-injection to collect peritoneal cells by lavage. Gene expression of IFNs, ISGs, and chemokines in peritoneal cells was measured using RT-qPCR and normalized to the geometric mean of housekeeping genes *Hprt* and *Gusb*. Statistical significance was determined by one-way ANOVA followed by a Dunnett's multiple comparisons test, comparing agonist treatment to control, at each timepoint. Data shown as mean \pm SEM. n = 4–5 per treatment condition. * $p < 0.05$; ** $p < 0.01$; *** $p < 0.001$; **** $p < 0.0001$.

Supernatants from the peritoneal washes were used for a Luminex assay to evaluate immune mediators at the protein level (**Figure 21**). At 2 hours, ADU-S100 treatment resulted in a significant increase in IFN- α and IFN- β production compared to vehicle-treated mice (**Figures 21D, E**). These IFNs were not observed at later time points (4 and 6 hours), possibly due to cellular uptake and protein degradation. This fleeting IFN response coincided with the gene expression data. CXCL10 production was observed at 2- and 4-hours following agonist injections (**Figure 21A**). CXCL10 is a cytokine produced downstream of type I IFNs that is important for the trafficking T cells and NK cells²⁰⁹. IL-6, a mediator downstream of NF- κ B activation, was also elevated at 2 hours (**Figure 21C**). There was also significant CXCL1 protein production at 2 hours post-ADU-S100 injection (**Figure 21B**), which may have contributed to the increase in neutrophil recruitment²⁴⁷ observed in flow cytometry data (**Figure 22**). Overall, these results indicate that STING activation rapidly activates innate and adaptive immunity through gene expression changes and mediator production. These findings corroborate immune-boosting effects of STING that is described in literature²⁰⁹.

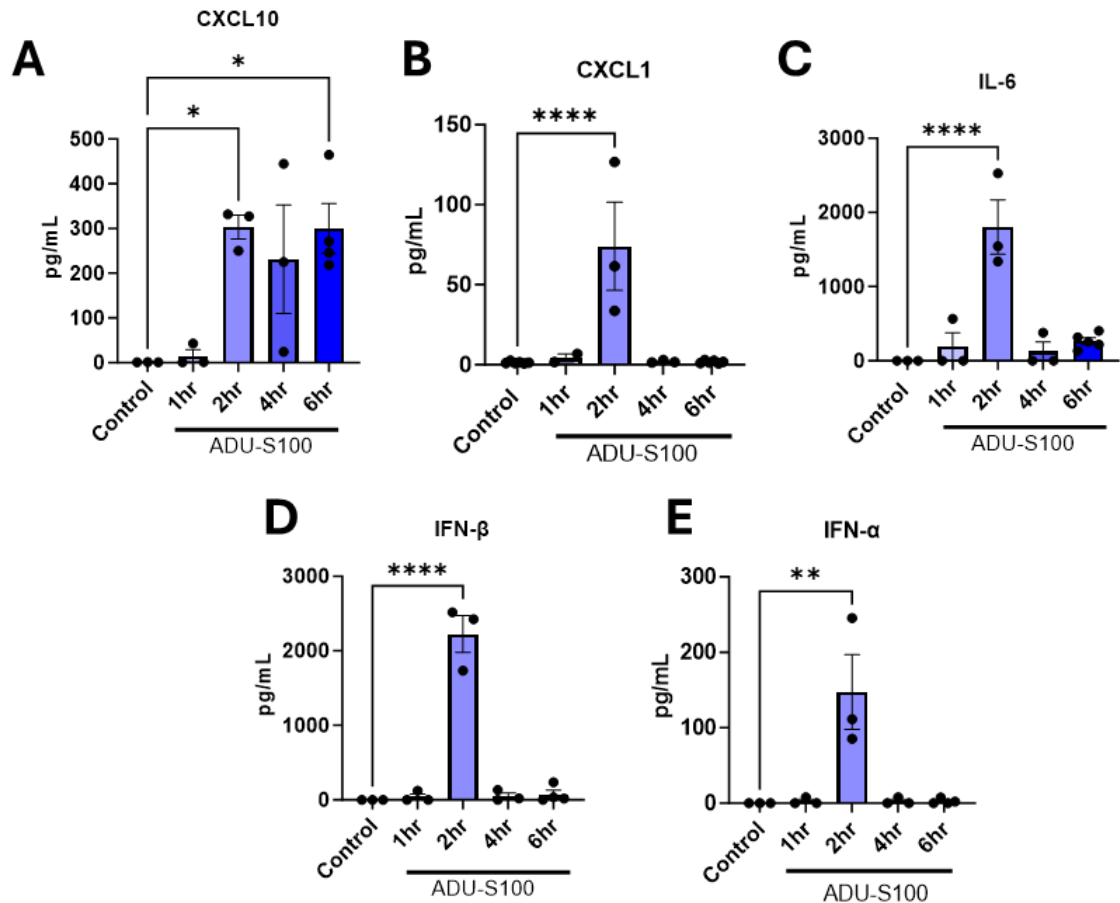


Figure 21. STING activation promotes the production of type I IFNs, CXCL10, CXCL1, and IL-6 by peritoneal cells.

C57BL/6 mice were injected (i.p.) with ADU-S100 (0.25 mg/kg) or vehicle control (H₂O in PBS). Mice were sacrificed at 1-, 2-, 4-, and 6-hours post-injection to collect peritoneal lavages. Protein levels of IFN-β, IFN-α, CXCL10, CXCL1, and IL-6 in the lavage were measured by Luminex. Statistical significance was determined by one-way ANOVA followed by a Dunnett's multiple comparisons test, comparing agonist treatment to control, at each timepoint. Data shown as mean ± SEM. n = 2–5 per treatment condition. **p* < 0.05; ***p* < 0.01; *****p* < 0.0001.

At the cellular level, following STING agonist administration, there were decreases in the counts and proportions of CD11b^{hi}F4/80^{hi} cells starting at 2 hours in mice treated with agonist compared to those given vehicle control. This suggested a decrease in resting and naïve peritoneal macrophages, which may be activated and exit the peritoneum (**Figure 22A and 22B**). At 2 hours, there was a transient increase in neutrophil cell counts (**Figure**

22A). A rise in CD4⁺ T cell counts was also observed at 2 hours (**Figure 23A**), which may be explained by recruitment associated with the production of CXCL10 detected in the peritoneal wash. The proportions of activated T cells (CD69⁺) within both the CD4⁺ and CD8⁺ populations were elevated at 6 hours (**Figure 23A**). However, no significant changes in B cell or NK cell infiltration were observed (**Figure 23B**). This may be dependent on the type, dose, or context in which the STING agonist used.

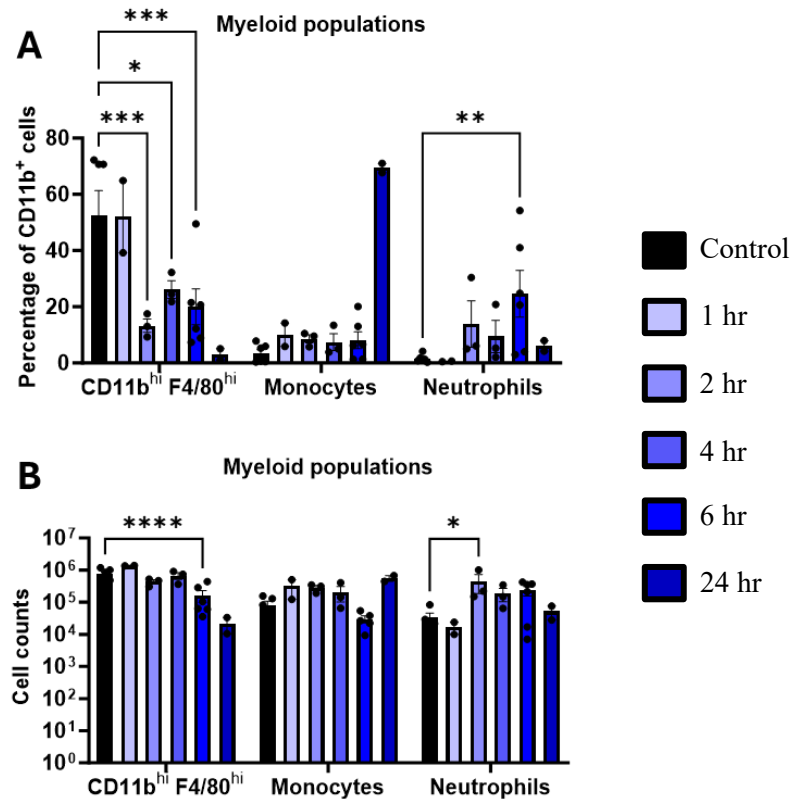


Figure 22. STING activation increases macrophage activation and neutrophil infiltration *in vivo*.

C57BL/6 mice were injected (i.p.) with ADU-S100 (0.25 mg/kg) or vehicle control (H₂O in PBS). Mice were sacrificed at 1-, 2-, 4-, 6- and 24-hours post-injection to collect peritoneal cells by lavage. Cells were stained with Panel 2 (**Table 5**) and fixed in 1% PFA to analyze innate immune cell proportions in the peritoneum by flow cytometry. (**A**) Percentages of myeloid cells from CD11b⁺ cells and (**B**) total cell counts are displayed. Statistical significance was determined by two-way ANOVA followed by a Dunnett's multiple comparisons test, comparing agonist treatment to control, at each timepoint, for each immune population. Data shown as mean \pm SEM. n=2-6 per treatment condition. * $p < 0.5$; ** $p < 0.01$; *** $p < 0.001$; **** $p < 0.0001$.

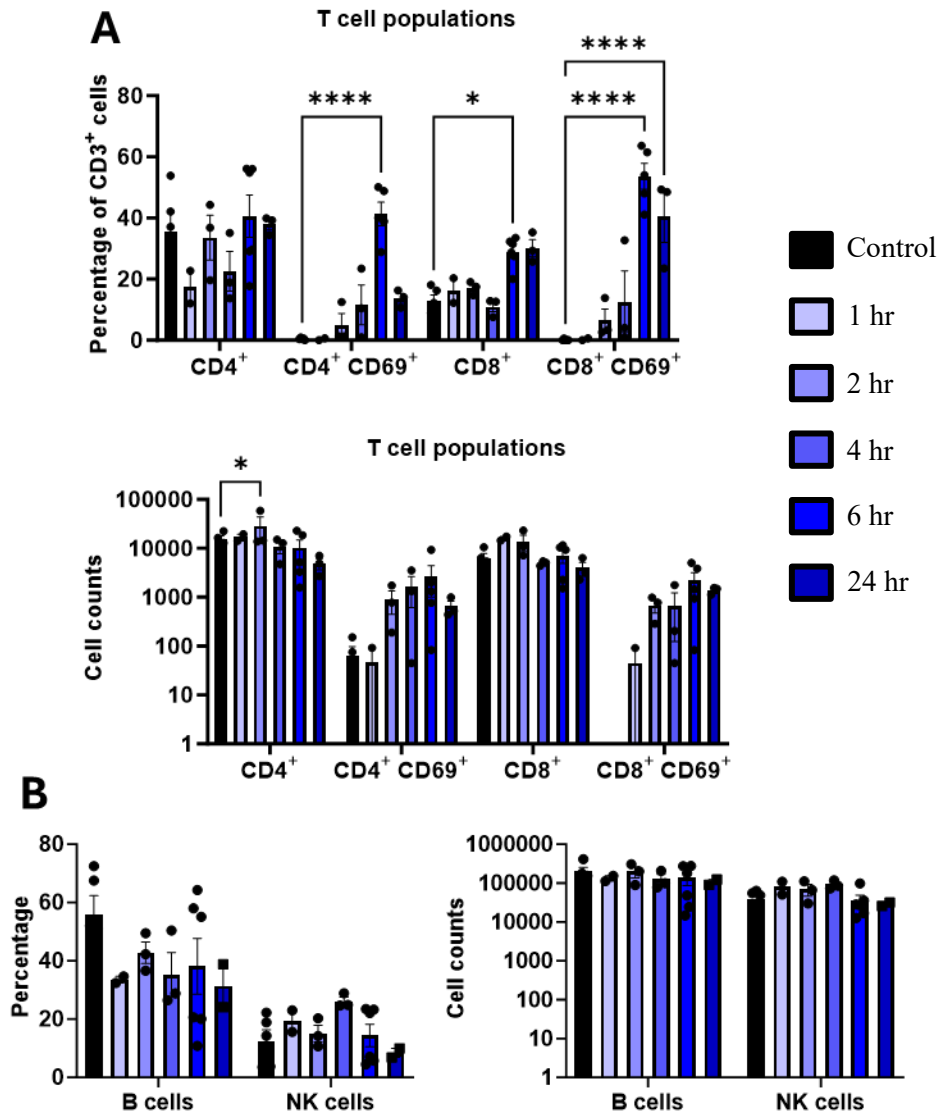


Figure 23. STING agonist treatment increases T cell activation *in vivo*.

C57BL/6 mice were injected (i.p.) with ADU-S100 (0.25 mg/kg) or vehicle control (H₂O in PBS). Mice were sacrificed at 1-, 2-, 4-, 6- and 24-hours post-injection to collect peritoneal cells by lavage. Cells were stained with Panel 1 (Table 4) and fixed in 1% PFA to analyze lymphoid immune cell proportions in the peritoneum by flow cytometry. Percentages of parent populations and total cell counts are shown of (A) T cells, (B) B cells, and NK cells. Statistical significance was determined by two-way ANOVA followed by a Dunnett's multiple comparisons test, comparing agonist treatment to control, at each timepoint, for each immune population. Data shown as mean \pm SEM. n=2-6 per treatment condition. * $p < 0.5$; **** $p < 0.0001$.

3.3.3 Assessing STING activation kinetics in mast cell-deficient mice

To determine the role of MCs in STING activation *in vivo*, the response to ADU-S100 in MC-deficient mice (*Cpa3-Cre; Mcl-1^{fl/fl}*, HK) was compared to their WT counterparts (HKLM). Mice were injected intraperitoneally with ADU-S100 (0.25 mg/kg) or vehicle control and peritoneal lavages collected at 1-, 2-, and 6-hour post-agonist treatment. At the gene expression level, *Il6* was higher in HKLMs at 2 hours which may suggest a pro-inflammatory role of MCs in response to STING activation (**Figure 24B**). No significant differences were observed in the transcription of *Ifnb1*, *Ifna6*, or *Ifna1* between mouse groups (**Figures 24C, E, F**). Since there are several immune and non-immune cells responding, MCs may be dispensable in the IFN response to STING activation at physiological levels. As a result, no differences were seen in the induction of *Ifit1*, which is downstream (**Figure 24D**). At the 2-hour timepoint, *Cxcl10* gene expression is higher in HKLMs, which may indicate that MCs play an important role in the production of the chemokine. To summarize, MCs may have a selective role in the gene expression of mediators in response to STING activation.

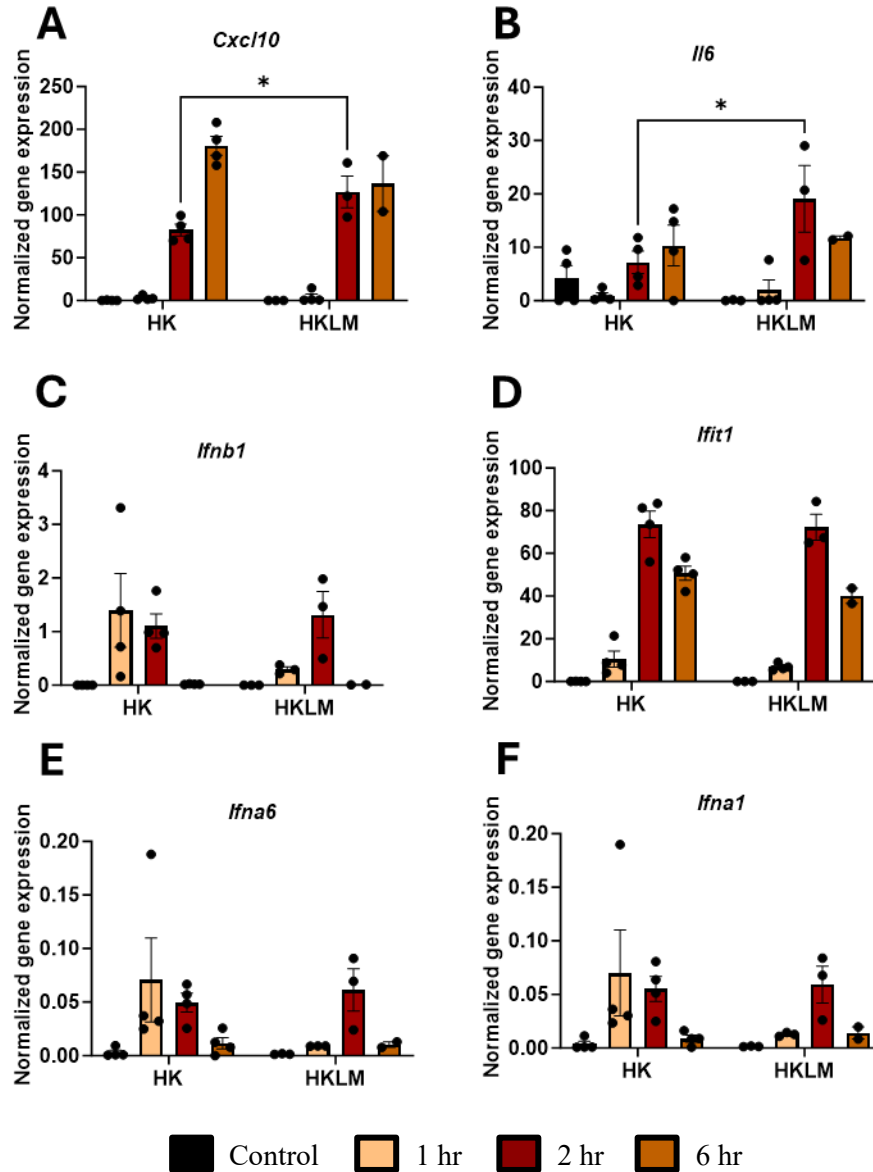


Figure 24. Mast cells play a selective role in transcriptional changes in response to STING activation *in vivo*.

MC-deficient mice (HK) and their wild-type counterparts (HKLM) were injected (i.p.) with ADU-S100 (0.25 mg/kg) or vehicle control (H₂O in PBS). Peritoneal cavity cells were isolated from peritoneal lavages at 1-, 2-, and 6-hours post-agonist treatment. Gene expression of type I IFNs and ISGs was measured using RT-qPCR and normalized to the geometric mean of housekeeping genes *Hprt* and *Gusb*. Statistical significance was determined by two-way ANOVA followed by a Dunnett's multiple comparisons test, comparing gene expression in HKs to HKLMs at each timepoint. Data shown as mean \pm SEM. n = 3-4 per treatment condition. * $p < 0.05$.

3.4 THE ROLE OF STING AGONIST THERAPY IN THE ID8 MODEL

3.4.1 ID8 survival in wild-type mice with STING agonist therapy

STING agonist therapy has been described to have therapeutic potential in the treatment of ovarian cancer. Studies have showed improved survival of murine ovarian cancer models with STING agonist therapy as a monotherapy or in combination with other targeted therapies^{248,249}. To confirm this in our model, wild-type mice (HK littermate controls) were intraperitoneally injected with ID8 ovarian cancer cells and a regimen of STING agonist ADU-S100 (0.25 mg/kg) or vehicle control (H₂O in PBS) starting at day 15 (**Figure 25A**). Mice were administered 3 doses, 3 days apart, as established by other researchers²⁴⁸, and monitored until endpoint for up to 100 days. Intraperitoneal administration of ID8 cells establishes a disseminated ovarian cancer model characterized by the formation of ascites, which resembles the cancer stage at diagnosis in most women^{234,250}. This approach is also particularly beneficial for studying MCs, as they are widely distributed throughout the peritoneum²⁵¹. Ascites development and endpoint is expected to develop around 35 to 40 days post-injection in untreated mice. We determined that mice treated with ADU-S100 exhibited longer survival times, with a median survival of 48 days, which was statistically significant compared to vehicle-treated mice that had a median survival of 40.5 ($p = 0.0264$) (**Figure 25B**). These results reinforce the therapeutic potential of STING agonist therapy in ovarian cancer.

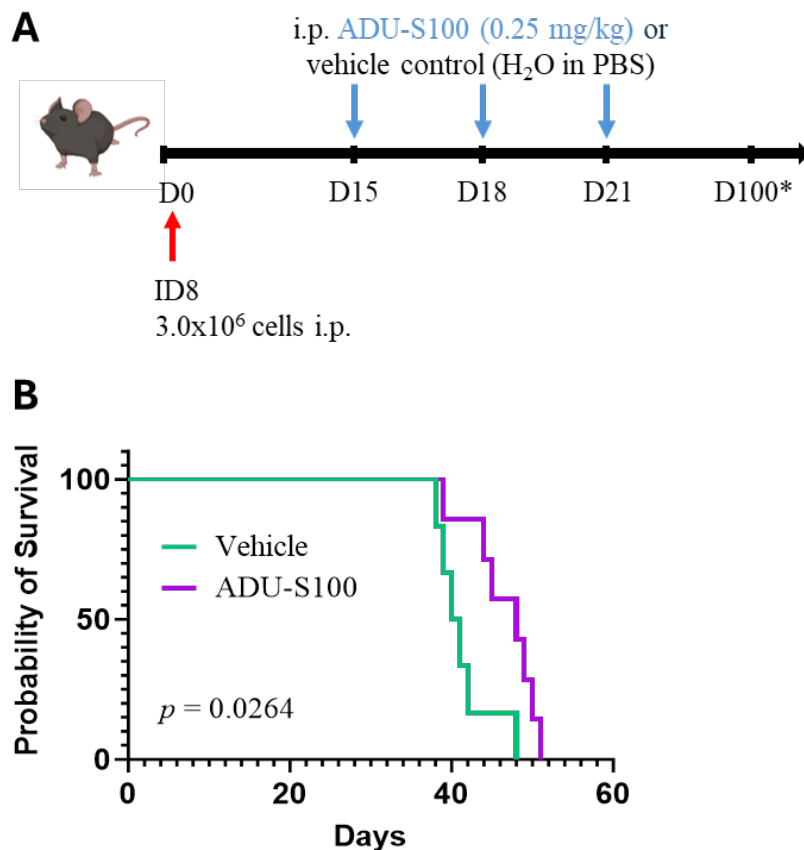


Figure 25. STING agonist therapy improves overall survival in the ID8 murine ovarian cancer model.

Wild-type mice (Hello Kitty littermate controls) were injected (i.p.) with 3.0x10⁶ ID8 cells, treated with ADU-S100 (0.25 mg/kg) or vehicle control (H₂O in PBS), and monitored until endpoint for up to 100 days. **(A)** A summary of experimental design to study the effect of STING agonist therapy in the treatment of the ID8 ovarian cancer model is shown. **(B)** Overall survival is represented through Kaplan-Meier survival curves. A Log-Rank (Mantel-Cox) Test was used to assess statistical significance between groups. n= 6-7 per treatment group.

3.5 THE ROLE OF MAST CELLS IN STING AGONIST EFFICACY IN THE ID8 MODEL

3.5.1 Survival of the ID8 model in MC-deficient mice

The impact of MCs on ovarian cancer growth and prognosis remains to be elucidated, with literature highlighting both detrimental and beneficial roles^{252–255}. However, studies that characterize the role of MCs in the ID8 ovarian cancer model are limited. To further investigate, two MC-deficiency models were used to evaluate the role of MCs on the overall survival of the ID8 model.

We initially utilized the Hello Kitty (HK) MC-deficiency model to assess the impact of MCs on survival at baseline. The overall survival was compared between vehicle-treated HK mice and their wild-type counterparts (HK littermates) as outlined in **Figure 26A**. Interestingly, HK mice survived significantly longer than wild-type littermates ($p = 0.0393$) (**Figure 26B, left**). To confirm MC-deficiency, gene expression levels of tryptase (*Tpsb2*) expression were determined in peritoneal cavity cells isolated at endpoint. Tryptase is an abundant serine protease found in MC granules and is mainly produced by MCs¹⁶. There were significantly higher transcript levels of *Tpsb2* in wild-type littermate controls compared to an absence in HKs, which confirms the depletion of MCs in HKs (**Figure 26B, right**). A similar trend was observed with the *Wsh* MC-deficient strain, where *Wsh* mice exhibited improved survival compared to in-house bred C57BL/6 mice (**Figure 26C**); however, further studies with additional mice are needed to determine statistical significance. Overall, these results suggest that MCs are detrimental in the ID8 ovarian cancer model.

To confirm that this phenotype of prolonged survival is due to the absence of MCs, adoptive transfers were performed. Mature MCs derived from wild-type bone marrow were injected into the peritoneum of MC-deficient mice. The MCs were allowed to reconstitute for four weeks to allow for establishment into the peritoneal cavity and phenotypic adaptation to the environment^{256,257}, prior to ID8 injections. To ensure successful reconstitution of the peritoneal cavity, we assessed *Tpsb2* expression levels and determined that reconstituted mice (R. HKs) had similar expression levels to wild-type littermate controls. This suggests that reconstitution led to similar quantities of MCs seen in the wild-type controls (**Figure 26B, right**). We assessed whether the survival of these reconstituted mice (R. HKs) would be similar to the wild-type controls. Interestingly, we observed that R. HKs have significantly improved survival compared to the wild-type littermates and do not recapitulate their survival trend ($p = 0.0038$). Instead, R. HK exhibit prolonged survival compared to MC-deficient mice as well, rather than worsened ($p = 0.0038$) (**Figure 26B, left**). This contradicts the previous findings that MCs are detrimental. These differences may be attributed to several factors, including variations in MC localization within the peritoneum following reconstitution, and will be discussed in later sections.

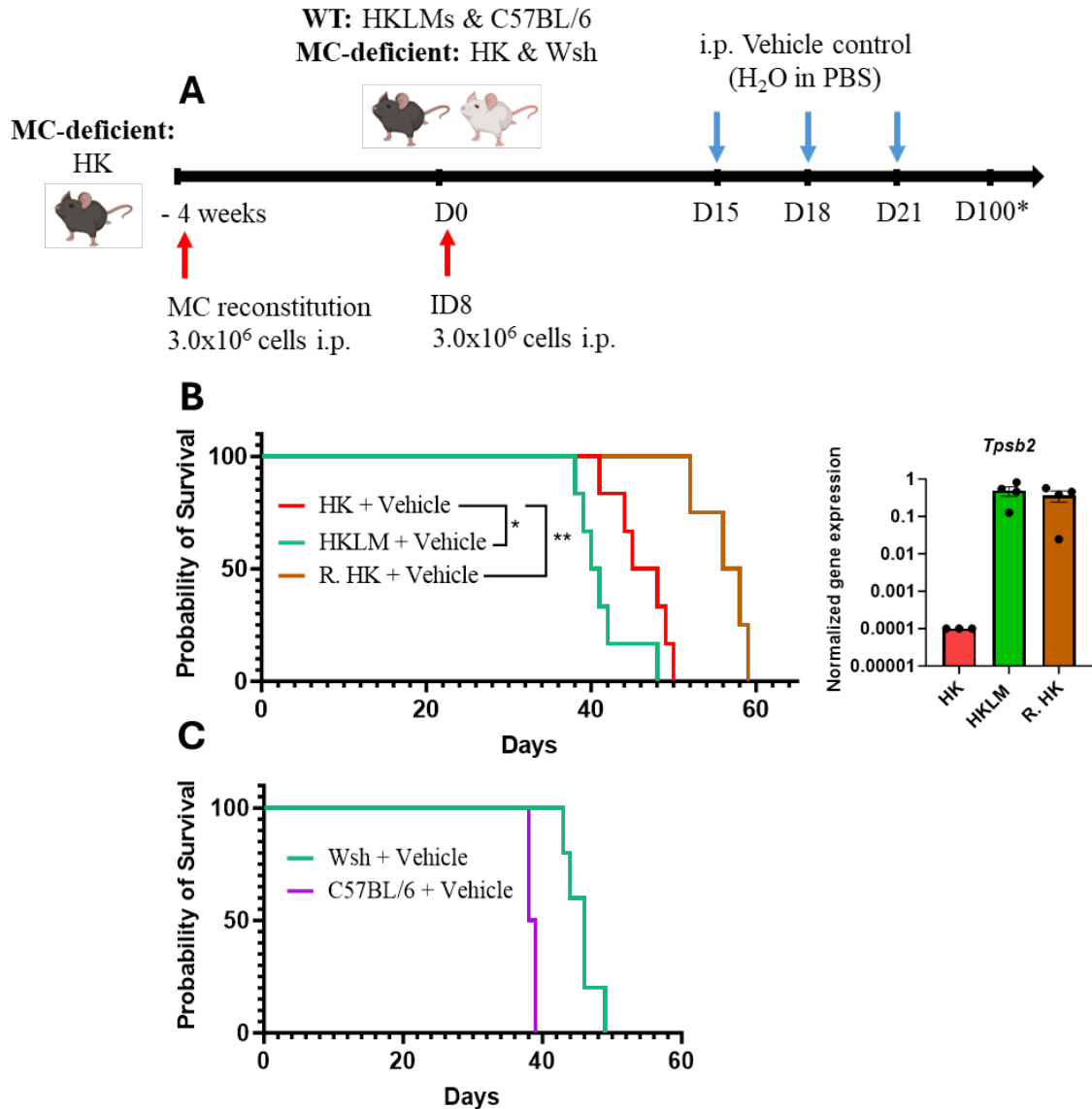


Figure 26. Mast cells influence the overall survival of the ID8 ovarian cancer model.

Wild-type MCs were adoptively transferred into MC-deficient mice (HK) and allowed to reconstitute for 4 weeks. MC-deficient mice, wild-type counterparts, and reconstituted mice were injected (i.p.) with ID8 ovarian cancer cells, treated with vehicle control, and monitored until endpoint for up to 100 days. **(A)** A summary of experimental design to study the role of MCs in the survival of the ID8 ovarian cancer model is shown. Kaplan-Meier survival curves of **(B, left)** HKs, R.HK and **(C)** Wsh mice compared to wild-type counterparts are shown. A Log-Rank (Mantel-Cox) Test was used to assess statistical significance between groups. **(B, right)** Gene expression of *Tpsb2* in PCCs was measured using RT-qPCR and normalized to reference genes *Hprt* and *Gusb*. Statistical significance was determined by one-way ANOVA followed by Tukey's multiple comparison test. Data shown as mean \pm SEM. n= 2-6 per treatment group.

3.5.2 The role of mast cells in STING agonist therapy on the survival of the ID8 model

To define the role of MC-specific STING activation in a cancer setting, we examined STING agonist efficacy in the treatment of the ID8 model in the presence and absence of MCs. MC-deficient mice (HKs) and littermates (HKLMs) were injected with ID8 cells and the previously described dosing regimen of STING agonist or vehicle control (**Figure 27A**). This would determine if the presence of MCs influences the immune response mounted to STING agonist therapy and whether it provides a survival advantage.

Consistent with our findings in **Section 3.4.1**, HK mice treated with the STING agonist survived significantly longer than HK mice treated with vehicle control ($p = 0.0023$) (**Figure 27B**), demonstrating that the efficacy of STING agonist therapy is consistent in the MC-deficient mice. More interestingly, the HK mice treated with STING agonist exhibited longer survival, with a median survival of 54 days, compared to the HKLMs treated with agonist that had a median survival of 48 days ($p = 0.0026$) (**Figure 27C**). This suggests there may be an immunomodulatory role for MCs that hinders the efficacy of STING agonist therapy. Once again, reconstituted HK mice were used to evaluate whether this result was MC-specific. The survival of R. HK mice treated with STING agonist did not significantly differ compared to the HK or HKLM mice ($p = 0.1206$, $p = 0.0688$, respectively) that were treated with STING agonist (**Figure 27C**). However, the significantly higher levels of *Tpsb2* detected in R.HK mice compared to wild-type littermates ($p = 0.0040$) suggests that there may be higher numbers of MCs in the former, thus skewing these results. Overall, these reconstituted mice do not recapitulate the survival

trend seen in the wild-type mice (HKLMs) and further experiments with more mice are needed to evaluate this.

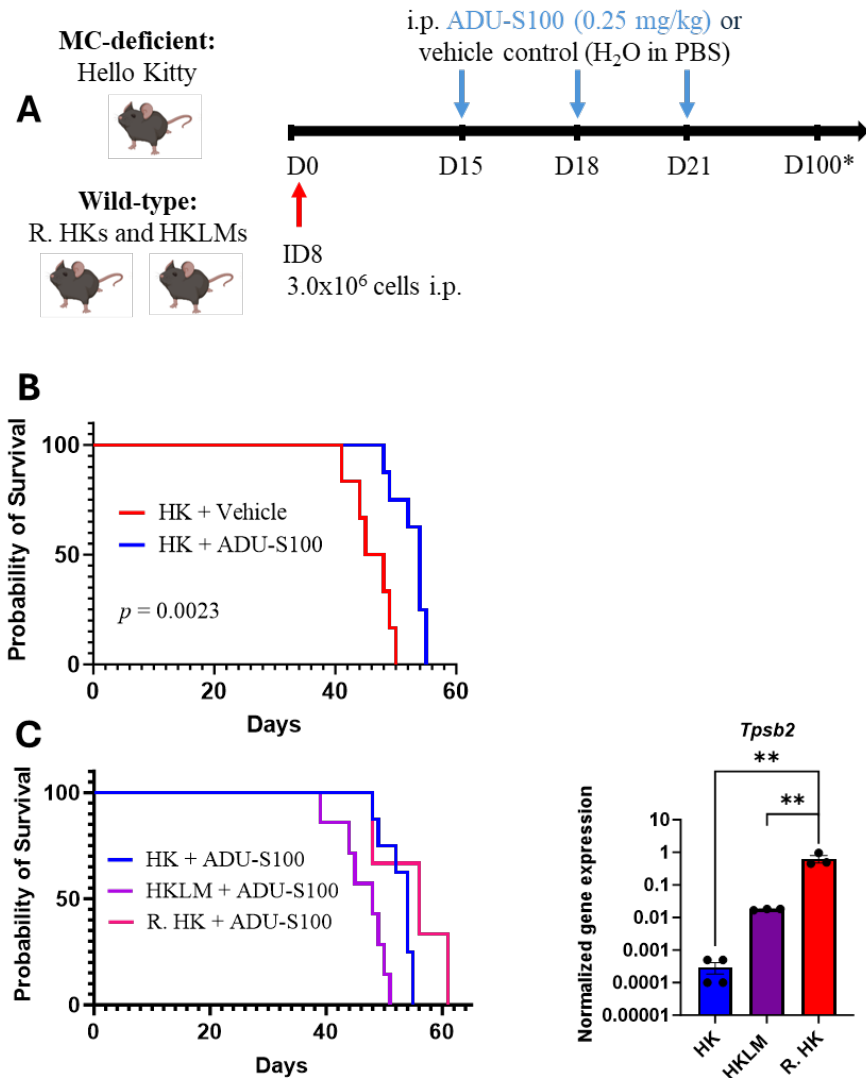


Figure 27. Mast cells do not provide a survival advantage with STING agonist therapy in the ID8 ovarian cancer model.

Wild-type MCs were adoptively transferred into MC-deficient mice (HK) and allowed to reconstitute for 4 weeks. Reconstituted HKs (R. HK), HKs, and littermate controls (HKLM) were injected (i.p.) with ID8 cells, treated with i.p. STING agonist ADU-S100 or vehicle control, and monitored until endpoint for up to 100 days. **(A)** An experimental timeline for ID8 ovarian cancer cell administration and STING agonist treatment is shown. **(B and C, left)** Kaplan-Meier survival curves of mice given are shown. A Log-Rank (Mantel-Cox) Test was used to assess statistical significance between groups. **(C, right)** Gene expression of *Tpsb2* in PCCs was measured using RT-qPCR and normalized to reference genes *Hprt* and *Gusb*. Statistical significance was determined by one-way ANOVA followed by Tukey's multiple comparison test. Data shown as mean \pm SEM. $n=3-7$ per treatment group. $**p < 0.01$

3.6 GENETIC MODIFICATION OF BMMCS BY TRANSDUCTION WITH LENTIVIRUSES EXPRESSING WILD-TYPE STING AND STING MUTANTS

Adoptive transfers of genetically modified immune cells have emerged as a novel strategy for treating diseases, particularly in cancer therapy. We focused on enhancing the STING pathway in MCs as a model for immunotherapy. This approach was particularly attractive given the widespread distribution of MCs throughout the body, their ability to produce a variety of potent mediators, and their long lifespan. Our goal was to establish a system for both inducible and constitutive activation of the STING pathway, which enables precise control over the production of inflammatory cytokines and chemokines. This would allow us to harness therapeutic benefits while preventing harmful overproduction. To achieve this, we used Tetracycline-On (Tet-on) lentiviruses expressing either wild-type STING (WT) or constitutively active mutants (V154M, N153S) for transductions. These STING mutants are well-characterized in the literature, with mouse models demonstrating phenotypes linked to constitutive activation^{117,258}, as discussed in **Section 1.3.4**. In the presence of doxycycline (DOX), a tetracycline-related antibiotic, the genes of interest are transcribed and expressed in the cells. As a control, we used lentiviruses expressing GFP, enabling us to assess the efficiency of transduction and ensure that any observed changes are due to the inserted genes rather than the lentiviral construct itself. Lentivirus was produced by standard molecular biology techniques using the pLJM1 lentiviral vector, as described in **Section 2.5** of the Materials and Methods.

This lentiviral transduction system, established by Dr. Ian Haidl, has been successfully applied in our lab to modify MCs to overexpress IFN α 1, which led to significantly increased survival in a mouse model of ovarian cancer. STING activation

would potentially induce the production of a broader range of type I IFNs, in addition to NF- κ B induced genes, thus was examined to see if it induced a more robust therapeutic response.

3.6.1 Testing induction of target genes and protein production in U-2 OS cells *in vitro*

To evaluate the functionality of these constructs, we first transduced U-2 OS cells, an osteosarcoma cell line known for its high transduction efficiency and expression of rtTA (reverse tetracycline-controlled transactivator). Gene expression of STING (*Tmem173*) was assessed at 24-, 48-, and 72-hours following DOX induction. In preliminary results, U-2 OS cells transduced with WT, V154M, or N153S STING showed an observable increase in *Tmem173* expression compared to both GFP-transduced and non-transduced (NT) cells at all timepoints (**Figure 28A**). Since this upregulation was also seen without DOX-treatment, there was some background expression from the lentiviral construct. To confirm these findings at the protein level, western blots were performed to detect total STING (35 kDa) using lysates from cells treated with DOX for 24 hours (**Figure 28B**). Increased STING protein was observed in the DOX-treated U-2 OS cells transduced with STING constructs (WT, V154M, N153S), while no STING was detected in the no-DOX control group despite the higher background levels of transcript. Additionally, no STING was observed in GFP-transduced or NT U-2 OS cells. These results demonstrate the transductions were successful and confirm that the lentiviral constructs increased STING expression.

3.6.2 Testing induction of target genes and protein production by transduced BMDCs *in vitro*

We then transduced BMDCs expressing rtTA (Rosa26-rtTA) and examined the same parameters. GFP-transduced BMDCs showed successful DOX-dependent increases in *Gfp* gene expression at all time points (**Figure 29A**). However, there was noticeable baseline *Gfp* expression even without DOX, further suggesting background activation of the construct. In BMDCs transduced with WT STING, there was significant DOX-induced increases in *Tmem173* gene expression (**Figure 29A**). In contrast, there was no *Tmem173* induction in DOX treated BMDCs expressing the constitutively active STING mutants, which differed from what was observed in U-2 OS cells.

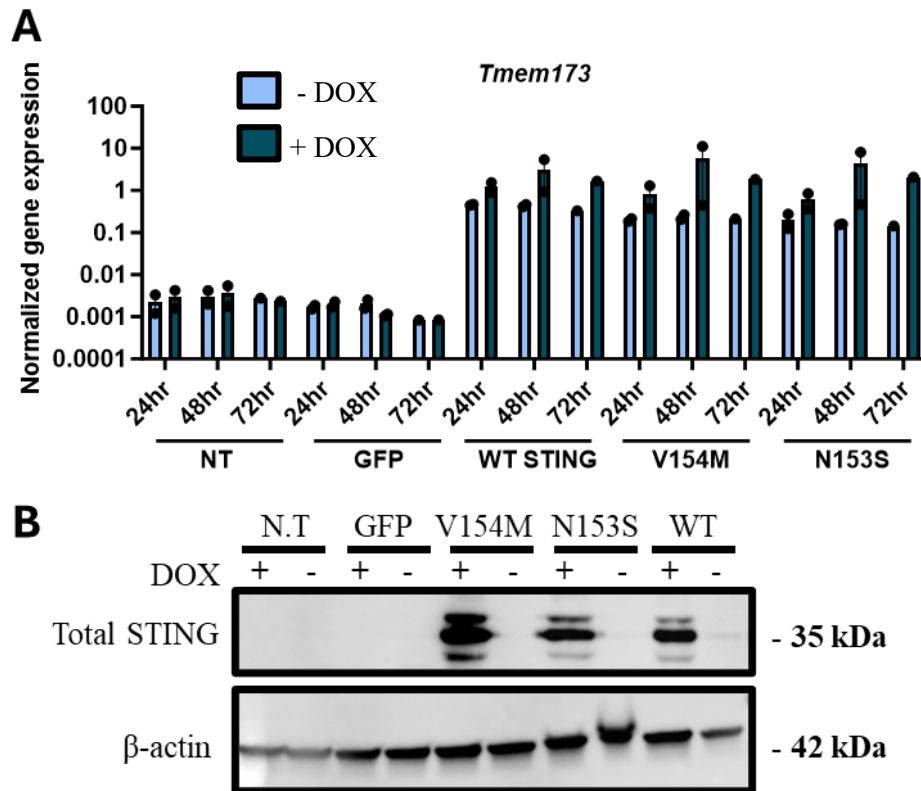


Figure 28. U-2 OS cells transduced with wild-type STING and constitutively active STING mutants (V154M, N153S) showed successful DOX-dependent increases of STING protein *in vitro*.

U-2 OS cells were either left untransduced (N.T) or transduced with GFP, wild-type STING, or constitutively active STING (V154M, N153S) constructs. The cells were then either left untreated or treated with 0.5 µg/mL of DOX for 24, 48, or 72 hours. **(A)** Gene expression of STING (*Tmem173*) was measured using RT-qPCR and normalized to reference genes *Hprt* and *Gusb*. **(B)** Representative western blots of cells treated for 24 hours, showing total STING (35 kDa) with β-actin (42 kDa) as loading control. Data shown as mean ± SEM. n= 1-2 per treatment.

These mutant-transduced BMSCs showed increased cell death under the microscope and through trypan blue staining, which may be due to toxicity associated with constitutive activation. As a result, these cells expanded poorly leading to limited cell numbers, even for analytical purposes.

At the protein level, WT STING-transduced MCs exhibited elevated STING levels, both with and without DOX treatment (**Figure 29B**). This was also observed with the FLAG tag, another indicator of successful construct expression, further implicating DOX-independent induction. No increase in total STING or FLAG tagged STING was detected in V154M-transduced MCs. Interestingly, phosphorylated STING was detected in WT STING MCs treated with DOX, indicating that overexpression of WT STING leads to pathway activation. This was further confirmed by significant increases in ISGs *Ifit1* and *Cxcl10* expression starting 48 hours post-DOX treatment (**Figure 30**). A smaller amount of phospho-STING was also seen in the V154M MCs (**Figure 29B**). Therefore, the WT STING-transduced MCs functioned in the way anticipated for the constitutively active mutants. Due to challenges faced with proliferation and survival of the MCs expressing the STING mutants, even without DOX induction, we decided to proceed with only the WT STING-transduced cells for further analysis.

To investigate the kinetics of DOX induction in the transduced cells, we assessed gene expression changes at 1-, 2-, 4-, 6-, 12-, and 24-hours post-DOX treatment. STING (*Tmem173*) transcript levels began to rise within 1 hour of DOX induction, with significant increases detectable as early as 2 hours (**Figure 31A**). No changes in *Ifnb1* transcript levels were observed at all time points. Significant upregulation of *Ifit1* and *Cxcl10* gene expression was observed after 24 hours of DOX treatment (**Figure 31C & 31D**), accounting for the time needed for STING transcripts to be translated and cause transcriptional changes following activation.

STING agonist activation was compared between transduced MCs and non-transduced C57BL/6 MCs to determine if elevated STING levels enhanced sensitivity to agonist activation. Twenty-four hours post-DOX induction, a titration experiment with the STING agonist ADU-S100 was performed, similar to the one described in **Section 3.1**. Six hours after agonist addition, transduced cells exhibited increased *Tmem173* expression following DOX treatment, confirming higher STING levels (**Figure 32A**). At the 10 µg/mL dose of ADU-S100, we observed slight but significant increases in *Ifit1* expression in transduced MCs, both with and without DOX induction (**Figure 32B**). However, there was no significant increase in the expression of *Cxcl10* or *Ifnb1* in the transduced cells compared to non-transduced MCs following agonist treatment (**Figure 32C and 32D**). As previously seen, *Cxcl10* expression was upregulated in STING-transduced MCs following DOX induction alone (mock treatment) (**Figure 32C**). Overall, these results suggest no substantial increase in sensitivity to the STING agonist in the transduced cells beyond the background activation observed with DOX induction alone.

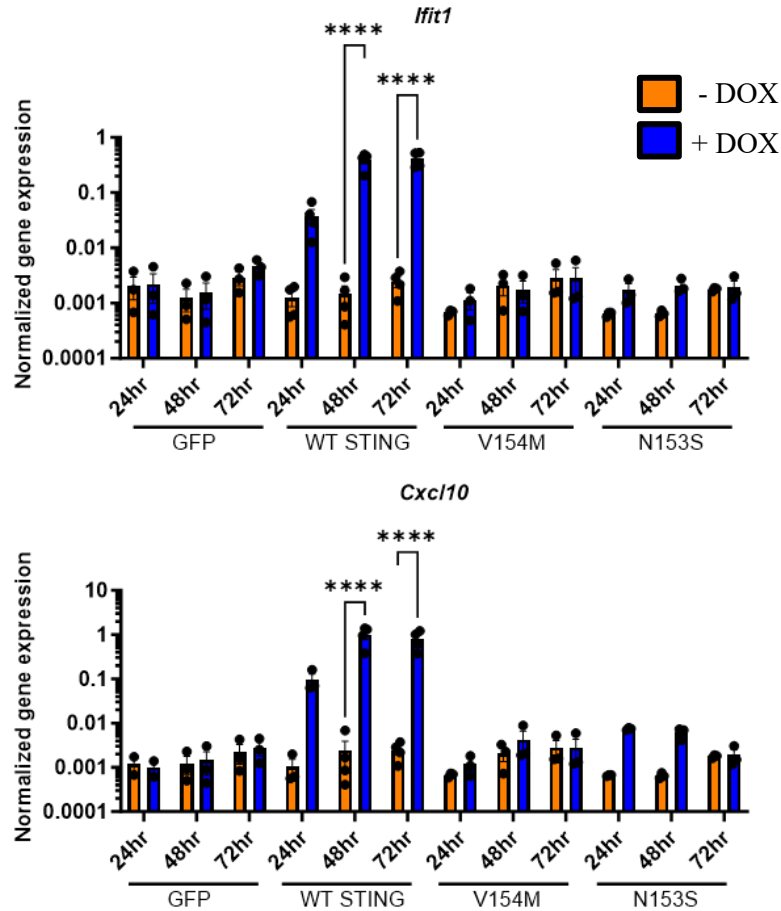


Figure 30. Mast cells transduced with WT STING showed DOX-dependent induction of ISG mRNA expression *in vitro*.

BMMCs were transduced with GFP, WT STING, or constitutively active STING (V154M, N153S) transcripts. Cells were either left untreated or treated with DOX (0.5 $\mu\text{g}/\text{mL}$) for 24, 48, or 72 hours. Gene expression of *Ifit1* and *Cxcl10* was measured using RT-qPCR and normalized to reference genes *Hprt* and *Gusb*. Statistical significance was determined by two-way ANOVA followed by Sidak's multiple comparisons test, comparing DOX treatment to unstimulated controls at each time point. Data shown as mean \pm SEM. $n=3-4$ per treatment. **** $p < 0.0001$.

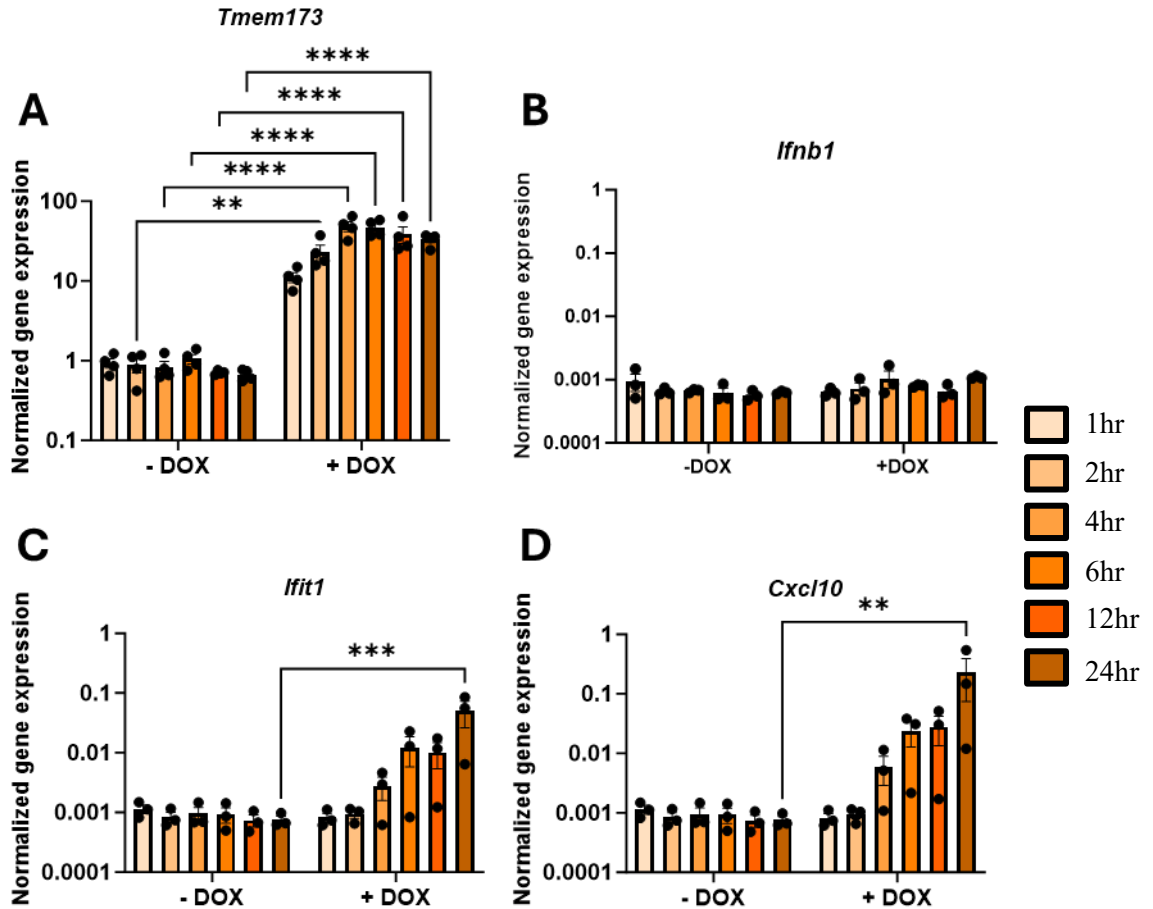


Figure 31. Mast cells transduced with WT STING showed rapid kinetics of DOX-dependent induction of STING (*Tmem173*) and ISG mRNA expression *in vitro*.

Cells were either left untreated or treated with DOX (0.5 $\mu\text{g}/\text{mL}$) for 1, 2, 4, 6, 12, or 24 hours. Gene expression of (A) *Tmem173*, (B) *Ifnb1*, (C) *Ifit1*, and (D) *Cxcl10* was measured using RT-qPCR and normalized to reference genes *Hprt* and *Gusb*. Statistical significance was determined by two-way ANOVA followed by Sidak's multiple comparisons test, comparing DOX treatment to unstimulated controls at each time point. Data shown as mean \pm SEM. $n = 3-4$ per treatment. ** $p < 0.01$; *** $p < 0.001$; **** $p < 0.0001$.

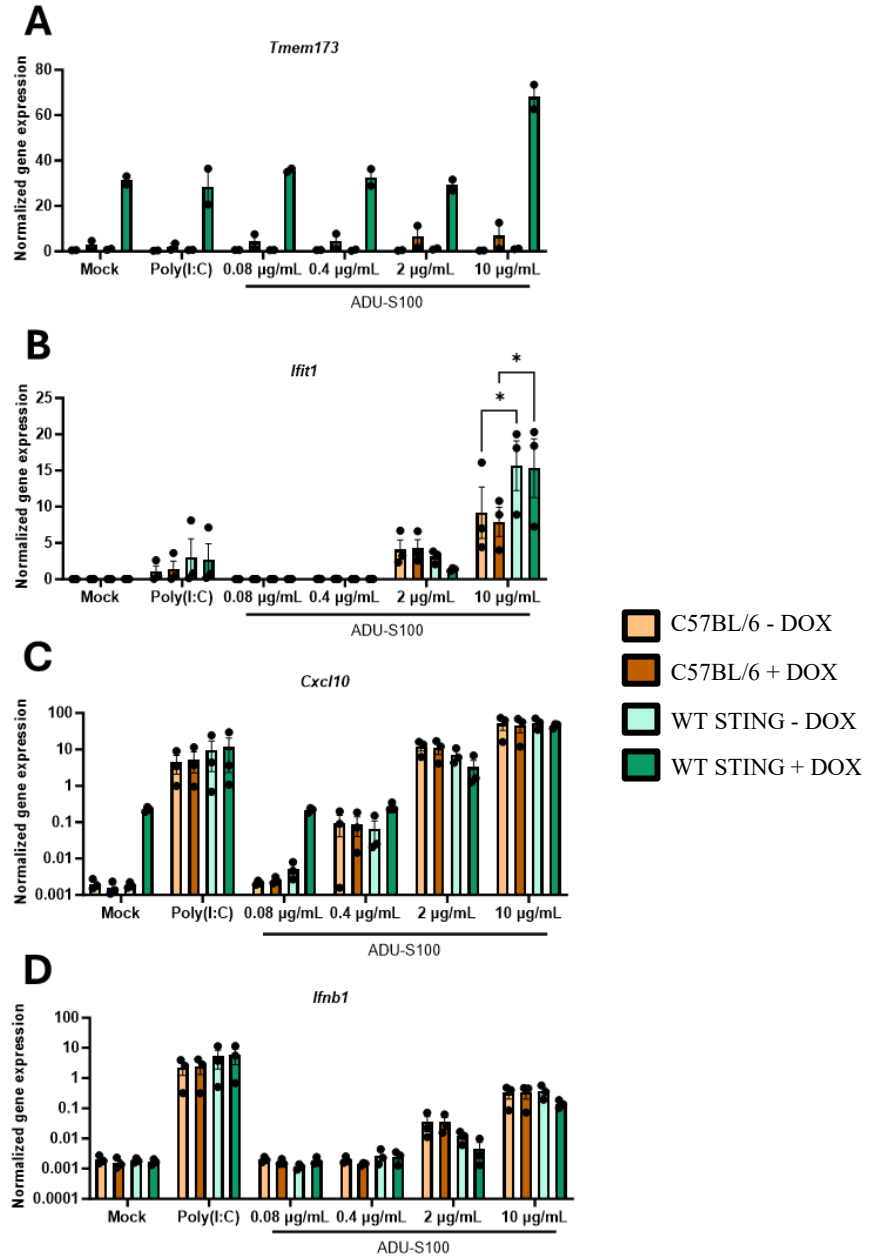


Figure 32. Mast cells transduced with WT STING do not exhibit enhanced sensitivity to STING agonist activation.

WT STING-transduced BMDCs and C57BL/6 BMDCs were pre-treated with DOX (0.5 µg/mL) for 24 hours. Cells were then either left untreated (mock), transfected with Poly(I:C) (10 µg/mL), or treated STING agonist ADU-S100 (0.08 µg/mL, 0.4 µg/mL, 2 µg/mL, 10 µg/mL) for 6 hours. Gene expression of (A) *Tmem173*, (B) *Ifit1*, (C) *Cxcl10*, and (D) *Ifnb1* was measured using RT-qPCR and normalized to reference genes *Hprt* and *Gusb*. Statistical significance was determined by two-way ANOVA followed by Sidak's multiple comparisons test, comparing cell groups at each agonist dose. Data shown as mean \pm SEM. n= 3 per treatment. * $p < 0.05$.

3.6.3 Testing induction of target genes by transduced BMMCs *in vivo*

After completing the *in vitro* characterization, we proceeded to test the WT STING-transduced MCs *in vivo*. The MCs were adoptively transferred into MC-deficient mice (HK) and allowed to reconstitute for 4 weeks. Reconstituted mice (R.HK) were either left untreated or given DOX chow for 6 or 24 hours to induce expression of the construct. Non-reconstituted Hello Kitty mice (NR) and littermate controls (HKLM) served as controls. Peritoneal cavity washes were collected to isolate peritoneal cells for qPCR analysis.

After 24 hours of DOX treatment, R. HK mice showed a significant increase in *Tmem173* gene expression compared to NR. HK and HKLM controls (**Figure 33A**). The more subtle changes in gene expression could be due to the fact that MCs represent only up to 5% of peritoneal cells, meaning gene expression changes in this population may be difficult to detect amidst the other cell types in the peritoneum. Additionally, there was a significant increase in *Cxcl10* gene expression in R. HKs treated with DOX for 24 hours, compared to non-reconstituted mice (**Figure 33B**). However, no significant differences were found in *Ifit1* expression (**Figure 33C**). Overall, these results suggest that reconstitution with the transduced MCs led to an increase in STING expression in the peritoneal cavity.

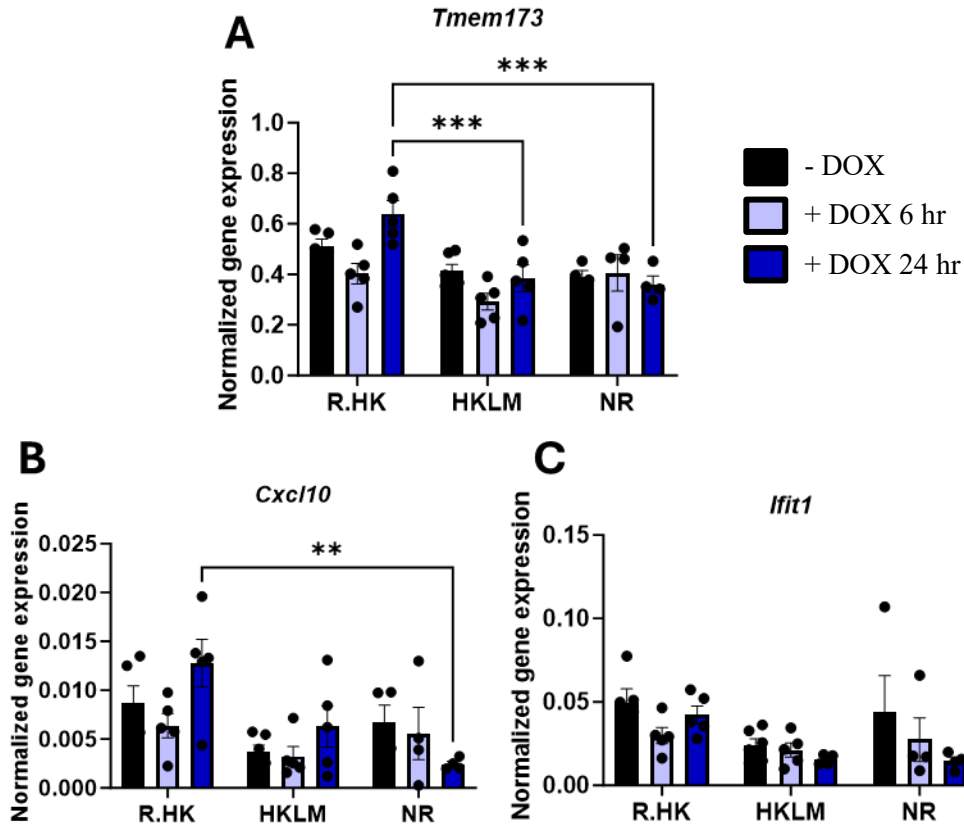


Figure 33. *In vivo* reconstitution with WT STING-transduced increases STING expression levels in the peritoneal cavity.

WT STING-transduced BMMCs (3×10^6) were adoptively transferred into MC-deficient mice (Hello Kitty) and allowed to reconstitute for 4 weeks. Reconstituted mice (R.HK), non-reconstituted mice (NR), and littermate controls (HKLM) were either left untreated or given DOX chow for 6 or 24 hours. Peritoneal cavity washes were then collected to isolate peritoneal cells. Gene expression of (A) *Tmem173*, (B) *Cxcl10*, and (C) *Ifit1* was measured using RT-qPCR and normalized to reference genes *Hprt* and *Gusb*. Statistical significance was determined by two-way ANOVA followed by Sidak's multiple comparisons test. Data shown as mean \pm SEM. $n = 4-6$ per treatment. ** $p < 0.01$; *** $p < 0.001$.

3.7 THE EFFECT OF WT STING-TRANSDUCED BMMCS ON ID8 SURVIVAL

IN VIVO

The therapeutic potential of the WT-STING transduced MCs was assessed in the ID8 ovarian cancer model. Four weeks following adoptive transfers of these cells into MC-

deficient mice (Wsh), ID8 cells were administered intraperitoneally. Reconstituted mice (R. Wsh) were either left untreated or given DOX chow throughout the ID8 experiment to induce expression of the STING construct and then monitored until end point at which time ascites was collected (**Figure 34A**). Overall, there was no significant difference in survival between DOX-treated reconstituted mice and untreated reconstituted mice ($p = 0.2721$) (**Figure 34B**). Expression of STING (*Tmem173*) in the peritoneum was similar in both untreated and DOX-treated mice, suggesting that the transduced MCs did not significantly enhance STING expression (**Figure 34C**). This lack of enhancement could be due to the cancer cells impairing the ability of transduced MCs to thrive and function effectively, a potential factor that will be discussed further. Additionally, some variations in the degree of MC reconstitution, as indicated by *Tpsb2* expression, may have contributed to the observed results (**Figure 34C**). Although no significant survival advantage was observed with DOX induction alone, it would be beneficial to repeat these experiments with larger sample sizes and consistent reconstitution levels to confirm these findings.

Despite DOX induction not improving survival alone, we sought out to investigate whether pulsing the transduced cells with a STING agonist could further improve the response to STING agonist therapy. Following reconstitution of Wsh mice with the transduced cells, we administered the previously established STING agonist regimen and provided DOX chow throughout the experiment (**Figure 35**). Non-reconstituted Wsh mice and C57BL/6 mice receiving DOX with or without agonist served as controls. The higher *Tpsb2* expression in reconstituted mice indicated successful transfer and retention of the MCs in the peritoneum until the end of the experiment (**Figure 35B, right**). However,

Tpsb2 expression in reconstituted mice treated with ADU-S100 slightly varied compared to those that received the vehicle control.

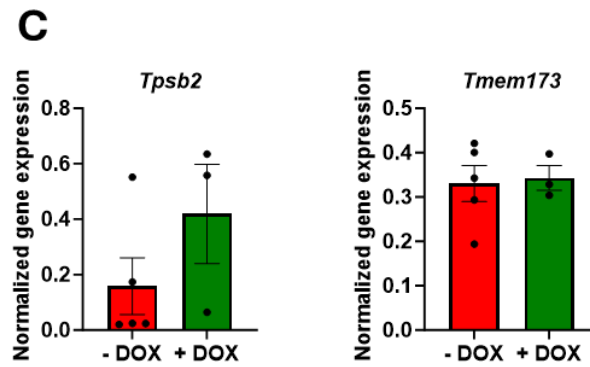
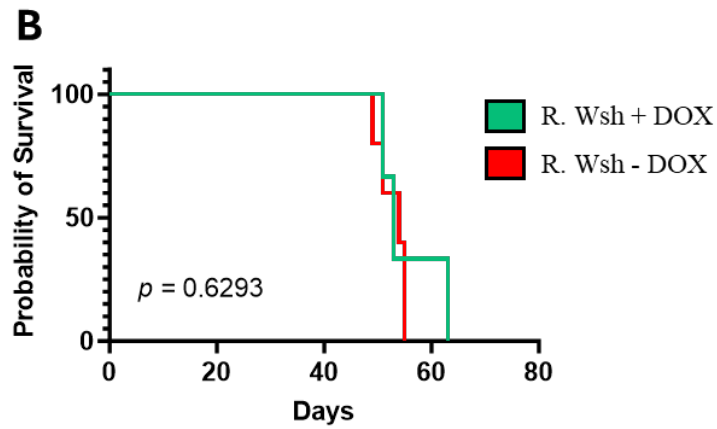
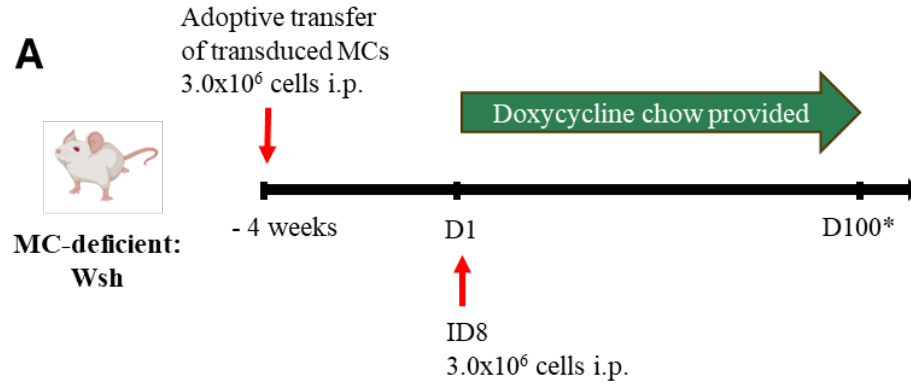


Figure 34. *In vivo* reconstitution of WT STING-transduced mast cells does not improve ID8 survival.

(A) A schematic of the experimental timeline is shown. WT STING-transduced BMMCs were adoptively transferred into MC-deficient mice (Wsh) and allowed to reconstitute for 4 weeks before ID8 cells were administered. Reconstituted mice (R. Wsh) were either left untreated or given DOX chow and monitored until endpoint up to day 100. (B) Overall survival is represented through Kaplan-Meier survival curves. A Log-Rank (Mantel-Cox) Test was used to assess statistical significance between groups. (C) Gene expression of *Tpsb2* and *Tmem173* in PCCs was measured using RT-qPCR and normalized to reference genes *Hprt* and *Gusb*. Statistical significance was determined by unpaired t tests comparing expression in untreated to DOX-treated mice. Data shown as mean \pm SEM. n= 3-5 per treatment.

In terms of survival, R. Wsh mice treated with the agonist showed significantly improved survival compared to mice that received the vehicle control ($p = 0.0058$), consistent with previous data that demonstrated the therapeutic effects of STING agonists (Figure 35B, left). Similar results were observed in non-reconstituted Wsh, where ADU-S100 treatment prolonged survival ($p = 0.0163$). Survival between R. Wsh and NR. Wsh mice treated with vehicle control and DOX chow were comparable, reinforcing that DOX induction alone does not affect outcomes (Figure 35B, left). However, there was also no difference in survival between R. Wsh and NR. Wsh mice that were treated with the agonist (Figure 35B, left). This result indicated that the presence of the transduced cells did not further enhance the efficacy of STING agonist therapy in improving ID8 survival. These results were further confirmed by data that demonstrated no survival difference with or without DOX induction in R. Wsh mice treated with ADU-S100 (Figure 35C, left). Overall, these results indicated that combining DOX induction and STING agonist did not provide any further survival advantage compared to the mice that receive STING agonist alone. However, more experiments should be conducted to increase mouse numbers for better evaluation and to examine the functionality of the transduced cells in the ID8 system.



Figure 35. *In vivo* reconstitution of WT STING-transduced mast cells does not enhance STING agonist therapy in the ID8 model.

(A) A schematic of the experimental timeline is shown. WT STING-transduced BMMCs were adoptively transferred into MC-deficient mice (Wsh) and allowed to reconstitute for 4 weeks. Reconstituted Wsh (R. Wsh), NR. Wsh, and C57BL/6 mice were administered ID8 cells and a regimen of ADU-S100 or vehicle control. Mice received either regular chow or DOX chow and were monitored until endpoint up to 100 days. (B, C left) Overall survival is represented through Kaplan-Meier survival curves. A Log-Rank (Mantel-Cox) Test was used to assess statistical significance between groups. (B, C right) Gene expression of *Tpsb2* in PCCs was measured using RT-qPCR and normalized to reference genes *Hprt* and *Gusb*. Statistical significance was determined one-way ANOVA followed by Tukey's multiple comparison test. Data shown as mean \pm SEM. n= 3-4 per treatment.

Chapter 4: DISCUSSION

Mast cells are tissue-resident innate immune cells that perform diverse and critical functions during immune responses. The STING pathway is an innate immune mechanism that responds to infection and cellular stress, triggering strong type I IFN and pro-inflammatory immune responses. Given that MCs are widely distributed across tissues and function as sentinel cells, we sought to explore the role of the STING pathway in MCs, which has not been characterized previously. Understanding this pathway not only sheds light on another mechanism by which MCs contribute to immunity during infections but also opens the door to evaluating MCs as potential targets for STING-mediated immunotherapies. In this research work, I hypothesized that activation of STING in MCs induces a type I IFN and NF- κ B-mediated response with therapeutic potential, particularly in the context of infection and cancer.

4.1 SUMMARY OF MAJOR FINDINGS

In this study, we demonstrated the functionality of the STING pathway in both murine and human MCs. Our findings revealed that MCs promote a type I IFN and NF- κ B response upon STING activation. However, we observed notable differences in the responses to STING agonist treatment between distinct MC populations. Specifically, human MCs exhibited a lower magnitude of response compared to murine MCs in response to agonist treatment. Furthermore, different STING agonists elicited varying kinetics and magnitudes of IFN and ISG responses. Nevertheless, these results highlight a previously undescribed mechanism for type I IFN expression in MCs and emphasize the impact of MC heterogeneity in shaping responses to immune stimuli.

In studies of the role of MC STING in response to bacterial infection, we demonstrated that MCs are susceptible to infection by *Shigella flexneri*. Our findings showed that BMMCs upregulate type I IFN and ISG expression in response to *Shigella* infection, in a process that depends on bacterial entry into the cell and is partially STING-dependent. Additionally, we found that extracellular receptors on MCs recognize *Shigella* and trigger downstream induction of *Cxcl10* gene expression. In contrast, PCMC *Cxcl10* upregulation was dependent on bacterial entry while CBMCs were observed to respond to *Shigella* primarily through extracellular recognition, thus independently of STING. These analyses revealed differences in infection responses between MC populations, including variations in infection kinetics. Together, these results suggest that both murine and human MCs play a role in the immune response to *Shigella* infection.

In a series of experiments using the murine ID8 ovarian cancer model, we investigated the impact of STING activation and MCs on overall survival. At baseline, MCs were found to influence survival outcomes in the context of ID8 tumor development. Specifically, the absence of MCs in MC-deficient models led to improved survival, while the reintroduction of MCs into MC-deficient mice significantly enhanced survival. Furthermore, treatment with a STING agonist regimen also improved overall survival. To explore the potential of STING-dependent MC-mediated immunotherapy, we genetically modified MCs to inducibly express STING by transducing them with a lentiviral vector with STING expression under the control of an inducible tetracycline promoter. While the transduced MCs demonstrated functionality *in vitro* and successfully reconstituted into MC-deficient mice, there was no significant improvement in mouse survival in the ID8 ovarian cancer model. However, the improvement of mouse survival with MC

reconstitution and STING agonist therapy underlines the therapeutic potential of the system. Further analyses into the mechanisms by which MC reconstitutions enhanced survival should be pursued.







Phenotype	Survival relative to wild-type
<p data-bbox="565 562 821 594">Mast cell-deficient</p> 	
<p data-bbox="435 758 964 789">Reconstituted with wild-type mast cells</p> 	
<p data-bbox="444 957 938 1031">Reconstituted with transduced mast cells expressing STING</p> 	

Figure 36. Summary of the impact of mast cells on ID8 ovarian cancer survival.

Mast cell-deficient mice (HK and Wsh) showed increased survival in the ID8 ovarian cancer model compared to wild-type mice. Reconstitution of mast cell-deficient mice with wild-type mast cells (HK) led to improved survival, while reconstitution with mast cells overexpressing STING (Wsh) had no effect on overall survival. These findings underscore the complex role of mast cells in ovarian cancer progression and suggest the need for further investigation into their contribution to tumor survival.

4.2 RESULTS IN THE CONTEXT OF ESTABLISHED LITERATURE

4.2.1 Activation and overexpression of STING in mast cells

There is limited literature describing the STING pathway in MCs. Two studies have suggested that MC cytokine responses to Influenza A and *S. aureus* infection are STING-dependent, using STING KO cells and inhibitors^{31,124}; however, these included no direct characterization of STING signaling. Here, we demonstrate that STING signaling in MCs follows the canonical pathway, with STING and TBK1 phosphorylation leading to type I IFN-related changes in gene expression²⁰³. This finding highlights the potential for MCs to serve as a, previously underappreciated, source of type I IFNs through STING activation. Moreover, MC production of CCL2 following STING agonist treatment suggests a role for MCs in recruiting other leukocytes, including monocytes²⁵⁹, in infection settings where STING is activated. More comprehensive analyses of other MC mediators, such as IL-6 and CCL1, should be conducted to fully capture the potential roles of MCs in physiological settings.

Our preliminary data suggests that STING activation, initiated by agonist treatment, does not induce overt cell death in MCs, in contrast to the apoptosis observed in T cells following STING agonist-induced ER stress¹⁰⁶. However, it is important to note that this cell death was observed with a different agonist and dose. Furthermore, STING-induced apoptosis is not limited to T cells. It has also been observed in monocytes during viral infection, potentially serving as a host defense mechanism to limit viral replication²⁶⁰. However, given the robust response observed with our agonist dose, these findings imply that a certain level of STING activation can elicit immune responses without triggering apoptosis in MCs.

The lower responses to STING agonists in human MCs may be attributed to the different affinity of the STING agonist for specific human STING isoforms. This observation has been described for the natural STING ligand 2'3'-cGAMP, which binds with lower affinity to certain isoforms²⁶¹. Additionally, DXMAA, the first STING agonist developed, potently induces IFN production in murine cells but fails to do so in human STING expressing cells²⁶². These observations suggest that further investigation into STING activation in human MCs is necessary, using alternative agonists or STING stimuli, to fully characterize the immune responses. Other potential explanations for these different responses include a higher threshold for activation or lower STING expression in human cells compared to murine cells, although this has yet to be explored.

There are also agonist-specific differences in the intensity and timing of STING activation, which can be attributed to the distinct chemical structures of the agonists. For instance, the degradation of total STING protein following treatment with ADU-S100 occurred more rapidly compared to cells treated with diABZI, possibly due to a shorter half-life of ADU-S100 or a higher binding affinity of diABZI for STING.

In our work, we found that overexpression of constitutively active STING mutants in MCs led to impaired proliferation and cell death. This effect was evident even with minimal background expression in the absence of DOX induction. This contrasted with the successful transduction and induction in U-2 OS cells without impairment. These findings suggest that MCs are particularly sensitive to mutant STING expression and cannot tolerate sustained activation. This may highlight a potential vulnerability in MCs in human conditions of constitutive STING activation, such as in patients with SAVI, who harbor gain-of-function mutations. It would be interesting to explore MC numbers in these patient

populations, which may be reduced similarly to the T cell cytopenia seen in SAVI¹¹⁷, and to investigate whether this has implications for diseases like allergies. One possible explanation is that continuous activation can overwhelm the cell's resources, which can interfere with other processes and lead to cellular stress and eventual cell death.

In MCs transduced with WT STING, we observed that overexpression resulted in pathway activation, which achieved the desired effect initially anticipated with the constitutively active mutants. Overexpression of a protein can activate its associated pathways by overcoming inhibitory or regulatory mechanisms, such as degradation, ultimately resulting in net activation of the pathway²⁶³. Moreover, we also observed no increased sensitivity to STING agonist treatment in MCs overexpressing WT STING. Since overexpression already induced pathway activation, the cells may have reached the maximum capacity for activation.

4.2.2 Mast cell responses to *Shigella* infection and the role of the STING pathway

The infection and activation of MCs by *Shigella* has not been extensively characterized. In adults, MCs are found in increased density in the rectal mucosa during the acute phase of *Shigella* infection which is followed by a decline during early convalescence²⁶⁴. However, in children, the elevated density of MCs persisted in the mucosa for a longer period. This early infiltration suggests that MCs may play a crucial role in initiating immune responses for bacterial clearance, such as promoting neutrophil recruitment^{265,266} and their production of NETs²⁶⁷. This corresponds to a notable increase in neutrophils observed during the acute phase of infection in both adult and pediatric patients²⁶⁴. Overall, Raqib *et al.* demonstrated the presence of MCs in biopsies from infected patients, showing that they localize to relevant tissue sites where *Shigella* infection

occurs. However, the mechanisms by which MCs are activated during *Shigella* infection remain to be investigated.

In addition to reinforcing that *Shigella* can elicit STING activation¹⁴⁷, our experiments confirm the relationship between MC phenotype and responses to stimuli. In BMMCs, *Cxcl10* gene induction was similar across cells infected with all three *Shigella* strains and appeared to be independent of bacterial entry. However, in PCMCs, *Cxcl10* expression was not upregulated in cells infected with the *mxiD* mutant, which lacks a functional T3SS for bacterial entry. This suggests that BMMCs may possess more diverse and/or higher levels of PRRs capable of detecting and responding to extracellular *Shigella* compared to PCMCs. Some candidate extracellular PRRs include TLR2 and TLR4 which can recognize lipoproteins and LPS from gram-negative bacteria^{167,168,268}. A transcriptomic study has also shown that BMMCs have higher levels of TLR4 transcripts compared to PCMCs⁷³. Another possibility is that BMMCs may have increased receptor sensitivity to activation. Since PCMCs are more skewed towards a connective-tissue phenotype, BMMCs may be a more suitable model for studying mucosal MC responses⁷³.

Moreover, the production of IL-6 and CCL2 suggests a pro-inflammatory role for MCs during *Shigella* infection. The recruitment of monocytes to the colonic mucosa via CCL2 contributes to crucial host defense against *Shigella* infection^{269,270}. In the case of *Klebsiella pneumoniae* infection, MC-derived IL-6 has been implicated in enhancing neutrophil-mediated bacterial killing and promoting host survival²⁷¹. Our findings may suggest a similar role for MCs in neutrophil recruitment and immune defense against *Shigella* infection. Given the central role of neutrophils in controlling *Shigella*, this

represents a potential avenue for further investigation into MC-neutrophil interactions during infection.

Interestingly in human MCs, the upregulation of *IFNB*, *IFIT1*, and *CXCL10* was similar across cells infected with all three bacterial strains, suggesting that type I IFN gene induction and downstream *IFIT1* expression are not primarily dependent on STING or bacterial entry. This could be also attributed to TLR4 and subsequent TRIF signaling for type I IFN induction, a mechanism that has been described in other bacterial infections²⁷².

Mast cells have been shown to respond to other intracellular enteric bacterial pathogens, including *Salmonella typhimurium*, which shares similarities with *Shigella*. Notably, one study demonstrated that MCs regulate their cytokine production based on the nature of bacterial entry²⁷³. For example, non-invasive *Salmonella* infection triggered a TLR4-dependent cytokine response, while intracellular invasion induced a much more robust inflammatory reaction. This aligns with our findings, which demonstrated that MCs employ multiple mechanisms to respond to *Shigella* infection, depending on bacterial entry. Additionally, increased numbers of MCs were found in the cecal mucosa and submucosa of infected mice, in close proximity to the *Salmonella*, demonstrating interactions between them.

In addition to *Salmonella*, MCs have been demonstrated to respond to other intracellular pathogens, such as *Chlamydia trachomatis*²⁷⁴, by upregulation of pro-inflammatory cytokines and chemokines, including IL-1 β , TNF, and CXCL8. These observations further support the concept that MCs play a critical sentinel role in acute inflammatory responses to intracellular bacterial infections. Interestingly, while *Chlamydia*

infected MCs, it did not replicate efficiently within these cells, suggesting that MCs may act as a barrier to bacterial propagation, thus limiting infection spread.

During *Listeria monocytogenes* infection, MCs produced ROS, TNF, CCL2, and IL-6²⁷⁵. This cytokine response was found to be partially TLR2-dependent. Since the STING pathway has been implicated in the host response to *Listeria* via CDN detection, it warrants further exploration of the STING pathway in the context of MC function during other bacterial infections.

Surprisingly, MCs were observed to survive following 18-hour *Shigella* infections. Mast cells did not exhibit cell death as analyzed with trypan blue staining. Of course, analyses of cell death and apoptotic processes should be conducted with greater sensitivity using techniques such as staining for Annexin V/7-AAD or with an FVD. However, this initial observation was interesting as other cell types are typically described as succumbing to *Shigella* infection quite rapidly. Dendritic cells that were infected with the same MOI we utilized (20) started exhibiting signs of cell death by the first hour of infection, with 50% cytotoxicity after four hours²⁷⁶. This is even observed in non-immune cells, for example, HeLa cells begin significantly dying 8 hours post-infection with the same M90T strain²⁷⁷. One study established a human MC culture isolated from intestinal tissues and infected them with the M90T strain of *Shigella* and observed that infected MCs exhibited cell death after 6 hours of infection. However, the cells were infected with a high MOI of 100. More notably, they found that MCs showed limited responsiveness to *Shigella* infection, as evidenced by minimal gene expression of *CXCL8*, *TNF*, and *IL5*²⁷⁸. It would be valuable to explore other cytokine responses in future studies.

4.2.3 The role of MCs and STING activation in ovarian cancer

In our *in vivo* studies of ovarian cancer, we found that STING agonist therapy improved survival in the ID8 model in WT mice. This result recapitulates previous findings using the same agonist in the ID8-*Trp53*^{-/-} model²⁴⁸. Treatment with ADU-S100 increased the activation of CD8⁺ T cells, as evidenced by elevated CD69 expression, similar to what we observed in our work. Additionally, they found that the STING agonist had synergistic effects with existing ovarian cancer treatments, such as carboplatin chemotherapy and PD-1 immune checkpoint blockade, significantly improving survival in the ID8 model. STING agonist therapy has been described as particularly beneficial in ovarian cancer by counteracting the immunosuppressive TME. For instance, STING agonist treatment has been shown to re-program tumor-associated macrophages to overcome resistance to PARP inhibitors in both syngeneic and PDX models of ovarian cancer²⁴⁹.

In the literature, MCs are found to accumulate around solid tumors where they exert contradictory roles. While their pro-tumorigenic properties are well-characterized, such as promoting angiogenesis and extracellular matrix degradation, their anti-tumorigenic functions remain less understood. The role of MCs in ovarian cancer is especially not well-studied, with most existing research focusing on correlations between MC infiltration and prognosis. In our investigation, we found that resident MCs may be detrimental in ovarian cancer using the ID8 model, using two MC-deficient models. A possible mechanism of this is via the release of histamine from granules, which was found to induce proliferation of ovarian cancer cells by regulating estrogen receptor expression²⁷⁹. Conversely, Meyer *et al.* examined the role of MCs in the ID8 model and found that MCs suppress ovarian tumor growth. However, their study administered ID8 cells subcutaneously into the flank, which

resulted in localized tumor formation at the injection site rather than metastasis throughout the peritoneum like in our intraperitoneal model of engraftment²⁵⁴. Additionally, their findings were based solely on the *Wsh* MC-deficient model, which carries MC-independent abnormalities due to its reliance on a KIT mutation, which will be discussed later.

In clinical samples, MCs are found within and around ovarian cancer tumors^{253–255}. Chan and colleagues observed that MC accumulation around ovarian cancer tumors with high vessel density is associated with improved survival in advanced stages (III-IV)²⁵⁵. Conversely, another study linked tumor-infiltrating MCs in the ovarian cancer stroma to an immunosuppressive microenvironment, which was associated with poorer prognosis in HGSC and reduced response to ICB therapy²⁵³. These conflicting findings suggest that the localization of MCs within the tumor microenvironment influences their contribution to disease progression.

In addition to variations in MC localization in tumors, MCs exhibit plasticity in their phenotype, which has subsequent effects on their association with clinical outcomes. Within ovarian cancer tumors, it was reported that tryptase- and carboxypeptidase A3-positive MCs post-chemotherapy were associated with poorer outcomes in HGSC. However, a higher proportion of tryptase-positive-only MCs demonstrated association with improved overall survival²⁵². This concept was further supported by a pan-cancer single-cell RNA sequencing analysis across 15 types of cancer, where MCs were classified into two subtypes based on low or high expression of TNF or VEGFA. TNF-positive MCs were linked to better prognosis, while VEGFA expression was associated with poorer outcomes²⁸⁰.

Mast cells are well implicated in tumor angiogenesis by releasing several pro-angiogenic factors including tryptase, VEGF, and heparin²⁸¹. Several studies have demonstrated that higher serum-tryptase and MC density are significantly correlated with microvascular density in cancer patients, implicating an involvement of MC tryptase in angiogenesis^{282–284}. However, appropriate MC activation can mediate antitumor functions by direct tumor cell cytotoxicity^{285,286}, secreting chemokines that mobilize anti-tumor immune effector cells to tumor sites^{51,60,287}, and modulating immune effector cell responses through the release of cytokines or cellular interactions^{288,289}. Overall, these findings support the potential idea of skewing the MC phenotype to promote the activation and production of specific mediators that favor anti-tumorigenic functions.

Interestingly, our results demonstrated significantly improved survival in MC-deficient mice compared to wild-type mice treated with the STING agonist regimen. However, since MC-deficient mice exhibit MC-independent abnormalities, baseline differences between the groups may have influenced these outcomes⁷⁸. Therefore, the use of MC-reconstitutions is an essential technique to determine whether the observed effects are specifically due to the absence of MCs. Given that MCs are involved in several physiological processes, their absence throughout development can contribute to these baseline differences. Using models of inducible MC-deficiency would reduce these limitations⁷⁸. Alternatively, this may suggest another contribution of MCs in impairing the efficacy of STING agonist therapy by exerting immunosuppressive effects on other cells that are responding to the agonis. For example, MC-derived IL-10 has been shown to promote pancreatic cancer progression and resistance to immunotherapy²⁹⁰.

4.3 CRITIQUES AND LIMITATIONS

Some limitations in our *in vivo* ID8 studies may contribute to the unexpected survival differences observed in reconstituted HK mice compared to wild-type littermates. One limitation is that the experiment with reconstituted HKs was not conducted in parallel with the other mice, meaning that different ID8 cells were used for injections. Although we strived to use the same batch of frozen ID8 cells to initiate culture, variations in passage numbers and health of ID8 cells can influence cellular proliferation and migration, which may impact metastasis and survival *in vivo*²⁹¹. Additionally, there may be differences in the distribution of reconstituted MCs within tissues following intraperitoneal injections, compared to their native localization in wild-type mice. Increasing evidence suggests that the micro-localization of MCs in tumors plays a significant role in their prognostic value. For example, intratumoral MCs are associated with improved outcomes in prostate cancer, whereas peritumoral MCs often exert pro-tumorigenic effects, such as promoting angiogenesis, which can lead to impaired survival²⁹².

We utilized two MC-deficient models, termed HK and Wsh, to study the effects of MCs in ovarian cancer. While these models provide valuable insights into the role of MCs in biological settings, each comes with limitations that must be considered. The Wsh model carries a KIT mutation, which is essential for other cell types, including hematopoietic stem cells, germ cells, and melanocytes⁷⁸. As a result, defects in these populations could lead to confounding results that are not specific to MCs. Additionally, increased neutrophil populations in this model may facilitate cancer progression²⁹³. On the other hand, the HK model is characterized by a partial reduction in basophil numbers, incomplete MC-deficiency across tissues (ranging from 92-100%), and mild anemia⁸⁰. These are all

potential confounding variables, making it more challenging to accurately determine the specific role of MCs in ovarian cancer. These limitations reinforce the need for MC reconstitutions to assess the specificity of results to the role of MCs. If reconstitutions of MCs into MC-deficient recapitulate the WT phenotype, it reaffirms the effects are MC-dependent.

A general limitation to consider for both models is compensatory mechanisms in MC-deficient models. The absence of MCs during development may trigger compensatory activity by other immune cells, which would mask the role of MCs⁷⁸. There are other MC-deficient models that involve inducible depletion before or during experimental timelines to circumvent this issue⁷⁸. Given these limitations, it is ideal to conduct experiments using more than one MC-deficiency model to assess whether the outcomes are consistent. However, due to limitations in available mouse numbers, we were unable to repeat all experiments in both the Wsh and HK models.

4.4 CLINICAL IMPLICATIONS

Current literature on MC-associated immunotherapies primarily focuses on counteracting their pro-tumorigenic features through population depletion or inhibition of degranulation. While MCs are often associated with promoting tumor progression, it may be worth exploring strategies that polarize their phenotype to limit cancer growth. Selectively activating MCs to produce anti-tumor mediators could be a strategy to boost anti-tumor responses. This approach could be accomplished with the use of agonists targeting MC receptors, a method that has been applied to MC TLR signaling and demonstrated therapeutic potential. MC TLR2 activation was shown to inhibit tumor growth of melanoma by promoting MC production of IL-6 and CCL3, leading to the

recruitment of NK and T cells⁶⁰. Similar findings were observed with TLR4 activation of MCs resulting in more effective tumor control, which was mediated by MC-derived CXCL10 production to recruit tumor-infiltration lymphocytes⁵¹.

STING agonists are being explored as adjuvants to improve the immunogenicity of vaccines against infections and cancer due to their ability to boost immune responses^{103,294}. For example, combining STING agonists with live-attenuated or inactivated viral vaccines can potentially increase the strength the immune response. This could occur through several mechanisms, one of which is the IFN-mediated activation and maturation of DCs, which are crucial for initiating adaptive immunity. Luo *et al.* demonstrated enhanced antibody titers and T cell responses when cGAMP was utilized as an adjuvant for Influenza vaccination²⁹⁵. Since MCs are key players in the immune system's initial defense, they may be instrumental in boosting responses to vaccines. Mast cells have been recognized for their role in mobilizing immune cells to sites of infection and to draining lymph nodes, including DCs, which are critical for antigen presentation and T cell priming. Because of this, compounds that activate MCs such as compound 48/80 have been investigated as vaccine adjuvants²⁹⁶. This has demonstrated enhanced humoral responses²⁹⁶ and further suggests that MCs may play a functional role in improving vaccine efficacy by facilitating immune cell recruitment and activation. Since MCs are implicated in the response to STING agonists, we could speculate they may play a functional role in IFN production and promoting more effective vaccination responses.

STING activation is linked to autoimmunity and interferonopathies, where excessive activation of the pathway can drive chronic inflammation and is typically seen in autoimmune conditions such as rheumatoid arthritis^{96,297}. This heightened immune

response is attributed to DNA accumulation or deficiencies in nuclease activity, resulting in excessive type I IFN production⁹⁶. MCs play a critical role in detecting PAMPs, including DNA. However, in autoimmune diseases, MCs can become activated by endogenous DAMPs such as self-DNA or other signals derived from tissue injury. This activation can perpetuate chronic inflammation. In fact, MCs are described to contribute to chronic inflammation in autoimmune diseases by releasing pro-inflammatory mediators and promoting angiogenesis²⁹⁸. If the STING pathway becomes overly activated or dysregulated in MCs, it could lead to exaggerated inflammatory immune responses that may contribute to pathological inflammation and tissue damage of these diseases.

Mast cells, being long-lived and capable of promoting inflammatory responses, can persist at sites of infection for extended periods and continuously secrete pro-inflammatory mediators²⁹⁹. A persistent activation of the STING pathway in MCs could contribute to a sustained, low-grade inflammatory environment, which may exacerbate chronic infections and prevent proper resolution of inflammation. For example, in chronic viral infections such as those caused by herpesviruses, intermittent STING activation in MCs could result in prolonged inflammation and tissue damage. Because MCs are involved in the regulation of other immune cells, the persistent activation of the STING pathway in MCs may also influence the broader immune response, leading to dysregulated immunity. This could hinder the resolution of infection and emphasizes the need for balanced activation of the STING pathway to induce effective immune responses with the prevention of excessive inflammation.

Our work has demonstrated that activation of STING is one potential approach to stimulate MC production of anti-tumorigenic type I IFNs. Given that MCs are long-lived⁴⁹,

radio-resistant³⁰⁰, and increased at tumor sites⁴⁸, they are an intriguing target for manipulation for immunotherapy. Although our transduced MCs did not exhibit therapeutic efficacy, investigating other systems of targeted MC-mediated STING therapy remains a valuable avenue for future research.

Additionally, our work with *Shigella* has highlighted the role of MCs as key players in infection. This is clinically relevant since MCs are present in all layers of the gastrointestinal tract, including in substantial density in the submucosa where *Shigella* enters after passing through M cells³⁰¹. We also demonstrated that MCs promote a type I IFN response; however, whether this response is beneficial or detrimental in physiological settings remains to be explored.

4.5 FUTURE RESEARCH DIRECTIONS

4.5.1 Characterization of STING signaling in mast cells

Although IFN- β protein was detected in the supernatant of BMMCs following treatment with the STING agonist, the levels were low to modest. The cells were cultured in media containing protease inhibitors, making degradation by MC-proteases less likely. Therefore, it is possible that MCs are taking up IFN- β in an autocrine fashion, which could explain the lower levels detected in the supernatant. To further investigate this, MCs should be pre-treated with an IFN receptor antagonist to block autocrine IFN signaling. If larger amounts of IFN- β are detected in the supernatant upon receptor blockade, it would suggest an autocrine mechanism in which MCs respond to STING activation, potentially reflecting a relevant process in physiological settings. This could also be investigated through intracellular cytokine staining to assess IFN and CXCL10 production by flow cytometry.

Although we have characterized some aspects of MC responses to STING activation, other facets of MC biology could be influenced by this pathway that remain to be explored. To gain a more comprehensive understanding, an unbiased approach such as RNA sequencing would be highly beneficial. By analyzing MCs treated with STING agonists, this method would allow for the identification of both known and novel pathways that may be modified, shedding light on how STING activation broadly alters MC gene expression. It could also reveal potential crosstalk between STING and other immune receptors. These comprehensive analyses will further our understanding of how STING contributes to immune function and disease.

4.5.2 Unraveling the role of mast cells in *Shigella* infection

To investigate the contribution of TLRs in *Shigella* infection, MC responses to the mxiD mutant could be evaluated following inhibition of TLRs or using MCs derived from different TLR KO mice. If pro-inflammatory cytokine and chemokine expression is dampened following inhibition or in the absence of specific TLR signal transduction, we would be able to identify the other PRRs involved during the MC response to infection. Additionally, MC survival during *Shigella* infection may be influenced by IFN-induced promotion of self-survival, as previously described in *S. aureus* infection¹²⁴. Blocking type I IFN binding to the IFNAR would provide insight into the impact of IFN signaling on cell-autonomous host defenses. Furthermore, it would be valuable to characterize the mechanisms by which MCs manage and eliminate intracellular infection, such as ROS production³⁰².

Another avenue for exploration includes studying the impact of MCs in *Shigella* infection using *in vivo* infection models. One challenge is the lack of murine models that

recapitulate the hallmarks of *Shigella* disease, as reviewed by Alphonse & Odendall³⁰³. Mice are typically resistant to gut colonization by *Shigella* by oral challenge, making it difficult to establish murine models³⁰³. More recently, mice deficient in the NAIP–NLRC4 inflammasome have been shown to be highly susceptible to oral *Shigella* infection and recapitulate the clinical features of human disease including colonization and replication within intestinal epithelial cells³⁰⁴. Another model includes intraperitoneal infection which results in a more systemic infection but mimics clinical dysentery with severe tissue destruction and inflammation²⁶⁹.

To assess the role of MCs, these models of *Shigella* infection model could be utilized to compare infection between MC-deficient and WT mice. Parameters to assess include the production of pro-inflammatory mediators, immune cell recruitment, tissue pathology, and infection resolution. Since MCs are involved in tissue remodeling and inflammation, it would be important to assess the extent of tissue damage by cross-sectional hematoxylin and eosin histological analyses of colon tissue sections, in addition to gross pathology. Furthermore, infection resolution could be examined by quantifying bacterial burden within the large intestine and feces to evaluate the ability of MCs to restrict bacterial propagation. Lastly, cytokine and chemokine expression in the intestines should be quantified to assess the contribution of MCs to the immune response. To further elucidate the role of MC-specific STING activation in this process, BMDCs could be cultured from STING KO mice and then used to reconstitute MC-deficient mice³⁰⁵. Overall, these assessments would provide further comprehensive analysis into the role of MCs in *Shigella* infection.

4.5.3 Elucidating the role of mast cells in ovarian cancer

Although the ID8 model was well-suited for our studies due to its relatively rapid time course and ability to represent metastatic ovarian cancer behavior, our findings regarding the effects of MCs may differ in other models of ovarian cancer. This is particularly relevant given the highly heterogeneous nature of ovarian cancer, which encompasses distinct genetic profiles and immune microenvironments³⁰⁶. To fully understand the role of MCs in ovarian cancer, it would be important to investigate their function in other cancer models, as these variables may influence MC activity and subsequent survival. Intrabursal ID8 injections could be used to recapitulate the mechanisms of ovarian cancer progression and dissemination from the ovaries²³¹. Additionally, there are altered ID8 cell lines possessing relevant mutations to the varying histological subtypes of ovarian cancer including *Trp53*, *Brca1*, *Pten*, or *Nfl*³⁰⁷. Perhaps the most clinically relevant model to explore would be PDXs, as they retain the molecular and genomic properties of ovarian cancer tumors that would reflect the complex relationship between tumor heterogeneity and responses to therapy. Overall, these factors can exhibit differing responses to immunotherapies³⁰⁶. Therefore, utilization of additional models would be beneficial to achieve a more accurate assessment of MCs in ovarian cancer.

We observed that the WT STING-transduced MCs did not improve survival in the ID8 ovarian cancer model. Although we successfully reconstituted MCs into MC-deficient mice, the functionality of these transduced cells may have been impaired within the ovarian cancer environment. It would be valuable to investigate the functionality of the STING-transduced MCs throughout the course of the ID8 model. This could be achieved by

collecting peritoneal cells at various time points during the experiment, including the endpoint, and performing flow cytometric analysis. Using intracellular FACS, the proportion of phosphorylated STING-positive cells within the MC population could be assessed to confirm their activation following DOX induction. This approach may provide greater sensitivity compared to evaluating changes in gene expression of STING (*Tmem173*) in peritoneal cells, especially since MCs typically comprise only 1-5% of the peritoneal cell population⁷¹.

To address the potential reasons behind the improved survival observed in MC reconstitutions within the ID8 model, further investigation into the localization and phenotype of the MCs is necessary. While BMDCs are generally known to phenotypically adapt to their environment, there are still concerns about whether reconstituted MC populations fully replicate the characteristics, distribution, and functional responses of native MCs in WT mice²⁵⁶. It would be crucial to assess the localization of MCs following reconstitution in comparison to their native tissue sites. Luciferase-expressing MCs could be tracked using IVIS to monitor their distribution post-reconstitution. Additionally, tissue sections from the peritoneum, including the peritoneal wall, could be stained with toluidine blue³⁰⁸ to evaluate the relative abundance of MCs in these tissues. Another factor to consider is the potential phenotypic differences between reconstituted and native MC populations, which could influence survival outcomes. To explore this, MCs should be isolated from the peritoneum of both WT and reconstituted mice for comparative profiling. Following peritoneal lavages, cells could be isolated and sorted using a cell sorter to obtain an enriched MC population for single-cell RNA sequencing to identify differentially expressed genes. Given that MCs are present in lower numbers in the peritoneum, pooling

samples from multiple mice may be required to obtain enough cells. These results would provide insight into the fundamental differences between the native and reconstituted MC populations and suggest potential factors contributing to the opposing results we observed in our model.

Alternative mechanisms for targeted activation of STING in MCs could be explored beyond tetracycline-dependent overexpression. One potential approach, independent of genetic modification, involves using targeted agonists for specific cell types. This can be achieved through antibody-drug conjugates, where a STING agonist is linked to a monoclonal antibody that selectively targets a receptor on MCs. Similar strategies have been used to direct STING agonists specifically to tumor cells and exhibited reduced tumor growth^{309,310}. This approach could minimize the risk of hyperinflammation associated with systemic STING agonist administration, as well as avoid potential complications from genetic modifications affecting other cellular processes.

4.6 CONCLUDING REMARKS

In summary, I have characterized the response of MCs to STING activation and its implications on immune responses. This work highlights the role of MCs as sentinel immune cells and their response to invading pathogens, which we have investigated in the specific context of *Shigella* infection. Furthermore, the production of type I IFNs by MCs via the STING pathway represents a novel avenue for further exploration in cancer immunotherapy. Taken together, these results provide evidence and establish a foundation for future research, emphasizing the potential of previously unexplored mechanisms in MCs in the context of infection and cancer.

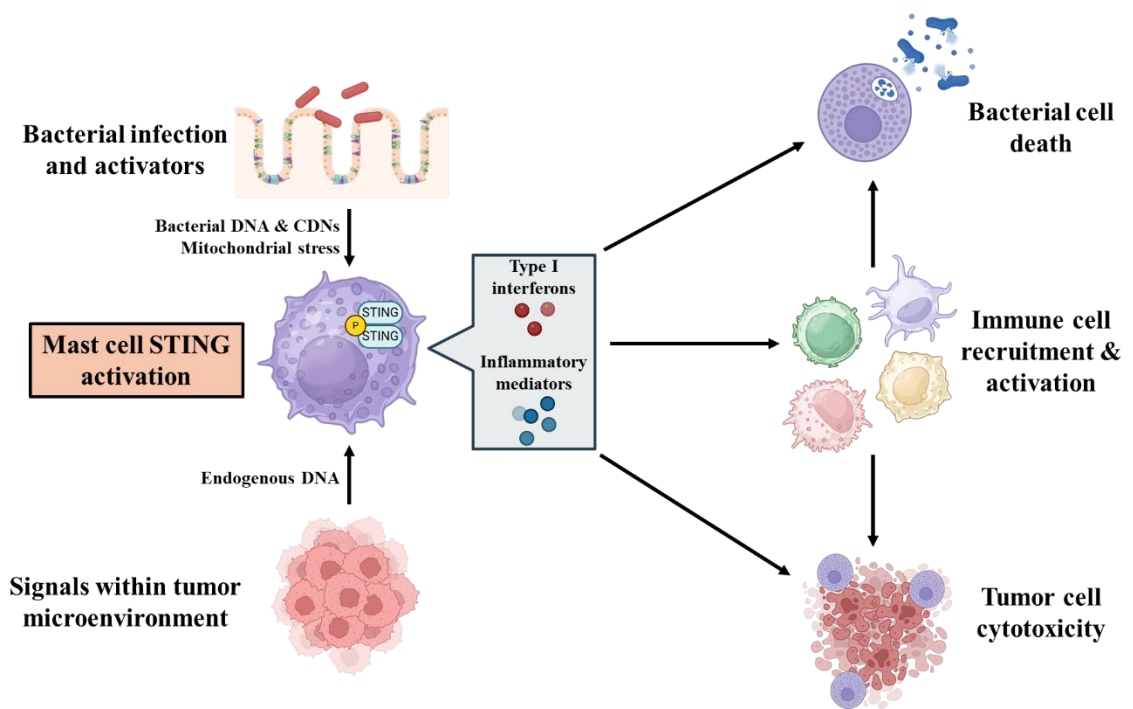


Figure 37. Schematic summary of findings on mast cell STING activation and the implications on bacterial and tumor immunity.

This illustration depicts how stimuli within bacterial infections and the tumor microenvironment, including bacterial or endogenous DNA, can stimulate STING activation in mast cells. Activation of STING within mast cells leads to the production of type I IFNs and pro-inflammatory mediators that can directly influence bacterial or tumor cell death, while also contributing to the recruitment and activation of other immune cells to enhance the overall immune response. Overall, this highlights a mechanism by which MCs can promote anti-bacterial and anti-tumor immunity.

REFERENCES

1. Lichterman, J.N., and Reddy, S.M. (2021). Mast Cells: A New Frontier for Cancer Immunotherapy. *Cells* 10, 1270. <https://doi.org/10.3390/cells10061270>.
2. Moon, T.C., St Laurent, C.D., Morris, K.E., Marcet, C., Yoshimura, T., Sekar, Y., and Befus, A.D. (2010). Advances in mast cell biology: new understanding of heterogeneity and function. *Mucosal Immunol* 3, 111–128. <https://doi.org/10.1038/mi.2009.136>.
3. Rathore, A.P., and St John, A.L. (2020). Protective and pathogenic roles for mast cells during viral infections. *Curr Opin Immunol* 66, 74–81. <https://doi.org/10.1016/j.coi.2020.05.003>.
4. Galli, S.J., and Tsai, M. (2012). IgE and mast cells in allergic disease. *Nat Med* 18, 693–704. <https://doi.org/10.1038/nm.2755>.
5. Marshall, J.S., Portales-Cervantes, L., and Leong, E. (2019). Mast Cell Responses to Viruses and Pathogen Products. *Int J Mol Sci* 20, 4241. <https://doi.org/10.3390/ijms20174241>.
6. Redegeld, F.A., Yu, Y., Kumari, S., Charles, N., and Blank, U. (2018). Non-IgE mediated mast cell activation. *Immunol Rev* 282, 87–113. <https://doi.org/10.1111/imr.12629>.
7. Lunderius-Andersson, C., Enoksson, M., and Nilsson, G. (2012). Mast Cells Respond to Cell Injury through the Recognition of IL-33. *Front Immunol* 3, 82. <https://doi.org/10.3389/fimmu.2012.00082>.
8. St. John, A.L., Rathore, A.P.S., and Ginhoux, F. (2023). New perspectives on the origins and heterogeneity of mast cells. *Nat Rev Immunol* 23, 55–68. <https://doi.org/10.1038/s41577-022-00731-2>.

9. Dahlin, J.S., and Hallgren, J. (2015). Mast cell progenitors: origin, development and migration to tissues. *Mol Immunol* *63*, 9–17. <https://doi.org/10.1016/j.molimm.2014.01.018>.
10. Dahlin, J.S., Malinowski, A., Öhrvik, H., Sandelin, M., Janson, C., Alving, K., and Hallgren, J. (2016). Lin- CD34hi CD117int/hi FcεRI+ cells in human blood constitute a rare population of mast cell progenitors. *Blood* *127*, 383–391. <https://doi.org/10.1182/blood-2015-06-650648>.
11. Tauber, M., Basso, L., Martin, J., Bostan, L., Pinto, M.M., Thierry, G.R., Houmadi, R., Serhan, N., Loste, A., Blériot, C., et al. (2023). Landscape of mast cell populations across organs in mice and humans. *Journal of Experimental Medicine* *220*, e20230570. <https://doi.org/10.1084/jem.20230570>.
12. McNeil, B.D., Pundir, P., Meeker, S., Han, L., Udem, B.J., Kulka, M., and Dong, X. (2015). Identification of a mast-cell-specific receptor crucial for pseudo-allergic drug reactions. *Nature* *519*, 237–241. <https://doi.org/10.1038/nature14022>.
13. Jiménez, M., Cervantes-García, D., Córdova-Dávalos, L.E., Pérez-Rodríguez, M.J., Gonzalez-Espinosa, C., and Salinas, E. (2021). Responses of Mast Cells to Pathogens: Beneficial and Detrimental Roles. *Front Immunol* *12*, 685865. <https://doi.org/10.3389/fimmu.2021.685865>.
14. Akula, S., Paivandy, A., Fu, Z., Thorpe, M., Pejler, G., and Hellman, L. (2020). Quantitative In-Depth Analysis of the Mouse Mast Cell Transcriptome Reveals Organ-Specific Mast Cell Heterogeneity. *Cells* *9*, 211. <https://doi.org/10.3390/cells9010211>.
15. Pejler, G., Rönnberg, E., Waern, I., and Wernersson, S. (2010). Mast cell proteases: multifaceted regulators of inflammatory disease. *Blood* *115*, 4981–4990. <https://doi.org/10.1182/blood-2010-01-257287>.

16. Moon, T.C., Befus, A.D., and Kulka, M. (2014). Mast Cell Mediators: Their Differential Release and the Secretory Pathways Involved. *Front Immunol* 5, 569. <https://doi.org/10.3389/fimmu.2014.00569>.
17. Ricciotti, E., and FitzGerald, G.A. (2011). Prostaglandins and inflammation. *Arterioscler Thromb Vasc Biol* 31, 986–1000. <https://doi.org/10.1161/ATVBAHA.110.207449>.
18. Cuzzo, B., and Lappin, S.L. (2025). Physiology, Leukotrienes (StatPearls Publishing).
19. Peters-Golden, M., Canetti, C., Mancuso, P., and Coffey, M.J. (2005). Leukotrienes: Underappreciated Mediators of Innate Immune Responses. *The Journal of Immunology* 174, 589–594. <https://doi.org/10.4049/jimmunol.174.2.589>.
20. Mukai, K., Tsai, M., Saito, H., and Galli, S.J. (2018). Mast cells as sources of cytokines, chemokines, and growth factors. *Immunol Rev* 282, 121–150. <https://doi.org/10.1111/imr.12634>.
21. Gri, G., Piconese, S., Frossi, B., Manfroi, V., Merluzzi, S., Tripodo, C., Viola, A., Odom, S., Rivera, J., Colombo, M.P., et al. (2008). CD4+CD25+ Regulatory T Cells Suppress Mast Cell Degranulation and Allergic Responses through OX40-OX40L Interaction. *Immunity* 29, 771–781. <https://doi.org/10.1016/j.immuni.2008.08.018>.
22. Lotfi-Emran, S., Ward, B.R., Le, Q.T., Pozez, A.L., Manjili, M.H., Woodfolk, J.A., and Schwartz, L.B. (2018). Human mast cells present antigen to autologous CD4+ T cells. *Journal of Allergy and Clinical Immunology* 141, 311-321.e10. <https://doi.org/10.1016/j.jaci.2017.02.048>.

23. Kambayashi, T., Allenspach, E.J., Chang, J.T., Zou, T., Shoag, J.E., Reiner, S.L., Caton, A.J., and Koretzky, G.A. (2009). Inducible MHC Class II Expression by Mast Cells Supports Effector and Regulatory T Cell Activation. *The Journal of Immunology* *182*, 4686–4695. <https://doi.org/10.4049/jimmunol.0803180>.
24. Stelekati, E., Bahri, R., D’Orlando, O., Orinska, Z., Mittrücker, H.-W., Langenhaun, R., Glatzel, M., Bollinger, A., Paus, R., and Bulfone-Paus, S. (2009). Mast Cell-Mediated Antigen Presentation Regulates CD8+ T Cell Effector Functions. *Immunity* *31*, 665–676. <https://doi.org/10.1016/j.immuni.2009.08.022>.
25. Barra, J., Liwski, C.R., Phonchareon, P., Portales-Cervantes, L., Gaston, D., Karakach, T.K., Haidl, I.D., and Marshall, J.S. (2025). Interleukin-5 enhances human mast cell survival and interferon responses to viral infection. *Journal of Allergy and Clinical Immunology*. <https://doi.org/10.1016/j.jaci.2025.02.025>.
26. Portales-Cervantes, L., Haidl, I.D., Lee, P.W., and Marshall, J.S. (2017). Virus-Infected Human Mast Cells Enhance Natural Killer Cell Functions. *J Innate Immun* *9*, 94–108. <https://doi.org/10.1159/000450576>.
27. Portales-Cervantes, L., Crump, O.M., Dada, S., Liwski, C.R., Gotovina, J., Haidl, I.D., and Marshall, J.S. (2020). IL-4 enhances interferon production by virus-infected human mast cells. *Journal of Allergy and Clinical Immunology* *146*, 675-677.e5. <https://doi.org/10.1016/j.jaci.2020.02.011>.
28. Zhou, J., Wang, Y., Chang, Q., Ma, P., Hu, Y., and Cao, X. (2018). Type III Interferons in Viral Infection and Antiviral Immunity. *Cellular Physiology and Biochemistry* *51*, 173–185. <https://doi.org/10.1159/000495172>.
29. McNab, F., Mayer-Barber, K., Sher, A., Wack, A., and O’Garra, A. (2015). Type I interferons in infectious disease. *Nat Rev Immunol* *15*, 87–103. <https://doi.org/10.1038/nri3787>.

30. Al-Afif, A., Alyazidi, R., Oldford, S.A., Huang, Y.Y., King, C.A., Marr, N., Haidl, I.D., Anderson, R., and Marshall, J.S. (2015). Respiratory syncytial virus infection of primary human mast cells induces the selective production of type I interferons, CXCL10, and CCL4. *Journal of Allergy and Clinical Immunology* *136*, 1346-1354.e1. <https://doi.org/10.1016/j.jaci.2015.01.042>.
31. Graham, A.C., Hilmer, K.M., Zickovich, J.M., and Obar, J.J. (2013). Inflammatory Response of Mast Cells during Influenza A Virus Infection Is Mediated by Active Infection and RIG-I Signaling. *The Journal of Immunology* *190*, 4676–4684. <https://doi.org/10.4049/jimmunol.1202096>.
32. King, C.A., Anderson, R., and Marshall, J.S. (2002). Dengue virus selectively induces human mast cell chemokine production. *J Virol* *76*, 8408–8419. <https://doi.org/10.1128/jvi.76.16.8408-8419.2002>.
33. Shelburne, C.P., Nakano, H., St. John, A.L., Chan, C., McLachlan, J.B., Gunn, M.D., Staats, H.F., and Abraham, S.N. (2009). Mast Cells Augment Adaptive Immunity by Orchestrating Dendritic Cell Trafficking through Infected Tissues. *Cell Host Microbe* *6*, 331–342. <https://doi.org/10.1016/j.chom.2009.09.004>.
34. Masri, M.F. Bin, Mantri, C.K., Rathore, A.P.S., and John, A.L. St. (2019). Peripheral serotonin causes dengue virus–induced thrombocytopenia through 5HT2 receptors. *Blood* *133*, 2325–2337. <https://doi.org/10.1182/blood-2018-08-869156>.
35. Rathore, A.P.S., Mantri, C.K., Aman, S.A.B., Syenina, A., Ooi, J., Jagaraj, C.J., Goh, C.C., Tissera, H., Wilder-Smith, A., Ng, L.G., et al. (2019). Dengue virus–elicited tryptase induces endothelial permeability and shock. *Journal of Clinical Investigation* *129*, 4180–4193. <https://doi.org/10.1172/JCI128426>.

36. Trivedi, N.H., Guentzel, M.N., Rodriguez, A.R., Yu, J.-J., Forsthuber, T.G., and Arulanandam, B.P. (2013). Mast cells: multitasking facilitators of protection against bacterial pathogens. *Expert Rev Clin Immunol* 9, 129–138. <https://doi.org/10.1586/eci.12.95>.
37. Chen, X., Feng, B.-S., Zheng, P.-Y., Liao, X.-Q., Chong, J., Tang, S.-G., and Yang, P.-C. (2008). Fc Gamma Receptor Signaling in Mast Cells Links Microbial Stimulation to Mucosal Immune Inflammation in the Intestine. *Am J Pathol* 173, 1647–1656. <https://doi.org/10.2353/ajpath.2008.080487>.
38. Malaviya, R., and Abraham, S.N. (2000). Role of mast cell leukotrienes in neutrophil recruitment and bacterial clearance in infectious peritonitis. *J Leukoc Biol* 67, 841–846. <https://doi.org/10.1002/jlb.67.6.841>.
39. Gekara, N.O., and Weiss, S. (2008). Mast cells initiate early anti-*Listeria* host defences. *Cell Microbiol* 10, 225–236. <https://doi.org/10.1111/j.1462-5822.2007.01033.x>.
40. Thakurdas, S.M., Melicoff, E., Sansores-Garcia, L., Moreira, D.C., Petrova, Y., Stevens, R.L., and Adachi, R. (2007). The Mast Cell-restricted Tryptase mMCP-6 Has a Critical Immunoprotective Role in Bacterial Infections. *Journal of Biological Chemistry* 282, 20809–20815. <https://doi.org/10.1074/jbc.M611842200>.
41. Dawicki, W., Jawdat, D.W., Xu, N., and Marshall, J.S. (2010). Mast Cells, Histamine, and IL-6 Regulate the Selective Influx of Dendritic Cell Subsets into an Inflamed Lymph Node. *The Journal of Immunology* 184, 2116–2123. <https://doi.org/10.4049/jimmunol.0803894>.
42. von Köckritz-Blickwede, M., Goldmann, O., Thulin, P., Heinemann, K., Norrby-Teglund, A., Rohde, M., and Medina, E. (2008). Phagocytosis-independent antimicrobial activity of mast cells by means of extracellular trap formation. *Blood* 111, 3070–3080. <https://doi.org/10.1182/blood-2007-07-104018>.

43. Abel, J., Goldmann, O., Ziegler, C., Höltje, C., Smeltzer, M.S., Cheung, A.L., Bruhn, D., Rohde, M., and Medina, E. (2011). Staphylococcus aureus Evades the Extracellular Antimicrobial Activity of Mast Cells by Promoting Its Own Uptake. *J Innate Immun* 3, 495–507. <https://doi.org/10.1159/000327714>.
44. Di Nardo, A., Yamasaki, K., Dorschner, R.A., Lai, Y., and Gallo, R.L. (2008). Mast Cell Cathelicidin Antimicrobial Peptide Prevents Invasive Group A *Streptococcus* Infection of the Skin. *The Journal of Immunology* 180, 7565–7573. <https://doi.org/10.4049/jimmunol.180.11.7565>.
45. Lin, T.-J., Garduno, R., Boudreau, R.T.M., and Issekutz, A.C. (2002). *Pseudomonas aeruginosa* Activates Human Mast Cells to Induce Neutrophil Transendothelial Migration Via Mast Cell-Derived IL-1 α and β . *The Journal of Immunology* 169, 4522–4530. <https://doi.org/10.4049/jimmunol.169.8.4522>.
46. Saxena, S., Singh, A., and Singh, P. (2020). Tumor associated mast cells: biological roles and therapeutic applications. *Anat Cell Biol* 53, 245–251. <https://doi.org/10.5115/acb.19.181>.
47. Derakhshani, A., Vahidian, F., Alihasanzadeh, M., Mokhtarzadeh, A., Lotfi Nezhad, P., and Baradaran, B. (2019). Mast cells: A double-edged sword in cancer. *Immunol Lett* 209, 28–35. <https://doi.org/10.1016/j.imlet.2019.03.011>.
48. Varricchi, G., Galdiero, M.R., Loffredo, S., Marone, G., Iannone, R., Marone, G., and Granata, F. (2017). Are Mast Cells MASTers in Cancer? *Front Immunol* 8, 261015. <https://doi.org/10.3389/fimmu.2017.00424>.
49. Oldford, S.A., and Marshall, J.S. (2015). Mast cells as targets for immunotherapy of solid tumors. *Mol Immunol* 63, 113–124. <https://doi.org/10.1016/j.molimm.2014.02.020>.

50. Burke, S.M., Issekutz, T.B., Mohan, K., Lee, P.W.K., Shmulevitz, M., and Marshall, J.S. (2008). Human mast cell activation with virus-associated stimuli leads to the selective chemotaxis of natural killer cells by a CXCL8-dependent mechanism. *Blood* *111*, 5467–5476. <https://doi.org/10.1182/blood-2007-10-118547>.
51. Kaesler, S., Wölbing, F., Kempf, W.E., Skabytska, Y., Köberle, M., Volz, T., Sinnberg, T., Amaral, T., Möckel, S., Yazdi, A., et al. (2019). Targeting tumor-resident mast cells for effective anti-melanoma immune responses. *JCI Insight* *4*, e125057. <https://doi.org/10.1172/jci.insight.125057>.
52. Drobits, B., Holcman, M., Amberg, N., Swiecki, M., Grundtner, R., Hammer, M., Colonna, M., and Sibilio, M. (2012). Imiquimod clears tumors in mice independent of adaptive immunity by converting pDCs into tumor-killing effector cells. *Journal of Clinical Investigation* *122*, 575–585. <https://doi.org/10.1172/JCI61034>.
53. Shikotra, A., Ohri, C.M., Green, R.H., Waller, D.A., and Bradding, P. (2016). Mast cell phenotype, TNF α expression and degranulation status in non-small cell lung cancer. *Sci Rep* *6*, 38352. <https://doi.org/10.1038/srep38352>.
54. Rabelo Melo, F., Santosh Martin, S., Sommerhoff, C.P., and Pejler, G. (2019). Exosome-mediated uptake of mast cell tryptase into the nucleus of melanoma cells: a novel axis for regulating tumor cell proliferation and gene expression. *Cell Death Dis* *10*, 659. <https://doi.org/10.1038/s41419-019-1879-4>.
55. Tchougounova, E., Lundequist, A., Fajardo, I., Winberg, J.-O., Åbrink, M., and Pejler, G. (2005). A Key Role for Mast Cell Chymase in the Activation of Pro-matrix Metalloprotease-9 and Pro-matrix Metalloprotease-2. *Journal of Biological Chemistry* *280*, 9291–9296. <https://doi.org/10.1074/jbc.M410396200>.

56. Tatler, A.L., Porte, J., Knox, A., Jenkins, G., and Pang, L. (2008). Tryptase activates TGF β in human airway smooth muscle cells via direct proteolysis. *Biochem Biophys Res Commun* 370, 239–242. <https://doi.org/10.1016/j.bbrc.2008.03.064>.
57. Chen, Y., Li, C., Xie, H., Fan, Y., Yang, Z., Ma, J., He, D., and Li, L. (2017). Infiltrating mast cells promote renal cell carcinoma angiogenesis by modulating PI3K→AKT→GSK3 β →AM signaling. *Oncogene* 36, 2879–2888. <https://doi.org/10.1038/onc.2016.442>.
58. Ammendola, M., Leporini, C., Marech, I., Gadaleta, C.D., Scognamillo, G., Sacco, R., Sammarco, G., De Sarro, G., Russo, E., and Ranieri, G. (2014). Targeting Mast Cells Tryptase in Tumor Microenvironment: A Potential Antiangiogenic Strategy. *Biomed Res Int* 2014, 1–16. <https://doi.org/10.1155/2014/154702>.
59. Komi, D.E.A., and Redegeld, F.A. (2020). Role of Mast Cells in Shaping the Tumor Microenvironment. *Clin Rev Allergy Immunol* 58, 313–325. <https://doi.org/10.1007/s12016-019-08753-w>.
60. Oldford, S.A., Haidl, I.D., Howatt, M.A., Leiva, C.A., Johnston, B., and Marshall, J.S. (2010). A Critical Role for Mast Cells and Mast Cell-Derived IL-6 in TLR2-Mediated Inhibition of Tumor Growth. *The Journal of Immunology* 185, 7067–7076. <https://doi.org/10.4049/jimmunol.1001137>.
61. Fereydouni, M., Motaghd, M., Ahani, E., Kafri, T., Dellinger, K., Metcalfe, D.D., and Kepley, C.L. (2022). Harnessing the Anti-Tumor Mediators in Mast Cells as a New Strategy for Adoptive Cell Transfer for Cancer. *Front Oncol* 12, 830199. <https://doi.org/10.3389/fonc.2022.830199>.
62. Liu, Z., Shi, M., Ren, Y., Xu, H., Weng, S., Ning, W., Ge, X., Liu, L., Guo, C., Duo, M., et al. (2023). Recent advances and applications of CRISPR-Cas9 in cancer immunotherapy. *Mol Cancer* 22, 35. <https://doi.org/10.1186/s12943-023-01738-6>.

63. Cao, M., and Gao, Y. (2024). Mast cell stabilizers: from pathogenic roles to targeting therapies. *Front Immunol* 15, 1418897. <https://doi.org/10.3389/fimmu.2024.1418897>.
64. Terhorst-Molawi, D., Hawro, T., Grekowitz, E., Kiefer, L., Merchant, K., Alvarado, D., Thomas, L.J., Hawthorne, T., Crowley, E., Heath-Chiozzi, M., et al. (2023). Anti-KIT antibody, barzolvolimab, reduces skin mast cells and disease activity in chronic inducible urticaria. *Allergy* 78, 1269–1279. <https://doi.org/10.1111/all.15585>.
65. Ma, Y., Hwang, R.F., Logsdon, C.D., and Ullrich, S.E. (2013). Dynamic Mast Cell–Stromal Cell Interactions Promote Growth of Pancreatic Cancer. *Cancer Res* 73, 3927–3937. <https://doi.org/10.1158/0008-5472.CAN-12-4479>.
66. Falcone, F.H., Wan, D., Barwary, N., and Sagi-Eisenberg, R. (2018). <sc>RBL</sc> cells as models for in vitro studies of mast cells and basophils. *Immunol Rev* 282, 47–57. <https://doi.org/10.1111/imr.12628>.
67. Staats, H.F., Kirwan, S.M., Choi, H.W., Shelburne, C.P., Abraham, S.N., Leung, G.Y.C., and Chen, D.Y.-K. (2013). A mast cell degranulation screening assay for the identification of novel mast cell activating agents. *Medchemcomm* 4, 88–94. <https://doi.org/10.1039/C2MD20073B>.
68. Wagner, A., Alam, S.B., and Kulka, M. (2023). The effects of age, origin, and biological sex on rodent mast cell (BMHC and MC/9) and basophil (RBL-2H3) phenotype and function. *Cell Immunol* 391–392, 104751. <https://doi.org/10.1016/j.cellimm.2023.104751>.
69. Yu, T., He, Z., Yang, M., Song, J., Ma, C., Ma, S., Feng, J., Liu, B., Wang, X., Wei, Z., et al. (2018). The development of methods for primary mast cells in vitro and ex vivo: An historical review. *Exp Cell Res* 369, 179–186. <https://doi.org/10.1016/j.yexcr.2018.05.030>.

70. West, P.W., and Bulfone-Paus, S. (2022). Mast cell tissue heterogeneity and specificity of immune cell recruitment. *Front Immunol* *13*, 932090. <https://doi.org/10.3389/fimmu.2022.932090>.
71. Malbec, O., Roget, K., Schiffer, C., Iannascoli, B., Dumas, A.R., Arock, M., and Daëron, M. (2007). Peritoneal cell-derived mast cells: an in vitro model of mature serosal-type mouse mast cells. *J Immunol* *178*, 6465–6475. <https://doi.org/10.4049/jimmunol.178.10.6465>.
72. Meurer, S.K., Neß, M., Weiskirchen, S., Kim, P., Tag, C.G., Kauffmann, M., Huber, M., and Weiskirchen, R. (2016). Isolation of Mature (Peritoneum-Derived) Mast Cells and Immature (Bone Marrow-Derived) Mast Cell Precursors from Mice. *PLoS One* *11*, e0158104. <https://doi.org/10.1371/journal.pone.0158104>.
73. Akula, S., Paivandy, A., Fu, Z., Thorpe, M., Pejler, G., and Hellman, L. (2020). How Relevant Are Bone Marrow-Derived Mast Cells (BMMCs) as Models for Tissue Mast Cells? A Comparative Transcriptome Analysis of BMMCs and Peritoneal Mast Cells. *Cells* *9*, 2118. <https://doi.org/10.3390/cells9092118>.
74. Arock, M., Wedeh, G., Hoermann, G., Bibi, S., Akin, C., Peter, B., Gleixner, K. V., Hartmann, K., Butterfield, J.H., Metcalfe, D.D., et al. (2018). Preclinical human models and emerging therapeutics for advanced systemic mastocytosis. *Haematologica* *103*, 1760–1771. <https://doi.org/10.3324/haematol.2018.195867>.
75. Guhl, S., Babina, M., Neou, A., Zuberbier, T., and Artuc, M. (2010). Mast cell lines HMC-1 and LAD2 in comparison with mature human skin mast cells--drastically reduced levels of tryptase and chymase in mast cell lines. *Exp Dermatol* *19*, 845–847. <https://doi.org/10.1111/j.1600-0625.2010.01103.x>.
76. Rådinger, M., Jensen, B.M., Kuehn, H.S., Kirshenbaum, A., and Gilfillan, A.M. (2010). Generation, Isolation, and Maintenance of Human Mast Cells and Mast Cell Lines Derived from Peripheral Blood or Cord Blood. *Curr Protoc Immunol* *90*, Unit 7.37. <https://doi.org/10.1002/0471142735.im0737s90>.

77. Bakhshab, S., Banafea, G.H., Ahmed, F., Alsehli, H., AlShaibi, H.F., Bagatian, N., Subhi, O., Gauthaman, K., Rasool, M., Schulten, H.-J., et al. (2023). Characterization of human umbilical cord blood-derived mast cells using high-throughput expression profiling and next-generation knowledge discovery platforms. *Exp Mol Pathol* 132–133, 104867. <https://doi.org/10.1016/j.yexmp.2023.104867>.
78. Reber, L.L., Marichal, T., and Galli, S.J. (2012). New models for analyzing mast cell functions in vivo. *Trends Immunol* 33, 613–625. <https://doi.org/10.1016/j.it.2012.09.008>.
79. Grimbaldston, M.A., Chen, C.-C., Piliponsky, A.M., Tsai, M., Tam, S.-Y., and Galli, S.J. (2005). Mast Cell-Deficient *W-sash c-kit* Mutant *Kit^{W-sh/W-sh}* Mice as a Model for Investigating Mast Cell Biology in Vivo. *Am J Pathol* 167, 835–848. [https://doi.org/10.1016/S0002-9440\(10\)62055-X](https://doi.org/10.1016/S0002-9440(10)62055-X).
80. Lilla, J.N., Chen, C.-C., Mukai, K., BenBarak, M.J., Franco, C.B., Kalesnikoff, J., Yu, M., Tsai, M., Piliponsky, A.M., and Galli, S.J. (2011). Reduced mast cell and basophil numbers and function in *Cpa3-Cre; Mcl-1^{fl/fl}* mice. *Blood* 118, 6930–6938. <https://doi.org/10.1182/blood-2011-03-343962>.
81. Didichenko, S.A., Spiegl, N., Brunner, T., and Dahinden, C.A. (2008). IL-3 induces a *Pim1*-dependent antiapoptotic pathway in primary human basophils. *Blood* 112, 3949–3958. <https://doi.org/10.1182/blood-2008-04-149419>.
82. Gaudenzio, N., Sibilano, R., Starkl, P., Tsai, M., Galli, S.J., and Reber, L.L. (2015). Analyzing the Functions of Mast Cells In Vivo Using “Mast Cell Knock-in” Mice. *J Vis Exp* 2015, e52753. <https://doi.org/10.3791/52753>.
83. Ishikawa, H., and Barber, G.N. (2008). STING is an endoplasmic reticulum adaptor that facilitates innate immune signalling. *Nature* 455, 674–678. <https://doi.org/10.1038/nature07317>.

84. Decout, A., Katz, J.D., Venkatraman, S., and Ablasser, A. (2021). The cGAS–STING pathway as a therapeutic target in inflammatory diseases. *Nat Rev Immunol* 21, 548–569. <https://doi.org/10.1038/s41577-021-00524-z>.
85. Ahn, J., and Barber, G.N. (2019). STING signaling and host defense against microbial infection. *Exp Mol Med* 51, 1–10. <https://doi.org/10.1038/s12276-019-0333-0>.
86. Motwani, M., Pesiridis, S., and Fitzgerald, K.A. (2019). DNA sensing by the cGAS–STING pathway in health and disease. *Nat Rev Genet* 20, 657–674. <https://doi.org/10.1038/s41576-019-0151-1>.
87. Zhang, X., Shi, H., Wu, J., Zhang, X., Sun, L., Chen, C., and Chen, Z.J. (2013). Cyclic GMP-AMP Containing Mixed Phosphodiester Linkages Is An Endogenous High-Affinity Ligand for STING. *Mol Cell* 51, 226–235. <https://doi.org/10.1016/j.molcel.2013.05.022>.
88. Marinho, F. V., Benmerzoug, S., Oliveira, S.C., Ryffel, B., and Quesniaux, V.F.J. (2017). The Emerging Roles of STING in Bacterial Infections. *Trends Microbiol* 25, 906–918. <https://doi.org/10.1016/j.tim.2017.05.008>.
89. Zhang, X., Bai, X., and Chen, Z.J. (2020). Structures and Mechanisms in the cGAS-STING Innate Immunity Pathway. *Immunity* 53, 43–53. <https://doi.org/10.1016/j.immuni.2020.05.013>.
90. Lam, E., Stein, S., and Falck-Pedersen, E. (2014). Adenovirus detection by the cGAS/STING/TBK1 DNA sensing cascade. *J Virol* 88, 974–981. <https://doi.org/10.1128/JVI.02702-13>.
91. Ishikawa, H., Ma, Z., and Barber, G.N. (2009). STING regulates intracellular DNA-mediated, type I interferon-dependent innate immunity. *Nature* 461, 788–792. <https://doi.org/10.1038/nature08476>.

92. Lio, C.-W.J., McDonald, B., Takahashi, M., Dhanwani, R., Sharma, N., Huang, J., Pham, E., Benedict, C.A., and Sharma, S. (2016). cGAS-STING Signaling Regulates Initial Innate Control of Cytomegalovirus Infection. *J Virol* *90*, 7789–7797. <https://doi.org/10.1128/JVI.01040-16>.
93. Gao, D., Wu, J., Wu, Y.-T., Du, F., Aroh, C., Yan, N., Sun, L., and Chen, Z.J. (2013). Cyclic GMP-AMP Synthase Is an Innate Immune Sensor of HIV and Other Retroviruses. *Science* (1979) *341*, 903–906. <https://doi.org/10.1126/science.1240933>.
94. Amurri, L., Horvat, B., and Iampietro, M. (2023). Interplay between RNA viruses and cGAS/STING axis in innate immunity. *Front Cell Infect Microbiol* *13*, 1172739. <https://doi.org/10.3389/fcimb.2023.1172739>.
95. Lanng, K.R.B., Lauridsen, E.L., and Jakobsen, M.R. (2024). The balance of STING signaling orchestrates immunity in cancer. *Nat Immunol* *25*, 1144–1157. <https://doi.org/10.1038/s41590-024-01872-3>.
96. Liu, Y., and Pu, F. (2023). Updated roles of cGAS-STING signaling in autoimmune diseases. *Front Immunol* *14*, 1254915. <https://doi.org/10.3389/fimmu.2023.1254915>.
97. Lukhele, S., Boukhaled, G.M., and Brooks, D.G. (2019). Type I interferon signaling, regulation and gene stimulation in chronic virus infection. *Semin Immunol* *43*, 101277. <https://doi.org/10.1016/j.smim.2019.05.001>.
98. Ji, L., Li, T., Chen, H., Yang, Y., Lu, E., Liu, J., Qiao, W., and Chen, H. (2023). The crucial regulatory role of type I interferon in inflammatory diseases. *Cell Biosci* *13*, 230. <https://doi.org/10.1186/s13578-023-01188-z>.
99. Schneider, W.M., Chevillotte, M.D., and Rice, C.M. (2014). Interferon-Stimulated Genes: A Complex Web of Host Defenses. *Annu Rev Immunol* *32*, 513–545. <https://doi.org/10.1146/annurev-immunol-032713-120231>.

100. Ou, L., Zhang, A., Cheng, Y., and Chen, Y. (2021). The cGAS-STING Pathway: A Promising Immunotherapy Target. *Front Immunol* *12*, 795048. <https://doi.org/10.3389/fimmu.2021.795048>.
101. Nicolai, C.J., Wolf, N., Chang, I.-C., Kirn, G., Marcus, A., Ndubaku, C.O., McWhirter, S.M., and Raulet, D.H. (2020). NK cells mediate clearance of CD8+ T cell-resistant tumors in response to STING agonists. *Sci Immunol* *5*, eaaz2738. <https://doi.org/10.1126/sciimmunol.aaz2738>.
102. Woo, S.-R., Fuertes, M.B., Corrales, L., Spranger, S., Furdyna, M.J., Leung, M.Y.K., Duggan, R., Wang, Y., Barber, G.N., Fitzgerald, K.A., et al. (2014). STING-dependent cytosolic DNA sensing mediates innate immune recognition of immunogenic tumors. *Immunity* *41*, 830–842. <https://doi.org/10.1016/j.immuni.2014.10.017>.
103. Gutjahr, A., Papagno, L., Nicoli, F., Kanuma, T., Kuse, N., Cabral-Piccin, M.P., Rochereau, N., Gostick, E., Lioux, T., Perouzel, E., et al. (2019). The STING ligand cGAMP potentiates the efficacy of vaccine-induced CD8+ T cells. *JCI Insight* *4*, e125107. <https://doi.org/10.1172/jci.insight.125107>.
104. Ohkuri, T., Kosaka, A., Ishibashi, K., Kumai, T., Hirata, Y., Ohara, K., Nagato, T., Oikawa, K., Aoki, N., Harabuchi, Y., et al. (2017). Intratumoral administration of cGAMP transiently accumulates potent macrophages for anti-tumor immunity at a mouse tumor site. *Cancer Immunology, Immunotherapy* *66*, 705–716. <https://doi.org/10.1007/s00262-017-1975-1>.
105. Nagata, M., Kosaka, A., Yajima, Y., Yasuda, S., Ohara, M., Ohara, K., Harabuchi, S., Hayashi, R., Funakoshi, H., Ueda, J., et al. (2021). A critical role of STING-triggered tumor-migrating neutrophils for anti-tumor effect of intratumoral cGAMP treatment. *Cancer Immunology, Immunotherapy* *70*, 2301–2312. <https://doi.org/10.1007/s00262-021-02864-0>.

106. Larkin, B., Ilyukha, V., Sorokin, M., Buzdin, A., Vannier, E., and Poltorak, A. (2017). Cutting Edge: Activation of STING in T Cells Induces Type I IFN Responses and Cell Death. *The Journal of Immunology* *199*, 397–402. <https://doi.org/10.4049/jimmunol.1601999>.
107. Kuhl, N., Linder, A., Philipp, N., Nixdorf, D., Fischer, H., Veth, S., Kuut, G., Xu, T.T., Theurich, S., Carell, T., et al. (2023). STING agonism turns human T cells into interferon-producing cells but impedes their functionality. *EMBO Rep* *24*, e55536. <https://doi.org/10.15252/embr.202255536>.
108. Cheng, Z., Dai, T., He, X., Zhang, Z., Xie, F., Wang, S., Zhang, L., and Zhou, F. (2020). The interactions between cGAS-STING pathway and pathogens. *Signal Transduct Target Ther* *5*, 91. <https://doi.org/10.1038/s41392-020-0198-7>.
109. Chauvin, S.D., Stinson, W.A., Platt, D.J., Poddar, S., and Miner, J.J. (2023). Regulation of cGAS and STING signaling during inflammation and infection. *Journal of Biological Chemistry* *299*, 104866. <https://doi.org/10.1016/j.jbc.2023.104866>.
110. Patel, S., and Jin, L. (2019). TMEM173 variants and potential importance to human biology and disease. *Genes Immun* *20*, 82–89. <https://doi.org/10.1038/s41435-018-0029-9>.
111. Patel, S., Blaauboer, S.M., Tucker, H.R., Mansouri, S., Ruiz-Moreno, J.S., Hamann, L., Schumann, R.R., Opitz, B., and Jin, L. (2017). The Common R71H-G230A-R293Q Human TMEM173 Is a Null Allele. *J Immunol* *198*, 776–787. <https://doi.org/10.4049/jimmunol.1601585>.
112. Jin, L., Xu, L., Yang, I. V, Davidson, E.J., Schwartz, D.A., Wurfel, M.M., and Cambier, J.C. (2011). Identification and characterization of a loss-of-function human MPYS variant. *Genes Immun* *12*, 263–269. <https://doi.org/10.1038/gene.2010.75>.

113. Ruiz-Moreno, J.S., Hamann, L., Shah, J.A., Verbon, A., Mockenhaupt, F.P., Puzianowska-Kuznicka, M., Naujoks, J., Sander, L.E., Witzenth, M., Cambier, J.C., et al. (2018). The common HAQ STING variant impairs cGAS-dependent antibacterial responses and is associated with susceptibility to Legionnaires' disease in humans. *PLoS Pathog* *14*, e1006829. <https://doi.org/10.1371/journal.ppat.1006829>.
114. Froechlich, G., Finizio, A., Napolano, A., Amiranda, S., De Chiara, A., Pagano, P., Mallardo, M., Leoni, G., Zambrano, N., and Sasso, E. (2023). The common H232 STING allele shows impaired activities in DNA sensing, susceptibility to viral infection, and in monocyte cell function, while the HAQ variant possesses wild-type properties. *Sci Rep* *13*, 19541. <https://doi.org/10.1038/s41598-023-46830-5>.
115. Dai, Y., Liu, X., Zhao, Z., He, J., and Yin, Q. (2020). Stimulator of Interferon Genes-Associated Vasculopathy With Onset in Infancy: A Systematic Review of Case Reports. *Front Pediatr* *8*, 577918. <https://doi.org/10.3389/fped.2020.577918>.
116. Valeri, E., Breggion, S., Barzaghi, F., Abou Alezz, M., Crivicich, G., Pagani, I., Forneris, F., Sartirana, C., Costantini, M., Costi, S., et al. (2024). A novel STING variant triggers endothelial toxicity and SAVI disease. *J Exp Med* *221*. <https://doi.org/10.1084/jem.20232167>.
117. Warner, J.D., Irizarry-Caro, R.A., Bennion, B.G., Ai, T.L., Smith, A.M., Miner, C.A., Sakai, T., Gonugunta, V.K., Wu, J., Platt, D.J., et al. (2017). STING-associated vasculopathy develops independently of IRF3 in mice. *Journal of Experimental Medicine* *214*, 3279–3292. <https://doi.org/10.1084/jem.20171351>.
118. Bouis, D., Kirstetter, P., Arbogast, F., Lamon, D., Delgado, V., Jung, S., Ebel, C., Jacobs, H., Knapp, A.-M., Jeremiah, N., et al. (2019). Severe combined immunodeficiency in stimulator of interferon genes (STING) V154M/wild-type mice. *Journal of Allergy and Clinical Immunology* *143*, 712-725.e5. <https://doi.org/10.1016/j.jaci.2018.04.034>.

119. Lohinai, Z., Dora, D., Caldwell, C., Rivard, C.J., Suda, K., Yu, H., Rivalland, G., Ellison, K., Rozeboom, L., Dziadziuszko, R., et al. (2022). Loss of STING expression is prognostic in non-small cell lung cancer. *J Surg Oncol* *125*, 1042–1052. <https://doi.org/10.1002/jso.26804>.
120. Kim, Y., Cho, N.-Y., Jin, L., Jin, H.Y., and Kang, G.H. (2023). Prognostic significance of STING expression in solid tumor: a systematic review and meta-analysis. *Front Oncol* *13*, 1244962. <https://doi.org/10.3389/fonc.2023.1244962>.
121. Della Corte, C.M., Sen, T., Gay, C.M., Ramkumar, K., Diao, L., Cardnell, R.J., Rodriguez, B.L., Stewart, C.A., Papadimitrakopoulou, V.A., Gibson, L., et al. (2020). STING Pathway Expression Identifies NSCLC With an Immune-Responsive Phenotype. *Journal of Thoracic Oncology* *15*, 777–791. <https://doi.org/10.1016/j.jtho.2020.01.009>.
122. Storozynsky, Q., and Hitt, M.M. (2020). The Impact of Radiation-Induced DNA Damage on cGAS-STING-Mediated Immune Responses to Cancer. *Int J Mol Sci* *21*, 8877. <https://doi.org/10.3390/ijms21228877>.
123. Xia, T., Konno, H., and Barber, G.N. (2016). Recurrent Loss of STING Signaling in Melanoma Correlates with Susceptibility to Viral Oncolysis. *Cancer Res* *76*, 6747–6759. <https://doi.org/10.1158/0008-5472.CAN-16-1404>.
124. Goldmann, O., Sauerwein, T., Molinari, G., Rohde, M., Förstner, K.U., and Medina, E. (2022). Cytosolic Sensing of Intracellular *Staphylococcus aureus* by Mast Cells Elicits a Type I IFN Response That Enhances Cell-Autonomous Immunity. *The Journal of Immunology* *208*, 1675–1685. <https://doi.org/10.4049/jimmunol.2100622>.
125. Dietrich, N., Rohde, M., Geffers, R., Kröger, A., Hauser, H., Weiss, S., and Gekara, N.O. (2010). Mast cells elicit proinflammatory but not type I interferon responses upon activation of TLRs by bacteria. *Proceedings of the National Academy of Sciences* *107*, 8748–8753. <https://doi.org/10.1073/pnas.0912551107>.

126. Chen, H., Sun, H., You, F., Sun, W., Zhou, X., Chen, L., Yang, J., Wang, Y., Tang, H., Guan, Y., et al. (2011). Activation of STAT6 by STING Is Critical for Antiviral Innate Immunity. *Cell* 147, 436–446.
<https://doi.org/10.1016/j.cell.2011.09.022>.
127. Martin, T.L., Jee, J., Kim, E., Steiner, H.E., Cormet-Boyaka, E., and Boyaka, P.N. (2017). Sublingual targeting of STING with 3'3'-cGAMP promotes systemic and mucosal immunity against anthrax toxins. *Vaccine* 35, 2511–2519.
<https://doi.org/10.1016/j.vaccine.2017.02.064>.
128. Valeri, V., Tonon, S., Vibhushan, S., Gulino, A., Belmonte, B., Adori, M., Karlsson Hedestam, G.B., Gautier, G., Tripodo, C., Blank, U., et al. (2021). Mast cells crosstalk with B cells in the gut and sustain IgA response in the inflamed intestine. *Eur J Immunol* 51, 445–458. <https://doi.org/10.1002/eji.202048668>.
129. Merluzzi, S., Frossi, B., Gri, G., Parusso, S., Tripodo, C., and Pucillo, C. (2010). Mast cells enhance proliferation of B lymphocytes and drive their differentiation toward IgA-secreting plasma cells. *Blood* 115, 2810–2817.
<https://doi.org/10.1182/blood-2009-10-250126>.
130. De Giovanni, M., Vykunta, V.S., Biram, A., Chen, K.Y., Taglinao, H., An, J., Sheppard, D., Paidassi, H., and Cyster, J.G. (2024). Mast cells help organize the Peyer's patch niche for induction of IgA responses. *Sci Immunol* 9, eadj7363.
<https://doi.org/10.1126/sciimmunol.adj7363>.
131. Liu, N., Pang, X., Zhang, H., and Ji, P. (2022). The cGAS-STING Pathway in Bacterial Infection and Bacterial Immunity. *Front Immunol* 12, 814709.
<https://doi.org/10.3389/fimmu.2021.814709>.
132. Boxx, G.M., and Cheng, G. (2016). The Roles of Type I Interferon in Bacterial Infection. *Cell Host Microbe* 19, 760–769.
<https://doi.org/10.1016/j.chom.2016.05.016>.

133. Danilchanka, O., and Mekalanos, J.J. (2013). Cyclic Dinucleotides and the Innate Immune Response. *Cell* 154, 962–970. <https://doi.org/10.1016/j.cell.2013.08.014>.
134. Louie, A., Bhandula, V., and Portnoy, D.A. (2020). Secretion of c-di-AMP by *Listeria monocytogenes* Leads to a STING-Dependent Antibacterial Response during Enterocolitis. *Infect Immun* 88. <https://doi.org/10.1128/IAI.00407-20>.
135. Shi, C., Hohl, T.M., Leiner, I., Equinda, M.J., Fan, X., and Pamer, E.G. (2011). Ly6G⁺ Neutrophils Are Dispensable for Defense against Systemic *Listeria monocytogenes* Infection. *The Journal of Immunology* 187, 5293–5298. <https://doi.org/10.4049/jimmunol.1101721>.
136. Gries, C.M., Bruger, E.L., Moormeier, D.E., Scherr, T.D., Waters, C.M., and Kielian, T. (2016). Cyclic di-AMP Released from *Staphylococcus aureus* Biofilm Induces a Macrophage Type I Interferon Response. *Infect Immun* 84, 3564–3574. <https://doi.org/10.1128/IAI.00447-16>.
137. Scumpia, P.O., Botten, G.A., Norman, J.S., Kelly-Scumpia, K.M., Spreafico, R., Ruccia, A.R., Purbey, P.K., Thomas, B.J., Modlin, R.L., and Smale, S.T. (2017). Opposing roles of Toll-like receptor and cytosolic DNA-STING signaling pathways for *Staphylococcus aureus* cutaneous host defense. *PLoS Pathog* 13, e1006496. <https://doi.org/10.1371/journal.ppat.1006496>.
138. Hansen, K., Prabakaran, T., Laustsen, A., Jørgensen, S.E., Rahbæk, S.H., Jensen, S.B., Nielsen, R., Leber, J.H., Decker, T., Horan, K.A., et al. (2014). *Listeria monocytogenes* induces IFN β expression through an IFI16-, cGAS- and STING-dependent pathway. *EMBO J* 33, 1654–1666. <https://doi.org/10.15252/embj.201488029>.
139. Zhou, C., Wang, B., Wu, Q., Lin, P., Qin, S., Pu, Q., Yu, X., and Wu, M. (2021). Identification of cGAS as an innate immune sensor of extracellular bacterium *Pseudomonas aeruginosa*. *iScience* 24, 101928. <https://doi.org/10.1016/j.isci.2020.101928>.

140. Watson, R.O., Bell, S.L., MacDuff, D.A., Kimmey, J.M., Diner, E.J., Olivas, J., Vance, R.E., Stallings, C.L., Virgin, H.W., and Cox, J.S. (2015). The Cytosolic Sensor cGAS Detects Mycobacterium tuberculosis DNA to Induce Type I Interferons and Activate Autophagy. *Cell Host Microbe* *17*, 811–819. <https://doi.org/10.1016/j.chom.2015.05.004>.
141. Gratz, N., Hartweger, H., Matt, U., Kratochvill, F., Janos, M., Sigel, S., Drobits, B., Li, X.-D., Knapp, S., and Kovarik, P. (2011). Type I Interferon Production Induced by Streptococcus pyogenes-Derived Nucleic Acids Is Required for Host Protection. *PLoS Pathog* *7*, e1001345. <https://doi.org/10.1371/journal.ppat.1001345>.
142. Castiglia, V., Piersigilli, A., Ebner, F., Janos, M., Goldmann, O., Damböck, U., Kröger, A., Weiss, S., Knapp, S., Jamieson, A.M., et al. (2016). Type I Interferon Signaling Prevents IL-1 β -Driven Lethal Systemic Hyperinflammation during Invasive Bacterial Infection of Soft Tissue. *Cell Host Microbe* *19*, 375–387. <https://doi.org/10.1016/j.chom.2016.02.003>.
143. Hu, X., Peng, X., Lu, C., Zhang, X., Gan, L., Gao, Y., Yang, S., Xu, W., Wang, J., Yin, Y., et al. (2019). Type I IFN expression is stimulated by cytosolic MtDNA released from pneumolysin-damaged mitochondria via the STING signaling pathway in macrophages. *FEBS J* *286*, 4754–4768. <https://doi.org/10.1111/febs.15001>.
144. Ning, L., Wei, W., Wenyang, J., Rui, X., and Qing, G. (2020). Cytosolic DNA-STING-NLRP3 axis is involved in murine acute lung injury induced by lipopolysaccharide. *Clin Transl Med* *10*, e228. <https://doi.org/10.1002/ctm2.228>.
145. Dey, B., Dey, R.J., Cheung, L.S., Pokkali, S., Guo, H., Lee, J.-H., and Bishai, W.R. (2015). A bacterial cyclic dinucleotide activates the cytosolic surveillance pathway and mediates innate resistance to tuberculosis. *Nat Med* *21*, 401–406. <https://doi.org/10.1038/nm.3813>.

146. Zhang, H., Zeng, L., Xie, M., Liu, J., Zhou, B., Wu, R., Cao, L., Kroemer, G., Wang, H., Billiar, T.R., et al. (2020). TMEM173 Drives Lethal Coagulation in Sepsis. *Cell Host Microbe* 27, 556-570.e6. <https://doi.org/10.1016/j.chom.2020.02.004>.
147. Dobbs, N., Burnaevskiy, N., Chen, D., Gonugunta, V.K., Alto, N.M., and Yan, N. (2015). STING Activation by Translocation from the ER Is Associated with Infection and Autoinflammatory Disease. *Cell Host Microbe* 18, 157–168. <https://doi.org/10.1016/j.chom.2015.07.001>.
148. Zheng, Z., Wei, C., Guan, K., Yuan, Y., Zhang, Y., Ma, S., Cao, Y., Wang, F., Zhong, H., and He, X. (2016). Bacterial E3 Ubiquitin Ligase IpaH4.5 of *Shigella flexneri* Targets TBK1 To Dampen the Host Antibacterial Response. *J Immunol* 196, 1199–1208. <https://doi.org/10.4049/jimmunol.1501045>.
149. Schnupf, P., and Sansonetti, P.J. (2019). *Shigella* Pathogenesis: New Insights through Advanced Methodologies. *Microbiol Spectr* 7. <https://doi.org/10.1128/microbiolspec.BAI-0023-2019>.
150. Aslam, A., Hashmi, M.F., and Okafor, C.N. (2025). *Shigellosis* (StatPearls Publishing).
151. Ashida, H., Mimuro, H., and Sasakawa, C. (2015). *Shigella* Manipulates Host Immune Responses by Delivering Effector Proteins with Specific Roles. *Front Immunol* 6, 219. <https://doi.org/10.3389/fimmu.2015.00219>.
152. Parsot, C. (2009). *Shigella* type III secretion effectors: how, where, when, for what purposes? *Curr Opin Microbiol* 12, 110–116. <https://doi.org/10.1016/j.mib.2008.12.002>.
153. Muthuramalingam, M., Whittier, S.K., Picking, W.L., and Picking, W.D. (2021). The *Shigella* Type III Secretion System: An Overview from Top to Bottom. *Microorganisms* 9, 451. <https://doi.org/10.3390/microorganisms9020451>.

154. Goldberg, M.B., and Theriot, J.A. (1995). *Shigella flexneri* surface protein IcsA is sufficient to direct actin-based motility. *Proceedings of the National Academy of Sciences* *92*, 6572–6576. <https://doi.org/10.1073/pnas.92.14.6572>.
155. Zaidi, M.B., and Estrada-García, T. (2014). *Shigella*: A Highly Virulent and Elusive Pathogen. *Curr Trop Med Rep* *1*, 81. <https://doi.org/10.1007/s40475-014-0019-6>.
156. Schroeder, G.N., and Hilbi, H. (2008). Molecular pathogenesis of *Shigella* spp.: controlling host cell signaling, invasion, and death by type III secretion. *Clin Microbiol Rev* *21*, 134–156. <https://doi.org/10.1128/CMR.00032-07>.
157. Ashida, H., Kim, M., and Sasakawa, C. (2014). Manipulation of the host cell death pathway by *Shigella*. *Cell Microbiol* *16*, 1757–1766. <https://doi.org/10.1111/cmi.12367>.
158. Weiner, A., Mellouk, N., Lopez-Montero, N., Chang, Y.-Y., Souque, C., Schmitt, C., and Enninga, J. (2016). Macropinosomes are Key Players in Early *Shigella* Invasion and Vacuolar Escape in Epithelial Cells. *PLoS Pathog* *12*, e1005602. <https://doi.org/10.1371/journal.ppat.1005602>.
159. Suzuki, S., Mimuro, H., Kim, M., Ogawa, M., Ashida, H., Toyotome, T., Franchi, L., Suzuki, M., Sanada, T., Suzuki, T., et al. (2014). *Shigella* IpaH7.8 E3 ubiquitin ligase targets glomulin and activates inflammasomes to demolish macrophages. *Proceedings of the National Academy of Sciences* *111*, E4254-63. <https://doi.org/10.1073/pnas.1324021111>.
160. Suzuki, S., Franchi, L., He, Y., Muñoz-Planillo, R., Mimuro, H., Suzuki, T., Sasakawa, C., and Núñez, G. (2014). *Shigella* Type III Secretion Protein MxiI Is Recognized by Naip2 to Induce Nlr4 Inflammasome Activation Independently of Pkc δ . *PLoS Pathog* *10*, e1003926. <https://doi.org/10.1371/journal.ppat.1003926>.

161. Storek, K.M., and Monack, D.M. (2015). Bacterial recognition pathways that lead to inflammasome activation. *Immunol Rev* 265, 112–129.
<https://doi.org/10.1111/imr.12289>.
162. Miao, E.A., Mao, D.P., Yudkovsky, N., Bonneau, R., Lorang, C.G., Warren, S.E., Leaf, I.A., and Aderem, A. (2010). Innate immune detection of the type III secretion apparatus through the NLRC4 inflammasome. *Proceedings of the National Academy of Sciences* 107, 3076–3080.
<https://doi.org/10.1073/pnas.0913087107>.
163. Ashida, H., Mimuro, H., and Sasakawa, C. (2015). Shigella Manipulates Host Immune Responses by Delivering Effector Proteins with Specific Roles. *Front Immunol* 6, 219. <https://doi.org/10.3389/fimmu.2015.00219>.
164. Sansonetti, P.J., Phalipon, A., Arondel, J., Thirumalai, K., Banerjee, S., Akira, S., Takeda, K., and Zychlinsky, A. (2000). Caspase-1 Activation of IL-1 β and IL-18 Are Essential for Shigella flexneri–Induced Inflammation. *Immunity* 12, 581–590.
[https://doi.org/10.1016/S1074-7613\(00\)80209-5](https://doi.org/10.1016/S1074-7613(00)80209-5).
165. Wu, Y., Zhang, J., Yu, S., Li, Y., Zhu, J., Zhang, K., and Zhang, R. (2022). Cell pyroptosis in health and inflammatory diseases. *Cell Death Discov* 8, 191.
<https://doi.org/10.1038/s41420-022-00998-3>.
166. Pore, D., Mahata, N., and Chakrabarti, M.K. (2012). Outer membrane protein A (OmpA) of Shigella flexneri 2a links innate and adaptive immunity in a TLR2-dependent manner and involvement of IL-12 and nitric oxide. *J Biol Chem* 287, 12589–12601. <https://doi.org/10.1074/jbc.M111.335554>.
167. Pore, D., Mahata, N., Pal, A., and Chakrabarti, M.K. (2010). 34 kDa MOMP of Shigella flexneri promotes TLR2 mediated macrophage activation with the engagement of NF-kappaB and p38 MAP kinase signaling. *Mol Immunol* 47, 1739–1746. <https://doi.org/10.1016/j.molimm.2010.03.001>.

168. Paciello, I., Silipo, A., Lembo-Fazio, L., Curcurù, L., Zumsteg, A., Noël, G., Ciancarella, V., Sturiale, L., Molinaro, A., and Bernardini, M.L. (2013). Intracellular *Shigella* remodels its LPS to dampen the innate immune recognition and evade inflammasome activation. *Proceedings of the National Academy of Sciences* *110*, E4345-54. <https://doi.org/10.1073/pnas.1303641110>.
169. Eislmayr, K.D., Langner, C., Liu, F.L., Yuvaraj, S., Babirye, J.P., Roncaioli, J.L., Vickery, J.M., Barton, G.M., Lesser, C.F., and Vance, R.E. (2025). Macrophages orchestrate elimination of *Shigella* from the intestinal epithelial cell niche via TLR-induced IL-12 and IFN- γ . *bioRxiv*, 2025.01.20.633976. <https://doi.org/10.1101/2025.01.20.633976>.
170. Kasper, C.A., Sorg, I., Schmutz, C., Tschon, T., Wischnewski, H., Kim, M.L., and Arrieumerlou, C. (2010). Cell-Cell Propagation of NF- κ B Transcription Factor and MAP Kinase Activation Amplifies Innate Immunity against Bacterial Infection. *Immunity* *33*, 804–816. <https://doi.org/10.1016/j.immuni.2010.10.015>.
171. Singer, M., and Sansonetti, P.J. (2004). IL-8 Is a Key Chemokine Regulating Neutrophil Recruitment in a New Mouse Model of *Shigella*- Induced Colitis. *The Journal of Immunology* *173*, 4197–4206. <https://doi.org/10.4049/jimmunol.173.6.4197>.
172. Sansonetti, P.J., Arondel, J., Huerre, M., Harada, A., and Matsushima, K. (1999). Interleukin-8 controls bacterial transepithelial translocation at the cost of epithelial destruction in experimental shigellosis. *Infect Immun* *67*, 1471–1480. <https://doi.org/10.1128/IAI.67.3.1471-1480.1999>.
173. François, M., Le Cabec, V., Dupont, M.A., Sansonetti, P.J., and Maridonneau-Parini, I. (2000). Induction of necrosis in human neutrophils by *Shigella flexneri* requires type III secretion, IpaB and IpaC invasins, and actin polymerization. *Infect Immun* *68*, 1289–1296. <https://doi.org/10.1128/IAI.68.3.1289-1296.2000>.

174. Weinrauch, Y., Drujan, D., Shapiro, S.D., Weiss, J., and Zychlinsky, A. (2002). Neutrophil elastase targets virulence factors of enterobacteria. *Nature* 417, 91–94. <https://doi.org/10.1038/417091a>.
175. Lemme-Dumit, J.M., Doucet, M., Zachos, N.C., and Pasetti, M.F. (2022). Epithelial and Neutrophil Interactions and Coordinated Response to Shigella in a Human Intestinal Enteroid-Neutrophil Coculture Model. *mBio* 13, e0094422. <https://doi.org/10.1128/mbio.00944-22>.
176. Brinkmann, V., Reichard, U., Goosmann, C., Fauler, B., Uhlemann, Y., Weiss, D.S., Weinrauch, Y., and Zychlinsky, A. (2004). Neutrophil Extracellular Traps Kill Bacteria. *Science* (1979) 303, 1532–1535. <https://doi.org/10.1126/science.1092385>.
177. Perdomo, O.J., Cavaillon, J.M., Huerre, M., Ohayon, H., Gounon, P., and Sansonetti, P.J. (1994). Acute inflammation causes epithelial invasion and mucosal destruction in experimental shigellosis. *J Exp Med* 180, 1307–1319. <https://doi.org/10.1084/jem.180.4.1307>.
178. Tavares, V., Marques, I.S., Melo, I.G. de, Assis, J., Pereira, D., and Medeiros, R. (2024). Paradigm Shift: A Comprehensive Review of Ovarian Cancer Management in an Era of Advancements. *Int J Mol Sci* 25, 1845. <https://doi.org/10.3390/ijms25031845>.
179. Garlisi, B., Lauks, S., Aitken, C., Ogilvie, L.M., Lockington, C., Petrik, D., Eichhorn, J.S., and Petrik, J. (2024). The Complex Tumor Microenvironment in Ovarian Cancer: Therapeutic Challenges and Opportunities. *Current Oncology* 31, 3826–3844. <https://doi.org/10.3390/curroncol31070283>.
180. Lheureux, S., Braunstein, M., and Oza, A.M. (2019). Epithelial ovarian cancer: Evolution of management in the era of precision medicine. *CA Cancer J Clin* 69, 280–304. <https://doi.org/10.3322/caac.21559>.

181. Matulonis, U.A., Sood, A.K., Fallowfield, L., Howitt, B.E., Sehouli, J., and Karlan, B.Y. (2016). Ovarian cancer. *Nat Rev Dis Primers* 2, 16061. <https://doi.org/10.1038/nrdp.2016.61>.
182. Veneziani, A.C., Gonzalez-Ochoa, E., Alqaisi, H., Madariaga, A., Bhat, G., Rouzbahman, M., Sneha, S., and Oza, A.M. (2023). Heterogeneity and treatment landscape of ovarian carcinoma. *Nat Rev Clin Oncol* 20, 820–842. <https://doi.org/10.1038/s41571-023-00819-1>.
183. Ali, A.T., Al-ani, O., and Al-ani, F. (2023). Epidemiology and risk factors for ovarian cancer. *Menopausal Review* 22, 93–104. <https://doi.org/10.5114/pm.2023.128661>.
184. Blanc-Durand, F., Clemence Wei Xian, L., and Tan, D.S.P. (2023). Targeting the immune microenvironment for ovarian cancer therapy. *Front Immunol* 14, 1328651. <https://doi.org/10.3389/fimmu.2023.1328651>.
185. Satora, M., Kułak, K., Zaremba, B., Grunwald, A., Świechowska-Starek, P., and Tarkowski, R. (2024). New hopes and promises in the treatment of ovarian cancer focusing on targeted treatment—a narrative review. *Front Pharmacol* 15, 1416555. <https://doi.org/10.3389/fphar.2024.1416555>.
186. Yang, Y., Yang, Y., Yang, J., Zhao, X., and Wei, X. (2020). Tumor Microenvironment in Ovarian Cancer: Function and Therapeutic Strategy. *Front Cell Dev Biol* 8, 548447. <https://doi.org/10.3389/fcell.2020.00758>.
187. Yang, L., Xie, H.-J., Li, Y.-Y., Wang, X., Liu, X.-X., and Mai, J. (2022). Molecular mechanisms of platinum-based chemotherapy resistance in ovarian cancer (Review). *Oncol Rep* 47, 82. <https://doi.org/10.3892/or.2022.8293>.
188. O’Malley, D.M., Krivak, T.C., Kabil, N., Munley, J., and Moore, K.N. (2023). PARP Inhibitors in Ovarian Cancer: A Review. *Target Oncol* 18, 471–503. <https://doi.org/10.1007/s11523-023-00970-w>.

189. Moufarrij, S., and O’Cearbhaill, R.E. (2023). Novel Therapeutics in Ovarian Cancer: Expanding the Toolbox. *Current Oncology* 31, 97–114. <https://doi.org/10.3390/currncol31010007>.
190. Wu, Y., Xu, S., Cheng, S., Yang, J., and Wang, Y. (2023). Clinical application of PARP inhibitors in ovarian cancer: from molecular mechanisms to the current status. *J Ovarian Res* 16, 6. <https://doi.org/10.1186/s13048-023-01094-5>.
191. Chandra, A., Pius, C., Nabeel, M., Nair, M., Vishwanatha, J.K., Ahmad, S., and Basha, R. (2019). Ovarian cancer: Current status and strategies for improving therapeutic outcomes. *Cancer Med* 8, 7018–7031. <https://doi.org/10.1002/cam4.2560>.
192. Birrer, M.J., Betella, I., Martin, L.P., and Moore, K.N. (2019). Is Targeting the Folate Receptor in Ovarian Cancer Coming of Age? *Oncologist* 24, 425–429. <https://doi.org/10.1634/theoncologist.2018-0459>.
193. Siminiak, N., Czepczyński, R., Zaborowski, M.P., and Iżycki, D. (2022). Immunotherapy in Ovarian Cancer. *Arch Immunol Ther Exp (Warsz)* 70, 19. <https://doi.org/10.1007/s00005-022-00655-8>.
194. Cutri-French, C., Nasioudis, D., George, E., and Tanyi, J.L. (2024). CAR-T Cell Therapy in Ovarian Cancer: Where Are We Now? *Diagnostics* 14, 819. <https://doi.org/10.3390/diagnostics14080819>.
195. Alturki, N.A. (2023). Review of the Immune Checkpoint Inhibitors in the Context of Cancer Treatment. *J Clin Med* 12, 4301. <https://doi.org/10.3390/jcm12134301>.
196. Eno, MS, PA-C, J. (2017). Immunotherapy Through the Years. *J Adv Pract Oncol* 8, 747. <https://doi.org/10.6004/jadpro.2017.8.7.8>.
197. Yoon, W.-H., DeFazio, A., and Kasherman, L. (2023). Immune checkpoint inhibitors in ovarian cancer: where do we go from here? *Cancer Drug Resistance* 6, 358–377. <https://doi.org/10.20517/cdr.2023.13>.

198. Pawłowska, A., Rekowski, A., Kuryło, W., Pańczyszyn, A., Kotarski, J., and Wertel, I. (2023). Current Understanding on Why Ovarian Cancer Is Resistant to Immune Checkpoint Inhibitors. *Int J Mol Sci* 24, 10859. <https://doi.org/10.3390/ijms241310859>.
199. Demaria, O., De Gassart, A., Coso, S., Gestermann, N., Di Domizio, J., Flatz, L., Gaide, O., Michielin, O., Hwu, P., Petrova, T. V., et al. (2015). STING activation of tumor endothelial cells initiates spontaneous and therapeutic antitumor immunity. *Proceedings of the National Academy of Sciences* 112, 15408–15413. <https://doi.org/10.1073/pnas.1512832112>.
200. Li, T., Cheng, H., Yuan, H., Xu, Q., Shu, C., Zhang, Y., Xu, P., Tan, J., Rui, Y., Li, P., et al. (2016). Antitumor Activity of cGAMP via Stimulation of cGAS-cGAMP-STING-IRF3 Mediated Innate Immune Response. *Sci Rep* 6, 19049. <https://doi.org/10.1038/srep19049>.
201. Song, C., Liu, D., Liu, S., Li, D., Horecny, I., Zhang, X., Li, P., Chen, L., Miller, M., Chowdhury, R., et al. (2022). SHR1032, a novel STING agonist, stimulates anti-tumor immunity and directly induces AML apoptosis. *Sci Rep* 12, 8579. <https://doi.org/10.1038/s41598-022-12449-1>.
202. Wang, B., Yu, W., Jiang, H., Meng, X., Tang, D., and Liu, D. (2024). Clinical applications of STING agonists in cancer immunotherapy: current progress and future prospects. *Front Immunol* 15, 1485546. <https://doi.org/10.3389/fimmu.2024.1485546>.
203. Zhu, Y., An, X., Zhang, X., Qiao, Y., Zheng, T., and Li, X. (2019). STING: a master regulator in the cancer-immunity cycle. *Molecular Cancer* 2019 18:1 18, 1–15. <https://doi.org/10.1186/S12943-019-1087-Y>.

204. Wang, H., Hu, S., Chen, X., Shi, H., Chen, C., Sun, L., and Chen, Z.J. (2017). cGAS is essential for the antitumor effect of immune checkpoint blockade. *Proceedings of the National Academy of Sciences* *114*, 1637–1642. <https://doi.org/10.1073/pnas.1621363114>.
205. Škrnjug, I., Guzmán, C.A., and Ruecker, C. (2014). Cyclic GMP-AMP Displays Mucosal Adjuvant Activity in Mice. *PLoS One* *9*, e110150. <https://doi.org/10.1371/journal.pone.0110150>.
206. Li, W., Lu, L., Lu, J., Wang, X., Yang, C., Jin, J., Wu, L., Hong, X., Li, F., Cao, D., et al. (2020). cGAS-STING-mediated DNA sensing maintains CD8+ T cell stemness and promotes antitumor T cell therapy. *Sci Transl Med* *12*, 9013. <https://doi.org/10.1126/scitranslmed.aay9013>.
207. Benoit-Lizon, I., Jacquin, E., Rivera Vargas, T., Richard, C., Roussey, A., Dal Zuffo, L., Martin, T., Melis, A., Vinokurova, D., Shahoei, S.H., et al. (2022). CD4 T cell-intrinsic STING signaling controls the differentiation and effector functions of TH1 and TH9 cells. *J Immunother Cancer* *10*, e003459. <https://doi.org/10.1136/jitc-2021-003459>.
208. Zhang, C., Ye, S., Ni, J., Cai, T., Liu, Y., Huang, D., Mai, H., Chen, Q., He, J., Zhang, X., et al. (2019). STING signaling remodels the tumor microenvironment by antagonizing myeloid-derived suppressor cell expansion. *Cell Death Differ* *26*, 2314–2328. <https://doi.org/10.1038/s41418-019-0302-0>.
209. Huang, R., Ning, Q., Zhao, J., Zhao, X., Zeng, L., Yi, Y., and Tang, S. (2022). Targeting STING for cancer immunotherapy: From mechanisms to translation. *Int Immunopharmacol* *113*, 109304. <https://doi.org/10.1016/j.intimp.2022.109304>.
210. Jiang, X., Wang, J., Zheng, X., Liu, Z., Zhang, X., Li, Y., Wilhelm, J., Cao, J., Huang, G., Zhang, J., et al. (2022). Intratumoral administration of STING-activating nanovaccine enhances T cell immunotherapy. *J Immunother Cancer* *10*, e003960. <https://doi.org/10.1136/jitc-2021-003960>.

211. Berger, G., Knelson, E.H., Jimenez-Macias, J.L., Nowicki, M.O., Han, S., Panagioti, E., Lizotte, P.H., Adu-Berchie, K., Stafford, A., Dimitrakakis, N., et al. (2022). STING activation promotes robust immune response and NK cell-mediated tumor regression in glioblastoma models. *Proc Natl Acad Sci U S A* *119*, e2111003119. <https://doi.org/10.1073/pnas.2111003119>.
212. Chon, H.J., Kim, H., Noh, J.H., Yang, H., Lee, W.S., Kong, S.J., Lee, S.J., Lee, Y.S., Kim, W.R., Kim, J.H., et al. (2019). STING signaling is a potential immunotherapeutic target in colorectal cancer. *J Cancer* *10*, 4932–4938. <https://doi.org/10.7150/jca.32806>.
213. Campisi, M., Sundararaman, S.K., Shelton, S.E., Knelson, E.H., Mahadevan, N.R., Yoshida, R., Tani, T., Ivanova, E., Cañadas, I., Osaki, T., et al. (2020). Tumor-Derived cGAMP Regulates Activation of the Vasculature. *Front Immunol* *11*, 2090. <https://doi.org/10.3389/fimmu.2020.02090>.
214. Jing, W., McAllister, D., Vonderhaar, E.P., Palen, K., Riese, M.J., Gershan, J., Johnson, B.D., and Dwinell, M.B. (2019). STING agonist inflames the pancreatic cancer immune microenvironment and reduces tumor burden in mouse models. *J Immunother Cancer* *7*, 115. <https://doi.org/10.1186/s40425-019-0573-5>.
215. Wang, Q., Bergholz, J.S., Ding, L., Lin, Z., Kabraji, S.K., Hughes, M.E., He, X., Xie, S., Jiang, T., Wang, W., et al. (2022). STING agonism reprograms tumor-associated macrophages and overcomes resistance to PARP inhibition in BRCA1-deficient models of breast cancer. *Nat Commun* *13*, 3022. <https://doi.org/10.1038/s41467-022-30568-1>.
216. Shi, F., Su, J., Wang, J., Liu, Z., and Wang, T. (2021). Activation of STING inhibits cervical cancer tumor growth through enhancing the anti-tumor immune response. *Mol Cell Biochem* *476*, 1015–1024. <https://doi.org/10.1007/s11010-020-03967-5>.

217. Lu, C., Guan, J., Lu, S., Jin, Q., Rousseau, B., Lu, T., Stephens, D., Zhang, H., Zhu, J., Yang, M., et al. (2021). DNA Sensing in Mismatch Repair-Deficient Tumor Cells Is Essential for Anti-tumor Immunity. *Cancer Cell* 39, 96-108.e6. <https://doi.org/10.1016/j.ccell.2020.11.006>.
218. Falahat, R., Perez-Villaruel, P., Mailloux, A.W., Zhu, G., Pilon-Thomas, S., Barber, G.N., and Mulé, J.J. (2019). STING Signaling in Melanoma Cells Shapes Antigenicity and Can Promote Antitumor T-cell Activity. *Cancer Immunol Res* 7, 1837–1848. <https://doi.org/10.1158/2326-6066.CIR-19-0229>.
219. Falahat, R., Berglund, A., Putney, R.M., Perez-Villaruel, P., Aoyama, S., Pilon-Thomas, S., Barber, G.N., and Mulé, J.J. (2021). Epigenetic reprogramming of tumor cell-intrinsic STING function sculpts antigenicity and T cell recognition of melanoma. *Proc Natl Acad Sci U S A* 118, e2013598118. <https://doi.org/10.1073/pnas.2013598118>.
220. Wang-Bishop, L., Wehbe, M., Shae, D., James, J., Hacker, B.C., Garland, K., Chistov, P.P., Rafat, M., Balko, J.M., and Wilson, J.T. (2020). Potent STING activation stimulates immunogenic cell death to enhance antitumor immunity in neuroblastoma. *J Immunother Cancer* 8, e000282. <https://doi.org/10.1136/JITC-2019-000282>.
221. Yang, H., Lee, W.S., Kong, S.J., Kim, C.G., Kim, J.H., Chang, S.K., Kim, S., Kim, G., Chon, H.J., and Kim, C. (2019). STING activation reprograms tumor vasculatures and synergizes with VEGFR2 blockade. *Journal of Clinical Investigation* 129, 4350–4364. <https://doi.org/10.1172/JCI125413>.
222. Garland, K.M., Sheehy, T.L., and Wilson, J.T. (2022). Chemical and Biomolecular Strategies for STING Pathway Activation in Cancer Immunotherapy. *Chem Rev* 122, 5977–6039. <https://doi.org/10.1021/acs.chemrev.1c00750>.

223. Motedayen Aval, L., Pease, J.E., Sharma, R., and Pinato, D.J. (2020). Challenges and Opportunities in the Clinical Development of STING Agonists for Cancer Immunotherapy. *J Clin Med* 9, 3323. <https://doi.org/10.3390/jcm9103323>.
224. Cerboni, S., Jeremiah, N., Gentili, M., Gehrman, U., Conrad, C., Stolzenberg, M.-C., Picard, C., Neven, B., Fischer, A., Amigorena, S., et al. (2017). Intrinsic antiproliferative activity of the innate sensor STING in T lymphocytes. *J Exp Med* 214, 1769–1785. <https://doi.org/10.1084/jem.20161674>.
225. Huang, L., Li, L., Lemos, H., Chandler, P.R., Pacholczyk, G., Baban, B., Barber, G.N., Hayakawa, Y., McGaha, T.L., Ravishankar, B., et al. (2013). Cutting Edge: DNA Sensing via the STING Adaptor in Myeloid Dendritic Cells Induces Potent Tolerogenic Responses. *The Journal of Immunology* 191, 3509–3513. <https://doi.org/10.4049/jimmunol.1301419>.
226. Lemos, H., Mohamed, E., Huang, L., Ou, R., Pacholczyk, G., Arbab, A.S., Munn, D., and Mellor, A.L. (2016). STING Promotes the Growth of Tumors Characterized by Low Antigenicity via IDO Activation. *Cancer Res* 76, 2076–2081. <https://doi.org/10.1158/0008-5472.CAN-15-1456>.
227. Bakhoun, S.F., Ngo, B., Laughney, A.M., Cavallo, J.-A., Murphy, C.J., Ly, P., Shah, P., Sriram, R.K., Watkins, T.B.K., Taunk, N.K., et al. (2018). Chromosomal instability drives metastasis through a cytosolic DNA response. *Nature* 553, 467–472. <https://doi.org/10.1038/nature25432>.
228. Chen, Q., Boire, A., Jin, X., Valiente, M., Er, E.E., Lopez-Soto, A., Jacob, L., Patwa, R., Shah, H., Xu, K., et al. (2016). Carcinoma-astrocyte gap junctions promote brain metastasis by cGAMP transfer. *Nature* 533, 493–498. <https://doi.org/10.1038/nature18268>.
229. Xia, Y., Shen, S., and Verma, I.M. (2014). NF- κ B, an Active Player in Human Cancers. *Cancer Immunol Res* 2, 823–830. <https://doi.org/10.1158/2326-6066.CIR-14-0112>.

230. Vasiyani, H., and Wadhwa, B. (2025). STING activation and overcoming the challenges associated with STING agonists using ADC (antibody-drug conjugate) and other delivery systems. *Cell Signal* 128, 111647.
<https://doi.org/10.1016/j.cellsig.2025.111647>.
231. Karakashev, S., and Zhang, R.-G. (2021). Mouse models of epithelial ovarian cancer for preclinical studies. *Zool Res* 42, 153–160.
<https://doi.org/10.24272/j.issn.2095-8137.2020.382>.
232. Ciucci, A., Buttarelli, M., Fagotti, A., Scambia, G., and Gallo, D. (2022). Preclinical models of epithelial ovarian cancer: practical considerations and challenges for a meaningful application. *Cellular and Molecular Life Sciences* 79, 364. <https://doi.org/10.1007/s00018-022-04395-y>.
233. Tsang, S.I., Hassan, A.A., To, S.K.Y., and Wong, A.S.T. (2022). Experimental models for ovarian cancer research. *Exp Cell Res* 416, 113150.
<https://doi.org/10.1016/j.yexcr.2022.113150>.
234. Roby, K.F., Taylor, C.C., Sweetwood, J.P., Cheng, Y., Pace, J.L., Tawfik, O., Persons, D.L., Smith, P.G., and Terranova, P.F. (2000). Development of a syngeneic mouse model for events related to ovarian cancer. *Carcinogenesis* 21, 585–591. <https://doi.org/10.1093/carcin/21.4.585>.
235. Walton, J., Blagih, J., Ennis, D., Leung, E., Dowson, S., Farquharson, M., Tookman, L.A., Orange, C., Athineos, D., Mason, S., et al. (2016). CRISPR/Cas9-Mediated Trp53 and Brca2 Knockout to Generate Improved Murine Models of Ovarian High-Grade Serous Carcinoma. *Cancer Res* 76, 6118–6129.
<https://doi.org/10.1158/0008-5472.CAN-16-1272>.

236. Walton, J.B., Farquharson, M., Mason, S., Port, J., Kruspig, B., Dowson, S., Stevenson, D., Murphy, D., Matzuk, M., Kim, J., et al. (2017). CRISPR/Cas9-derived models of ovarian high grade serous carcinoma targeting *Brcal*, *Pten* and *Nf1*, and correlation with platinum sensitivity. *Sci Rep* 7, 16827. <https://doi.org/10.1038/s41598-017-17119-1>.
237. de Witte, C.J., Kutzera, J., van Hoeck, A., Nguyen, L., Boere, I.A., Jalving, M., Ottevanger, P.B., van Schaik-van de Mheen, C., Stevense, M., Kloosterman, W.P., et al. (2022). Distinct Genomic Profiles Are Associated with Treatment Response and Survival in Ovarian Cancer. *Cancers (Basel)* 14, 1511. <https://doi.org/10.3390/cancers14061511>.
238. Alsop, K., Fereday, S., Meldrum, C., deFazio, A., Emmanuel, C., George, J., Dobrovic, A., Birrer, M.J., Webb, P.M., Stewart, C., et al. (2012). *BRCA* Mutation Frequency and Patterns of Treatment Response in *BRCA* Mutation-Positive Women With Ovarian Cancer: A Report From the Australian Ovarian Cancer Study Group. *Journal of Clinical Oncology* 30, 2654–2663. <https://doi.org/10.1200/JCO.2011.39.8545>.
239. Liao, J.B., Ovenell, K.J., Curtis, E.E.M., Cecil, D.L., Koehnlein, M.R., Rastetter, L.R., Gad, E.A., and Disis, M.L. (2015). Preservation of tumor-host immune interactions with luciferase-tagged imaging in a murine model of ovarian cancer. *J Immunother Cancer* 3, 16. <https://doi.org/10.1186/s40425-015-0060-6>.
240. Gitto, S.B., Kim, H., Rafail, S., Omran, D.K., Medvedev, S., Kinose, Y., Rodriguez-Garcia, A., Flowers, A.J., Xu, H., Schwartz, L.E., et al. (2020). An autologous humanized patient-derived-xenograft platform to evaluate immunotherapy in ovarian cancer. *Gynecol Oncol* 156, 222–232. <https://doi.org/10.1016/j.ygyno.2019.10.011>.
241. Stein, S.C., and Falck-Pedersen, E. (2012). Sensing Adenovirus Infection: Activation of Interferon Regulatory Factor 3 in RAW 264.7 Cells. *J Virol* 86, 4527–4537. <https://doi.org/10.1128/JVI.07071-11>.

242. Gonugunta, V.K., Sakai, T., Pokatayev, V., Yang, K., Wu, J., Dobbs, N., and Yan, N. (2017). Trafficking-Mediated STING Degradation Requires Sorting to Acidified Endolysosomes and Can Be Targeted to Enhance Anti-tumor Response. *Cell Rep* 21, 3234–3242. <https://doi.org/10.1016/j.celrep.2017.11.061>.
243. Parungo, C.P., Soybel, D.I., Colson, Y.L., Kim, S.-W., Ohnishi, S., De Grand, A.M., Laurence, R.G., Soltész, E.G., Chen, F.Y., Cohn, L.H., et al. (2007). Lymphatic Drainage of the Peritoneal Space: A Pattern Dependent on Bowel Lymphatics. *Ann Surg Oncol* 14, 286–298. <https://doi.org/10.1245/s10434-006-9044-6>.
244. Lazear, H.M., Schoggins, J.W., and Diamond, M.S. (2019). Shared and Distinct Functions of Type I and Type III Interferons. *Immunity* 50, 907–923. <https://doi.org/10.1016/j.immuni.2019.03.025>.
245. Ank, N., West, H., Bartholdy, C., Eriksson, K., Thomsen, A.R., and Paludan, S.R. (2006). Lambda Interferon (IFN- λ), a Type III IFN, Is Induced by Viruses and IFNs and Displays Potent Antiviral Activity against Select Virus Infections In Vivo. *J Virol* 80, 4501–4509. <https://doi.org/10.1128/JVI.80.9.4501-4509.2006>.
246. Li, M., Ferretti, M., Ying, B., Descamps, H., Lee, E., Dittmar, M., Lee, J.S., Whig, K., Kamalia, B., Dohnalová, L., et al. (2021). Pharmacological activation of STING blocks SARS-CoV-2 infection. *Sci Immunol* 6, eabi9007. <https://doi.org/10.1126/sciimmunol.abi9007>.
247. Sawant, K. V., Poluri, K.M., Dutta, A.K., Sepuru, K.M., Troshkina, A., Garofalo, R.P., and Rajarathnam, K. (2016). Chemokine CXCL1 mediated neutrophil recruitment: Role of glycosaminoglycan interactions. *Sci Rep* 6, 33123. <https://doi.org/10.1038/srep33123>.

248. Ghaffari, A., Peterson, N., Khalaj, K., Vitkin, N., Robinson, A., Francis, J.-A., and Koti, M. (2018). STING agonist therapy in combination with PD-1 immune checkpoint blockade enhances response to carboplatin chemotherapy in high-grade serous ovarian cancer. *Br J Cancer* *119*, 440–449. <https://doi.org/10.1038/s41416-018-0188-5>.
249. Ding, L., Wang, Q., Martincuks, A., Kearns, M.J., Jiang, T., Lin, Z., Cheng, X., Qian, C., Xie, S., Kim, H.-J., et al. (2023). STING agonism overcomes STAT3-mediated immunosuppression and adaptive resistance to PARP inhibition in ovarian cancer. *J Immunother Cancer* *11*, e005627. <https://doi.org/10.1136/jitc-2022-005627>.
250. Rickard, B.P., Conrad, C., Sorrin, A.J., Ruhi, M.K., Reader, J.C., Huang, S.A., Franco, W., Scarcelli, G., Polacheck, W.J., Roque, D.M., et al. (2021). Malignant Ascites in Ovarian Cancer: Cellular, Acellular, and Biophysical Determinants of Molecular Characteristics and Therapy Response. *Cancers (Basel)* *13*, 4318. <https://doi.org/10.3390/cancers13174318>.
251. Jamur, M.C., Moreno, A.N., Mello, L.F., Souza Júnior, D.A., Campos, M.R.C., Pastor, M.V.D., Grodzki, A.C.G., Silva, D.C., and Oliver, C. (2010). Mast cell repopulation of the peritoneal cavity: contribution of mast cell progenitors versus bone marrow derived committed mast cell precursors. *BMC Immunol* *11*, 32. <https://doi.org/10.1186/1471-2172-11-32>.
252. McAdams, J., Ebott, J., Jansen, C., Kim, C., Maiz, D., Ou, J., Hanley, L.C., Cruz, P.D. La, and James, N.E. (2024). Neoadjuvant chemotherapy induces phenotypic mast cell changes in high grade serous ovarian cancer. *J Ovarian Res* *17*, 192. <https://doi.org/10.1186/s13048-024-01516-y>.

253. Cao, K., Zhang, G., Zhang, X., Yang, M., Wang, Y., He, M., Lu, J., and Liu, H. (2021). Stromal infiltrating mast cells identify immunoevasive subtype high-grade serous ovarian cancer with poor prognosis and inferior immunotherapeutic response. *Oncoimmunology* *10*, 1969075. <https://doi.org/10.1080/2162402X.2021.1969075>.
254. Meyer, N., Hinz, N., Schumacher, A., Weißenborn, C., Fink, B., Bauer, M., von Lenthe, S., Ignatov, A., Fest, S., and Zenclussen, A.C. (2023). Mast Cells Retard Tumor Growth in Ovarian Cancer: Insights from a Mouse Model. *Cancers (Basel)* *15*, 4278. <https://doi.org/10.3390/cancers15174278>.
255. Chan, J.K., Magistris, A., Loizzi, V., Lin, F., Rutgers, J., Osann, K., DiSaia, P.J., and Samoszuk, M. (2005). Mast cell density, angiogenesis, blood clotting, and prognosis in women with advanced ovarian cancer. *Gynecol Oncol* *99*, 20–25. <https://doi.org/10.1016/J.YGYNO.2005.05.042>.
256. Rodewald, H.-R., and Feyerabend, T.B. (2012). Widespread immunological functions of mast cells: fact or fiction? *Immunity* *37*, 13–24. <https://doi.org/10.1016/j.immuni.2012.07.007>.
257. Wolters, P.J., Mallen-St Clair, J., Lewis, C.C., Villalta, S.A., Baluk, P., Erle, D.J., and Caughey, G.H. (2005). Tissue-selective mast cell reconstitution and differential lung gene expression in mast cell-deficient Kit(W-sh)/Kit(W-sh) sash mice. *Clin Exp Allergy* *35*, 82–88. <https://doi.org/10.1111/j.1365-2222.2005.02136.x>.
258. Bouis, D., Kirstetter, P., Arbogast, F., Lamon, D., Delgado, V., Jung, S., Ebel, C., Jacobs, H., Knapp, A.M., Jeremiah, N., et al. (2019). Severe combined immunodeficiency in stimulator of interferon genes (STING) V154M/wild-type mice. *J Allergy Clin Immunol* *143*, 712-725.e5. <https://doi.org/10.1016/J.JACI.2018.04.034>.

259. Jia, T., Serbina, N. V., Brandl, K., Zhong, M.X., Leiner, I.M., Charo, I.F., and Pamer, E.G. (2008). Additive Roles for MCP-1 and MCP-3 in CCR2-Mediated Recruitment of Inflammatory Monocytes during *Listeria monocytogenes* Infection. *The Journal of Immunology* *180*, 6846–6853.
<https://doi.org/10.4049/jimmunol.180.10.6846>.
260. Sze, A., Belgnaoui, S.M., Olganier, D., Lin, R., Hiscott, J., and van Grevenynghe, J. (2013). Host restriction factor SAMHD1 limits human T cell leukemia virus type 1 infection of monocytes via STING-mediated apoptosis. *Cell Host Microbe* *14*, 422–434. <https://doi.org/10.1016/j.chom.2013.09.009>.
261. Yi, G., Brendel, V.P., Shu, C., Li, P., Palanathan, S., and Cheng Kao, C. (2013). Single Nucleotide Polymorphisms of Human STING Can Affect Innate Immune Response to Cyclic Dinucleotides. *PLoS One* *8*, e77846.
<https://doi.org/10.1371/journal.pone.0077846>.
262. Conlon, J., Burdette, D.L., Sharma, S., Bhat, N., Thompson, M., Jiang, Z., Rathinam, V.A.K., Monks, B., Jin, T., Xiao, T.S., et al. (2013). Mouse, but not human STING, binds and signals in response to the vascular disrupting agent 5,6-dimethylxanthenone-4-acetic acid. *J Immunol* *190*, 5216–5225.
<https://doi.org/10.4049/jimmunol.1300097>.
263. Prelich, G. (2012). Gene Overexpression: Uses, Mechanisms, and Interpretation. *Genetics* *190*, 841–854. <https://doi.org/10.1534/genetics.111.136911>.
264. Raqib, R., Moly, P.K., Sarker, P., Qadri, F., Alam, N.H., Mathan, M., and Andersson, J. (2003). Persistence of Mucosal Mast Cells and Eosinophils in *Shigella* -Infected Children. *Infect Immun* *71*, 2684–2692.
<https://doi.org/10.1128/IAI.71.5.2684-2692.2003>.

265. Dudeck, J., Kotrba, J., Immler, R., Hoffmann, A., Voss, M., Alexaki, V.I., Morton, L., Jahn, S.R., Katsoulis-Dimitriou, K., Winzer, S., et al. (2021). Directional mast cell degranulation of tumor necrosis factor into blood vessels primes neutrophil extravasation. *Immunity* 54, 468-483.e5. <https://doi.org/10.1016/j.immuni.2020.12.017>.
266. De Filippo, K., Dudeck, A., Hasenberg, M., Nye, E., van Rooijen, N., Hartmann, K., Gunzer, M., Roers, A., and Hogg, N. (2013). Mast cell and macrophage chemokines CXCL1/CXCL2 control the early stage of neutrophil recruitment during tissue inflammation. *Blood* 121, 4930–4937. <https://doi.org/10.1182/blood-2013-02-486217>.
267. Pejler, G., Alanazi, S., Grujic, M., Adler, J., Olsson, A.-K., Sommerhoff, C.P., and Rabelo Melo, F. (2022). Mast Cell Tryptase Potentiates Neutrophil Extracellular Trap Formation. *J Innate Immun* 14, 433–446. <https://doi.org/10.1159/000520972>.
268. Ray, A., Chatterjee, N.S., Bhattacharya, S.K., and Biswas, T. (2003). Porin of *Shigella dysenteriae* enhances mRNA levels for Toll-like receptor 2 and MyD88, up-regulates CD80 of murine macrophage, and induces the release of interleukin-12. *FEMS Immunol Med Microbiol* 39, 213–219. [https://doi.org/10.1016/S0928-8244\(03\)00233-5](https://doi.org/10.1016/S0928-8244(03)00233-5).
269. Yang, J.-Y., Lee, S.-N., Chang, S.-Y., Ko, H.-J., Ryu, S., and Kweon, M.-N. (2014). A Mouse Model of Shigellosis by Intraperitoneal Infection. *J Infect Dis* 209, 203–215. <https://doi.org/10.1093/infdis/jit399>.
270. Hathaway, L.J., Griffin, G.E., Sansonetti, P.J., and Edgeworth, J.D. (2002). Human Monocytes Kill *Shigella flexneri* but Then Die by Apoptosis Associated with Suppression of Proinflammatory Cytokine Production. *Infect Immun* 70, 3833–3842. <https://doi.org/10.1128/IAI.70.7.3833-3842.2002>.

271. Sutherland, R.E., Olsen, J.S., McKinstry, A., Villalta, S.A., and Wolters, P.J. (2008). Mast Cell IL-6 Improves Survival from *Klebsiella* Pneumonia and Sepsis by Enhancing Neutrophil Killing. *The Journal of Immunology* *181*, 5598–5605. <https://doi.org/10.4049/jimmunol.181.8.5598>.
272. Yamamoto, K., Kondo, Y., Ohnishi, S., Yoshida, M., Sugiyama, T., and Sakamoto, N. (2021). The TLR4–TRIF–type 1 IFN–IFN- γ pathway is crucial for gastric MALT lymphoma formation after *Helicobacter suis* infection. *iScience* *24*, 103064. <https://doi.org/10.1016/j.isci.2021.103064>.
273. von Beek, C., Fahlgren, A., Geiser, P., Di Martino, M.L., Lindahl, O., Prensa, G.I., Mendez-Enriquez, E., Eriksson, J., Hallgren, J., Fällman, M., et al. (2024). A two-step activation mechanism enables mast cells to differentiate their response between extracellular and invasive enterobacterial infection. *Nat Commun* *15*, 904. <https://doi.org/10.1038/s41467-024-45057-w>.
274. Mayavannan, A., Shantz, E., Haidl, I.D., Wang, J., and Marshall, J.S. (2023). Mast cells selectively produce inflammatory mediators and impact the early response to *Chlamydia* reproductive tract infection. *Front Immunol* *14*, 1166068. <https://doi.org/10.3389/fimmu.2023.1166068>.
275. Soria-Castro, R., Alfaro-Doblado, Á.R., Rodríguez-López, G., Campillo-Navarro, M., Meneses-Preza, Y.G., Galán-Salinas, A., Alvarez-Jimenez, V., Yam-Puc, J.C., Munguía-Fuentes, R., Domínguez-Flores, A., et al. (2021). TLR2 Regulates Mast Cell IL-6 and IL-13 Production During *Listeria monocytogenes* Infection. *Front Immunol* *12*, 650779. <https://doi.org/10.3389/fimmu.2021.650779>.
276. Edgeworth, J.D., Spencer, J., Phalipon, A., Griffin, G.E., and Sansonetti, P.J. (2002). Cytotoxicity and interleukin-1 β processing following *Shigella flexneri* infection of human monocyte-derived dendritic cells. *Eur J Immunol* *32*, 1464–1471. [https://doi.org/10.1002/1521-4141\(200205\)32:5<1464::AID-IMMU1464>3.0.CO;2-G](https://doi.org/10.1002/1521-4141(200205)32:5<1464::AID-IMMU1464>3.0.CO;2-G).

277. Carneiro, L.A.M., Travassos, L.H., Soares, F., Tattoli, I., Magalhaes, J.G., Bozza, M.T., Plotkowski, M.C., Sansonetti, P.J., Molkentin, J.D., Philpott, D.J., et al. (2009). Shigella Induces Mitochondrial Dysfunction and Cell Death in Nonmyeloid Cells. *Cell Host Microbe* 5, 123–136. <https://doi.org/10.1016/j.chom.2008.12.011>.
278. Krämer, S., Sellge, G., Lorentz, A., Krueger, D., Schemann, M., Feilhauer, K., Gunzer, F., and Bischoff, S.C. (2008). Selective Activation of Human Intestinal Mast Cells by *Escherichia coli* Hemolysin. *The Journal of Immunology* 181, 1438–1445. <https://doi.org/10.4049/jimmunol.181.2.1438>.
279. Liu, M., Zhang, Y., Xu, Q., Liu, G., Sun, N., Che, H., and He, T. (2021). Apigenin Inhibits the Histamine-Induced Proliferation of Ovarian Cancer Cells by Downregulating ER α /ER β Expression. *Front Oncol* 11, 682917. <https://doi.org/10.3389/fonc.2021.682917>.
280. Cheng, S., Li, Z., Gao, R., Xing, B., Gao, Y., Yang, Y., Qin, S., Zhang, L., Ouyang, H., Du, P., et al. (2021). A pan-cancer single-cell transcriptional atlas of tumor infiltrating myeloid cells. *Cell* 184, 792-809.e23. <https://doi.org/10.1016/j.cell.2021.01.010>.
281. Ribatti, D., and Crivellato, E. (2012). Mast cells, angiogenesis, and tumour growth. *Biochimica et Biophysica Acta (BBA) - Molecular Basis of Disease* 1822, 2–8. <https://doi.org/10.1016/J.BBADIS.2010.11.010>.
282. Marech, I., Ammendola, M., Sacco, R., Capriuolo, G.S., Patruno, R., Rubini, R., Luposella, M., Zuccalà, V., Savino, E., Gadaleta, C.D., et al. (2014). Serum tryptase, mast cells positive to tryptase and microvascular density evaluation in early breast cancer patients: possible translational significance. *BMC Cancer* 14, 534. <https://doi.org/10.1186/1471-2407-14-534>.

283. Ammendola, M., Sacco, R., Sammarco, G., Donato, G., Zuccalà, V., Luposella, M., Patruno, R., Marech, I., Montemurro, S., Zizzo, N., et al. (2014). Mast Cells Density Positive to Tryptase Correlates with Angiogenesis in Pancreatic Ductal Adenocarcinoma Patients Having Undergone Surgery. *Gastroenterol Res Pract* 2014, 1–7. <https://doi.org/10.1155/2014/951957>.
284. Ammendola, M., Sacco, R., Sammarco, G., Donato, G., Montemurro, S., Ruggieri, E., Patruno, R., Marech, I., Cariello, M., Vacca, A., et al. (2014). Correlation between Serum Tryptase, Mast Cells Positive to Tryptase and Microvascular Density in Colo-Rectal Cancer Patients: Possible Biological-Clinical Significance. *PLoS One* 9, e99512. <https://doi.org/10.1371/journal.pone.0099512>.
285. Fereydouni, M., Ahani, E., Desai, P., Motaghd, M., Dellinger, A., Metcalfe, D.D., Yin, Y., Lee, S.H., Kafri, T., Bhatt, A.P., et al. (2022). Human Tumor Targeted Cytotoxic Mast Cells for Cancer Immunotherapy. *Front Oncol* 12, 871390. <https://doi.org/10.3389/fonc.2022.871390>.
286. Plotkin, J.D., Elias, M.G., Fereydouni, M., Daniels-Wells, T.R., Dellinger, A.L., Penichet, M.L., and Kepley, C.L. (2019). Human Mast Cells From Adipose Tissue Target and Induce Apoptosis of Breast Cancer Cells. *Front Immunol* 10, 432943. <https://doi.org/10.3389/fimmu.2019.00138>.
287. Bodduluri, S.R., Mathis, S., Maturu, P., Krishnan, E., Satpathy, S.R., Chilton, P.M., Mitchell, T.C., Lira, S., Locati, M., Mantovani, A., et al. (2018). Mast Cell-Dependent CD8⁺ T-cell Recruitment Mediates Immune Surveillance of Intestinal Tumors in ApcMin/+ Mice. *Cancer Immunol Res* 6, 332–347. <https://doi.org/10.1158/2326-6066.CIR-17-0424>.
288. Vosskuhl, K., Greten, T.F., Manns, M.P., Korangy, F., and Wedemeyer, J. (2010). Lipopolysaccharide-Mediated Mast Cell Activation Induces IFN- γ Secretion by NK Cells. *The Journal of Immunology* 185, 119–125. <https://doi.org/10.4049/JIMMUNOL.0902406>.

289. Dudeck, A., Suender, C.A., Kostka, S.L., von Stebut, E., and Maurer, M. (2011). Mast cells promote Th1 and Th17 responses by modulating dendritic cell maturation and function. *Eur J Immunol* *41*, 1883–1893. <https://doi.org/10.1002/EJI.201040994>.
290. Ma, Y., Zhao, X., Feng, J., Qiu, S., Ji, B., Huang, L., Hwu, P., Logsdon, C.D., and Wang, H. (2024). Tumor-infiltrating mast cells confer resistance to immunotherapy in pancreatic cancer. *iScience* *27*, 111085. <https://doi.org/10.1016/j.isci.2024.111085>.
291. Prasad, C.P., Tripathi, S.C., Kumar, M., and Mohapatra, P. (2023). Passage number of cancer cell lines: Importance, intricacies, and way-forward. *Biotechnol Bioeng* *120*, 2049–2055. <https://doi.org/10.1002/bit.28496>.
292. Johansson, A., Rudolfsson, S., Hammarsten, P., Halin, S., Pietras, K., Jones, J., Stattin, P., Egevad, L., Granfors, T., Wikström, P., et al. (2010). Mast Cells Are Novel Independent Prognostic Markers in Prostate Cancer and Represent a Target for Therapy. *Am J Pathol* *177*, 1031–1041. <https://doi.org/10.2353/ajpath.2010.100070>.
293. Lee, W., Ko, S.Y., Mohamed, M.S., Kenny, H.A., Lengyel, E., and Naora, H. (2019). Neutrophils facilitate ovarian cancer premetastatic niche formation in the omentum. *Journal of Experimental Medicine* *216*, 176–194. <https://doi.org/10.1084/jem.20181170>.
294. Van Herck, S., Feng, B., and Tang, L. (2021). Delivery of STING agonists for adjuvanting subunit vaccines. *Adv Drug Deliv Rev* *179*, 114020. <https://doi.org/10.1016/j.addr.2021.114020>.
295. Luo, J., Liu, X., Xiong, F., Gao, F., Yi, Y., Zhang, M., Chen, Z., and Tan, W. (2019). Enhancing Immune Response and Heterosubtypic Protection Ability of Inactivated H7N9 Vaccine by Using STING Agonist as a Mucosal Adjuvant. *Front Immunol* *10*, 2274. <https://doi.org/10.3389/fimmu.2019.02274>.

296. McLachlan, J.B., Shelburne, C.P., Hart, J.P., Pizzo, S. V, Goyal, R., Brooking-Dixon, R., Staats, H.F., and Abraham, S.N. (2008). Mast cell activators: a new class of highly effective vaccine adjuvants. *Nat Med* *14*, 536–541. <https://doi.org/10.1038/nm1757>.
297. Crow, Y.J., and Stetson, D.B. (2022). The type I interferonopathies: 10 years on. *Nat Rev Immunol* *22*, 471–483. <https://doi.org/10.1038/s41577-021-00633-9>.
298. Xu, Y., and Chen, G. (2015). Mast Cell and Autoimmune Diseases. *Mediators Inflamm* *2015*, 246126. <https://doi.org/10.1155/2015/246126>.
299. Abraham, S.N., and St. John, A.L. (2010). Mast cell-orchestrated immunity to pathogens. *Nat Rev Immunol* *10*, 440–452. <https://doi.org/10.1038/nri2782>.
300. Soule, B.P., Brown, J.M., Kushnir-Sukhov, N.M., Simone, N.L., Mitchell, J.B., and Metcalfe, D.D. (2007). Effects of Gamma Radiation on FcεRI and TLR-Mediated Mast Cell Activation. *The Journal of Immunology* *179*, 3276–3286. <https://doi.org/10.4049/jimmunol.179.5.3276>.
301. Albert-Bayo, M., Paracuellos, I., González-Castro, A.M., Rodríguez-Urrutia, A., Rodríguez-Lagunas, M.J., Alonso-Cotoner, C., Santos, J., and Vicario, M. (2019). Intestinal Mucosal Mast Cells: Key Modulators of Barrier Function and Homeostasis. *Cells* *8*, 135. <https://doi.org/10.3390/cells8020135>.
302. Li, H., Zhou, X., Huang, Y., Liao, B., Cheng, L., and Ren, B. (2021). Reactive Oxygen Species in Pathogen Clearance: The Killing Mechanisms, the Adaption Response, and the Side Effects. *Front Microbiol* *11*, 622534. <https://doi.org/10.3389/fmicb.2020.622534>.
303. Alphonse, N., and Odendall, C. (2023). Animal models of shigellosis: a historical overview. *Curr Opin Immunol* *85*, 102399. <https://doi.org/10.1016/j.coi.2023.102399>.

304. Mitchell, P.S., Roncaioli, J.L., Turcotte, E.A., Goers, L., Chavez, R.A., Lee, A.Y., Lesser, C.F., Rauch, I., and Vance, R.E. (2020). NAIP–NLRC4-deficient mice are susceptible to shigellosis. *Elife* *9*, e59022. <https://doi.org/10.7554/eLife.59022>.
305. de Jonge, W.J., The, F.O., van der Coelen, D., Bennink, R.J., Reitsma, P.H., van Deventer, S.J., Van den Wijngaard, R.M., and Boeckxstaens, G.E. (2004). Mast cell degranulation during abdominal surgery initiates postoperative ileus in mice. *Gastroenterology* *127*, 535–545. <https://doi.org/10.1053/j.gastro.2004.04.017>.
306. Balan, D., Kampan, N.C., Plebanski, M., and Abd Aziz, N.H. (2024). Unlocking ovarian cancer heterogeneity: advancing immunotherapy through single-cell transcriptomics. *Front Oncol* *14*, 1388663. <https://doi.org/10.3389/fonc.2024.1388663>.
307. Cook, D.P., Galpin, K.J.C., Rodriguez, G.M., Shakfa, N., Wilson-Sanchez, J., Echaibi, M., Pereira, M., Matuszewska, K., Haagsma, J., Murshed, H., et al. (2023). Comparative analysis of syngeneic mouse models of high-grade serous ovarian cancer. *Commun Biol* *6*, 1152. <https://doi.org/10.1038/s42003-023-05529-z>.
308. Ribatti, D. (2018). The Staining of Mast Cells: A Historical Overview. *Int Arch Allergy Immunol* *176*, 55–60. <https://doi.org/10.1159/000487538>.
309. Wu, Y.-T., Fang, Y., Wei, Q., Shi, H., Tan, H., Deng, Y., Zeng, Z., Qiu, J., Chen, C., Sun, L., et al. (2022). Tumor-targeted delivery of a STING agonist improves cancer immunotherapy. *Proc Natl Acad Sci U S A* *119*, e2214278119. <https://doi.org/10.1073/pnas.2214278119>.
310. Malli Cetinbas, N., Monnell, T., Soomer-James, J., Shaw, P., Lancaster, K., Catcott, K.C., Dolan, M., Mosher, R., Routhier, C., Chin, C.-N., et al. (2024). Tumor cell-directed STING agonist antibody-drug conjugates induce type III interferons and anti-tumor innate immune responses. *Nat Commun* *15*, 5842. <https://doi.org/10.1038/s41467-024-49932-4>.